

Design and Evaluation of a Novel Motion Cueing Algorithm for the Desdemona Simulator

Bruno Jorge Correia Grácio

March 10, 2009



# Advanced Driving in the Desdemona Simulator

Design and Evaluation of a Novel Motion Cueing Algorithm for the Desdemona Simulator

MASTER OF SCIENCE THESIS

For obtaining the degree of Master of Science in Aerospace Engineering at Delft University of Technology

Bruno Jorge Correia Grácio

March 10, 2009



#### **Delft University of Technology**

Copyright  $\odot$  Control and Simulation division, Delft University of Technology All rights reserved.

## DELFT UNIVERSITY OF TECHNOLOGY DEPARTMENT OF CONTROL AND SIMULATION

The undersigned hereby certify that they have read and recommend to the Faculty of Aerospace Engineering for acceptance a thesis entitled "Advanced Driving in the Desdemona Simulator" by Bruno Jorge Correia Grácio in partial fulfillment of the requirements for the degree of Master of Science.

	Dated: March 10, 2009
Supervisor:	
	prof. dr. ir. J. A. Mulder
Readers:	prof. dr. ir. M. Mulder
	dr. ir. M. M. van Paassen
	dr. ir. M. Wentink
	dr. ir. P. Feenstra

## Acknowledgements

I want to start my acknowledgments by expressing my gratitude to prof. dr. ir. Max Mulder. He supported my stay in the Netherlands for the MSc program and recommended me for an internship at TNO Defence, Security and Safety. The comments and advices that he gave during my thesis were very important to improve not only my work, but also my skills and competences. I want to thank dr. ir René van Paasen for all the good ideas he gave me during our meetings.

A special thanks to Rita Pais for the help with the painful LaTeX, for having the patience to read my documents and for all the great laughs during our car trips from Delft to Soesterberg (when she was able to stay awake...).

I also want to thank prof. dr. ir. J. A. Mulder for giving me the opportunity to do my MSc at the Control and Simulation Division.

The present work was performed at TNO Defence, Security and Safety in Soesterberg. During my stay there I had the opportunity to meet and work with amazing people. I want to thank Bart Kappé for being a great roommate, Wim Bles for his stories and advices, Philippus Feenstra for his support, Paul Bakker for the help during the experiment in the Desdemona, Ingmar for his problem solving skills, Jelte Bos and Suzanne Nooij for all the lunch conversations, Nicolet Theunissen for explaining me the steps to design an effective questionnaire and Martin van Schaik for his help with factor analysis. A special thanks to all my colleagues at Training and Instruction for accepting in their department the only non-dutch speaker at TNO. I also want to thank all the participants of my experiment for their willingness to drive in the Desdemona.

I would like to express my most sincere gratitude to Mark Wentink. He was my first contact with TNO and has been my supervisor and mentor during my internship and MSc thesis at TNO. Without him, the outcome of the present work would have been totally different. I cannot thank him enough for what he has taught, for all the trust he has put on me and on my work, and above all, for his friendship.

I also want to thank Instituto Superior Técnico for making me the engineer I am today. It was there were I learnt how to exceed myself and to learn something out of nothing. For that

M.Sc. thesis

I have to thank all my colleagues from Aerospace Engineering. Thanks for the support in the long nights, for the help during difficult assignments, for all the lunches at Pizza Hut, for the card games at Civil and Química, for the beach days and mainly, for being the best friends one could ask when facing such a demanding challenge as are the Aerospace Engineering studies.

A special thanks goes to my closest friends for their support during these years. I want to thank Posturas for his special temper, Catroga for her nice stories, Madeiras for our trips, Julio for his sense of humor, Paulo for the great dinners at his house, Boavida for his friendship, Diogo and Gil for the great workgroup we were, Serra for being Serra, GT for his musical skills, Escórcio for showing us great spots, Tatiana for her accent, Nuno for his wisdom, Fred for being always ready, Mário for his pictures, Inês for her crazy ideas, Mathilde for her energy, Christina for the movie nights, Mauro, Emanuela and Kakin for the poker nights, and Miguel and Pires for the Sunday afternoons.

I want to thank Maria for being always there for me. She was the one who had to bear my bad temper during the difficult times and still was able to do it with a smile. Thanks to her I was able to feel at home even though Portugal is so far away. She is simply the best. I want also to thank my sister, my mother, my father, my grandparents and my uncle for making me the person I am today. If I am successful today it is thanks to you all. To finish, I still want to thank my mother for having the patience to raise both me and my sister, and my father for being the best role model ever and advising me to choose Aerospace instead of Electro technical Engineering.

Quero agradecer à Maria por estar sempre lá para mim. Foi ela que teve de aturar o meu mau feitio durante os tempos difíceis e foi capaz de o fazer com um sorriso. Graças a ela sentime sempre em casa mesmo que Portugal estivesse tão longe. Ela é simplesmente a melhor. Também quero agradecer à minha irmã, à minha mãe, ao meu pai, aos meus avós e ao meu tio por fazerem de mim a pessoa que sou hoje. Se tenho sucesso é graças a vocês todos. Para acabar, ainda quero agradecer à minha mãe por ter a paciência de criar-me a mim e à minha irmã e ao meu pai por ser o melhor modelo de sempre e por me aconselhar a escolher Engenharia Aeroespacial ao invés de Electrotécnica.

Delft, University of Technology March 10, 2009

Bruno Jorge Correia Grácio

## Table of Contents

	Acknowledgements	V
	Acronyms	xvi
I	MSc Article	1
	I DSC Europe 2009 paper Motion Feedback in Advanced Driving Manoeuvres	35
	II DSC Europe 2009 paper Effect of Simulator Motion Space on Realism in the Desdemona Simulat	or 51
		01 31
IV	V Preliminary Thesis	65
Ι <b>V</b> 1	V Preliminary Thesis	
	V Preliminary Thesis	65 67
	V Preliminary Thesis Introduction	<b>65</b> <b>67</b>
	V Preliminary Thesis Introduction 1-1 Background	<b>65 67</b> 68
	V Preliminary Thesis  Introduction 1-1 Background 1-2 Research Aims and Objectives 1-3 Research Methodology	<b>65 67</b> 68
1	V Preliminary Thesis  Introduction  1-1 Background  1-2 Research Aims and Objectives  1-3 Research Methodology	65 67 68 69
1	V Preliminary Thesis  Introduction 1-1 Background 1-2 Research Aims and Objectives 1-3 Research Methodology  Motion Cueing Algorithms	65 67 68 69 71
1	V Preliminary Thesis  Introduction 1-1 Background 1-2 Research Aims and Objectives 1-3 Research Methodology  Motion Cueing Algorithms 2-1 Classical Washout	65 67 68 69 71 73

M.Sc. thesis

3	Mot	ion Cu	eing Evaluation	79
	3-1	Motion	n Cue Errors	81
	3-2	Object	ive Evaluation	81
		3-2-1	Mathematical Measurement	83
			Graphical Comparison	83
			Performance Indicator	
		3-2-2	Behavioural measurements	101
			Power Spectral Density Analysis	
			Statistical Analysis of Mathematical Variables	
	3-3	Subjec	tive Evaluation	
		3-3-1	Rating Scales	
		3-3-2	Subjective Comments	
			Pairwise Comparison	
4	Extr	eme M	lanoeuvres in Curve Driving	129
	4-1	Slippin	g	129
	4-2	Sliding		131
	4-3	Unders	steer/Oversteer	132
		4-3-1	Position of the center of gravity (CG)	132
		4-3-2	Torque	132
		4-3-3	Wheight transfer	133
	4-4	Overst	eer dynamics	133
5	Desi	gn of F	Racing Motion Cueing Algorithms for Desdemona	137
	5-1	Desder	mona Specifications	137
	5-2	Motion	Cueing Solutions	137
		5-2-1	Solution 1:	137
		5-2-2	Solution 2:	
		5-2-3	Solution 3:	
		5-2-4	Solution 4:	
	5-3		inary motion cueing analysis	
		5-3-1	Car model	
		5-3-2	Datasets	
			Car model	
		5-3-3	Solution 1:	
		5-5-5	Car model results	
			Roundabout dataset results	
		5-3-4	Solution 2:	
			Car model results	

Table of Contents ix

		Roundabout dataset results	
	5-3-5		
		Car model results	165
		Roundabout dataset results	167
	5-3-6	Solution 4:	169
		Car model results	169
		Roundabout dataset results	171
6	Conclusion	and Future Guidelines	173
	6-1 Literat	ure Research	173
	6-2 Prelim	inary Analysis	174
V	Appendic	ces	183
Α	Car model	radius calculation	185
В	Questionna	nires (Dutch)	187

Table of Contents

## List of Figures

1-1	Document structure
2-1	General structure of a motion cueing algorithm [Wu and Cardullo, 1997]
2-2	Classical Washout Algorithm structure [Nahon and Reid, 1990]
2-3	Coordinate Adaptive algorithm structure [Nahon and Reid, 1990]
2-4	Aircraft simulation problem structure [Telban et al., 2000b]
2-5	Optimal Control algorithm structure [Nahon and Reid, 1990]
3-1	Objective evaluation structure
3-2	Motion fidelity criterion for different gains and phase distortions [Sinacori, 1977] $97$
3-3	Modified motion fidelity criterion [Schroeder, 1999]
3-4	Beneficial motion cues criterion for scaling [White and Rodchenko, 1999] 99
3-5	Negative motion cues criterion for scaling [White and Rodchenko, 1999] 100
3-6	Tilting coordination criterion [White and Rodchenko, 1999]
3-7	Subjective evaluation structure
3-8	Handling qualities rating scale
3-9	NASA TLX rating descriptions
3-10	NASA TLX rating sheet
3-11	UTIAS rating scale [Reid and Nahon, 1988]
3-12	MIT rating scale [Reid and Nahon, 1988]
3-13	Two-level assessment scale [Brünger-Koch et al., 2006a]
4-1	a) The Force F will disalign the planes of symmetry of the wheel and of the contact area. b) Slip angle of the whell when a lateral force F is applied

M.Sc. thesis

4-2	Example of slip angle versus available traction	130
4-3	Total force acting on a wheel due to torque and centrifugal forces. The circle aroung the wheel represents the total adhesion of the wheel (This circle is also known as traction circle).	131
4-4	Neutral steering on the left, understeering in the middle and oversteering on the right	
4-5	Center of gravity position. $F_c$ is the centrifugal force of the curve applied in the car CG during a curve. $F_r$ is the wheels reaction force. Note that $F_c$ is an imaginary force and does not exist in an inertial frame of reference.	
4-6	Weight transfers in a car. On the left we have weight transfer to the front or rear of the car while in the right we have lateral weight transfer. The yellow tire is the one supporting more weight.	133
4-7	On the left, the car is in a normal steer situation. On the right, the car oversteers during the curve	134
4-8	On the left, the car is in a curve without oversteering. On the right, the car is in a curve with oversteering.	135
5-1	Desdemona DoF's	138
5-2	Solution 1 block diagram	139
5-3	Solution 2 block diagram	140
5-4	Desdemona top view. Desdemona cabin is represented in dark blue while Desdemona radius is represented in light blue. The z axis is perpendicular to x and y and is represented as a point in the origin.	141
5-5	Desdemona top view. In red we have the Desdemona cabin reference frame and in black we have the Desdemona inertial reference frame.	141
5-6	Rotation of a mass point (yellow) on the tip of a string. The blue arrow stands for the particle velocity, the green arrow shows the centrifugal force (which is a fictional force, that has to be considered in non-inertial frames of reference) and the red arrow shows the centripetal force. R stands for the radius of the circle that the mass point is doing and $\omega$ stands for the angular velocity	142
5-7	Solution 3 block diagram	144
5-8	Total force decomposed into lateral force and gravity.	145
5-9	Solution 4 block diagram	146
5-10	Desdemona frame of reference	146
5-11	Desdemona pitch rotation. $x$ and $z$ represent Desdemona frame of reference while $x'$ and $z'$ represent Desdemona cabin position	147
5-12	Desdemona yaw rotation. x and y represent Desdemona frame of reference while x' and y' represent Desdemona cabin position.	148
5-13	Desdemona roll rotation. y and z represent Desdemona frame of reference while y' and z' represent Desdemona cabin position.	148
5-14	Car model	151
5-15	Radius of a curve. The blue vector represents the tire in a time instant. The green vector represents the tire in a future time instant, making an angle $\alpha$ with the blue vector. The orange line is proportional to the real curve radius	152
5-16	Steering wheel input.	153
5-17	Velocity input	154

5-18	Car model lateral specific force	154
5-19	Car model yaw rate	155
5-20	Roundabout dataset steering wheel angle.	156
5-21	Roundabout dataset lateral specific force.	156
5-22	Roundabout dataset yaw rate	157
5-23	Specific forces of the car model data versus simulated data using motion cueing solution 1	157
5-24	Angular rates of the car model data versus simulated data using motion cueing solution 1	158
5-25	Desdemona displacement using motion cueing solution 1 (car model data)	158
5-26	Specific forces of the roundabout data versus simulated data using motion cueing solution 1	159
	Angular rates of the roundabout data versus simulated data using motion cueing solution 1	
5-28	Desdemona displacement using motion cueing solution 1 (roundabout data)	160
	Specific forces of the car model data versus simulated data using motion cueing solution 2	161
	Angular rates of the car model data versus simulated data using motion cueing solution 2	
5-31	Desdemona displacement using motion cueing solution 2 (car model data)	162
	Specific forces of the roundabout data versus simulated data using motion cueing solution 2	163
	Angular rates of the roundabout data versus simulated data using motion cueing solution 2	164
5-34	Desdemona displacement Desdemona displacement using motion cueing solution 2 (roundabout data)	164
5-35	Specific forces of the car model data versus simulated data using motion cueing solution 3	165
5-36	Angular rates of the car model data versus simulated data using motion cueing solution 3	166
5-37	Desdemona displacement using motion cueing solution 3 (car model data)	166
	Specific forces of the roundabout data versus simulated data using motion cueing solution 3	167
5-39	Angular rates forces of the roundabout data versus simulated data using motion cueing solution 3	168
5-40	Desdemona displacement using motion cueing solution 3 (roundabout data)	168
5-41	Specific forces of the car model data versus simulated data using motion cueing solution 4	169
5-42	Angular rates of the car model data versus simulated data using motion cueing solution 4	170
5-43	Desdemona displacement using motion cueing solution 4 (car model data)	170
	Specific forces of the roundabout data versus simulated data using motion cueing solution 4	171
5-45	Angular rates of the roundabout data versus simulated data using motion cueing solution 4	172

xiv List of Figures

5-46	Desdemona displacement using motion cueing solution 4 (roundabout data) 173
	Radius of a curve. The blue vector represents the tire in a time instant. The green vector represents the tire in a future time instant, making an angle $\alpha$ with the blue vector. The orange line is proportional to the real curve radius

## List of Tables

3-1	Rating scale used during the experiment [Fortmüller and Meywerk, 2005] 1	22
5-1	Desdemona technical specifications	.38

M.Sc. thesis Bruno Jorge Correia Grácio

xvi List of Tables

## Acronyms

MCA Motion Cueing Algorithm

MDA Motion Drive Algorithm

**PSD** Power Spectral Density

**DUT** Delft University of Technology

TNO Netherlands Organization for Applied Scientific Research

AMST AUSTRIA METALL SYSTEMTECHNIK GmbH

**DSC** Driving Simulation Conference

Desdemona DESoriëntatie DEMONstrator Amst

xviii Acronyms

# Part I MSc Article

### Design and Evaluation of a Motion Cueing Algorithm for Advanced Driving Maneuvers

B. J. Correia Grácio,\*

Delft University of Technology, Delft, The Netherlands

M. Wentink,†

TNO Defence, Security and Safety, Soesterberg, The Netherlands

A. R. Valente Pais,‡ M. Mulder,§ and M. M. van Paassen¶

Delft University of Technology, Delft, The Netherlands

During advanced driving maneuvers, such as a slalom maneuver, drivers can be hypothesized to use all the available cues to optimize their performance. These type of maneuvers generate linear acceleration amplitudes and angular displacements (mainly in yaw) that most motion simulators cannot present. The innovative design of the Desdemona simulator seems adequate to simulate such motion cues. Features like the absence of angular displacement constraints, and having an 8 meter radius sledge to deliver high amplitude specific forces seem important to simulate such maneuvers. The first goal of this project was to develop a motion cueing algorithm that is capable of handling motion cues inherent to advanced driving maneuvers. The second goal was to study the effect of motion feedback in these extreme maneuvers. We hypothesize that motion feedback improves driver performance and affects the driving control strategy during advanced driving maneuvers when compared to a situation without motion feedback. To test the hypothesis, a comparison between no-motion car-driving simulation and motion-feedback car-driving simulation is done, by measuring driver performance and control behavior in a fast slalom. In the designed fast slalom, a car drives at 70 Km/h around pylons spaced quite closely from each other. Twenty subjects successfully drove the fast slalom in both conditions. The results from a paired comparison show that subjects prefer driving with motion feedback. Significant differences in the average speed between the two motion conditions were found. From the results we conclude that there is a difference in driving advanced maneuvers in a fixed based simulator as compared to a motion simulator. This difference influences driving behavior with respect to keeping control over the car. From the results it is also clear that drivers change their control strategy from one motion condition to the other.

#### I. Introduction

Motion feedback has been used in flight simulators for many years. For example Hosman, howed that this feedback has a beneficial effect on the pilot control performance. Also in the flight simulation domain, Telban et al. stated that the addition of motion cues with visual cues produces a rapid onset of vection, reducing the delay observed with visual cues alone. In driving simulation, visual cues are assumed to be the primary source of information. However, the role of motion feedback during a driving maneuver was proved to be relevant for subjects' motion perception. Research has been conducted to study the impact

<sup>\*</sup>MSc student, Control and Simulation Division.

 $<sup>^\</sup>dagger Researcher, mark.wentink@tno.nl, P.O. Box 23, 3769 ZG Soesterberg, The Netherlands$ 

<sup>&</sup>lt;sup>‡</sup>PhD student, Control and Simulation Division, A.R. ValentePais@tudelft.nl, P.O. Box 5058, 2600 GB Delft, The Netherlands

<sup>§</sup> Professor, Control and Simulation Division, M.Mulder@tudelft.nl, P.O. Box 5058, 2600 GB Delft, The Netherlands

<sup>¶</sup>Associate Professor, Control and Simulation Division, M.M.vanPassen@tudelft.nl, P.O. Box 5058, 2600 GB Delft, The Netherlands

of motion feedback in driving performance and driving behavior.<sup>6–9</sup> The used maneuvers on these studies were based in elementary driving tasks like braking, cornering, rural and city driving.

The most challenging situation for a driving simulator would be to simulate advanced driving maneuvers. Advanced driving maneuvers are maneuvers that are usually close to the car dynamic traction limits, <sup>10</sup> like fast slaloms or fast curves present in racing circuits. Under- and/or oversteer events can occur during these type of maneuvers due to the high amplitude of the forces applied on the tires. In this study it is investigated how motion feedback affects driver response in these extreme events.

To simulate advanced driving maneuvers, a new Motion Cueing Algorithm (MCA) was developed. A MCA transforms vehicle motion cues to simulator motion cues. This transformation has to be performed since simulators have limited motion space when compared with the real vehicle. Therefore, MCAs are used to present subjects with the necessary/possible motion cues while keeping the simulator within its physical limits. The new MCA developed for advanced driving maneuvers had to deal with the high amplitude specific forces and angular rates of these maneuvers, without losing important cues for the perception of overand understeer events. The Classical Washout<sup>11</sup> algorithm is one of the most used MCAs in commercial simulators.<sup>12</sup> Given its easy implementation and tuning, the Classical Washout is one of the first choices of engineers when choosing/designing a MCA for a simulator. However, Wentink et al.<sup>13</sup> showed that using a typical Classical Washout algorithm in Desdemona would not take advantage of the available motion space. This is because the most common MCAs are designed for hexapod simulators. Therefore new MCAs are needed to fully explore the potential of the Desdemona simulator. Desdemona already proved to be an effective simulator for driving research.<sup>14,15</sup> Therefore we believe that the Desdemona motion platform, with its unlimited rotation features and high amplitude specific force capabilities, can be used as a tool to assess how motion feedback influences driving in advanced maneuvers.

The goal of this study is to develop a new motion cueing algorithm for the Desdemona research simulator and assess the effect of motion feedback on driver performance and behavior during advanced driving maneuvers. Fixed-base simulators or simulators with low motion capabilities are the most used in driving and advanced driving training.<sup>16</sup> Therefore, differences in car handling and task performance between a condition with motion feedback (motion simulator) and a condition without motion (fixed-base simulator) during advanced maneuvers was analyzed. The used maneuver was a fast slalom because it can lead to under- and/or oversteer events, it is usually used in advanced driving courses and the results are comparable with other driving simulation studies.<sup>17, 18</sup> Our first hypothesis is that simulator motion cues improve driving performance during advanced driving maneuvers. We expect that motion feedback helps drivers in controlling the car during an extreme maneuver. Secondly, we hypothesize that with motion cues available, drivers are better able to identify events like understeer and oversteer. Differences in driving behavior are differences in the vehicle control inputs induced by motion feedback, vehicle model, control inputs dynamics among others. We assume it is possible to deduce driving behavior differences from performance measures like average speed or steering wheel angle. See Brünger-Koch et al.<sup>8</sup> for examples of performance measures used to study differences in driving behavior.

The paper will start with a brief description of the Desdemona simulator followed by the motion cueing algorithm description. In the last sections, the experimental method and the results are presented, followed by the discussion of the results and the conclusions of the study.

#### II. Motion Cueing Algorithm

The present study uses the 6 DoF Desdemona simulator, Figure 1. Desdemona has a cabin that is suspended in a gimballed 3 DoF system which gives it the capability to rotate freely around any axis in space. These 3 DoF's are denominated by cabin roll  $(\phi_{cab})$ , cabin yaw  $(\psi_{cab})$ , cabin pitch  $(\theta_{cab})$ . The gimballed system is mounted in a heave axis (H) that provides the simulator with vertical translation capabilities (2 meter stroke). The system moves horizontally over an 8 meter sledge. This DoF is denominated as radius (R). The 8 meter sledge can rotate around its center to provide sustained centripetal acceleration, denominated as central yaw( $\psi_{centr}$ ). Table 1 shows the Desdemona actuator limits (position, velocity and acceleration). More details regarding the motion system can be found in Roza et al.<sup>19</sup>

Two different motion conditions were used to test the influence of motion feedback in advanced driving maneuvers. The first condition, denoted as "No Motion", only used Desdemona actuators when subjects drove over a pylon (an upward cue was triggered to notify the driver of the event). For the rest of the simulation, Desdemona behaved like a fixed-base simulator. The second condition, denoted as "Motion",



Figure 1. Desdemona simulator developed by AMST Systemtechnik (Austria) and TNO Human Factors (Netherlands).

R Η  $\theta_{cab}$  $\psi_{centr}$  $\phi_{cab}$ Max. Position >360 °  $\pm 4~\mathrm{m}$  $\pm 1 \text{ m}$ >360° >360 ° >360° 180 °/s 180 °/s 180 °/s Max. Velocity 155 °/s  $3.2 \mathrm{m/s}$ 2 m/s $90^{\circ}/s^{2}$ Max. Acceleration  $45 \, ^{\circ}/\mathrm{s}^{2}$  $4.9 \text{ m/s}^2$  $4.9 \text{ m/s}^2$ 

Table 1. Desdemona technical specifications.

used a Desdemona motion cueing algorithm designed specifically for advanced driving simulation. The next sections explain in more detail the two MCAs used in both motion conditions.

#### A. No Motion

The MCA used in this motion condition was composed by a collision algorithm (that detects when subjects drive over a pylon) in series with a third order high-pass filter. The third order high-pass filter was created using a second order high-pass filter in series with a first order high-pass filter. Figure 2 shows a block diagram of the MCA used in the No Motion condition. The inputs of the MCA were the car x and y positions in the virtual world while the outputs were the position, velocity and acceleration of Desdemona's Heave drive. The collision algorithms verified the car position and the pylon position and calculated the difference between them. Figure 3 shows the principle of the collision algorithm, where R is the collision radius and d is the distance between the center of the car and the center of the pylon. If d is smaller than R, an acceleration impulse is generated by the algorithm and sent to the block HP Filter 3 order represented in Figure 2. The HP Filter 3 order block is defined by Eq. 1, where  $\omega$  is the second order high-pass filter natural frequency,  $\varsigma$  is the second order high-pass filter damping and  $\omega_b$  is the first order high-pass filter natural frequency.



Figure 2. Block diagram of the motion cueing algorithm used in the No Motion condition.

$$H(s) = \frac{s^2}{s^2 + 2s\omega\varsigma + \omega^2} \frac{s}{s + \omega_b} \tag{1}$$

The collision algorithm was implemented to give subjects a better perception of their own performance. This was implemented to decrease driving path differences between subjects. In this way, drivers were punished if they drove over a pylon. This algorithm helped to prevent large discrepancies between the two

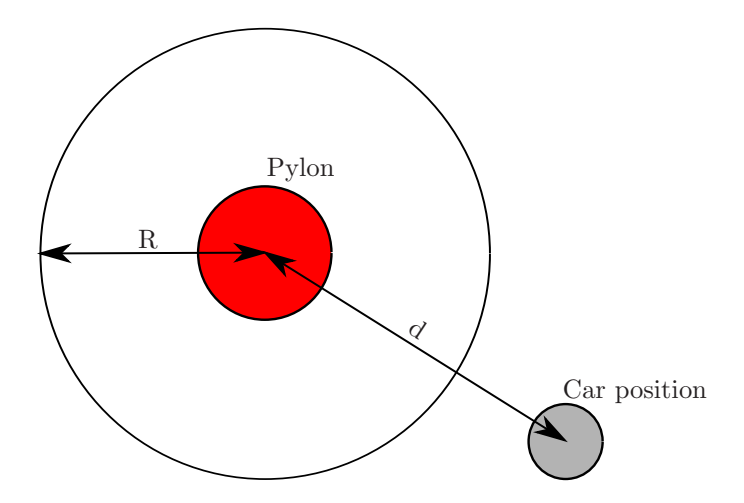


Figure 3. Collision detection algorithm principle.

different motion conditions. If no pylons were hit during the simulation, Desdemona behaved like a fixed base simulator.

#### B. Motion

The Motion condition uses a MCA designed for advanced driving maneuvers. Previous solutions developed for Desdemona<sup>14,15</sup> were not able to deliver lateral specific forces with amplitudes higher than  $\approx 3m/s^2$ . This is because these solutions were designed for city driving, with focus on low speed curve driving. Therefore, the amplitude of the lateral specific force for city driving is below the one needed for advanced driving.

For the advanced driving MCA a new reference frame was defined. It is referred to as the Desdemona frame of reference,  $\mathcal{F}^d = x^d y^d z^d$  (Figure 4). The reference axis is fixed to the heave sledge (see Figure 4), meaning that when the sledge moved, the axis moved with it.

Figure 5, shows the block diagram of the MCA used in the Motion condition. The inputs of this motion filter were car specific forces  $(f_x, f_y \text{ and } f_z)$ , the car positions (x and y) and the car longitudinal velocity. The outputs were the position, velocity and acceleration of all Desdemona's six actuators. The filter is divided into two channels: specific force channel and angular rate channel.

#### 1. Specific force channel

In this channel, the car specific forces were first scaled using the Scaling Factor block and then were sent to the Car2Desdemona block. The Car2Desdemona block transformed the specific forces from the vehicle reference frame into Desdemona reference frame. In this way, the specific forces will be filtered at the actuator level as can be seen in Figure 5. Because the g earth component is parallel to the g axis of the Desdemona reference frame, we transformed the specific forces coming from the Car2Desdemona block into accelerations by subtracting the gravitational component. Note that the Heave, Radius and Central Yaw channels of Figure 5 are aligned with the Desdemona frame of reference g, g and g axis respectively.

HEAVE CHANNEL The z acceleration coming from the Car2Desdemona block is summed with the acceleration from the Collision Algorithm block. The Collision Algorithm was equal to the one used in the No Motion condition. The acceleration signals are filtered using a third order high-pass filter (HP Filter 3order) with the same structure of the one used in the No Motion condition (Eq. 1). The Road Rumble block was used to create the oscillations generated by road irregularities. This algorithm was already used in a previous Desdemona study.<sup>14</sup> The accelerations generated by the Road Rumble algorithm are summed to the ones coming from the high-pass filter. The acceleration signals are sent to a Limiter block that examined if the signals were within the Desdemona's limits.

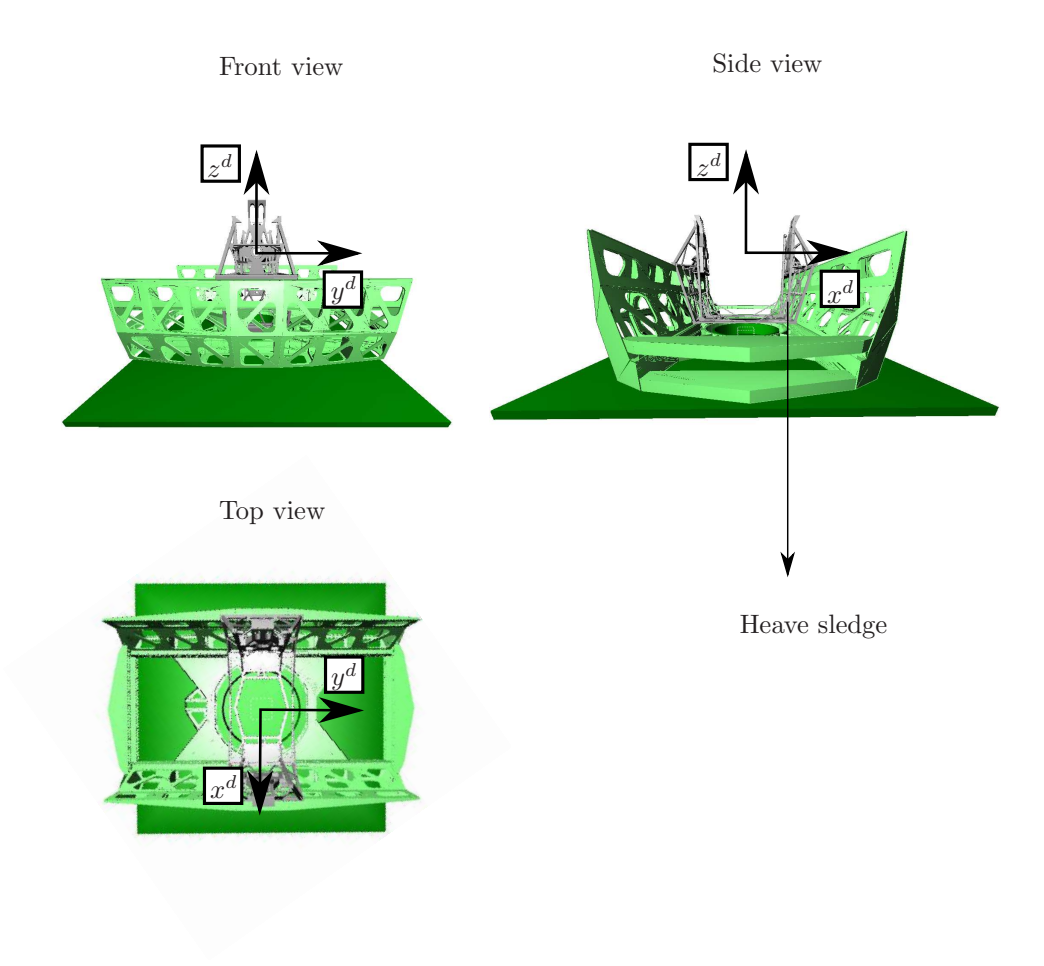


Figure 4. Desdemona frame of reference.

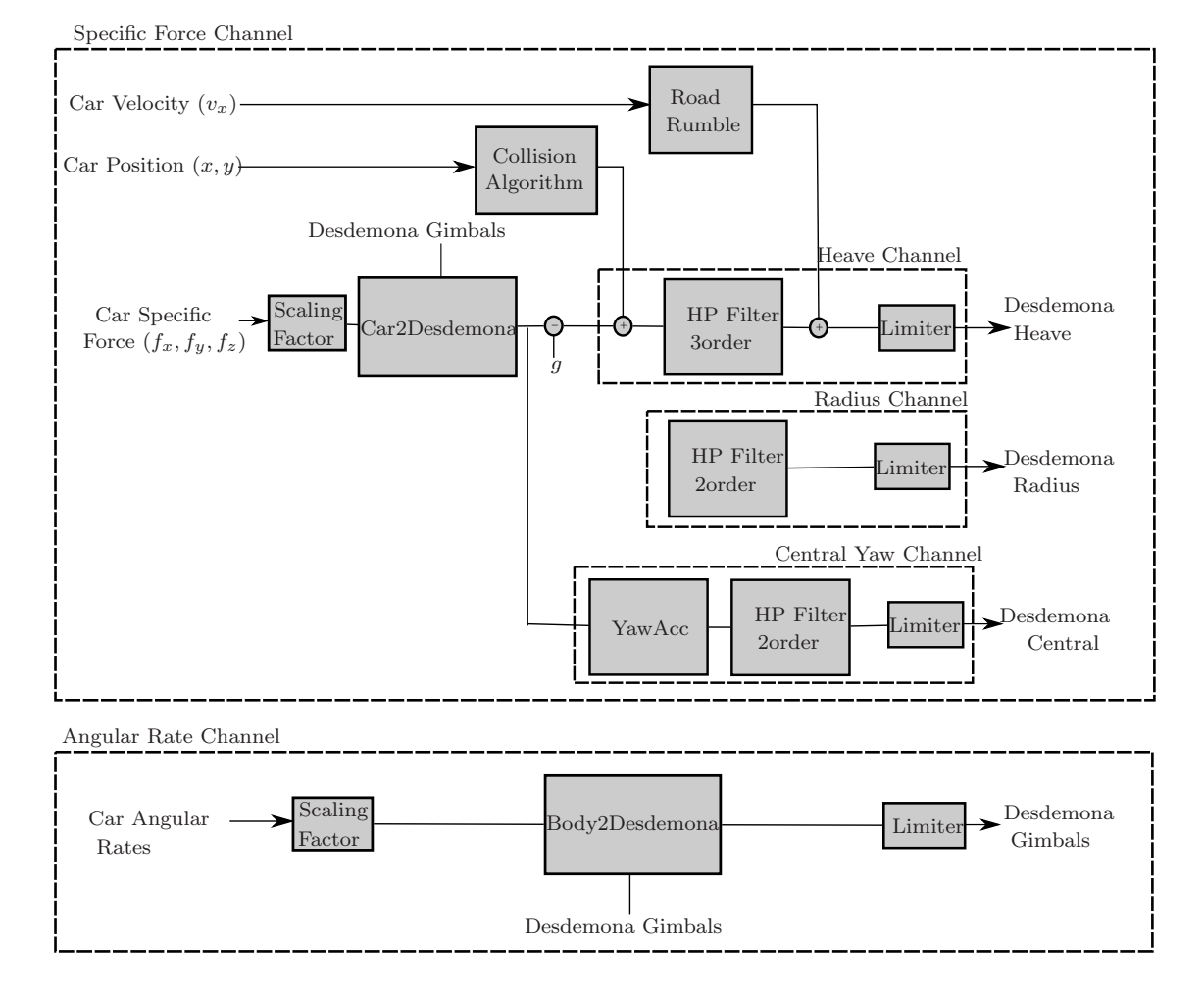


Figure 5. Block diagram of the MCA used in the No Motion condition.

RADIUS CHANNEL The y acceleration coming from the Car2Desdemona block is filtered using a second order high-pass filter (HP Filter 2 order) defined by Eq. 2, where  $\omega$  is the second order high-pass filter natural frequency and  $\varsigma$  is the second order high-pass filter damping. The Limiter block was again used to examine the signal limits before sending it to the actuator.

$$H(s) = \frac{s^2}{s^2 + 2s\omega\varsigma + \omega^2} \tag{2}$$

CENTRAL YAW CHANNEL The central yaw actuator is used to generate longitudinal acceleration. In contrast to the radius and heave actuators, the central yaw  $(\psi_c)$  is a rotation actuator instead of a translational actuator. Therefore, the simulation of longitudinal specific force cannot be so straightforward as for the other actuators. By rotating  $\psi_c$ , centripetal and tangential accelerations are generated. This can be seen in Figure 6, where  $\vec{ac}$  is the centripetal acceleration,  $\vec{at}$  is the tangent acceleration,  $\omega$  is the central yaw angular velocity and R is the current cabin radius.

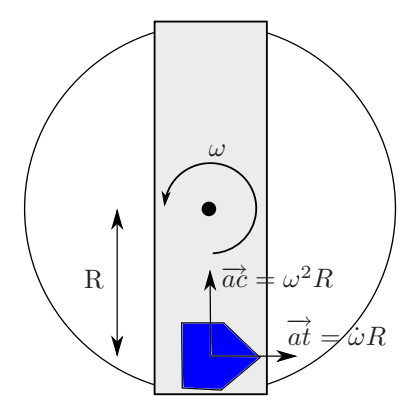


Figure 6. Accelerations generated by the central yaw actuator.

The tangent acceleration will be used to cue the longitudinal acceleration coming from the Car2Desdemona block. The tangent acceleration is given by Eq. 3, where  $\vec{at}$  is the tangent acceleration,  $\dot{\omega}$  is the angular acceleration of the central yaw and R is the current cabin radius.

$$\vec{at} = \dot{\omega}R$$
 (3)

Consider now that the longitudinal acceleration from the Car2Desdemona block  $(\vec{a_{xi}})$  equals  $\vec{at}$  and that Eq. 3 is resolved in order to the angular acceleration creating Eq. 4. Eq. 4 is then the needed angular acceleration by the  $\psi_c$  to generate a longitudinal force equal to  $\vec{a_{xi}}$ .

$$\dot{\omega} = \frac{\vec{a_{xi}}}{R} \tag{4}$$

The YawAcc block (Figure 5) used Eq. 4 to transform linear acceleration into angular acceleration. Note that this method will also generate centripetal acceleration (Figure 6). Because this technique is used to generate onset cues, we expect low angular velocities and also limited centripetal acceleration components. Note that if the radius is constant, the centripetal acceleration is proportional to the angular velocity squared.

From Figure 5 it can be seen that the angular acceleration is filtered (HP Filter 2 order) by a second order high-pass filter defined by Eq. 2. The Limiter block was used at the end of the channel to guarantee that Desdemona limits were not violated.

#### 2. Angular rate channel

The angular rates coming from the car model are scaled in the Scaling Factor block. The scaled angular rates are then transformed from body rates into Desdemona angle rates in the Body2Desdemona block. The Limiter block was used to guarantee that the signals sent to the simulator are within limits. The fact that filtering was not performed in this channel, guarantees that the shape of the signal coming from the vehicle model is maintained.

#### 3. Pre-position of the MCA

To explain the pre-position property of the MCA a new frame of reference was defined. The Cabin frame of reference,  $\mathcal{F}^c = x^c y^c z^c$ , is defined in Figure 7.

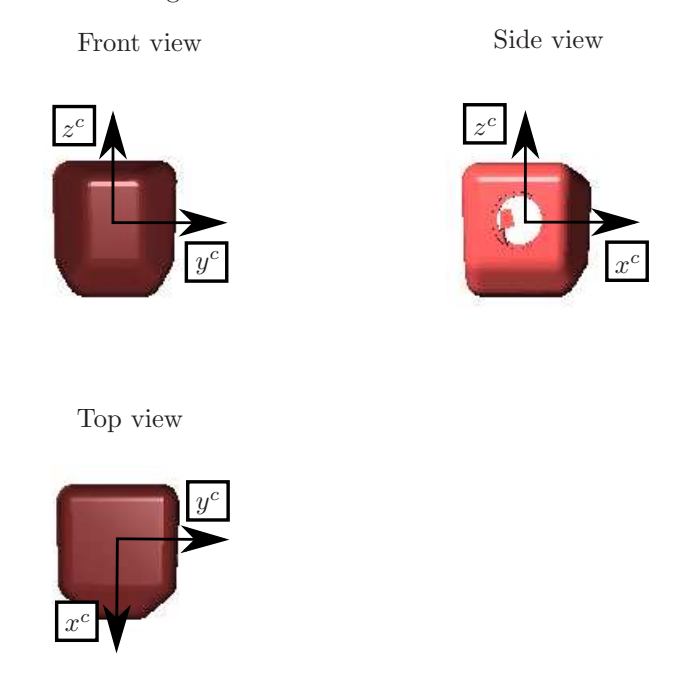


Figure 7. Cabin frame of reference.

If at the initial cabin position, the Cabin frame of reference is aligned with the Desdemona frame of reference, a longitudinal input in the cabin frame of reference will be equal to a longitudinal displacement in the Desdemona frame of reference. This example is shown in Figure 8.

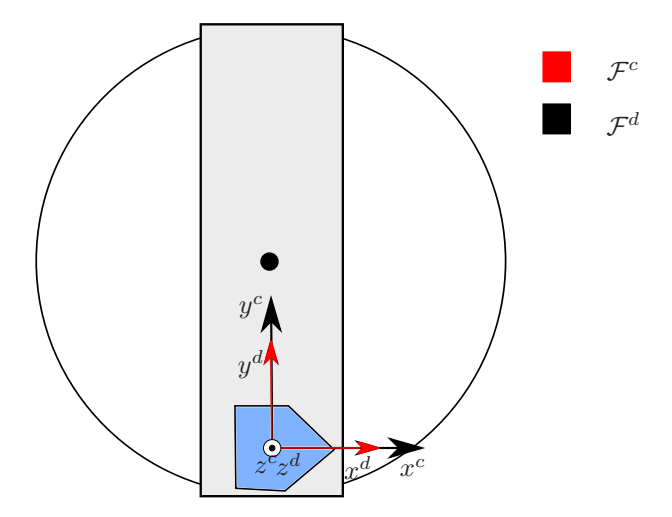


Figure 8. Desdemona and Cabin frame of references when the Radius is used for lateral cueing and the central yaw is used for longitudinal cueing.

Now consider the case when the two frame of reference are misaligned, for example 90° in yaw angle, as shown in Figure 9. In this case, a longitudinal input in the Cabin frame of reference would mean a lateral displacement in the Desdemona frame of reference. In this way, the radius actuator would be used for longitudinal displacement instead of lateral displacement. Therefore, when defining the cabin initial attitude, one is also defining which actuators are used to cue a certain direction.

For the slalom maneuver, the Cabin frame of reference was aligned with the Desdemona frame of reference.

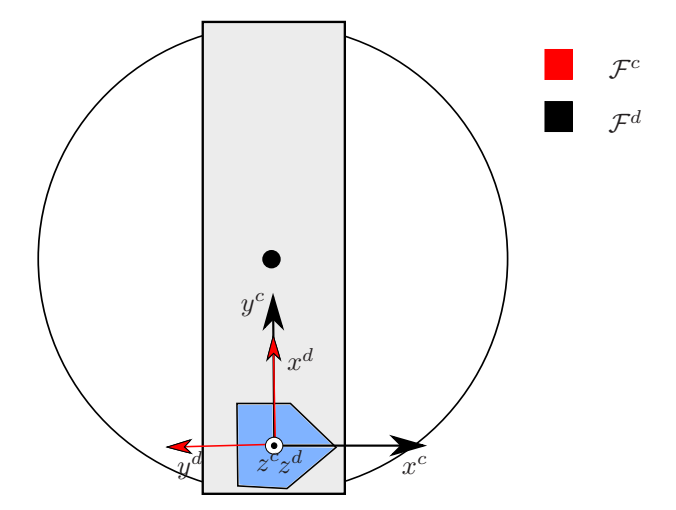


Figure 9. Desdemona and Cabin frame of references when the Radius is used for longitudinal cueing and the central yaw is used for lateral cueing.

In this way the radius actuator was used to cue the lateral specific force coming from the vehicle model. This is done because the lateral specific force is dominant in a slalom maneuver. The longitudinal specific force coming from the car model will not be cued. In this way, it is possible to use the full length of the radius sledge. By not cueing longitudinal cues, we can use the center of the radius as the initial position for the simulator cabin. Note that at this position it is not possible to generate longitudinal specific force (see Eq. 4), meaning that one has to choose a new initial position if longitudinal cueing was to be taken into account. Therefore, the only time that the  $\psi_c$  is used is when the Cabin frame of reference gets misaligned with the Desdemona frame of reference due to vehicle model yaw rotations.

#### 4. Tuning the MCA for the slalom maneuver

With the initial actuator positions discussed before, the simulator movement for a slalom right curve was similar to the schematic shown in Figure 10. While the virtual vehicle approached the pylon (1 in Figure 10), Desdemona cabin remained at the neutral position. When the vehicle started turning to the right (2), Desdemona moved along the radius sledge to the right. The cabin rotated along its z axis to follow the same rotation happening in the virtual vehicle. With this movement, the cabin y axis is no longer aligned with Desdemona radius, therefore the central yaw actuator moved to keep the lateral specific force generated by the simulator aligned with the one of the virtual vehicle. When the virtual vehicle turned to the left (3), the simulator changed its movement also to the left along the radius sledge.

Although possible, tilting coordination was not implemented in this MCA. Tilting coordination is a technique that generates sustained specific forces without driving the simulator out of its limits. In this method, the motion platform is tilted to generate a specific force. This specific force is generated using the gravity vector acting on the motion platform. In this way, the gravity vector direction matches the direction of the vehicle specific force that one wants to simulate. This technique provides good results as long as the angular rates used for tilting are below the human semicircular canals (human organs that perceive angular motion) perception threshold.<sup>12</sup> Initial tests performed with the advanced driving MCA showed that the tilt rate limitation introduced delay in the system and that the extra sustained cues were not an improvement in the specific forces delivered by the simulator. This had to do with the amplitude and frequency of a slalom maneuver. To compensate the lack of tilting coordination, the vehicle roll rate was amplified in the Scaling Factor block (Figure 5) of the MCA. This "false cue" was not disturbing as we confirmed during the initial tests. Table 2 shows the values of the scaling factors used in the Scaling Factor blocks of the MCA. The filter parameters of the MCA obtained during the initial tests are shown in Table 3. Note that there is no filtering in the yaw rate. This means that the only difference between the signal from the car model and the signal rendered by Desdemona is the amplitude. In this way, the frequency component is equal to the one of the vehicle model. We believe that this is an important feature for advanced driving simulation because during oversteer events, the loss of traction on the rear tires would lead to high frequency variations in the

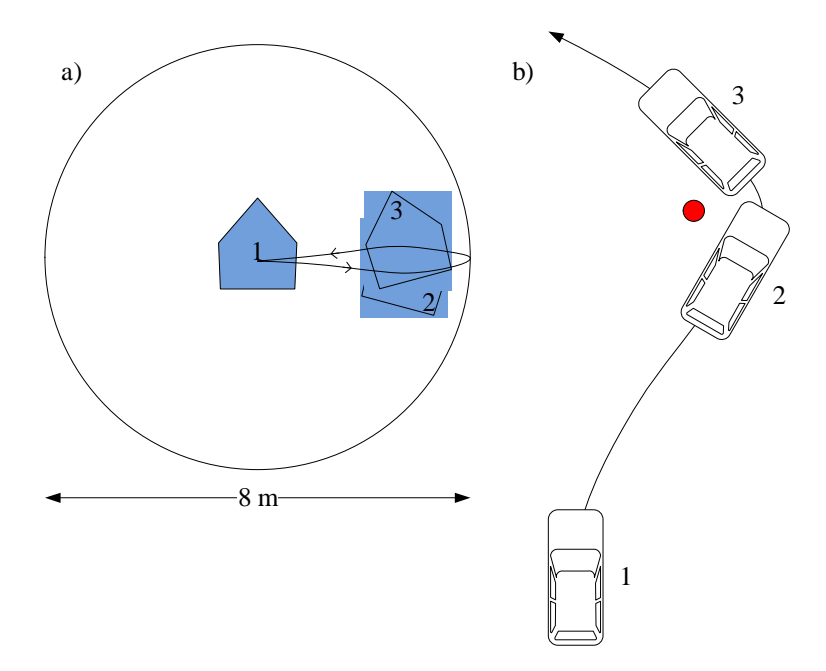


Figure 10. Schematic of Desdemona cabin motion during a slalom right curve. a) Desdemona movement. b) Car movement in the virtual world.

car yaw rate. We believe that subjects had the necessary cues in the simulator to judge oversteer events.

 ${\bf Table~2.~~Motion~Cueing~Algorithm~scaling~factors.}$ 

	Scaling Factor
Lateral specific force	0.75
Vertical specific force	1
Roll rate	2
Pitch rate	0.8
Yaw rate	0.8

 ${\bf Table~3.~~Motion~Cueing~Algorithm~characteristics.}$ 

Desdemona Actuators	$\omega$	ς	$\omega_b$
Central Yaw ( $x$ direction in the Cabin frame)	$1 \text{ rad/s}^2$	1	-
Radius ( $y$ direction in the Cabin frame)	$0.2 \text{ rad/s}^2$	1	-
Heave ( $z$ direction in the Cabin frame)	$1 \text{ rad/s}^2$	2	$2 \text{ rad/s}^2$

#### III. Method

#### A. Apparatus

#### 1. Desdemona cabin

Figure 11 shows a schematic of the car mock-up used in the experiment. The car mock-up contained a steering wheel and two pedals (gas and brake) with force-feedback. The sampling frequency was 1 KHz for the pedals and 100 Hz for the steering wheel. The steering wheel had a diameter of 40 centimeters. The steering column inertia, damping and hysteresis were respectively  $0.1 \ kg.m^2$ ,  $0.025 \ Nm.s/deg$  and  $1.5 \ Nm$ . A fourteen inches LCD screen was present in the mock-up and was used to display the car instrument

panel (speedometer and tachometer). The force-feedback system was powered by electrical drives. These drives enabled changes in the loading characteristics used in the steering wheel and pedals. An I/O computer coupled to the car mock-up controlled the control loadings and generated the instruments panel display. This computer was inside the cabin for high bandwidth purposes. The outside visual was displayed using three projectors and a three part flat screen where the images were projected. The refresh rate was 60 Hz. Subjects were at approximately 1.5 meters from the central screen with a field-of-view of 120 horizontal degrees and 32 vertical degrees. The projectors were connected to three computers on the top of the simulator cabin. The sound system only reproduced the engine sound based on the car engine RPM.

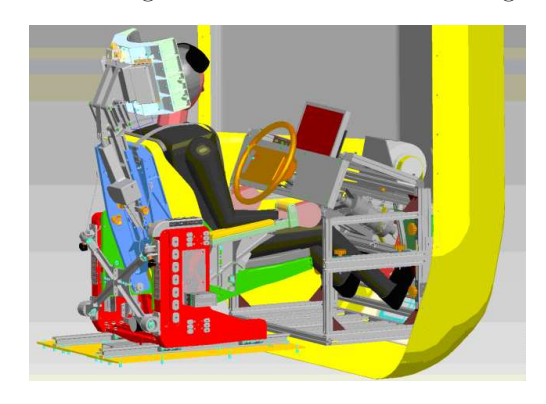


Figure 11. Schematic of Desdemona car mock-up.

#### 2. Car model

In this study, we used Carsim  $7.01b^{20}$  as the car model for the experiment. The vehicle dynamics were similar to a Volkswagen Passat wagon, which is the instrumented car present at TNO Soesterberg. The car model had automatic gear shift since the Desdemona car mock-up does not have a gear stick implemented. The speed was limited to 70 Km/h due to the experiment design.

#### B. Slalom Maneuver

The slalom designed for this study is based on the one used in the MOVES (MOtion cueing for VEhicle Simulators) Eureka project.<sup>17</sup> The maneuver was designed according to the theoretical sinusoidal path of Figure 12, where a is the sinusoidal path amplitude and d is the distance between pylons.

The amplitude of the theoretical lateral acceleration achieved in this slalom is given by Eq. 5, where a is the sinusoidal path amplitude, d is the distance between pylons and v is the car velocity.

$$a_y = a \left(\frac{\pi}{d}v\right)^2 \tag{5}$$

Nine different pylon sections were created using Eq. 5, each of them containing six pylons. Figure 12 shows a pylon section example. To create the nine different pylon sections, the sinusoidal path amplitude, a and the car velocity, v in Eq. 5 were kept constant. Their values were respectively 1.25 m and 70 Km/h. Distance between the pylons, d was the variable used to differentiate between the pylon sections. Table 4 shows the characteristics of the nine pylon sections.

The nine sections are 200 meters apart from each other to cancel dynamic driving effects between sections. The pylons are at 0.5 meters from the centerline of the road as is shown in Figure 12.

This slalom was designed with the intent of inducing under- and oversteer events. For that, the theoretical lateral specific force of the slalom increased up to  $5m/s^2$ . It is expected that drivers achieve specific forces that are above the car traction limit. The traction limit is the maximum force that a tire can be subjected before losing adhesion with the road. It is likely that motion feedback helps drivers to better identify and recover from under- and oversteer events. This is expected because of the extra sensory information that is fed to the driver which would give him a better perception of the current car cues (like speed perception or total force acting on the car). The use of no filtering in the vehicle yaw rate was important to cue the large angle variations occurring during oversteer. The yaw rate variation also generates variations in the

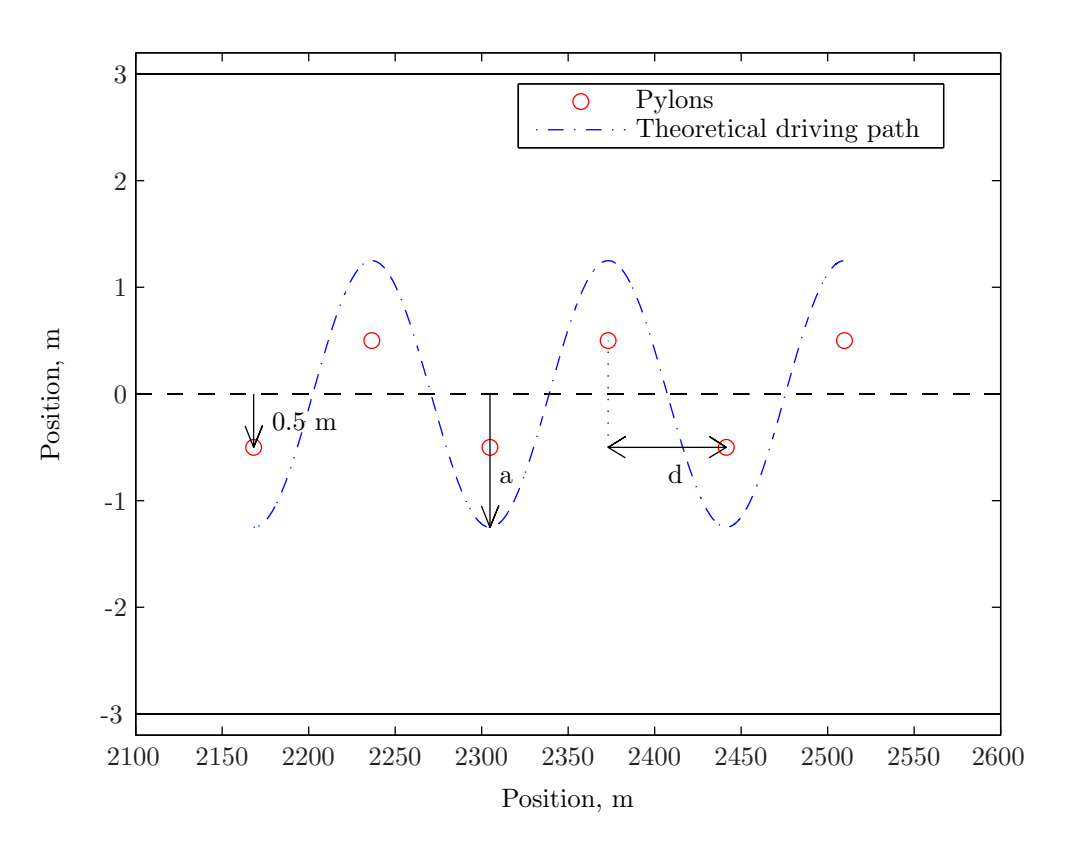


Figure 12. Schematic of the driving path.

Table 4. Slalom characteristics.

Section	Theoretical lateral force	Distance between pylons
1	$1 \mathrm{m/s^2}$	68.30  m
2	$1.5 \mathrm{m/s^2}$	$55.76 \mathrm{m}$
3	$2 \mathrm{m/s^2}$	48.29 m
4	$2.5 \mathrm{m/s^2}$	43.19 m
5	$3 \mathrm{m/s^2}$	39.43 m
6	$3.5 \mathrm{m/s^2}$	36.51 m
7	$4 \mathrm{m/s^2}$	34.15 m
8	$4.5 \text{ m/s}^2$	32.20 m
9	$5 \mathrm{m/s^2}$	$30.54~\mathrm{m}$
	<del>_</del>	

lateral specific force. These motion cues would be felt in the simulator, helping the subject to identify and counteract the oversteer event. Other cues are also used by drivers to identify under- and oversteer events like changes in steering wheel torque. For example, during understeer the car loses traction in the front tires. This means that control inputs on the steering wheel do not change the car direction. This "lack of control" is felt by differences in the steering wheel torque. The steering wheel torque in this simulation was generated by Carsim 7.01b.<sup>20</sup>

#### C. Procedure

The experiment started with a practice run as it can be seen in Figure 13. In this run, the easiest slalom section was driven until subjects felt familiarized with the driving task. Subjects were instructed to drive through the slalom as fast as possible; however, the velocity was limited to a maximum speed of 70 Km/h. They were told only to lower the car velocity (using the brake pedal or releasing the gas pedal) when the car was near hitting the guard rail or if they felt losing the control over the car.

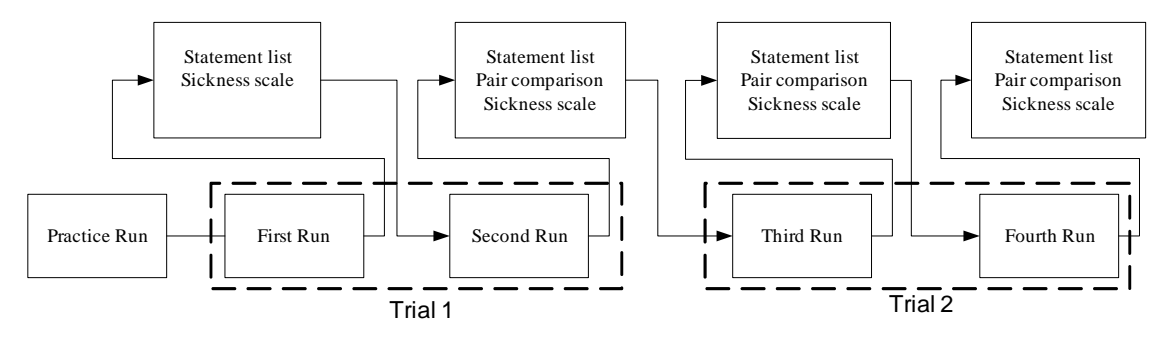


Figure 13. Experimental order.

After the practice run, subjects had to drive through the slalom (all the nine pylon sections) four times. Two times for the Motion condition and two for the No Motion condition. The repetition of the conditions was only introduced to observe if driving behavior was influenced by any training effect. If training effects affect subject's driving, it is expected that their driving behavior is more constant during the repetition. To decrease order effects subjects were divided into two randomized groups, <sup>21</sup> shown in Table 5, where NM refers to the No Motion condition and M refers to the condition with motion feedback. In Table 5. The first time a condition was run corresponds to Trial 1 and its repetition corresponds to Trial 2.

	т.	ial 1	Т";	ial 2
Group				
0 v 0.F	First run	Second run	Third run	Fourth run
1	NM	M	NM	M
2	M	NM	M	NM

Table 5. Motion condition order.

#### D. Subjects

Twenty two participants (15 males and 7 females) participated in the experiment. Data from two subjects had to be discarded due to motion sickness issues. Of the twenty remaining subjects, ten participants started with the no motion condition (Group 1 of Table 5) while the other ten participants started with the motion feedback condition (Group 2 of Table 5). The participants were all TNO employees. None of them had driving experience with advanced maneuvers. The average age of the participants was 38 years old ( $\sigma = \pm 11$  years); the average driving experience was 18 years ( $\sigma = \pm 11$  years) with an average mileage per year of 18000 Km ( $\sigma = \pm 16000$  Km).

#### E. Dependent measures

#### 1. Subjective measures

A paired comparison technique was used to test if the condition with motion feedback is preferred to the no motion condition. Subjects had to compare the current run with the previous run in terms of overall impression of realism by saying which condition they preferred. Subjects indicated the overall impression between two motion conditions three times during the experiment. They compared the first run with the second, the second run with the third and the third run with the last one.

After each run, subjects had to fill in a questionnaire. A questionnaire to measure simulation realism was not found in the literature, therefore it was decided to design a new questionnaire that can measure simulation realism in the way we needed. The questionnaire was developed such that it can be re-used in future simulator studies that want to measure the same. In our opinion, simulation realism cannot be directly measured and can be influenced by variables like subjects immersion, controllability of the vehicle, task performance among others. Therefore, 26 statements were created in order to measure simulation realism. The statements were based on the variables we thought were important to measure simulation realism. Table 6 contains the 26 statements, as well as the variables we though the statements were measuring. These variables are shown just to explain the reasoning behind the statements. Note that the original statements were in Dutch which means that part of the meaning can be lost in translation. Subjects had to agree or disagree with the statements using a 7 point "Likert<sup>22</sup>-type" scale like the one in Table 7.

Table 6. Statement list.

	Statements	Measured variable		
1	I felt I was really driving.			
2	I forgot that I was inside a simulator.	•		
3	I drove like I usually would do.	Immersion		
4	I felt that I could get injured during the driving task.	- Illinicision		
5	I felt quite anxious while conducting the driving task.			
6	I enjoyed driving.			
7	The car steered normally, as I am used to.			
8	The motion of the car felt like I am used to.			
9	I felt confident with the car.	- Vehicle Controlability		
10	I sometimes had the feeling of losing control over the car.	- Vehicle Controlability		
11	I felt that I was driving near the car performance limit.			
12	It felt as if I was controlling a real car.			
13	The task was easy.			
14	I had to adapt task-execution to the limitations of the simulator.	- - Task Performance		
15	I performed the task well.	Task i citorinance		
16	The motions and forces helped me conducting the task.			
17	The simulation was realistic.			
18	The simulator motion and forces felt realistic.	- Simulator cues		
19	The outside visual of the simulator was realistic.	Simulator cues		
20	The field-of-view in the simulator was large enough.			
21	I was really focused.			
22	I have really pushed it.	Motivation		
23	I was really challenged to perform well.	-		
24	I continuously became better.			
25	After this experience, I can perform the task better in the real world.	Training Value		
26	This experience helped me to develop the required driving skills.	- 		

A six point sickness scale<sup>23,24</sup> (Table 8) was used to check the sickness levels of subjects during the

Table 7. Seven point Likert scale.

Strongly Disagree 1 2 3 4 5 6 7 Strongly Ag	Strongly Disagree	1	2	3	4	5	6	7	Strongly Agre
---	-------------------	---	---	---	---	---	---	---	---------------

experiment. Subjects were asked to indicate their level of sickness after each run through the inter-com. If their level was higher or equal to four, the experiment stopped.

Score Symptom

1 feeling OK, no symptoms
2 initial symptoms, such as stomach awareness, but no nausea
3 mild nausea
4 moderate nausea
5 severe nausea and /or retching
6 vomiting

Table 8. Six point motion sickness scale.

#### 2. Objective measures

Objective measures were used to draw conclusions regarding car handling differences in the two motion conditions. For that, car variables such as car speed, specific forces, steering wheel angle were recorded. In addition, we observed that the number of accidents occurring was different for both motion conditions, so these results were also reported. We considered that an accident occurred whenever subjects hit the guard rail or lose the control over the vehicle. Note that in all conditions, the only difference was the motion feedback while other simulator characteristics such as steering wheel dynamics and visual scene were kept equal.

#### IV. Results

#### A. Simulator motion

In the No Motion condition, the simulator behaved like a fixed-base simulator except when a pylon was hit. Therefore the simulator only used vertical motion space. In the Motion condition the implemented MCA took advantage of all Desdemona actuators. Figure 14 shows an example of the motion space used by the MCA during a full slalom run, i.e. during a run where the nine pylon sections were driven.

Figure 15 shows an example of lateral and vertical specific forces generated by the vehicle model versus the ones generated by the Desdemona simulator in the Motion condition. The analysis is done for pylon section one and pylon section eight to show how the MCA handles the motion cues in a slower and in a faster pylon section.

From Figures 15(a) and 15(b) it follows that the slalom amplitude and frequency were higher for pylon section 8 as it was predicted when designing the slalom maneuver. In pylon section 8, the simulator was able to follow the shape of the car model signal. For this pylon section, the simulator lateral specific forces reached amplitudes in the same order of magnitude of the ones from the car model signal. For pylon section one, the lateral specific force only differed a little in amplitude from the one of the car model due to the used scaling factor.

In Figure 15(c), it is possible to see that for section one, the vertical specific force was nearly constant in terms of amplitude during a significant part of the maneuver. For section eight, we can notice some sinusoidal variation due to the high roll rates that the car model was facing. In both pylon sections, the MCA was able to correctly follow the vehicle signal in terms of amplitude and timing. In Figures 15(c) and 15(d), we can also observe a peak on the simulator specific force. This peak was caused by hitting a pylon during the simulation.

Figure 16 shows the roll and yaw rates of the vehicle model versus the ones rendered by Desdemona. As given in Table 2, the roll rate of the MCA was scaled with a factor of two in order to generate higher

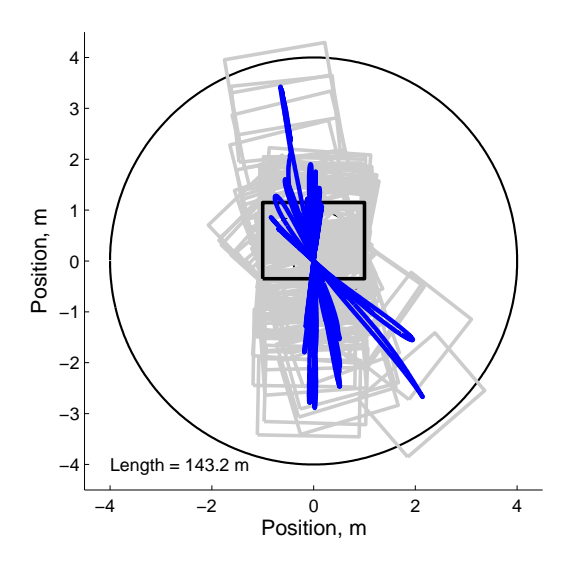


Figure 14. Motion space used by the MCA during the nine slalom sections. The blue line represents the cabin center motion path.

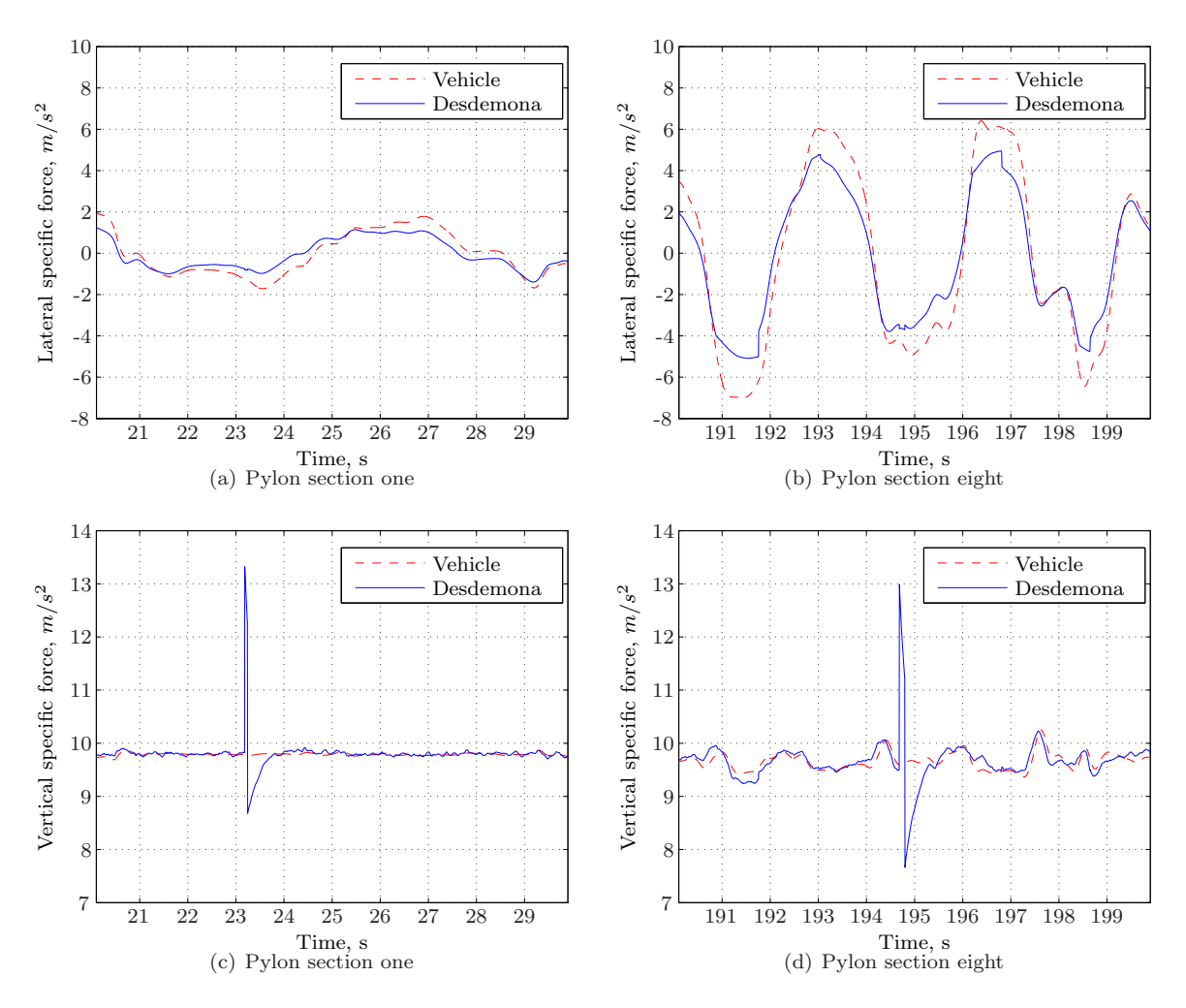


Figure 15. Specific forces of the vehicle model (dashed line) versus the specific forces generated by Desdemona simulator (solid line) for sections one and eight of the slalom maneuver.

lateral specific forces to compensate the lack of tilt coordination. This can be seen in Figure 16(b) where the simulator roll rates had clearly higher amplitude than the vehicle model roll rates. It is also noticeable both in Figures 16(a) and 16(b) a small delay of the simulator signal in comparison to the one of the vehicle model. This delay was created by the MCA limiters. Again, one can see that the roll rate of section eight was higher in terms of amplitude and frequency than the roll rate of section one.

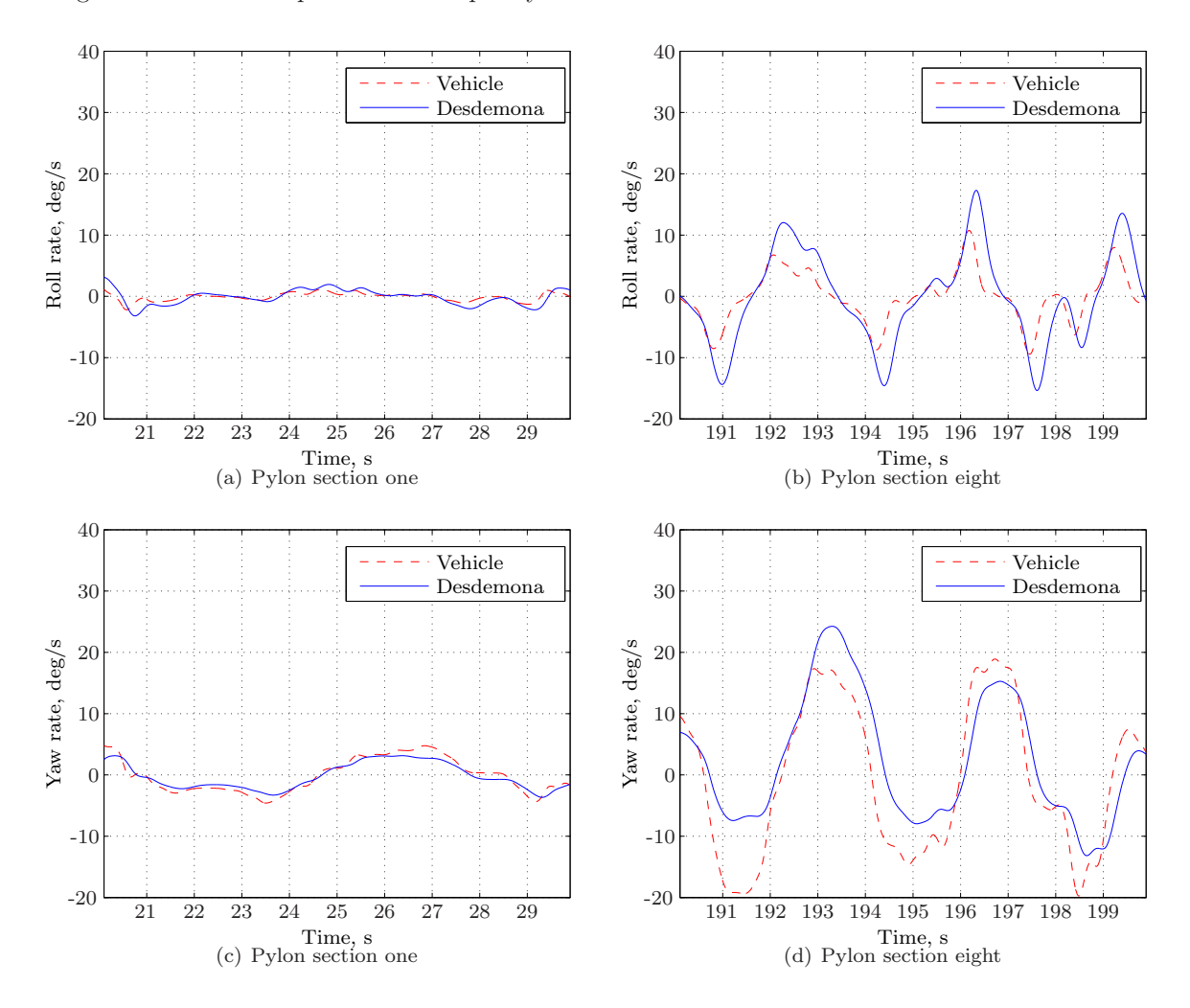


Figure 16. Angular rates of the vehicle model (dashed line) versus the angular rates generated by Desdemona simulator (solid line) for sections one and eight of the slalom maneuver.

The simulator yaw rate of pylon section one (Figure 16(c)) correctly followed in amplitude and frequency the one generated by the vehicle model. For pylon section eight small delays are noticeable due to the MCA limiters. Near  $t \approx 193s$ , the simulator yaw rate had higher amplitude than the one of the vehicle model. This happened because the central yaw actuator was also moving at that time. Therefore, the extra amplitude was coming from the rotation of the central yaw.

#### B. Paired Comparison

Figure 17 shows the total scores for each of the comparisons. The score is the number of times that a condition was preferred over the other.<sup>25</sup> A chi-square test was used to verify the significance of the paired comparison analysis. In the first comparison (1 vs 2 in Figure 17) there was not a significant effect of the motion condition in the subject's overall impression,  $\chi^2(1) = 3.2, p = 0.074$ . A total number of 14 subjects preferred the condition with motion, while 6 subjects preferred the no motion condition. For the second and third comparisons it was found a significant effect of the motion condition at the 5% level, respectively  $\chi^2(1) = 5, p = 0.025$  and  $\chi^2(1) = 9.8, p = 0.02$ . For the second comparison, fifteen subjects preferred the

motion condition. For the third comparison, seventeen subjects preferred the condition with motion.

The effects of subjects' groups (whether subjects start with Motion or No Motion) was only considerable for the first comparison. From the fourteen subjects that preferred the Motion condition in the first comparison, six of them were from Group 1 and eight were from Group 2. From the fifteen subjects that preferred the Motion condition in the second comparison, seven of them were from Group 1 and eight were from Group 2. From the seventeen subjects that preferred the Motion condition in the third comparison, eight of them were from Group 1 and nine were from Group 2.

When the scores of the paired comparison are accumulated, the result is a total score of 46 for the Motion condition and a total score of 14 for the No Motion condition. In this case there is a significant effect of the motion condition at the 1% level,  $\chi^2(1) = 17.067, p < 0.01$ .

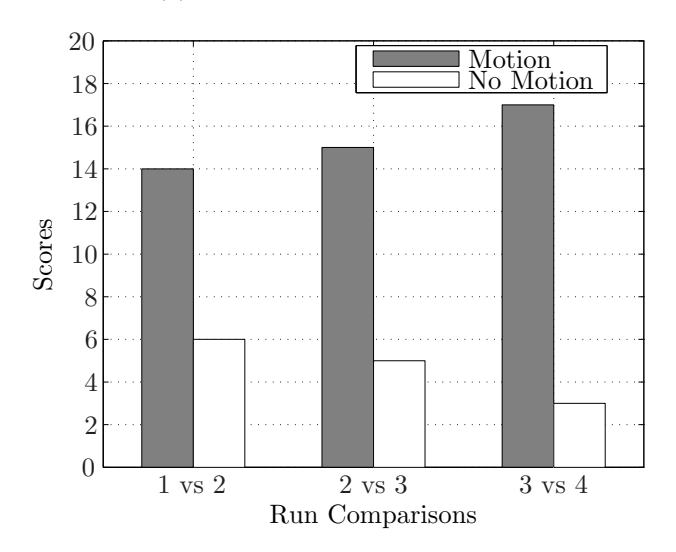


Figure 17. Paired comparison total scores for each run.

#### C. Questionnaires

#### 1. Factor analysis

To analyze the results from the questionnaire, a factor analysis was performed. A factor analysis<sup>21</sup> is a technique used to identify groups of variables. It examines how the variables correlate with each other, grouping the ones with higher correlation. In our case, we will use the factor analysis to see how the statements are grouping together. If the statements group like in Table 6, it means that our initial predictions were correct, i.e., the variables we thought the statements were measuring were correct. The factor analysis results showed that the statements did not group as it was predicted. We can conclude that the questionnaire needs to be re-designed so that we can measure some of the simulation realism variables that did not group in the way it was predicted.

Two statements had to be removed from the analysis because they were not grouping with any other statements, creating two separate factors. These were statements eleven ("I felt that I was driving near the car performance limit.") and fourteen ("I had to adapt task-execution to the limitations of the simulator.").

#### 2. Reliability analysis

A reliability analysis<sup>21</sup> was performed to verify how reliable was the scale we used in the questionnaire. Field<sup>21</sup> argues that a Cronbach's alpha value lower than 0.7 normally indicates an unreliable scale. A value between 0.7 and 0.8 is acceptable. Field states that leaving out some variables can increase dramatically the Cronbach's alpha value, meaning that the reliability of the scale increases. This means that the quality of the questionnaire also increases. With the purpose of increasing the reliability of the scale, the following statements were left out: 2-I forgot that I was inside a simulator, 3-I drove like I usually would do, 4-I felt that I could get injured during the driving task, 20-The field-of-view in the simulator was large enough, 21-I was really focused, 24-I continuously became better.

The results from the factor analysis and the reliability analysis are summarized in Table 9. Table 9 shows how the statements grouped together as well as their Cronbach's alpha value. Because Factor 5 had a low Cronbach's alpha value, no further analysis was made using it.

Table 9. Factor and Reliability analyses results.

Factor	Statements	Cronbach's alpha	
	01 - I felt I was really driving.		
	07 - The car steered normally, as I am used to.		
	08 - The motion of the car felt like I am used to.	-	
1	12 - It felt as if I was controlling a real car.	0.947	
	16 - The motions and forces helped me conducting the task.	-	
	17 - The simulation was realistic.		
	18 - The simulator motion and forces felt realistic.	-	
	06 - I enjoyed driving.		
2	19 - The outside visual of the simulator was realistic.	- 0.763	
2	22 - I have really pushed it.	0.100	
	23 - I was really challenged to perform well.		
	09 - I felt confident with the car.		
3	13 - The task was easy.	0.787	
	15 - I performed the task well.		
4	25 - After this experience, I can perform the task better in the real world.	- 0.915	
	26 - This experience helped me to develop the required driving skills.	0.910	
5	05 - I felt quite anxious while conducting the driving task.	- 0.565	
	10 - I sometimes had the feeling of losing control over the car.	0.000	

#### 3. Result analysis

From the grouping obtained in Table 9, we tried to reason why the statements were grouping in that way. The statements of factor one appear to be measuring how subjects felt the car motion cues (driving feeling/motion perception) in relation with the control inputs. Factor two seems related with subject motivation but the fact that statement 19 ("The outside visual of the simulator was realistic.") is coupled with the other statements of this factor cannot be explained. Factor three appears to be related with task performance, and factor four with training value or skill transfer to the real world.

Figure 18 shows the average factor ratings for the five factors found in the factor analysis. A repeated-measures ANOVA between the two independent variables, motion condition and trial number, was performed. Interactions of the motion condition and/or trial with the two different subjects' groups were only found for the task performance factor. Therefore, a three-way mixed ANOVA was used in the analysis of this factor to take into account the group effect. The ANOVA results can be found in Table 10 for the motion independent variable and in Table 11 for the trial independent variable.

From Figure 18(a) it is possible to see that the driving feeling was higher for the motion condition. The condition with motion scored  $\approx 4.5$  and  $\approx 4.8$ , respectively for trials 1 and 2, while the no motion condition scored  $\approx 3.4$  both for trials 1 and 2.

For the factor measuring motivation, Figure 18(b), motion also scored better than no motion for both trials.

Regarding task performance, two significant interactions were found. The first is related with a significant interaction between the motion condition and the subject's group, F(1,18) = 5.049, p = 0.037. The second was a sginificant interaction between the motion condition and the subjects' group and at which trial subjects' were, F(1,18) = 5.835, p = 0.027. Figure 19 shows these interactions. From Figure 19(a) one can observe that subjects from Group 1 (start with the No Motion condition) felt that their performance was better in the No Motion condition than in the Motion condition. Their average scores were  $\approx 3.3$  and  $\approx 4.0$  respectively for the No Motion and Motion condition. On the other hand, subjects from Group 2 felt that

their performance was better in the Motion condition. Their average scores were  $\approx 4.4$  and  $\approx 3.2$  respectively for the No Motion and Motion condition. For Trial 2, one can observe from Figure 19(b) subjects felt that their performance was similar in both conditions. The results were also similar between the two subject's groups.

In terms of training value, the motion condition scored  $\approx 3.5$  in trial 1 and  $\approx 4.0$  in trial 2. For the same factor, the no motion scored  $\approx 2.9$  and  $\approx 3.3$ , respectively, for trials 1 and 2. The training value was the only factor with a significant main effect of the trial.

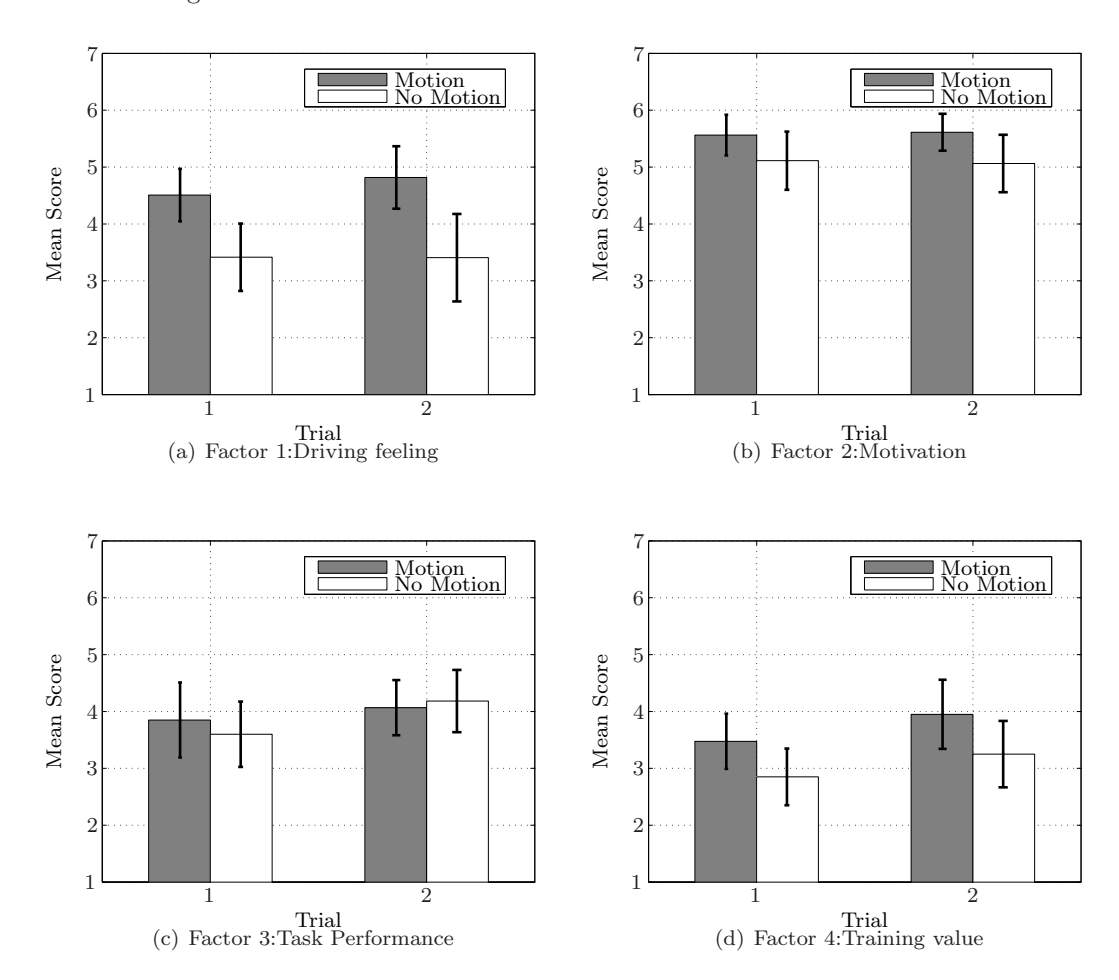


Figure 18. Average factor scores and 95% confidence intervals for the five factors.

Table 10. Repeated-measures ANOVA results of the factor scores for the motion variable (\* = p < 0.05).

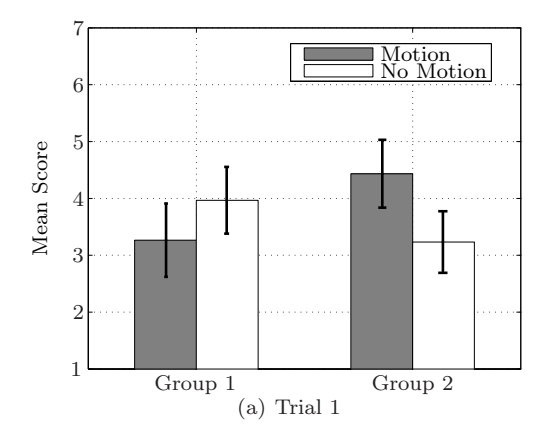
Factor	F	p	sig.
1	F(1,19) = 11.007	0.004	*
2	F(1,19) = 13.511	0.002	*
3	F(1,18) = 0.091	0.767	-
4	F(1,19) = 6.532	0.019	*

#### D. Motion sickness scale

The motion sickness scale was used to observe the subject's sickness level during the experiment. Figure 20 shows the average sickness scores of all motion conditions for trials 1 and 2. A repeated-measure ANOVA was performed to check for significant effects of the motion condition or the trial. There was a significant

Table 11. Repeated-measures ANOVA results of the factor scores for the trial variable (\* = p < 0.05).

Factor	F	p	sig.
1	F(1,19) = 0.481	0.496	-
2	F(1,19) = 0.000	1.000	-
3	F(1,18) = 3.734	0.069	-
4	F(1,19) = 10,414	0.004	*



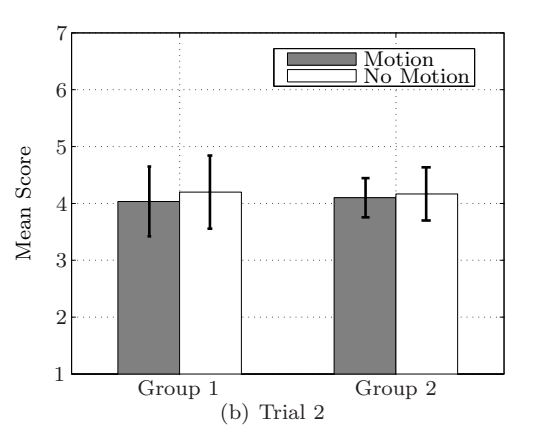


Figure 19. Average factor scores and 95% confidence intervals for the task performance factor.

main effect of the motion condition on the motion sickness score, F(1,19) = 5,444, p = 0.031. A significant main effect of the trial on the motion sickness scale was not found. However, note that the motion sickness average scores are low for all the conditions (below two in a scale of one to six), which indicates that motion sickness was not an issue during the experiment.

#### E. Subjective comments

The only results obtained regarding under- and/or oversteer events were obtained during the de-briefing phase. Subjects that have previously experienced oversteer events were able to identify those in the Motion condition. In some cases, motion feedback helped them to recover from these events without crashing. However, it was difficult to identify under- and oversteer events from the objective data due to the experiment design. These events happened only to some subjects and it was difficult to find a relation in the data to explain differences observed in both motion conditions. In order to study these events more in-depth, an experiment should be designed where under- and oversteer events are induced. For example, a clothoid curve as suggested by Fortmüller, 5 can be used to study these events and to better understand how vehicle handling in simulation can be improved by motion feedback.

During the de-briefing, subjects commented that they were surprised when they lost control over the car during the condition without motion. On the other hand, during the motion condition, subjects did feel that they were losing control over the vehicle, which made accidents more expected events.

#### F. Number of pylon sections accomplished

The slalom got increasingly more difficult with each pylon section. Table 12 shows the number of participants that were able to drive through the nine slalom sections without crashing the car. The runs were again divided in two groups, to show the difference between the first time a motion condition was driven (Trial 1) and its repetition (Trial 2). This means that for the first trial, 55% of the participants were able to finish the slalom. For Trial 2, subjects were more consistent and 75% were able to finish the slalom. Differences between Motion and No Motion are only considerable for trial one. In this trial, 65% of the participants experiencing

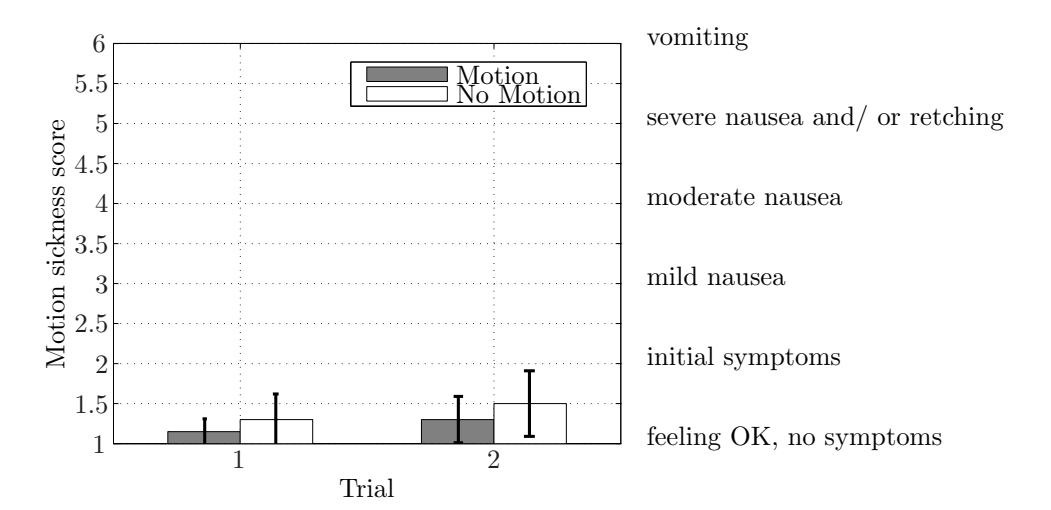


Figure 20. Average scores and 95% confidence intervals of the motion sickness scale for trials 1 and 2.

the motion condition were able to finish the slalom against 45% experiencing the condition without motion feedback. No considerable differences were found between the two subject's groups as one can observe from Table 12. Table 13 shows in which pylon section accidents occurred. Note that because of the number of accidents, the total number of participants is lower in the last pylon sections.

Table 12. Number of participants out of 20 that finished the nine pylon sections.

	Tri	al 1	Tria	al 2
	Group 1	Group 2	Group 1	Group 2
Motion	7	6	8	8
No Motion	4	5	8	7

Table 13. Number of accidents per total participants in each section.

	rial 2	Τ	rial 1	Pylon section	
otion	No Mot	Motion	No Motion	Motion	1 yion section
0	0/20	0/20	0/20	0/20	1
0	0/20	0/20	0/20	0/20	2
0	0/20	0/20	0/20	0/20	3
0	1/20	0/20	0/20	0/20	4
9	0/19	0/20	0/20	0/20	5
9	0/19	1/20	2/20	1/20	6
9	1/19	1/19	5/18	2/19	7
8	3/18	1/18	1/13	4/17	8
5	0/15	1/17	3/12	0/13	9
9	1/19 3/18	1/19 1/18	5/18 1/13	2/19 4/17	7 8

#### G. Average speed

The average speeds were analyzed to check differences in driving strategy between the two motion conditions. Subjects had a more constant driving behavior in Trial 2 than in Trial 1. For trial one, the total number of accidents was higher and the standard deviations of the average speeds were also higher. For example, in pylon section nine, the standard deviations for the Motion condition are 4.84 for trial one and 1.33 for trial two. This means that the practice run was not enough for subjects to develop a constant driving behavior.

For the objective measures, we want subjects to have a more constant driving behavior, so that we can analyze differences between motion and no motion without external factors interfering in subjects' driving behavior, like the lack of training. Figure 21 shows the mean car speed and the 95% confidence intervals for the nine pylon sections. From Figure 21 one can observe that the average speed decreases with the pylon sections, since they got increasingly difficult. The Motion condition average speeds are smaller than the No Motion condition average speeds. A repeated measures ANOVA was performed with the intent of studying the effect of motion on the car average speed. Significant main effects were found starting on pylon section five. The ANOVA results can be found in Table 14.

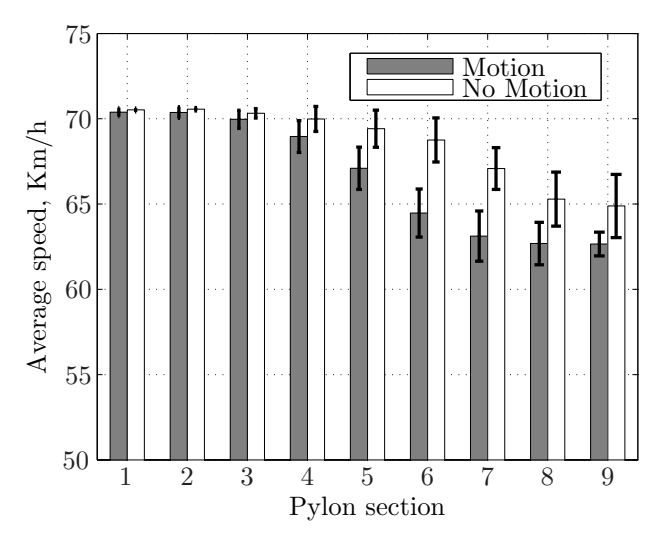


Figure 21. Average car speed and 95% confidence interval for all pylon sections in Trials 2.

Table 14. Repeated-measures ANOVA results of the average speed for the motion independent variable (\* = p < 0.05).

Section	F	p	sig.
5	F = (1, 18) = 8.697	0.009	*
6	F = (1, 18) = 19.278	0.000	*
7	F = (1, 17) = 25.306	0.000	*
8	F = (1, 14) = 5.940	0.029	*
9	F = (1,4) = 5.352	0.041	*

#### H. Vehicle model measures

Subjects were able to control the vehicle velocity up to a maximum of 70 km/h. In this way subjects could naturally control their speed. Therefore, the time that a subject took to drive the full slalom was different from participant to participant. Consequently, comparing time plots of car variables is not correct. This is because at a certain time instant, subjects are in different slalom positions. In order to compare averages of car variables, we used longitudinal spatial plots. In this way, we can compare the differences of a certain car variable for a certain road section (e.g., what happens to the lateral specific force when the car is near a pylon). This analysis was performed in two different section of the slalom: pylon sections two and nine. Pylon section two was preferred to pylon section one to decrease subjects' variance on the control inputs due to adaptation to the driving task. By comparing a slalom section demanding lower frequency control inputs with a slalom section demanding higher frequency control inputs, one can study the driving behavior evolution in the slalom.

#### 1. Driving path

The driving path was analyzed to observe if subjects had a different driving strategy (like distance to the pylons) when motion feedback was present. Figure 22 shows the average driving path for pylon section two and nine. Pylon positions are also represented in the plot. The average was calculated by combining data from all participants for trial 2. Trial one data was not included because subjects' driving behavior was more variable there. From Figure 22(a) it is observable that the driving path is lagging in the motion condition when compared with the no motion condition. A zoom near the fourth pylon (Figure 23) showed that the standard deviations of the two motion conditions slightly intersect each other. The same delay was observable in pylon section nine. However in this pylon section, the standard deviations of both driving paths fully intersected each other, meaning large driving path variations between subjects. Although the frequency of the driving path was higher in pylon section nine, the path amplitude was similar in both sections.

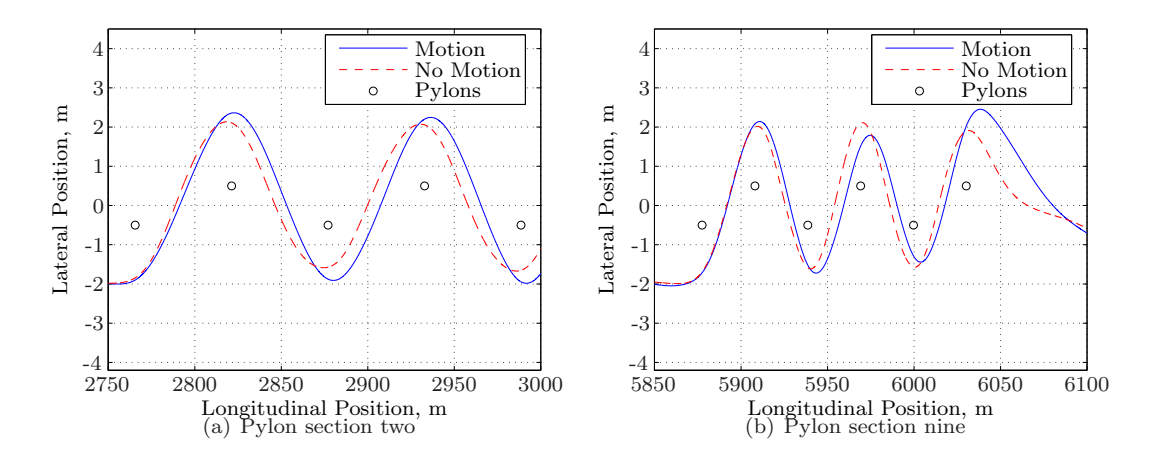


Figure 22. Average driving path for sections two and nine.

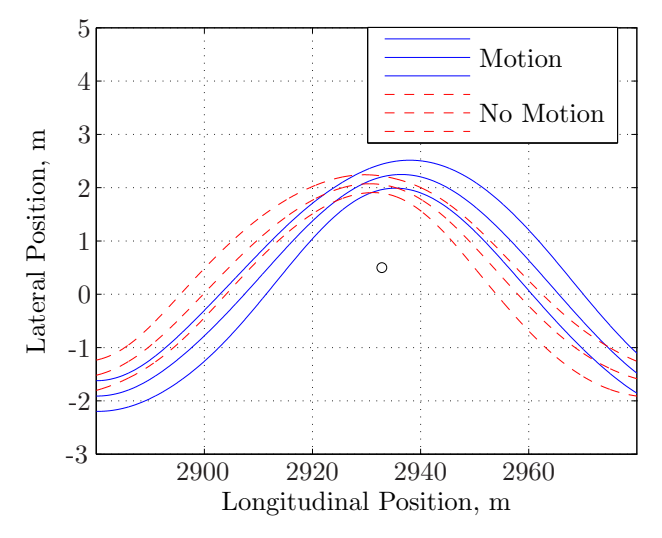


Figure 23. Zoom of the average driving path and standard deviations for section two.

#### 2. Steering wheel angle

The steering wheel angle was analyzed to observe the effort that subjects had put into the car control inputs for the different motion conditions. Figure 24 shows the average steering wheel angle for pylon section two and nine. The average was calculated using all participants' data for trial 2. In Figure 24(a) it is possible to observe that the signal amplitude is similar for Motion and No Motion. However, the No Motion signal seems to have a higher frequency component on top of the main sinusoidal component. This high frequency

component was not observable in the Motion condition. In Figure 24(b) the high frequency component of the No Motion condition is no longer noticeable. In this pylon section, a delay of the Motion condition in comparison with the No Motion condition was visible. The standard deviations of the steering wheel angle for this pylon section are too high to draw any conclusions.

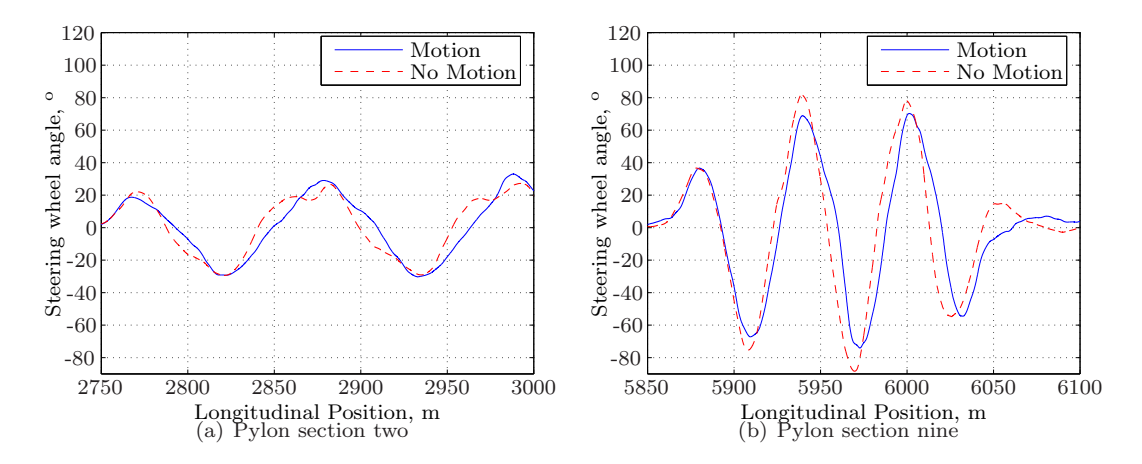


Figure 24. Car model steering wheel angle average for sections two and nine.

#### I. Power spectral density analysis

A Power Spectral Density (PSD) analysis was performed to examine the control effort differences between the tested motion conditions. PSD analysis has already been used to check differences in motion conditions for flight simulators.<sup>26–28</sup> Telban et al.<sup>27</sup> used this technique to study pilot performance variations and which motion cueing algorithm demanded a higher pilot workload. In this study we used this technique to draw conclusions not only about the control effort but also to investigate changes in control behavior by studying the frequency content of the control input signals for the different motion conditions.

Figure 25 shows the results obtained from the PSD analysis. The PSD was calculated for every subject and then averaged. Again, only the results of trial two were used. The total time in a pylon section depends from pylon section to pylon section since the distance between pylons is different for all the nine pylon sections. This means that the results of pylon section two had a lower frequency resolution than the ones of pylon section nine. The total time used to calculate the PSD was measured from the second last pylon in the pylon section. In this way, one obtains a total time of two periods of the pylon section driving path. Ideally, the frequency of the control input is equal to the frequency of the driving path. From Figures 25(a) and 25(b) it follows that pylon section nine required higher control effort since the power of the main frequency peak is much higher than the one of pylon section two. In pylon section nine, the Motion condition main frequency peak has less power and seems to be at a lower frequency than the one of the No Motion condition. A zoom on the PSD of pylon second two (Figure 26(a)) shows a high frequency component on the No Motion condition nonexistent on the Motion condition. This was also investigated for pylon section nine (Figure 26(b)). To check if these high frequency differences on both motion conditions were statistically significant, a dependent t-test was performed. For pylon section two, the average of the individual PSD's was computed from 0.3 to 0.6 Hz which was where this high frequency peak on the No Motion condition was noticeable. The same was done for pylon section nine but from 0.6 to 1.0 Hz. The dependent t-test results can be found in Table 15.

Table 15. Dependent t-test results for the mean PSD in the frequency range of 0.3-0.6 Hz in pylon section two and 0.6-1 Hz in pylon section nine (\* = p < 0.05).

Pylon section	Mea	an PSD	Standard error	+	n	eio
1 yion section –	Motion	No Motion	Standard error	U	Р	sig.
2	0.0101	0.0341	0.0058	t(19) = -4.157	0.001	*
9	0.0267	0.0455	0.0122	t(13) = -1.536	0.149	-

For all the pylon sections, the subjects' control input is between 0 and 1 Hz. This interval is congruent with what was reported by Guo et al.<sup>26</sup> To study the control effort, the PSD plots were integrated. The integrals were calculated from 0 to 1 Hz using Euler integration. Figures 25(c) and 25(d) show the average integral power and its standard deviations respectively for pylon section two and nine. It follows that pylon section nine required higher control effort than pylon section two. The control effort for the Motion condition in this pylon section was lower than the one of the No Motion condition. Note that the same results can be obtained by calculating the variance of the steering wheel angle.

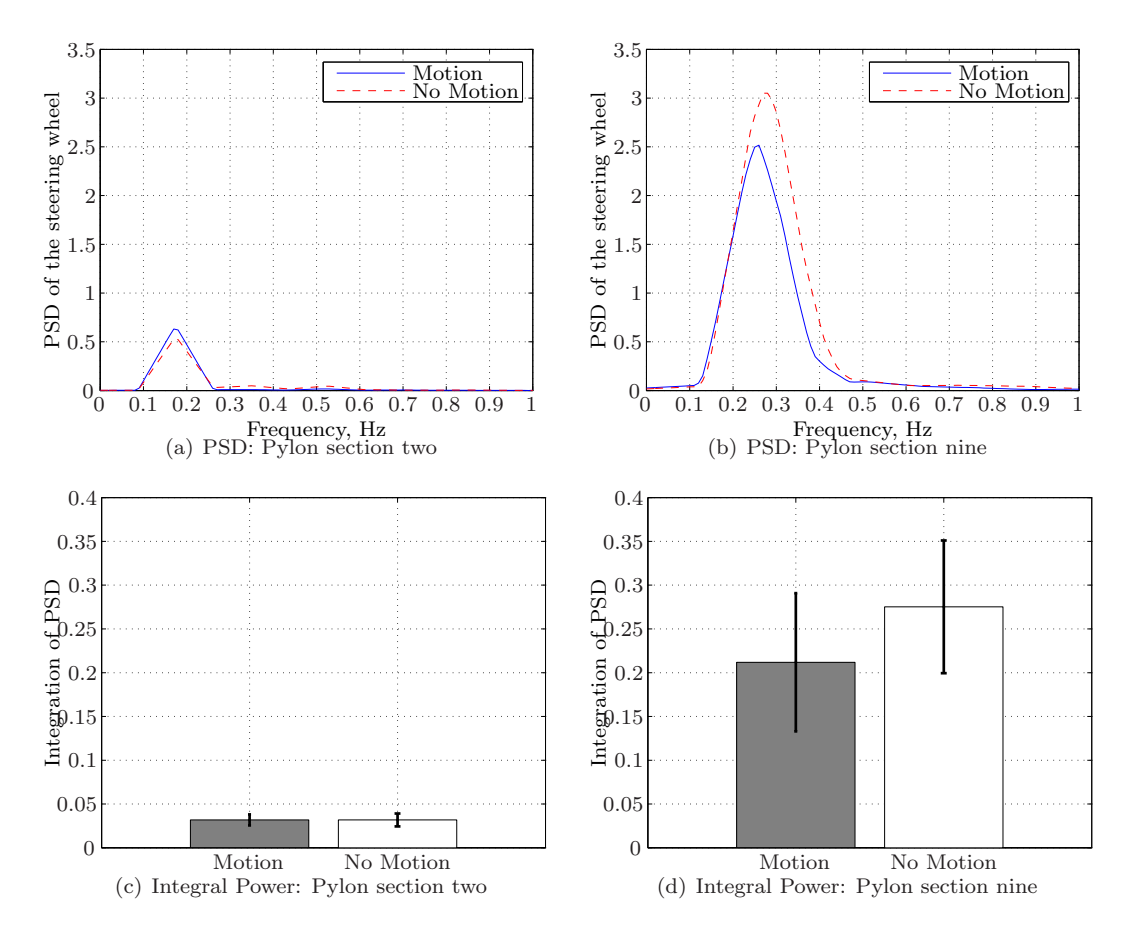


Figure 25. Average PSD (top figures) and average integral power and standard deviations (bottom figures) of the steering wheel input for pylon section two and nine.

#### V. Discussion

#### A. Simulator motion

Desdemona is a simulator with a special motion platform. This motion platform allows new approaches to simulate motion, not possible in more conventional motion platforms. The main effort during the development of the advanced driving MCA was in simulating the main motion features of a slalom maneuver while having an MCA capable of adapting to other kind of maneuvers/simulations. Desdemona's gimballed system allows full rotations around the three axes of the Desdemona frame of reference. Because of this, tuning of the rotational channel was not an issue. Therefore, the main focus during the tuning of the MCA was in achieving specific forces in the same order of magnitude of the ones of the real vehicle. The lateral specific force is the one with the higher amplitude during a slalom maneuver. The MCA was able to follow this specific force both in amplitude and frequency. The 0.75 lateral gain was chosen based on the results obtained from other studies<sup>17,18,29,30</sup> where it was found that a scaling factor of one is not preferred by subjects in a simulation environment. These studies indicated that subjects perceive the one to one condition as too strong.

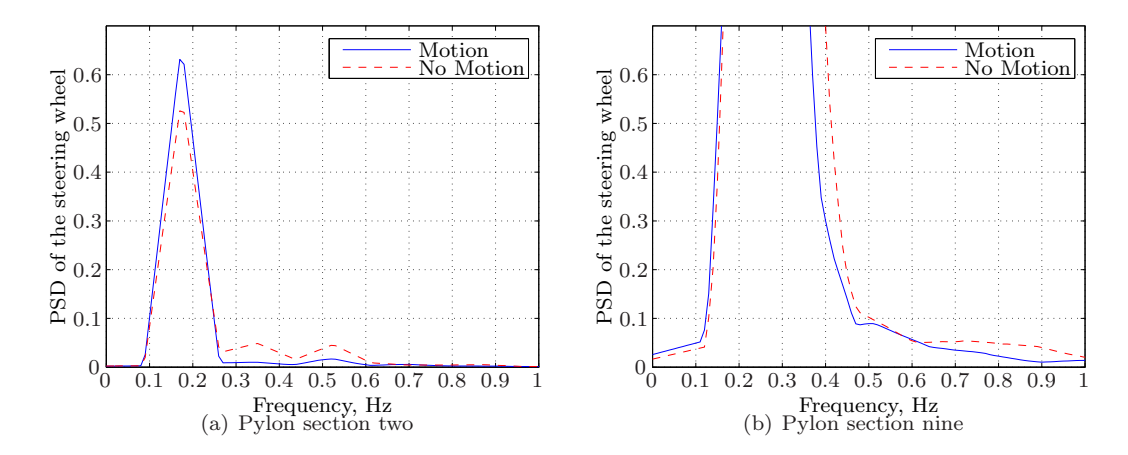


Figure 26. Zoom of the average PSD for pylon section two and nine.

The MCA structure is similar to the Classical Washout algorithm.<sup>11</sup> An advantage of this property is that the filter is easy to tune. It is also computationally fast due to its simple mathematics. Unfortunately the MCA also had some of the disadvantages present in the Classical Washout algorithm, such as the need to tune for the worst case scenario since its filter parameters are fixed during the entire simulation. Nevertheless future updates can be made to this MCA to include new features like high pass filters with adaptive parameters or blocks containing mathematical functions of the human perception organs to optimize motion space usage. Tilt coordination can also be easily implemented in this design.

The design decision of using a zero gain on the longitudinal scaling created some discomfort whenever subjects had to use the brake pedal. Subjects complained that they missed a longitudinal specific force input whenever they had to brake to lower the vehicle speed. They also stated that the lack of longitudinal cueing when they lowered speed made it more difficult for them to infer the current vehicle velocity. A suggestion to overcome this situation is to use a floating neutral position instead of a fixed neutral position. A floating neutral position would change the neutral positions of the actuators during the simulation. In this way, the neutral position would adapt depending on current simulation requirements.

Some authors<sup>31,32</sup> are using predictive algorithms to calculate the best neutral position to handle the next simulator maneuver. Other authors like Chapron et al.<sup>33</sup> use a gain scheduling algorithm to change between two different motion cueing algorithms within the simulation. This solution has the advantage of being able to use two MCAs specifically tuned for two different maneuvers. In their case,<sup>33</sup> they had a situation where the vehicle had to perform a lane change and some seconds after had to do a curve. Two algorithms were used: a lane position algorithm (LPA) and a Classical Washout algorithm. During the lane change the LPA was used. After, the LPA is changed into the Classical Washout by a pre-positioning algorithm so that the vehicle performs the curve with the Classical Washout instead of the LPA. The main disadvantage of this scheme is that the pre-positioning algorithm takes time to change from one algorithm to another which could generate false cues if the algorithms are not changed when the vehicle is already on the curve.

In our opinion an online algorithm that changes the neutral position of the simulator would be a good feature to implement in this MCA. In this way one would have a better use of Desdemona motion space, and in the particular case of the slalom maneuver it would be possible to generate longitudinal cues. For the slalom maneuver, the neutral positions could oscillate between -2 and 2 meters of the radius sledge, which would enable the use of the central yaw to generate longitudinal onset cues. The filter parameters could also adapt with the change of neutral positions to guarantee that the simulator stays within its physical limits (e.g., if the cabin is at 2 meters of radius, movements in one lateral direction have to be more conservative than movements in the other direction).

#### B. Paired comparison

From the paired comparison analysis we can see that the condition with motion was much more preferred by the subjects than the condition with no motion. It can also be observed that with the progression of the experiment, the No Motion condition was rated best fewer times (Figure 17). This had to do mainly with the subjects that started the experiment with the No Motion condition. In the first paired comparison four subjects of this group preferred the No Motion condition while in the last comparison only two subjects continued to prefer this condition.

By accumulating the preferrences from the three paired comparisons together, the difference between the two motion conditions was highly significant, showing that subjects much prefer the condition with motion feedback. It can be concluded that for advanced maneuvers like this slalom, subjects prefer to have a simulatior with motion feedback, rather than a fixed based simulator. Some of the participants commented that it was much easier to "catch up with the cadence" (the sinusoid) of the slalom when motion was present.

#### C. Questionnaires

The factor analysis conducted in this study tried to reveal the subject's subjective impression about the realism of the simulation. Factor one, which had to do with driving feeling, showed that subjects had a better perception of how the car was reacting to the control inputs in the motion condition. This means that in the subjects' point of view, motion feedback enhances driving feeling. However, some subjects said that they perceived motion in the No Motion condition.<sup>34</sup> This phenomenon of perceiving motion in a no-motion condition was already reported by Wentink et al.<sup>14</sup> Nevertheless, according to the results of the driving feeling factor motion feedback is needed in order to have a better perception of the vehicle one is controlling. This could mean that motion feedback in simulation helps subjects to build a better internal model of the vehicle they are controlling.

Factor two was a measure of subjects' motivation to perform the task. In both conditions, subjects were motivated to perform the task, but in the Motion condition this motivation was higher than in the No Motion. These results showed that the driving task was motivating for subjects and that with motion feedback, their motivation increased.

Task performance (factor 3) was the only factor influenced by whether the first motion condition was Motion or No Motion. Both subjects' groups felt that their performance decreased in the second time they drove the full slalom. However, one can observe that for Trial 2, subjects felt that their performance did not change regardless the motion condition.

The fourth factor has to do with training value, i.e., with the subjective account to wether skills learned in the simulator transferred to skills in the real world. From the obtained results it is possible to observe that for the first trial, subjects did not feel that the experiment helped develop car driving skills. Nevertheless, we can observe that the condition with motion feedback had a higher score. For trial two we noticed an increase of the average scores meaning that training effects had an influence in the skills developed in the simulator.

Some issues with the questionnaire arose in this experiment. Therefore we would suggest some corrections of the questionnaire for future studies. First we should leave out all the statements that were not grouping with other statements and all the statements that failed the reliability test. The factors measuring simulation realism need to be rewritten based on how statements were grouping together in the factor analysis results. In the questionnaire, every factor should have a small introduction explaining to the subject what we want to measure with the statements. It would be useful to conduct small experiments to validate the questionnaire where the objective would be to improve/correct the questionnaire instead of trying to validate a hypothesis. These measures would improve the method and guarantee better results in future experiments.

#### D. Motion sickness scale

The motion sickness scale was used in this experiment to monitor the subject's sickness level. In this way it is possible to observe if there is a condition that raises the sickness level of subjects which can affect the results of the other measures. The sickness scores were very low for all the motion conditions which is good since higher motion sickness scores could bias the other measures.

Despite the low scores, there was a significant effect of the motion condition in the motion sickness scores. The No Motion condition was more sickening than the Motion condition. A possibility for this has to do with the fact that in the No Motion condition the human vestibular organs are not activated, which is incongruent with what is happening in the visual channel. It is also possible to note a slight increase of the sickness scores with the trials, nevertheless the repeated measures ANOVA did not show any significant effect of the trial in the sickness scores.

#### E. Number of sections finished

The number of accidents was dependent on training effects since there were more accidents in trial 1 than in trial 2. In the first pylon sections the task was easy and no accidents occurred. When the task became more difficult, accidents started occurring mainly in the No Motion condition. In trial 2, the number of accidents decreased in both conditions since subjects were more aware of the difficulty of the task. Therefore, subjects driving behavior was more constant in trial 2. This shows that the practice run at the beginning of the experiment was not enough to stabilize subjects' driving behavior. Note that the slalom in the practice run induced a lower lateral specific force on the vehicle when compared to some pylon sections of the full slalom.

#### F. Average speed

Motion feedback changed driving behavior as one can see from the average speed differences between the two motion conditions. Subjects had a lower average speed in the Motion condition when compared to the No Motion condition. This means that with motion feedback, in the more difficult pylons sections, subjects were more aware of how the car was reacting and drove it more carefully to prevent a crash with the guardrail. The speed difference was always significant (starting on pylon section 5) which seems to indicate that subjects learned how to use the motion feedback cues. In this case, motion is helping subjects in better perceiving the car speed and not exceeding the car limits. These speed differences are congruent with results found in other studies.<sup>6,8,9</sup> Brünger-Koch et al.<sup>8</sup> were able to compare the results obtained in the simulator with results obtained during real car driving. The results showed that the average speed in simulator is much higher than that in real driving. Siegler et al.<sup>6</sup> used two motion conditions (motion and no motion) to draw conclusions about subjects braking behavior in a simulator. They found differences in the subject's decelerations, concluding that motion prevented subjects from reaching high decelerations, producing a more realistic driving behavior.

One can also argue that the differences in average speed between the two motion conditions are related with driver comfort. Since none of the subjects had experience in advanced maneuvers, the information provided by motion feedback was used to improve comfort instead of performance. Therefore, one can link the decrease of speed in the No Motion condition with the increase of task difficulty, and link the extra decrease of speed in the Motion condition with the increase of comfort during the maneuver.

#### G. Vehicle model measures

The average driving path is similar for both motion conditions. However, one can observe that the sinusoidal peak of the motion condition has some delay when compared with the one of the no motion condition. Pretto et al. 18 found similar results for the average driving path that subjects had during their slalom maneuver. It was reported that this driving path delay varies with the lateral gain of the vehicle specific force used has input for the motion cueing algorithm of the simulator. For pylon section two, the lateral amplitude of the driving path sinusoid is higher for the motion condition than for the no motion condition. For pylon section nine this changes since the driving path amplitude is lower for the motion condition. This difference is clearer between pylons 3 and 5 since the other pylons were affected by subjects entering and exiting the pylon sections. A longer pylon section would be needed to study in more detail the sinusoidal differences between the two motion conditions.

The steering wheel angle plots showed that in the earlier pylon sections the control inputs were similar, indicating similar driving behavior in both motion conditions. This is no longer true in the fastest sections where the control inputs for each motion condition were different in amplitude and frequency. In the earlier pylon sections, it was also observed during the No Motion condition a high frequency behavior on the steering wheel. This behavior was observed while conducting the experiment where subjects overcompensated their movements.

#### H. Power spectral density analysis

The PSD analysis was used to check control effort differences between the two motion conditions. The integral of the PSD was used as a workload measure. Telban et. al.<sup>27</sup> stated that a motion condition having a higher integration means that subjects spent more power on that condition than on the other. The integral plots show that pylon section nine had higher workload than pylon section two.

From the PSD plots it is possible to observe a high frequency behavior during the No Motion condition in pylon section two. The high frequency behavior is around 0.3 and 0.6 Hz. This high frequency behavior was not observed in the Motion condition. For pylon section nine, the main frequency peak of the Motion condition was at a smaller frequency than the one of the No Motion condition. This was expected since in the No Motion condition the average speeds were higher, meaning that the steering wheel input needs a higher frequency behavior in order to drive through the slalom.

#### VI. Conclusion

This experiment showed that it is important to have motion feedback in the simulation of advanced driving maneuvers. Subjects much prefer the condition with motion feedback as one can observe from the paired comparison results. From the questionnaire results one can conclude that subjects found that motion enhances their driving feeling and also keeps them more motivated to perform the task. From the objective measures it follows that with motion subjects drove more carefully and had better control of the car; therefore they could anticipate on the car dynamic behavior better and were less surprised when the car did crash. In trial one, where subjects had not crashed before, the Motion condition registered less accidents than the No Motion condition. One can deduce that during unexpected events, motion can help to decrease the accident rate. Motion feedback also decreased subjects' workload during the last pylon sections.

The questionnaire used in this experiment proved to be a good tool to understand the subject's preference of the condition with motion feedback. It helped to pinpoint what variables made subjects prefer the motion condition. Future work should be done in improving the questionnaire.

Motion feedback had an effect on driver performance and driving behavior, especially on the fastest sections of the slalom. This means that drivers adopted different strategies when they were fed with extra sensory information. In flight simulation, it was already shown that motion feedback had a beneficial influence on pilot control performance.<sup>1</sup> A similar effect seems to be present in simulating advanced driving maneuvers. Research using driver-on-the-loop would also be affected if a fixed based simulator is used whenever extreme maneuvers are present. This could happen in road safety research or research that explores driving disturbances, since advanced driving maneuvers are normally required to overcome difficult driving situations. Therefore, if motion is not present, drivers are losing important information that ultimately would make them react to the situation in a totally different way. Future experiments should focus on investigating the most important cues for driver control in advanced driving maneuvers.

#### References

<sup>1</sup>Hosman, R. J. A. W., *Pilot's perception and control of aircraft motions*, Ph.D. thesis, Faculty of Aerospace Engineering, Delft University of Technology, 1996.

<sup>2</sup>Telban, R. J., Cardullo, F. M., and Houck, J. A., "Developments in human centered cueing algorithms for control of flight simulator motion systems," *Modeling and Simulation Technologies Conference and Exhibit*, No. 99-4328, AIAA, Portland, OR, August 1999.

<sup>3</sup>Kemeny, A. and Panerai, F., "Evaluating perception in driving simulation experiments," *TRENDS in Cognitive Sciences*, Vol. 7, 2003, pp. 37–37.

<sup>4</sup>Fortmüller, T. and Meywerk, M., "The influence of Yaw Movements on the Rating of the Subjective Impression of Driving," *DSC2005 North America*, Orlando, November 2005.

<sup>5</sup>Fortmüller, T., Tomaske, W., and Meywerk, M., "The Influence of Sway Accelerations on the Perception of Yaw Movements," DSC 2008 Europe, Monaco, January-February 2008, pp. 161–170.

<sup>6</sup>Siegler, I., Reymond, G., Kemeny, A., and Berthoz, A., "Sensorimotor integration in a driving simulator: contributions of motion cueing in elementary driving tasks," *DSC2001*, Sophia Antipolis, September 2001.

<sup>7</sup>Brünger-Koch, M., Briest, S., and Vollrath, M., "Virtual driving with different motion characteristics - braking manoeuvre analysis and validation," 2006 Driving Simulation Conference, 2006.

<sup>8</sup>Brünger-Koch, M., Briest, S., and Vollrath, M., "Do you feel the difference? - A motion assessment study," *Driving Simulation Conference - Asia/Pacific*, Tsubaka, Japan, May-June 2006.

<sup>9</sup>Colombet, F., Dagdelen, M., Reymond, G., Pere, C., Merienne, F., and Kemeny, A., "Motion Cueing: what is the impact on the driver's behaviour?" *DSC 2008 Europe*, Monaco, January-February 2008, pp. 171–181.

<sup>10</sup>Milliken, W. and Milliken, D., Race Car Vehicle Dynamics, SAE International, Warrendale, PA., 1995.

<sup>11</sup>Reid, L. D. and Nahon, M. A., "Flight simulation motion-base drive algorithms: part 1 - developing and testing the equations," Tech. Rep. 296, Institute for Aerospace Studies, University of Toronto, December 1985.

<sup>12</sup>Nahon, M. A. and Reid, L. D., "Simulator Motion-Drive Algorithms: A Designer's Perspective," *Journal of Guidance, Control and Dynamics*, Vol. 13, No. 2, March-April 1990, pp. 356–362.

- <sup>13</sup>Wentink, M., Bles, W., Hosman, R. J. A. W., and Mayrhofer, M., "Design & evaluation of spherical washout algorithm for Desdemona simulator," *Modeling and Simulation Technologies Conference and Exhibit*, San Francisco, CA, August 2005.
- <sup>14</sup>Wentink, M., Valente Pais, A. R., Mayrhofer, M., Feenstra, P., and Bles, W., "First Curve Driving Experiments in the Desdemona Simulator," *DSC 2008 Europe*, Monaco, January-February 2008, pp. 135–146.
- <sup>15</sup>Valente Pais, A. R., Wentink, M., van Paasen, M. M., and Mulder, M., "Comparison of Three Motion Cueing Algorithms for Curve Driving in an Urban Environment," *PRESENCE: Teleoperators and Virtual Environments*, 2009, Accepted for publication.
- <sup>16</sup>Kappé, B. and van Emmerik, M., "Mogelijkheden van rijsimulatoren in de rijopleiding en het rijexamen," Tech. rep., TNO Defence, Security and Safety, 2005, (in Dutch).
- $^{17} {\rm Feenstra},$  P., Wentink, M., Correia Grácio, B. J., and Bles, W., "Effect of Simulator Motion Space on Realism in the Desdemona Simulator," DSC 2009 Europe, 2009.
- <sup>18</sup>Pretto, P., Nusseck, H. G., Teufel, H. J., and Bülthoff, H. H., "Effect of lateral motion on driver's performance in the MPI motion simulator," DSC 2009 Europe, 2009.
- <sup>19</sup>Roza, M., Wentink, M., and Feenstra, P., "Performance Testing of the Desdemona Motion System," *Modeling and Simulation Technologies Conference and Exhibit*, 2007.
  - <sup>20</sup> "http://www.carsim.com/," January 2009.
  - $^{21}{\rm Field,\,A.,\,}$   $Discovering\,\,Statistics\,\,Using\,\,SPSS,\,$  Sage Publications Ltd, 2nd ed., 2005.
  - <sup>22</sup>Likert, R., "A technique for the measurement of attitudes," Archives of Psychology, Vol. 22, No. 140, 1932, pp. 1–55.
- <sup>23</sup>Golding, J., "Motion sickness susceptibility questionnaire revised and its relationship to other forms of sickness Facilitation of the emetic response to poisons," *Brain Research Bulletin*, Vol. 47, 1998, pp. 507–516.
- <sup>24</sup>Mert, A., Bles, W., and Nooij, S. A., "Hyperventilation in a Motion Sickness Desensitization Program," Aviation, Space, and Environmental Medicine, Vol. 78, 2007, pp. 505–509.
- <sup>25</sup>Grant, P. R., Blommer, M., Cathey, L., Artz, B., and Greenberg, J., "Analyzing Classes of Motion Drive Algorithms Based on Paired Comparison Techniques," DSC North America 2003 Proceedings, October 2003.
- <sup>26</sup>Guo, L., Cardullo, F. M., Telban, R. J., Houck, J. A., and Kelly, L. C., "The Results of a Simulator Study to Determine the Effects on Pilot Performance of Two Different Motion Cueing Algorithms and Various Delays, Compensated and Uncompensated," Modeling and Simulation Technologies Conference, AIAA, Austin, TX, 2003.
- $^{27}$  Telban, R. J., Cardullo, F. M., and Kelly, L. C., "Motion Cueing Algorithm Development: Piloted Performance Testing of the Cueing Algorithms," Tech. Rep. CR-2005-213748, Nasa, May 2005.
- <sup>28</sup>Soparkar, S. and Reid, L. D., "The Influence of Simulator Motion on Handling Qualities," *Canadian Aeronautics and Space Journal*, Vol. 52, No. 1, March 2006, pp. 21–29.
- <sup>29</sup>Groen, E. L., Clari, M. S. V. V., and Hosman, R. J. A. W., "Evaluation of perceived motion during a simulated takeoff run," *Journal of Aircraft*, Vol. 38, No. 4, 2001, pp. 600 606.
- <sup>30</sup>Groen, E. L., Smaïli, M. H., and Hosman, R. J. A. W., "Simulated decrab maneuvers evaluation with a pilot perception model," AIAA Modeling and Simulation Technologies Conference and Exhibit, 2005.
- <sup>31</sup>Wang, S.-C. and Fu, L.-C., "Predictive Washout Filter Design for VR-based Motion Simulator," *International Conference on Systems, Man and Cybernetics*, Vol. 7, IEEE, The Hague, The Netherlands, October 2004, pp. 6291 6295.
- <sup>32</sup>Chen, S.-H. and Fu, L.-C., "Predictive Washout Filter Design Using the Forward Kinematics and a Kalman Filter," Control Applications, IEEE, Singapore, October 2007.
- <sup>33</sup>Chapron, T. and Colinot, J.-P., "The new PSA Peugeot-Citroën Advanced Driving Simulator Overall design and motion cue algorithm," DSC 2007 North America, Iowa City, September 2007.
- <sup>34</sup>Correia Grácio, B. J., Wentink, M., Feenstra, P., Mulder, M., van Paassen, M. M., and Bles, W., "Motion Feedback in Advanced Driving Manoeuvres," DSC 2009 Europe, Monaco, 2009.

## Part II

# DSC Europe 2009 paper Motion Feedback in Advanced Driving Manoeuvres

# MOTION FEEDBACK IN ADVANCED DRIVING MANOEUVRES

B. J. Correia Grácio\*, M. Wentink\*, P. Feenstra\*, M. Mulder† M. M. van Paassen†, W. Bles\*

\*TNO Defence, Security and Safety Human Factors 3769 ZG Soesterberg, the Netherlands

†Control and Simulation Department, Aerospace Engineering, Delft University of Technology P.O. Box 5058, 2600 GB Delft, the Netherlands

bruno.correiagracio@tno.nl

#### **Abstract**

During advanced driving manoeuvres, drivers can be hypothesized to use all the available cues to optimize their performance. Fixed-base simulators are commonly used for training of these advanced driving manoeuvres, despite the fact that motion cues are not present. In this experiment we hypothesize that motion feedback improves driver performance and affects the driving control strategy during advanced driving manoeuvres when compared to a situation without motion feedback. A comparison between no-motion car-driving simulation and motion-feedback car-driving simulation is done, by measuring driver performance and control behaviour in a fast slalom. In the fast slalom designed for this experiment, a car drives at 70 Km/h around pylons spaced quite closely at approximately 30 meters apart.

The advanced Desdemona motion platform was used in this study. Desdemona's unique motion system allowed us to create a motion simulation that was almost one-to-one regarding the specific forces and angular rates in the actual car. A new motion cueing algorithm was developed to handle advanced driving manoeuvres like this fast slalom.

Twenty subjects successfully drove the fast slalom in both conditions. The results from a paired comparison show that subjects prefer driving with motion feedback. Motion feedback also helped subjects conducting the driving task. The number of accidents was significantly lower in the motion condition, as compared to the no-motion condition. Significant differences in the maximum lateral specific force and in the average speed between the two motion conditions were found also. From the experimental results we conclude that there is a difference in driving advanced manoeuvres in a fixed based simulator as compared to a motion simulator. This difference influences driving behaviour with respect to keeping control over the car and also it is clear that the driver changes his control strategy.

#### Résumé

#### Introduction

The number of simulators with motion feedback has increased in the past few years. Due to their physical limitations, one-to-one motion is often not possible to render in current simulators. These motion limitations introduce false cues in the simulation, such as the motion responsible for bringing the simulator cabin back to the neutral position. False cues can be very disturbing [1], degrading the simulator fidelity. Clearly, within the constraints of the simulator motion space the negative effects on simulation fidelity must be minimized.

The goal of this study is to assess the effect of motion feedback on driver performance in advanced driving manoeuvres. Advanced driving manoeuvres are usually close to the car dynamic traction limits [2], like fast slaloms or fast curves (like those in racing circuits) that can induce under- and/or oversteer in the car. Fixed-base simulators or simulators with low motion capabilities are the most used in driving and advanced driving training [3]. With this experiment we want to investigate the difference of using a fixed based simulator or a simulator with motion feedback in advanced manoeuvres. The manoeuvre used will be a fast slalom for two reasons: to compare the results with other experiments in the MOVES (MOtion cueing for VEhicle Simulators) Eureka project [4], and because this type of manoeuvre is usually used in advanced driving courses.

This research aims to understand whether motion feedback is an advantage in advanced driving simulation. Our first hypothesis is that simulator motion cues improve driving performance during advanced driving manoeuvres. We expect that motion feedback will help the driver in controlling the car during an extreme manoeuvre. Secondly, we hypothesize that with motion cues available, drivers are better able to identify events like understeer and oversteer.

The paper will start with a brief description of the Desdemona simulator followed by the explanation of the experimental method. The motion cueing filter for Desdemona is explained here as well. Next the results are presented and discussed followed by conclusions.

#### **Desdemona**

The present study uses the 6 DoF Desdemona simulator at TNO Human Factors, The Netherlands [5]. The Desdemona motion platform, with its unlimited rotation and high specific force capabilities, can be used as a tool to assess how motion feedback influences drivers in advanced manoeuvres. A first driving simulation experiment was already carried out in Desdemona on the topic of cornering [5]. In the current study a motion cueing algorithm will be developed for slalom driving with the objective of providing realistic motion cues without violating Desdemona physical limits. In the development of the algorithm, an effort is made to guarantee that the necessary motion cues for advanced driving are present, like cues that indicate over- and understeer.

#### Method

#### **Motion Cueing Algorithm**

Two different motion conditions were used in this experiment. The first condition, denoted as "No Motion", only used Desdemona actuators when subjects drove over a pylon (an upward cue was triggered to notify the driver of the event). For the rest of the simulation Desdemona behaved like a fixed-base simulator. The second condition, denoted as "Motion", used a Desdemona motion cueing algorithm that was designed specifically for advanced driving simulation. The next sections explain in more detail the two motion conditions.

#### No Motion

This motion condition contains an algorithm that activates the Heave drive every time a subject hits a pylon, giving the subject a feeling of actually driving over the pylon. In this way, subjects had a better perception of their own performance. If no pylons were hit during the simulation, Desdemona behaved like a fixed base simulator.

#### Motion

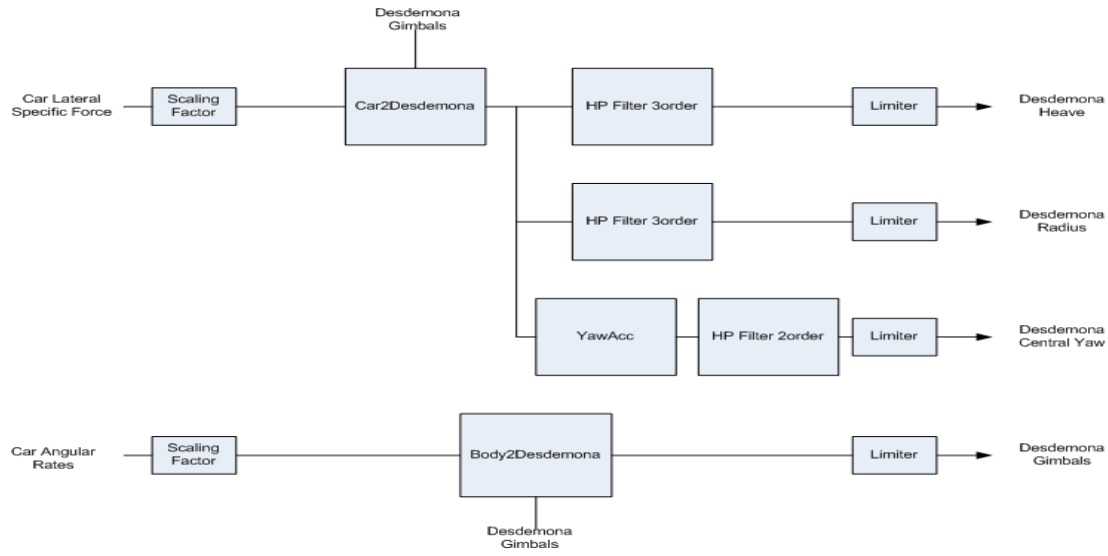


Figure 1 - Motion Cueing Algorithm.

The motion cueing algorithm is based on the principles of the Classical Washout filter [6, 7]. It uses rotation matrices (blocks Car2Desdemona and Body2Desdemona in Figure 1) to transform the car specific forces and angular rates from the car reference frame into Desdemona reference frame. This motion condition also contains the "hitting pylon" algorithm coupled to the Heave drive. The road rumble algorithm of [5] was also used in this condition. Figure 2 shows the car specific forces and angular rotations versus the ones rendered by the simulator for a given pylon section.

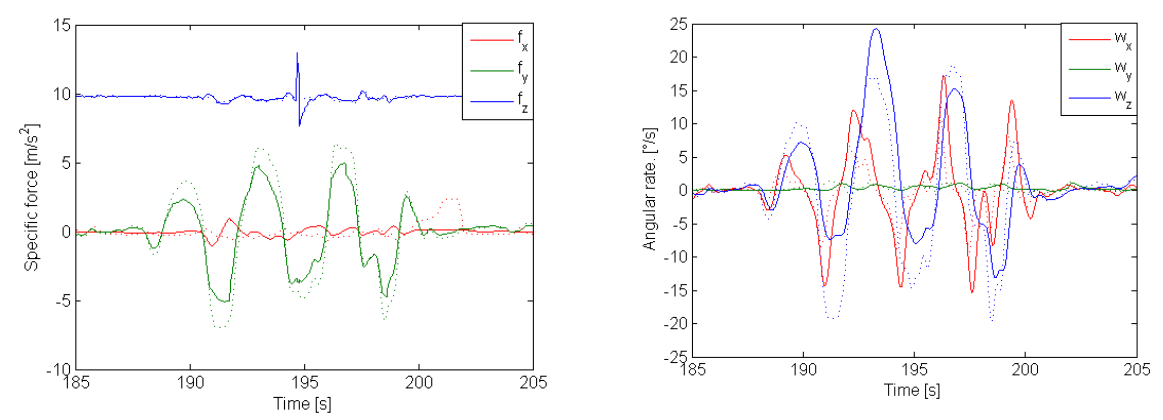


Figure 2 - Specific forces (on the left) and angular rates (on the right) of the car model (dotted lines) versus the simulator (solid lines) in one of the fastest sections of the slalom manoeuvre. The peak in fz is caused by hitting a pylon.

#### **Slalom Manoeuvre**

The slalom designed for this study is an extension to the one used in the MOVES (MOtion cueing for VEhicle Simulators) Eureka project [4]. The manoeuvre was created based on a car sinusoidal path like the one in Figure 3, where a is the sinusoidal path amplitude and d is the distance between pylons.

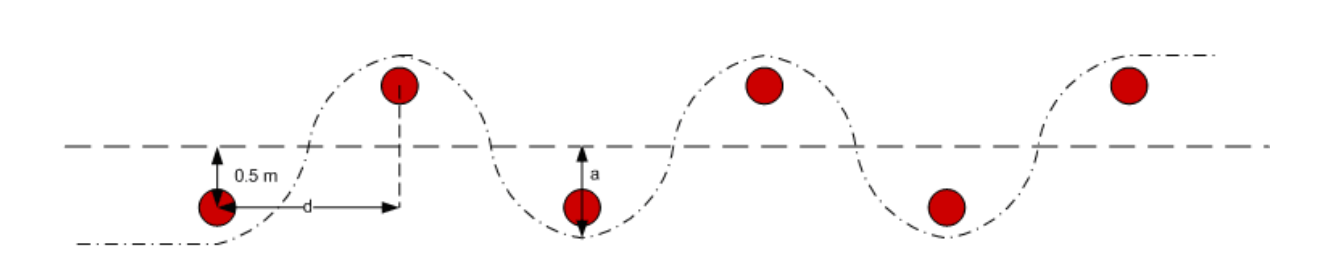


Figure 3 - Theoretical driving path.

The amplitude of the lateral force is given by equation

(1), where a is the sinusoidal path amplitude, d is the distance between pylons and v is the car velocity.

$$a_{y} = a \left(\frac{\pi}{d}v\right)^{2} \tag{1}$$

Nine different pylon sections were created using equation

(1), each of them containing six pylons. The constant parameters of equation

(1) were the sinusoidal path amplitude, a (1.25 meters) and the car velocity v (70 Km/h). Distance between the pylons was the variable parameter. Table 1 shows the characteristics of the pylon sections.

Section	Theoretical lateral	Distance between pylons (m)
	force (m/s <sup>2</sup> )	
1	1	68.30
2	1.5	55.76
3	2	48.29
4	2.5	43.19
5	3	39.43
6	3.5	36.51
7	4	34.15
8	4.5	32.20
9	5	30.54

Table 1 – Slalom characteristics.

The nine sections are 200 meters apart from each other to cancel dynamic driving effects between sections. The pylons are at 0.5 meters from the centreline of the road as is shown in Figure 3.

#### **Procedure**

The experiment started with a practice run. In this run, the easiest slalom section was driven multiple times, since the objective was to familiarize subjects with the driving task. Subjects were instructed to drive through the slalom as fast as possible; however, the velocity was saturated at a maximum speed of 70km/hour. They were told only to lower the car velocity (using the brake pedal or releasing the gas pedal) when the car was near hitting the guard rail or if they felt losing the control over the car.

After the practice run, subjects had to drive through the slalom (all the nine pylon sections) in the two different conditions. Drivers had to drive each condition twice to test if their driving is influenced by any training effect. This means that subjects had to drive the slalom four times in total. To decrease order effects subjects were divided into two randomized groups, shown in Table 2, where NM refers to the no motion condition and M refers to the condition with motion feedback.

Group	First run	Second run	Third run	Fourth run
1	NM	M	NM	M
2	M	NM	M	NM

Table 2 - Motion condition order.

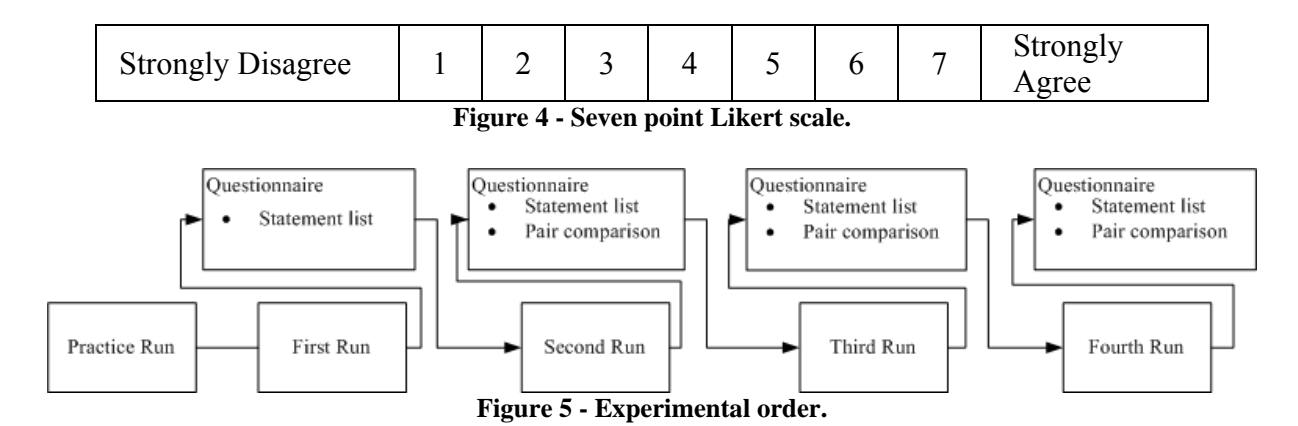
#### **Experimental Design**

Twenty-two participants (15 males and 7 females) participated in the experiment, with an average age of 38 years. Two had to be discarded due to motion sickness issues. Of the twenty remaining subjects, ten started with the no motion condition (Group 1 of Table 2) while the other ten participants started with the motion feedback condition (Group 2 of Table 2).

Starting in the second run, a paired comparison technique was used to test if the condition with motion feedback is preferred to the no motion condition. Subjects had to compare the current run with the previous run in terms of overall impression of realism by forcing them to say which condition they preferred.

After each run, subjects had to fill in a questionnaire that dealt with the following topics: immersion in the simulator task, controllability of the car, slalom performance, simulation realism, motion realism and training value.

In the questionnaire we used a list of statements on which subjects had to agree or disagree using a 7 point Likert scale. See Figure 4. Figure 5 shows in which order the experiment was conducted.



#### **Objective measures**

The objective measures used in this study were the car average speed and the lateral specific forces generated by the car model. From these measures it is possible to draw conclusions about the subjects' driving behaviour. In our study, we assume that differences in driving behaviour show up as differences in measurable car variables such as car speed, car specific forces and driving trajectory. In addition, we observed that the number of accidents occurring was different for both motion conditions, so these results were also reported. Note that in all conditions, the only difference was the motion feedback while all other simulator characteristics such as steering wheel dynamics and visual scene were kept equal.

#### **Results**

#### Paired comparison

Subjects indicated the overall impression between two motion conditions three times during the experiment. They compared the first run with the second, the second run with the third and the third run with the last one. Figure 6 shows the total scores for each of the comparisons. Like stated in Grant et al. [8], the score is the number of times that a condition was preferred over the other. A chi-square test was used to check the significance of the paired comparison analysis. In the first comparison (1 vs 2 in Figure 6) there was not a significant effect of the motion condition in the subject's overall impression,  $\chi^2(1)=3.2$ , p=0.074. For the second and third comparisons it was found a significant effect of the motion condition at the 5% level, respectively  $\chi^2(1)=5$ , p=0.025 and  $\chi^2(1)=9.8$ , p=0.02. When the scores of the paired comparison are accumulated, the result is a total score of 46 for the Motion condition and a total score of 14 for the No Motion condition. In this case there is a significant effect of the motion condition at the 1% level,  $\chi^2(1)=17.067$ , p<0.001.

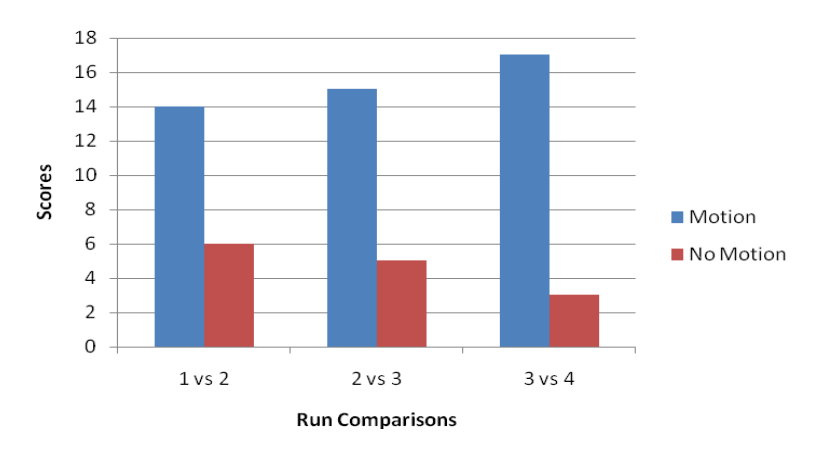


Figure 6 - Paired comparison total scores for each run.

#### **Questionnaires**

From this section on, we will define Trial 1 as run one and two and Trial 2 as run three and four. This is done to show the difference between the first time a motion condition was driven and its repetition. The questionnaire used in this experiment contained 26 statements, where subjects had to indicate whether they agreed or not with the statement. Because of time issues only four statements were analysed. The statements are:

- "The motions and forces helped me conducting the task".
- "The simulator motion and forces felt realistic".
- "I sometimes had the feeling of losing control over the car".
- "I was really focused".

The choice of these statements is related with the experiment hypothesis since they show how motion feedback can influence driving behaviour in terms of task performance, realism, control and concentration. Note that the original statements were in Dutch, which means that part of the meaning can be lost in translation.

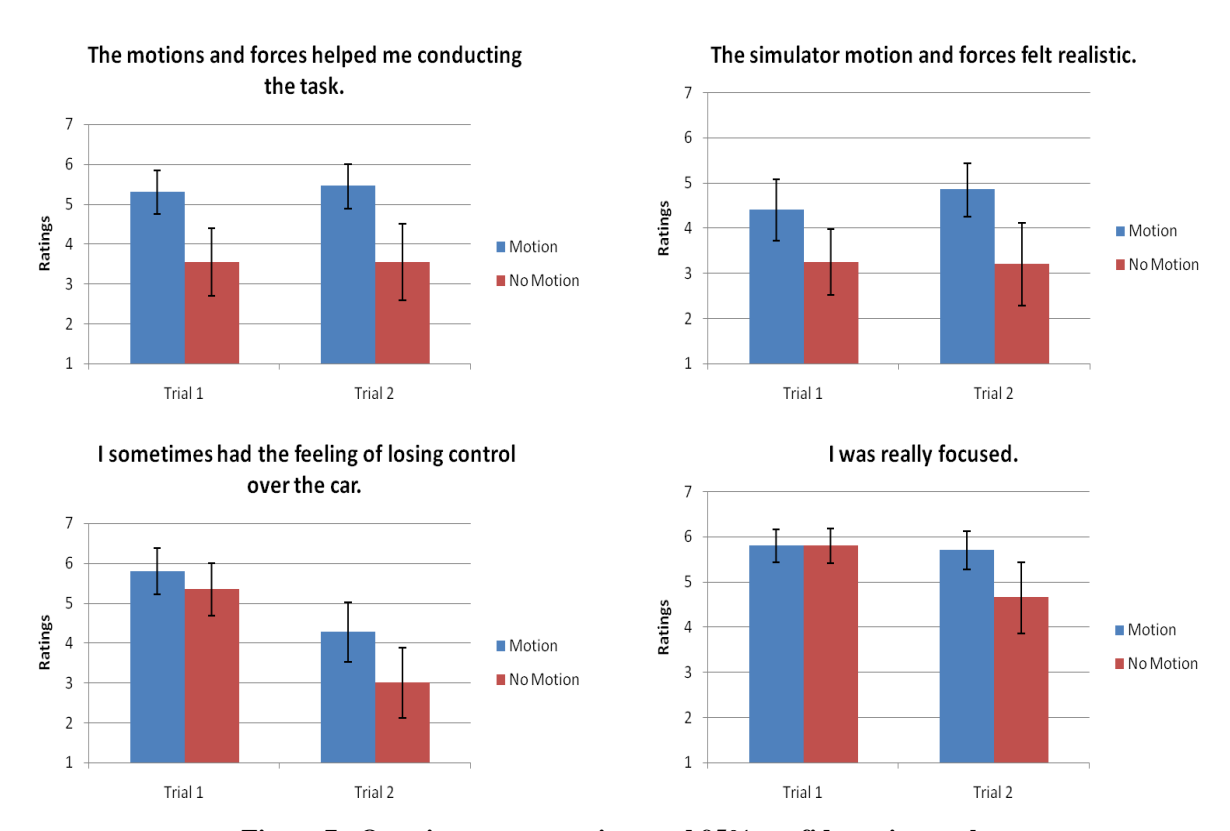


Figure 7 - Question average ratings and 95% confidence intervals.

Figure 7 shows the subject's ratings for the four chosen statements. A repeated measure ANOVA with contrasts focusing on the differences between the two independent variables (motion condition and Trial number) was performed. For the statement, "The motions and forces helped me conducting the task" there was a significant main effect of the motion condition on questionnaire ratings, F(1,19) = 13.589, p = 0.002. Contrasts revealed that the effect of the motion condition in the subject ratings was significant for Trial 1, F(1,19) =9.404, p = 0.006 and for Trial 2, F(1,19) = 14.625, p = 0.001. The statement, "The simulator motion and forces felt realistic" also showed a significant main effect of the motion condition on questionnaire ratings, F(1,19) = 11.406, p = 0.003. Contrasts showed significant effects of the motion condition in the subjects ratings for Trial 1, F(1,19) = 5.550, p = 0.029 and for Trial 2, F(1,19) = 10.715, p = 0.004. For the statement, "I sometimes had the feeling of losing control over the car" there was a significant main effect of the motion condition on questionnaire ratings, F(1,19) = 7.452, p = 0.013. There was also a significant main effect of the trial number on the questionnaire ratings, F(1,19) = 30.523, p < 0.001. Contrasts showed a significant effect of the motion condition on the subjects ratings for Trial 2, F(1,19) = 4.952, p = 0.038, but not for Trial 1. In the statement "I was really focused" there was a significant main effect of the motion condition on questionnaire ratings, F(1,19) = 7.356, p = 0.014. There was also a significant effect of the trial number on the questionnaire ratings, F(1,19) =12.435, p = 0.002. There was a significant interaction between the motion condition and the run number, F(1,19) = 6.450, p = 0.020. Contrasts revealed a significant effects of the motion condition in the subjects rating for Trial 1, F(1,19) = 7.912, p = 0.011, but not for Trial 1.

#### **Objective Measurements**

#### Number of sections finished

In the experiment the slalom got increasingly more difficult with each section (see Table 1). The runs were again divided in two groups (Trial 1 and Trial 2), to show the difference between the first time a motion condition was driven and its repetition. For Trial 1, thirteen subjects out of twenty were able to drive through the nine slalom sections without crashing the car in the Motion condition. For the No Motion condition only nine subjects out of twenty were able to drive the slalom without crashing. For Trial 2, sixteen out of twenty subjects finished the full slalom for the Motion condition while for the No Motion condition fifteen out of twenty subjects were able to finish the slalom. Table 3 shows in which pylon section accidents occurred.

Dylon section	Т	rial 1	Trial 2		
Pylon section	Motion	No Motion	Motion	No Motion	
1	0	0	0	0	
2	0	0	0	0	
3	0	0	0	0	
4	0	0	0	1	
5	0	0	0	0	
6	1	2	1	0	
7	2	5	1	1	
8	4	1	1	3	
9	0	3	1	0	

Table 3 - Number of accidents in each section.

#### Average speed

The average speeds were analysed to check differences in driving strategy between the two motion conditions. Figure 8 shows the mean car speed and the 95% confidence intervals for the nine pylon sections. From Figure 8 one can observe that the average speed decreases with the pylon sections, since they got increasingly difficult. The Motion condition average speeds are slightly smaller than the No Motion condition average speeds.

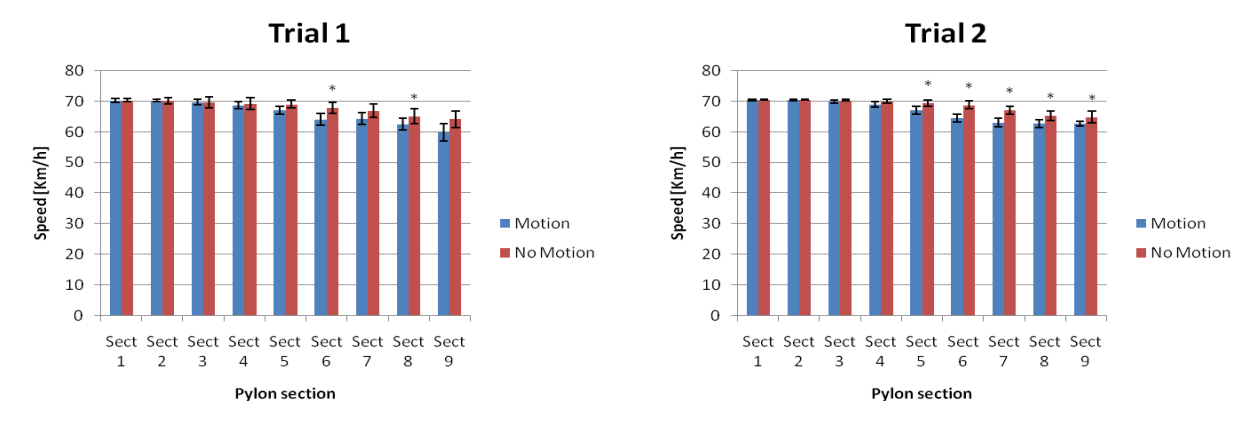


Figure 8 - Average car speed and 95% confidence interval for all pylon sections in Trial 1 and 2.

Significant differences between motion conditions for the average car speed were found from section 5 to section 9. The available data decreases with the section number because of the occurred accidents. Since we are only interested in the differences between Motion and No Motion for Trial 1 and 2, a dependent t-test will be used in the analysis instead of a repeated measure ANOVA. Note that the results for Trial 2 will have more statistical power than the ones of Trial 1 since there were fewer accidents in the last runs. Table 4 shows the results of the dependent t-test. Significant effects (at the 5% level) of the motion condition in the car average speed were found for the highlighted rows in Table 4, and indicated by asterisks (\*) in Figure 8.

Section		ΜΔ	SE	t	p
5	Trial1	-2.017	0.981	t(19) = -2.056	0.054
	Trial 2	-2.101	0.712	t(18) = -2.949	0.009
6	Trial1	-3.522	1.579	t(17) = -2.230	0.039
	Trial 2	-4.179	0.952	t(18) = -4.391	0.000
7	Trial1	-2.513	1.983	t(14) = -1.267	0.226
	Trial 2	-3.808	0.757	t(17) = -5.030	0.000
8	Trial1	-4.947	2.148	t(10) = -2.303	0.044
	Trial 2	-2.851	1.170	t(14) = -2.437	0.029
9	Trial1	-5.713	3.409	t(6) = -1.676	0.145
	Trial 2	-2.577	1.114	t(11) = -2.313	0.041

Table 4 - Mean difference, standard error, t-test score and significance of the car speed for the last 5 pylon sections.

#### Car model specific forces

Figure 9 shows the average specific force generated by the car model. The average was calculated using all the participants in all the four runs

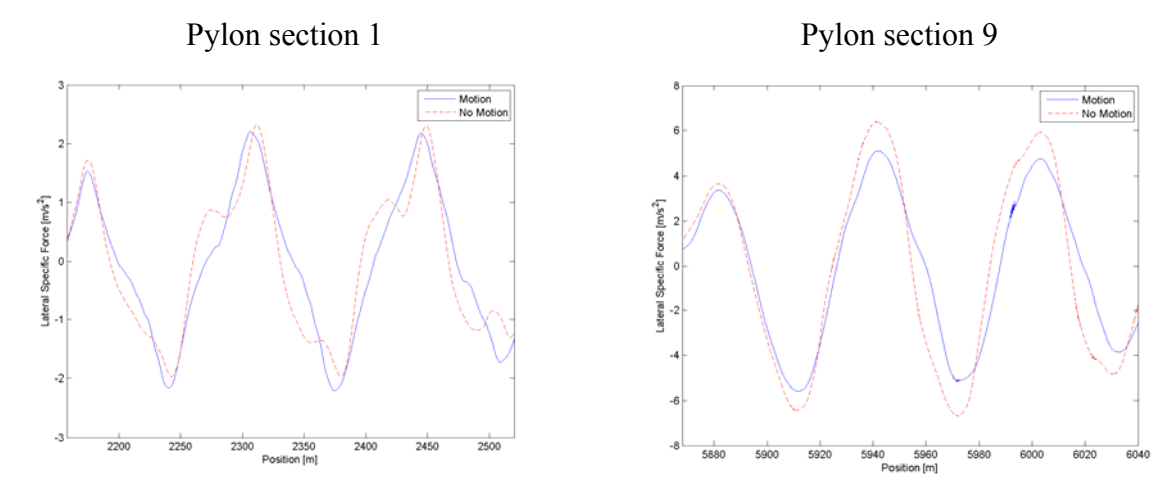


Figure 9 - Car model average specific forces for pylon section 1 (on the left) and pylon section 9 (on the right). The averages are calculated using all the participants in all runs.

#### **Discussion**

Motion feedback has been used in flight simulation for many years. It has been shown that this feedback has beneficial effects on pilot performance [9]. In driving simulation, visual feedback is assumed to be the primary source of information [10], nevertheless several studies that assess the effect of motion in a driving task have already been performed [11,12]. In this study, we also want to investigate the effect of motion feedback, but this time in advanced driving manoeuvres.

The condition with motion was much more preferred by the subjects than the condition with no motion. From the 14 subjects that rated the Motion condition the best when the first run was compared with the second run, only one subject changed its opinion in the other comparisons (rated No Motion better when comparing the second run with the third run). It can also be seen that with progression of the experiment, the No Motion condition was rated best fewer times (Figure 6). At the end of the experiment, the difference between the two motion conditions was highly significant as one can see from the paired comparison results. This means that for advanced manoeuvres like this slalom, subjects prefer to have a simulation with motion feedback, rather than a fixed based simulator. Some of the participants commented that it was much easier to "catch up with the cadence" (the sinusoid) of the slalom when motion was present.

Motion seems also necessary to help subjects conducting the driving task better as can be seen from the questionnaire results. The participants agreed that motion helped them in the driving since the average rating for the statement "The motions and forces helped me conducting the task" in the Motion condition was 5.30 for Trial 1 and 5.45 for Trial 2. Regarding how realistic the motion was, it can be seen that subjects in the Motion condition were undecided whether what they were feeling was realistic or not (the ratings for this statement were 4.4 for Trial 1 and 4.85 for Trial 2). This had to do mainly with control differences of their car and the used car model (some subjects did not have power steering in their car for example) and also because the used manoeuvre was not comparable with the type of manoeuvres they normally do in their car. For the No Motion condition, subjects rated it unrealistic (3.25 in Trial 1 and 3.20 in Trial 2) even though that some of them believed that simulator movements were present in this condition. This phenomenon of reporting the presence of motion in a no-motion condition was already reported by Wentink et al. [5]

Motion feedback changes driving behaviour as one can see from the average speed differences between the two motion conditions. Subjects had a lower average speed in the Motion condition compared to the No Motion condition. This means that with motion feedback, in the harder pylons sections (which is where this difference is noticeable) subjects are more aware of how the car is reacting and drive it more carefully to prevent a crash. Figure 9 shows that in the earlier pylon sections (section 1 in this case) the car model specific forces are very similar, which indicates that the driving behaviour of subjects in both motion conditions is the same. This is no longer true in the fastest sections (section 9 in Figure 9) where the car model specific forces have different amplitudes. The Motion condition has smaller force amplitudes than the No Motion condition since subjects have feedback about the magnitude of the specific forces and try to drive with smaller lateral forces. Nevertheless this data has to be analysed in more detail to draw more conclusions about how subjects drove the slalom manoeuvre.

Motion feedback has an effect on driver performance and driving behaviour, especially on the fastest sections of the slalom. This means that drivers adopt different strategies when they are feed with extra sensorial information (motion cues in this case). In flight simulation, it was already shown that motion feedback has a beneficial influence on pilot control performance [9]. A similar effect seems to be present in extreme driving simulation. This has consequences in training, since advanced driving training is still mainly performed with fixed based simulators [3]. Research using driver-on-the-loop would also be affected if a fixed based simulator is used whenever extreme manoeuvres are present. This could happen in road safety research or research that explores driving disturbances, since advanced driving manoeuvres are normally required to overcome difficult driving situations. Therefore, if motion is not present, drivers are losing important information that ultimately would make them react to the situation in a totally different way.

#### **Conclusions**

This experiment showed that it is important to have motion feedback in the simulation of advanced driving manoeuvres. From the results we see that subjects much prefer the condition with motion feedback and that motion supports them in conducting the task better. In the fixed base condition, the participants had difficulties to keep the control over the car and therefore the number of crashes was higher. Motion feedback also influences driving behaviour as can be concluded from the differences in the car average velocity for both motion conditions. With motion feedback, subjects drove more carefully and had better control of the car; therefore they could anticipate on the car dynamic behaviour better and were not that surprised when the car did crash.

Motion feedback is desirable in this type of manoeuvres since it helps drivers in their driving task. With motion it was easier for subjects to catch up the correct sinusoidal path of the slalom as well as to predict when control actions were needed. It also helped to reduce the accident rate since participants had a better control approach due to the extra feedback that motion produces. With motion, subjects also identified situations of under- and oversteer better and some of them were able to recover without crashing the car. Without motion, subjects failed to identify these events, making accidents an unexpected occurrence.

Further analysis of other objective measurements like the steering wheel angle and the specific forces has to be done in order to draw more conclusions about the driving control behaviour differences. Future experiments should focus on investigating the most important cues for driver control in advanced driving manoeuvres, since from this experiment one can conclude that motion feedback is very important in these types of manoeuvres.

#### Acknowledgements

This work was conducted in the framework of the MOVES (Motion cueing for Vehicle Simulators) Eureka #3601 European research project, which aims at increasing the scientific knowledge on the human multi-sensory perception of motion in virtual environments, and to explicitly define the possibilities and limitations of several high-end European driving simulators. The MOVES consortium is composed of LPPA/CNRS, Renault, TNO Human Factors, MPI-Biological Cybernetics, AMST, and collaborates with DLR and SIMTEC.

#### References

- [1] Grant, P. R. & Reid, L. D., "Motion Washout Filter Tuning: Rules and Requirements", *Journal of Aircraft*, **1997**, *34*, 145-151
- [2] Milliken, W. & Milliken, D., "Race Car Vehicle Dynamics", SAE International, Warrendale, PA., 1995
- [3] Kappé, B. & van Emmerik, M. Mogelijkheden van rijsimulatoren in de rijopleiding en het rijexamen TNO Defence, Security and Safety, **2005**
- [4] Feenstra, P.; Wentink, M.; Correia Grácio, B. J. & Bles, W. "Effect of Simulator Motion Space on Realism in the Desdemona Simulator" DSC 2009 Europe, **2009** (presented in this conference)
- [5] Wentink, M.; Valente Pais, A. R.; Mayrhofer, M.; Feenstra, P. & Bles, W., "First Curve Driving Experiments in the Desdemona Simulator", *DSC 2008 Europe*, **2008**, 135-146
- [6] Conrad, B.; Schmidt, S. F. & Douvillier, J. G. "Washout circuit design for multi-degrees-of-freedom moving base simulators." *Visual and Motion Simulation Conference, AIAA*, **1973**
- [7] Reid, L. D. & Nahon, M. A. "Flight simulation motion-base drive algorithms: part 1 developing and testing the equations", Institute for Aerospace Studies, University of Toronto, 1985
- [8] Grant, P. R.; Blommer, M.; Cathey, L.; Artz, B. & Greenberg, J. "Analyzing Classes of Motion Drive Algorithms Based on Paired Comparison Techniques", DSC North America 2003 Proceedings, **2003**
- [9] Hosman, R.J.A.W. "Pilot's perception and control of aircraft motions", Ph.D. Thesis, Faculty of Aerospace Engineering, Delft University of Technology, **1996**
- [10] Kemeny, A. & Panerai, F. "Evaluating perception in driving simulation experiments" TRENDS in Cognitive Sciences, **2003**, 7, 37-37
- [11] Fortmüller, T.; Tomaske, W. & Meywerk, M. "The Influence of Sway Accelerations on the Perception of Yaw Movements" DSC 2008 Europe, **2008**
- [12] Brünger-Koch, M.; Briest, S. & Vollrath, M. "Do you feel the difference? A motion assessment study" Driving Simulation Conference Asia/Pacific, **2006**

## Part III

## DSC Europe 2009 paper Effect of Simulator Motion Space on Realism in the Desdemona Simulator

# EFFECT OF SIMULATOR MOTION SPACE ON REALISM IN THE DESDEMONA SIMULATOR

Philippus Feenstra, Mark Wentink, Bruno Correia Grácio and Wim Bles

TNO Defence, Security and Safety
Human Factors
3769 ZG Soesterberg
Netherlands
philippus.feenstra @tno.nl

## **Abstract**

The goal of this study was to assess the effect of an increasing motion space on the fidelity of driving simulation in the Desdemona research simulator. The experimental task was a standardized slalom maneuver where the car velocity was limited to 70 km/h.

Subjective measures, which included eight statements on realism and task performance were used to assess simulation fidelity. The slalom task was driven in four conditions: 1) one-to-one motion space, 2) 0.7 times the motion space, 3) 0.4 times the motion space, and 4) no-motion. The conditions were compared pair-wise. In total 16 participants completed the experiment. Compared to the no-motion condition, driving a slalom maneuver in Desdemona was judged more realistic when motion cues were available, where the magnitude of the motion, within the range of 0.4 to 1, has less to no effect on the realism compared to the issue of motion versus no-motion. Furthermore, the participants indicated that motion and forces actuated by Desdemona helped to conduct their task better.

## Introduction

The goal of this study was to assess the effect of an increasing motion space on the fidelity of driving simulation in the Desdemona simulator. Subjective variables, e.g. realism, and the objective driver performance were used as measures of simulation fidelity. The subjective measures are described in this paper. A standardized slalom maneuver is simulated while varying the simulator motion space across conditions, ranging from no-motion to one-to-one motion.

In flight simulation it has been shown that motion has a beneficial effect on pilot performance, especially in high-gain control tasks where the pilot has to stabilize the aircraft during (atmospheric) disturbances [Hosman 1996, Pool 2007]. In those conditions, the inertial motion perceived by the equilibrium system provides phase-lead over the motion information perceived by the visual system (i.e. the information is faster). In addition, the delay time in the vestibular pathway is shorter than the delay in the visual pathway. Already in the 1960's, McRuer showed that phase-lead from motion feedback improves control performance [McRuer et al., 1965, 1967, Weir & McRuer 1968]. Over the years, the motion cueing systems of full flight simulators were more or less optimized to render disturbance motion correctly in order to achieve comparable pilot behavior in the simulator.

Although it is generally assumed that visual feedback is the primary source of information when driving a car [Kemeny & Panerai, 2003], motion feedback will most probably help the driver to stabilize the car and to keep it on track. It is hypothesized that the role of motion in driving simulation is equivalent to that in flight simulation, and that the addition of motion in demanding, simulated driving tasks improves control performance and realism. Since driving simulators are far from standardized, the question that arises is: how much simulator motion and what type of motion platform and cueing logic is required to provide realistic motion feedback.

Among others, [Groen et al., 2001] found in their study that the simulator motion was perceived as too strong when in fact the motion was already scaled-down and filtered. Therefore, it is expected to find the best driver performance and the highest degree of realism in a scaled motion space condition, and the worst results in the no-motion condition.

The work described in this paper is carried out in the framework of the MOVES (MOtion cueing for VEhicle Simulators) Eureka project. One of the main purposes of the project is to evaluate and compare simulation fidelity of different driving simulators. Driving simulators involved are KUKA (Max Planck Institute), Ultimate (Renault), CarSim (DLR) and Desdemona (TNO, AMST). A comparable experiment on driver performance in a standard slalom maneuver was carried out on each of these simulators. In addition to the study described in this paper, an extended slalom driving experiment was performed. This addition addresses Advanced Driving Simulation that involved faster slalom maneuvers and higher accelerations and forces [Correia Grácio et al., 2009].

## Method

## **Apparatus**

The Desdemona simulator (Figure 1) was utilized for the slalom experiment. Desdemona is a moving-base research-simulator located at TNO (Soesterberg, The Netherlands) that was designed with a special focus on spatial disorientation demonstrations, flight simulation, and driving simulation. It was built in close co-operation with AMST (Ranshofen, Austria). The simulator has 6 Degrees of Freedom (DoF). The cabin is mounted in a gimbaled system (3 DoF,  $>2\pi$  radians), which as a whole can move vertically along a heave axis (1 DoF,  $\pm 1$ m) and horizontally along a linear arm (1 DoF,  $\pm 4$ m). This structure can as a whole rotate around a central axis to facilitate centrifugal motion (1 DoF,  $\leq 3$ G). For the experiment, the Desdemona cabin was equipped with a generic car cockpit. The cockpit contains force-feedback on steering wheel, and on gas and brake pedals. Direct drive electrical motors generate the control loading for the steering wheel and pedals. The out-the-window visuals have a width of 120x40 degrees visual angle.



Figure 1 The Desdemona Research simulator

The vehicle dynamics were calculated by a Carsim vehicle model (Ann Arbor, MI, USA) and were comparable with the dynamics of a Volkswagen Passat with automatic gear shift. In the experiment, the velocity was limited to 70 km/h. The vehicle model ran in a Matlab-Simulink thread using shared memory [Hogema et al., 2004].

The motion cueing filter ran in a separate Matlab-Simulink thread as well. Figure 2 shows the global structure of the applied filter. The lateral position – and thereby the lateral acceleration – of the vehicle was cued by the 8 m linear arm. The width of the road is 6m, which enables the possibility to cue one-to-one. Pilot tests showed that participants were able to drive the

slalom trail with the maximum velocity of 70 km/h. Therefore, the longitudinal force was not cued. The roll and pitch vehicle motions were cued directly by the corresponding Desdemona gimbals. The paths only contain a scaling gain and a limiter block. The car heading was cued by two degrees of freedom, i.e., the high frequencies were cued by the cabin yaw and the remaining low frequencies were cued by the central yaw. The lateral cues by the linear arm remain in the proper direction when only high frequencies are actuated by the cabin yaw. The high and low pass filters were complementary, i.e., the output of the two filters add up to 1 such that the total heading is also cued directly. Finally, a velocity depending road rumble and a stimulus when hitting a pylon were applied by the heave axis. Note that the filter does not contain tilt coordination. A previous experiment on curve driving [Wentink et al., 2008] suggested that false cues were receiving more attention than correct cues. Tilt coordination or rather the washout associated with tilt coordination is an example of a false cue, which could disturb the judgment of a condition.

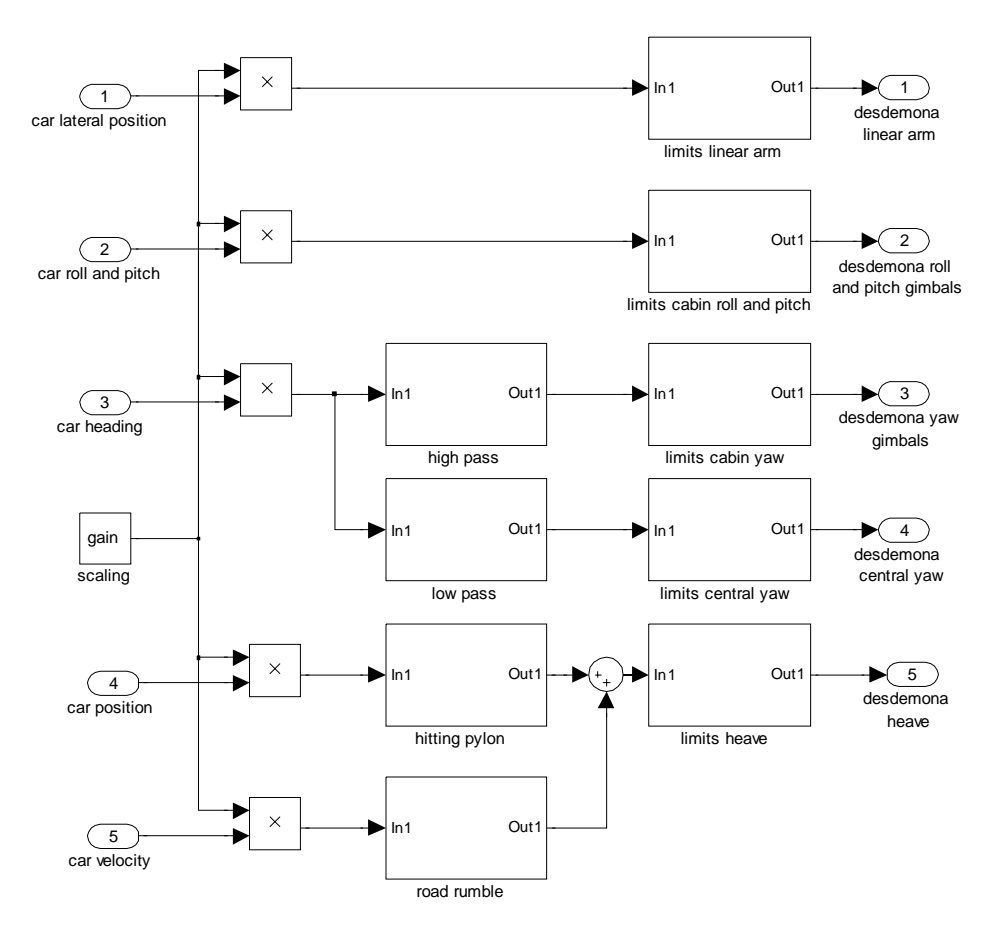


Figure 2 Global structure of the applied motion cueing filter

## Scenario and conditions

The experiment took place at a two-lane rural road (Figure 3). The lane width was (3 m). Guardrails were placed at both sides of the road. During the experiment, the participants had to drive multiple times the slalom trail that was indicated by the pylons. The pylons were alternately placed at 0.5 m to the right and left of the road centerline. Within each trail, the distance between the first nine pylons was 62.5 m and the distance between the last three

pylons was 50 m. The change of the spatial frequency in a slalom prevents that the driver can drive the whole slalom with the same cadence.

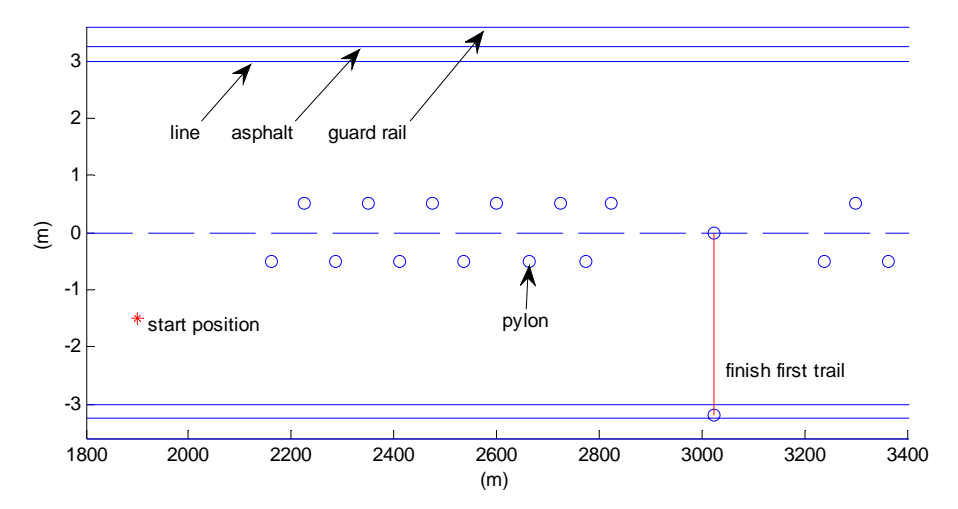


Figure 3 The road geometry (the axes are not scaled)

In total four gain settings (conditions) of the motion cueing filter (Figure 2) were compared. The gains were 0 for no-motion and 0.4, 0.7 and 1 for motion. In terms of lateral displacement, the motion space used was 0, <2.8, <4.2 and <6 m, respectively. Twelve different pairs can be composed out of four conditions. These 12 pairs were assigned to two sets such that per set all gains were compared (but not in all orders). One group of participants tested set 1 and the second group of participants tested set 2. In one run, one pair was driven, i.e., one gain setting for the first trail and another gain setting for the second trail. Each participant compared six pairs in six runs in a randomized order.

#### Participants, procedures and data registration

Sixteen participants (4 female and 12 male) completed the experiment. Two participants did not finish the experiment due to motion sickness. They were all TNO employees and not professional drivers. The average age was 36 (s.d. – standard deviation – 10) years, the average mileage per year was 14281 (s.d. 9252) km and the average driving simulator experience was 28 (s.d. 65) hours.

After arrival, the participant was briefed about the experiment. The goal was to complete a run in the lowest possible time. That was, to drive as fast as possible (maximum was 70 km/h), without damaging the car. It was allowed to reduce the velocity when he/she expected to loose the control of the car. For example, when the car was going to leave the road or when they were hitting pylons. The experimenter answered questions that the participant might have. Subsequently, the participant signed an informed consent (stating that he/she was in good health, had understood the instructions and participated voluntarily).

To get used to the simulator and the car dynamics, the experiment started with a practice slalom run (gain 0.5 with a rather similar filter). Next the real runs started. A pylon at the right side of the road indicated the finish of a trail (Figure 3).

Both objective and subjective data was collected during the experiment. The objective data included the position, velocities, accelerations and the control inputs of the car. This paper

does not include the results of the objective data. The subjective data were collected by means of a questionnaire. After each trail, a questionnaire with 8 statements and a misery-score was filled-out. Regarding the statements, so-called *constructs* have been used [Field, 2005]. Variables that cannot be measured directly like realism are called constructs. Firstly one has to determine which observable 'variables' can be measured that represent the construct. Therefore, different statements have been used that have an association with one construct, for example realism. The validation of the constructs is not covered in this paper. The participants had to agree or disagree with the statements using a 7-point Likert scale (Figure 4). The misery score is a 6-point scale, ranging from 'feeling OK, no symptoms' to 'vomiting'. After each pair, the participant did a pair-wise comparison, that is, the participant indicated which of the two trails was the most realistic. Finally, at the end of the total run the participant could give general comments.

Strongly Disagree	1	2	3	4	5	6	7	Strongly Agree
Strongly Bisagree	1	_	J		-	0	,	Subligity rigide

Figure 4 The 7-point Likert scale to judge the statements

## **Results**

## Pair-wise comparison

After each pair, the participant was asked to indicate which of the two trails he found the most realistic. Figure 5 shows the result for the four gain settings. The value at the vertical axis indicates the number of times the particular gain setting was preferred. The sum of all preferences is 96, which corresponds to 16 participants times 6 pairs.

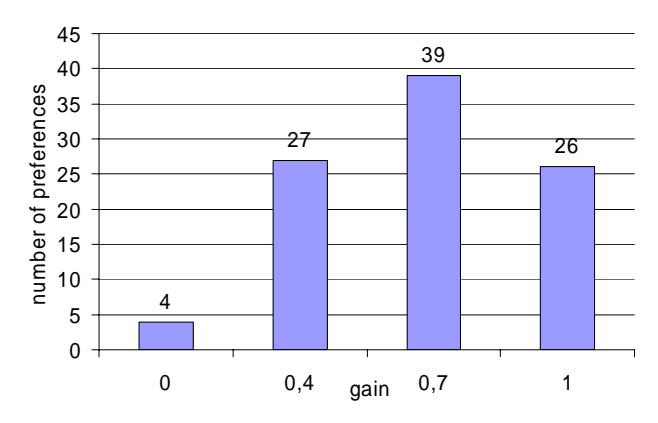


Figure 5 Result of a pair-wise comparison on realism between 4 different gain settings

A significant effect was found by comparing all four gains in one Chi-square test ( $\chi^2$ = 26.58, df = 3, p < 0.01). This implies that a difference was found in realism between the different gain settings. In order to differentiate between the gain settings, 6 separate (6 combinations) Chi-square tests were done. Consequently the significance level reduces according to the Bonferroni correction, i.e. there is a difference between two setting when p < 0.05/6 = p < 0.008. Table 1 shows the results. It can be concluded that the gain setting 0 (no-motion) differs with the other 3 gains setting. The remaining gain settings are not found to be different.

Table 1 Pair-wise	comporison on	rooliem	botwoon the	A gain	cattings (	** - n < 0.01
Table I I all wise	Cumpai isun un	i i cansin	netween the	→ gam	scungs (	- h<0.01)

Compared gains	$\chi^2$	df	p	significance
0 and 0.4	17.06	1	0.000036	**
0 and 0.7	28.49	1	0.000000	**
0 and 1	16.13	1	0.000059	**
0.4 and 0.7	2.18	1	0.139650	-
0.4 and 1	0.02	1	0.890746	-
0.7 and 1	2.60	1	0.106865	-

#### **Statements**

After each trail, a questionnaire with 8 statements was filled-out. Each participant rated the 4 gain settings 3 times (6 pairs/4 gains = 12 trails/4 gains). The 4 gain settings, 8 statements and 4 repetitions where tested in a repeated measures ANOVA. No effect for the repetitions was found for the statements; therefore the influence of the repetition was left out of the analysis. Figure 6 shows the mean scores for the statement for each gain setting. A post-hoc Tukey HSD test showed a significant effect between gain 0 and the other gains for the statements. This implies that slalom driving with motion was experienced as more realistic and helped the participants by conducting their task better as compared to the no-motion condition. In this experiment, no statistical significant differences in realism and conducting the task were found between the gain settings 0.4, 0.7 and 1, except for the utmost right statement in Figure 6. A significant effect (p<0.05) was found between gain 0.4 and gain 0.7. The forces for gain-setting 0.7 were found to be more realistic compared to gain setting 0.4. A trend or a marginal effect (p<0.1) was found for the statement that 'motion and forces helped conducting the task' between gain setting 0.4 and 0.7.

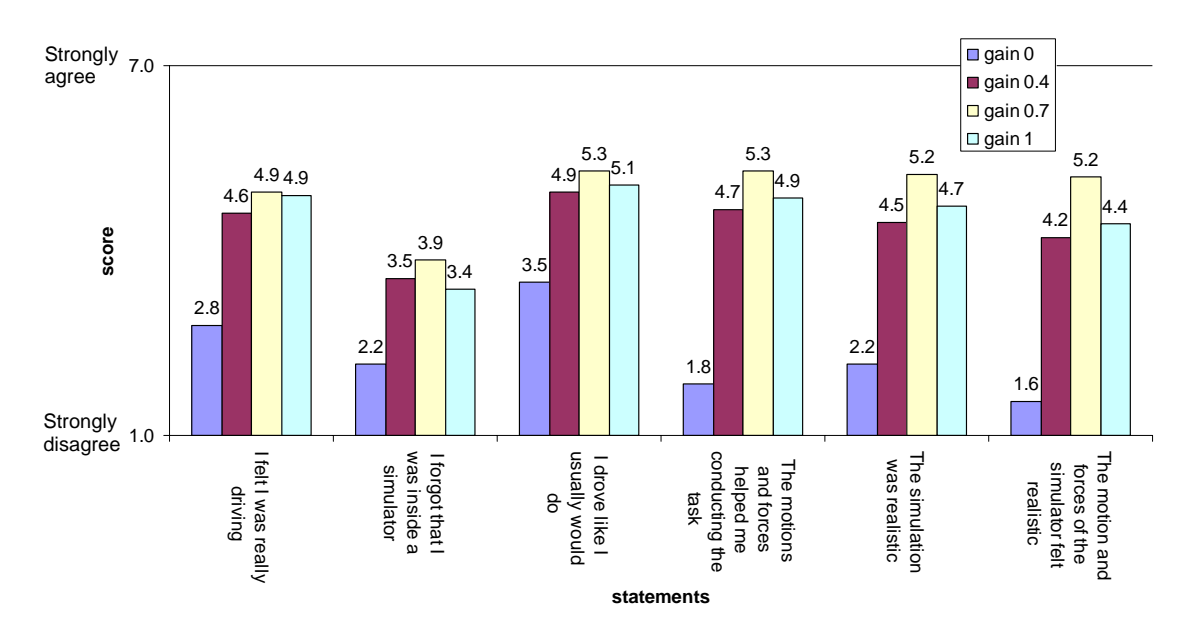


Figure 6 The mean scores for 6 statements

The overall result is in line with the pair-wise comparison. Although, for both the pair-wise comparison (Figure 5) and the statements (Figure 6), a visual inspection indicates a slight preference for a gain setting of 0.7.

## **Misery Score**

After each trail, the participant indicated the MISC (misery score). The mean MISC was 1.35 (for the 16 participants that completed all runs). The mean value was between 'feeling OK, no symptoms' and 'initial symptoms, such as stomach awareness, but no nausea'.

The MISC was analyzed with an ANOVA and a post-hoc Tukey test. The sequence of gain settings were randomized among the participants and the time-constant of misery is relatively low compared to the duration of a trail. Therefore, no effect was found for the Misery Score as a function of the gain settings.

For the repetition, a significant effect (p<0.01) for the MISC was found between repetition 2 and 3 (for all conditions together). Hence, during the experiment the MISC changed from 1 (feeling OK) to 2 (initial symptoms).

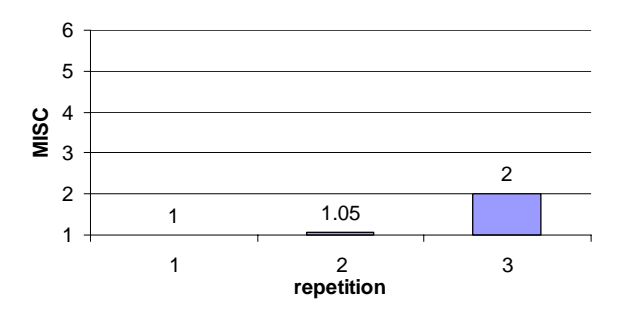


Figure 7 The (misery score) MISC as a function of the repetition

## **Discussion**

The participants had rather limited to no experience with real slalom driving. However, one can assume that they have driven similar kind of maneuvers, such as sudden lane changes and driving a roundabout with a relative high velocity. Comparable lateral forces and roll rates are present in these maneuvers. This indicates that the participants were able to differentiate between the conditions.

Compared to the no-motion condition, the analysis showed that driving a slalom trail has been judged more realistic when motion cues were available. The pair-wise comparison and the statements showed this. It also appeared that the magnitude of this motion, within the range of 0.4 to 1, is less important compared to issue of motion versus no-motion. Only for one statement a distinction between motion gain 0.4 and 0.7 was found, where a motion gain of 0.7 was found to be more realistic. As mentioned earlier, the cueing filter did not provide false cues due to washout effects associated with tilt coordination. In a previous experiment concerning curve driving [Wentink et al., 2008], the participants criticized false cues, which influenced the judgment between no-motion and motion. The participants did not mention false cues in the present experiment. Consequently, absence of washout is likely to be a reason for the clear distinction between the motion and no-motion conditions.

The experiment described in this paper applied a road rumble that was scaled with the gain setting. This implies no road rumble for the gain 0 condition and maximal road rumble in the

one-to-one motion condition. The effect of road rumble is important for driving immersion. Therefore, the absence of road rumble in no-motion condition has influenced the results.

It was found that the motion and forces actuated by Desdemona helped the participants to conduct their task better. This is a first result regarding the effect of motion on driver performance. Motion feedback will most probably help the driver to stabilize the car and to keep it on track. It is hypothesized that the role of motion in driving simulation is equivalent to that in flight simulation, and that the addition of motion in demanding, simulated driving tasks improves control performance. In ongoing work, we will verify this hypothesis by analyzing the objective data.

Finally, no effect has been found for the Misery Score as a function of the gain settings because the 'time-constant of misery' is relatively low compared to the duration of a trail. Only a slight increase of the Misery Score over time was found.

## **Conclusions**

The present study showed the following results:

- 1) Compared to the no-motion condition, driving a slalom trail in Desdemona has been judged more realistic when motion cues were available, where the magnitude of the motion, within the range of 0.4 to 1, has less effect on the realism compared to issue of motion versus no-motion.
- 2) The participants indicated that motion and forces actuated by Desdemona helped to conduct their task better. An analysis of the objective data will be performed to strengthen this conclusion.

## Acknowledgements

This work was conducted in the framework of the MOVES (Motion cueing for Vehicle Simulators) Eureka #3601 European research project, which aims at increasing the scientific knowledge on the human multi-sensory perception of motion in virtual environments, and to explicitly define the possibilities and limitations of several high-end European driving simulators. The MOVES consortium is composed of LPPA/CNRS, Renault, TNO Human Factors, MPI-Biological Cybernetics, AMST, and collaborates with DLR and SIMTEC. The standard slalom manoeuvre described here was designed in agreement with this consortium.

#### References

Correia Grácio, B., Wentink M., Feenstra, P., Mulder M., van Paassen M., Bles W. (2009). Motion feedback in advanced driving manoeuvres, *Driving Simulator Conference DSC*, Monaco, France (In this proceeding)

Hosman, R. (1996). *Pilot's perception and control of aircraft motions*. Ph.D. Thesis, Faculty of Aerospace Engineering, Delft University of Technology

Kemeny, A., Panerai, F. (2003). Evaluating perception in driving simulation experiments. *Trends in Cognitive Sciences*, 7(1) 31-37

Field, A. (2005), Discovering Statistics Using SPSS, Sage Publications Ltd

Groen, E. L.,, Clari, M. S. V. V., and Hosman, R. J. A. W. (2001). Evaluation of Perceived Motion During Simulated Takeoff Run, *AIAA Journal of Aircraft*, Vol. 38, No. 4, July-August, pp. 600-606.

Hogema, J.H., Hoekstra, W., & Stel, I. (2004). *On-line vehicle model coupling Driving Simulator - ADVANCE* (TNO Memorandum TNO DV3 2004-M 059). Soesterberg: TNO Defence, Security and Safety.

McRuer, D., Graham, D., Krendel, E., Reisener, Jr W. (1965). *Human pilot dynamics in compensatory systems*. Tech. Rep. AFFDL-TL-65-15, Systems Technology Inc. & The Franklin Institute

McRuer, D., Jex, H. (1967). *A review of quasi-linear pilot models*. IEEE Transactions on Human Factors in Electronics, Vol. HFE-8, No. 3, pp. 231-249
Pool, D., Mulder, M., Paassen, M. (2007). A review of the Hosman and Van der Vaart Tracking Experiment. *AIAA Modeling and Simulation Technologies Conference and Exhibit*, August, Hilton Head, USA

Weir, D., McRuer, D. (1968). A Theory for Driver Steering Control of Motor Vehicles. Highway Research Record, Vol. 247

Wentink, M., Pais, R., Mayrhofer, M., Feenstra, P., Bles, W. (2008). First curve driving experiments in the Desdemona simulator. *9th Driving Simulator Conference DSC*, January 2008, Monaco, France

# Part IV Preliminary Thesis

## Chapter 1

## Introduction

## 1-1 Background

Vehicle simulators are nowadays being used more and more as test and training platforms. For example, driving simulators can be used to test new car technologies, like navigation systems, active driving pedals, speed control mechanisms among others. Other examples of functions performed by vehicle simulators enclose pilot/driver training, vehicle research, human factors research and others.

Dynamic simulators introduce motion into the simulation, which has the objective of increasing the simulation fidelity. However, the motion cues generated by dynamic simulators are different from the ones of the vehicles that they are simulating. This has to do with the physical limitations (actuator maximal displacements, available motion space of the simulator, etc.) that a simulator has. Therefore, dynamic flight simulators need an algorithm that transforms vehicle motion into simulator motion. These algorithms are normally denominated by motion cueing algorithms, but we can also find them in the literature referred as washout filters, motion drive algorithms or motion filters.

Desdemona (Figure 1-1) is a new research simulator located at TNO Soesteberg. This simulator has 6 Degrees-of-Freedom (DoF's) and is based on a centrifuge design. The simulator was developed by AMST Systemtechnik in cooperation with TNO Human Factors. Desdemona can be used in the following research areas as can be found in Wentink et al. [Wentink et al., 2008a]: motion simulation and cueing, driving (simulation) research, flight (simulation) research, motion perception, mission simulation, space physiology and motion comfort.

In this study, Desdemona will be used as a racing simulator. Therefore, a new motion cueing algorithm that contains the motion cues necessary for a race driver needs to be developed. We believe that the unique motion capabilities of Desdemona will bring new opportunities in cueing extreme race manoeuvres, like understeer and oversteer situations. A motion cueing algorithm evaluation will have to be conducted to choose the algorithm that best suits the needs of a racing environment.

68 Introduction



Figure 1-1: Desdemona simulator.

## 1-2 Research Aims and Objectives

This study started with the need to develop a new racing simulation that takes advantage of Desdedemona motion capabilities. Such study created new questions and objectives that will take a part in this research, since one of the functions of this racing simulator will be to use it as a training tool for extreme manoeuvres, specially in curves. The following questions are used as guidelines in this research:

- How can a motion cueing algorithms be evaluated?
- How can motion cueing algorithm's performance be measured?
- Which motion cues are more important to have in a racing simulator?
- What motion cues trigger the drivers feeling of understeer or oversteer?

Therefore this research will try to accomplish the following objectives:

- Develop a protocol that helps choosing the best motion cueing algorithm for a certain situation.
- Identify the required motion cues for driving a race car in its limit.
- Develop a motion cueing algorithm for a racing simulation that can be used as an effective training tool.

The completion of these objectives would open new research opportunities in the domain of racing simulation and motion cueing algorithms development and assessment.

## 1-3 Research Methodology

This document encloses the first part of my Msc Thesis, containing a literature research and a preliminary analysis. The literature research had a main focus on how motion cueing algorithms were evaluated in other simulations. This research arose with the need to choose a motion cueing solution that best suits race driving specifications from different motion solutions that will be develop in this project. The bibliography used in this study was mainly composed by articles and conference papers of how researchers conducted assessment studies in theirs simulator. The main source came from the AIAA conferences and scientific articles and the Driving Simulation Conferences. A literature research in race driving was also performed to gain some insight in the physics of race driving, specially in driving in the traction limit. The preliminary analysis contains some motion cueing algorithm designs as well as some performance analysis using two different datasets.

The document is structured into six chapters. The first chapter corresponds to the introduction of this research. The second chapter contains a brief description of what is a motion cueing algorithm, giving a short explanation of the three most famous motion cueing algorithms (Classical Washout Algorithm, Coordinate Adaptive Algorithm and Optimal Control Algorithm). The third chapter encloses the literature research on motion cueing evaluation methods. Each evaluation method described in this section contains an extensive explanation of how the method was used for each study where it was found in the literature. The explanation includes the manoeuvres used in the assessment, the platforms where the study was made, how the data was presented to the reader and future suggestions made by the authors. The studies are organized in a chronological way in order to show the evolution of the each method. The fourth chapter contains a small description of the physics behind extreme driving manoeuvres found in the literature. Examples of some of these type of manoeuvres are understeer and oversteer. The fifth chapter has a description of the developed motion cueing solutions that will be used in Desdemona as well as preliminary results using the graphical comparison evaluation method. The last chapter contains the conclusions gathered in the first part of the Msc Thesis as well as guidelines for future work in the second part of the Thesis. This structure is shown in Figure 1-2.

70 Introduction

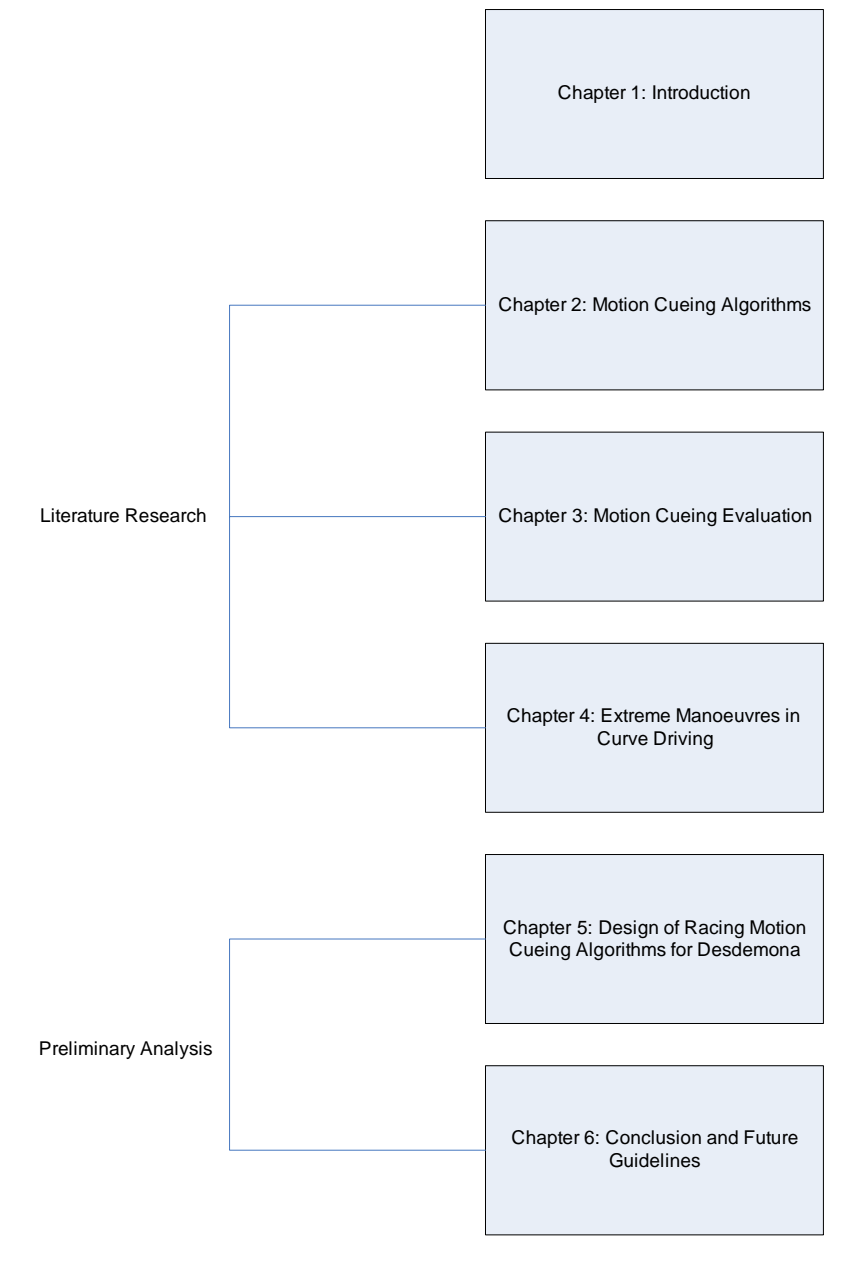


Figure 1-2: Document structure.

# Motion Cueing Algorithms

Inertial motion was introduced in flight simulators to improve the motion sensations of simulated flight. It was thought that pilots would use a more realistic flying control strategy in the presence of motion cues. According to Grant and Reid [Grant and Reid, 1997] a motion cue is "a signal generated by motion relative to inertial space which is sensed by the pilot and/or guides the pilot's behaviour". The existence of motion cues in simulators would decrease the perception gap existent between them and airplanes. Therefore, for the first time motion cues could be used by pilots in flight simulators. Gundry [Gundry, 1976] was one of the first investigators to study the beneficial effects of having motion in control tasks. Nevertheless the benefits of motion continues to be discussed today. Nowadays, not only flight simulators have motion, but also other type of simulators, like car and motorcycle simulators.

Baarspul [Baarspul, 1990] divided the existent cues in a simulator into Environmental cues and Equipment cues. Equipment cues are the ones that provide a duplication of the form and feeling of all the equipment present in the real vehicle. Environmental cues are the ones that provide the duplication of the environment. These can be divided in four groups:

- Alerting cues: cues sensed because of initial effects of disturbance motions, e.g. turbulence or engine failure.
- Onset cues: the initial cues instantaneously felt after a control command generated by the pilot/driver.
- Sustained cues: cues felt due to the long or quasi-static effects generated by the pilot/driver commands or by the disturbance motions.
- Transient cues: cues that occur between on-set and sustained cues.

Environmental cues are the cues that should be taken into account when designing a motion cueing algorithm.

A feature that is common to all the dynamic flight simulators is the motion cueing algorithm. These algorithms can also be designated by Washout filters since one of its properties is to

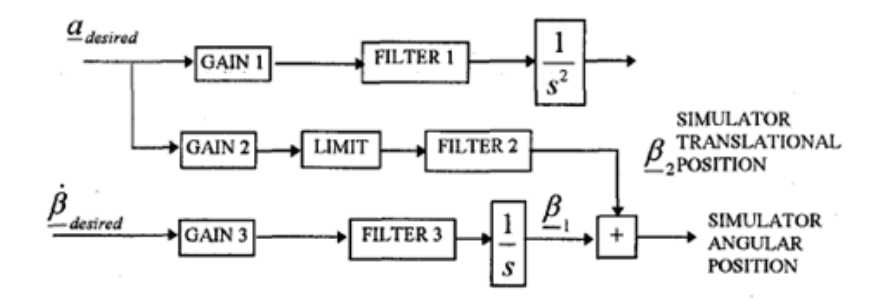


Figure 2-1: General structure of a motion cueing algorithm [Wu and Cardullo, 1997].

"washout" the simulator back to the neutral position. Neutral position is the position where the simulator cabin should return after each simulator movement. This position is defined by the designer and most of the times is at the centre of the motion system. The motion cueing algorithm transforms real vehicle motions into simulator motions. This is needed because all the simulators have a limited motion space, when compared to the one of the real vehicle. The major simulation problem has to do with the low frequency characteristic of the motion cues, which cause huge displacements, impossible to reproduce in a simulator. To counteract this, high pass filters are included in the washout algorithm, since they cancel the low frequency components of any signal that passes through them. These filters are used to simulate the onset cue of the motion bringing then the cabin back to neutral position without pilot's awareness. This ensures that the simulator remains within the motion envelope. These high pass filters are used to filter the translational and angular motions of the vehicle.

Because of the high pass filters used in the motion cueing algorithm, the low frequency component of the motion cues is lost. Therefore sustained cues are not present in the simulation. In order not to lose all the sustained cues in this process, tilting coordination is commonly used in simulators. Tilting coordination is a trick used in motion cueing algorithms to generate sustained specific forces without driving the simulator out of its limits. Total specific force applied on a vehicle is equal to the gravity plus an external specific force used to move the vehicle. The total specific force will then have a direction different than the one of the gravity vector. What tilting coordination does is to match the total specific force direction using the gravity vector. Therefore the pitch and roll angles of the simulator are used to orient the gravity vector in the same direction as the total force vector. Then the person in the simulator would feel the total force in the same direction as it should be in the real vehicle. We can use this tilt mechanism thanks to the human perception organs. The human being perceives linear motion with the otolith organs located in the inner ear. These organs cannot differentiate between acceleration and tilt [Telban et al., 2000a] without the aid of other sensors. Therefore this situation can be used to give to the pilot the sensation of linear accelerations using simulator tilting. This technique provides good results as long as the angular rates used for tilting are below the human semicircular canals perception threshold [Nahon and Reid, 1990]. The semicircular canals are the human organs that perceive angular motion.

Figure 2-1 shows the typical structure of a motion cueing algorithm. The motion cueing structure is similar for most of the washout filters that are referred in this document. The high pass filters that handle the onset cues are designated by FILTER 1 and FILTER 3

in Figure 2-1. The former filter is responsible for the translational cues while the latter is responsible for the angular cues. Blocks GAIN 1, FILTER 1 and the block containing the double integrator form the high-pass translational channel while blocks GAIN 3, FILTER 3 and the block containing the integrator form the high-pass rotational channel. Blocks GAIN 2, LIMIT and FILTER 2 form the low pass translational channel. It is in this channel where the tilting coordination is included (normally in the LIMIT block). FILTER 2 is a low pass filter used to cut off the high frequency characteristics of the motion cue (The high frequency characteristic is already simulated in the high-pass translational channel).

The following sections will contain a brief explanation of the three motion cueing algorithms that seem to be the ones that designers prefer, based in the frequency with which they appear in the literature. The motion cueing algorithms are the Classical Washout algorithm, the Coordinate Adaptive algorithm and Optimal Control algorithm. Nevertheless other interesting algorithms were also found during research like the Robust Control Algorithm designed by Idan et al. [Idan and Sahar, 1996, Idan et al., 1998, Idan and Nahon, 1999], the Nonlinear Algorithm designed by Telban and Cardullo [Telban and Cardullo, 2005] and the hybrid adaptive algorithm developed by Nahon et al. [Nahon et al., 1992].

## 2-1 Classical Washout

The Classical Washout (CW) was the first motion cueing algorithm to be developed. The algorithm final form is based on designs proposed in references [Conrad and Schmidt, 1970, Conrad et al., 1973]. The transparent tuning features of the algorithm allied with the simple computational and mathematical model makes it one of the most used algorithms in commercial simulators [Nahon and Reid, 1990]. One of the shortcomings of the CW is that the tuning has to be performed for the "worst case scenario". This makes the algorithm too conservative. The CW algorithm description will be based in the Reid and Nahon [Reid and Nahon, 1985] design. The CW block diagram is shown in Figure 2-2.

The CW inputs are specific forces and body rates from the real vehicle (or vehicle model). From Figure 2-2 we see that the algorithm is divided into three different channels: the high-pass translational channel and the high-pass rotational channel.

The high-pass translational channel is composed by the following blocks: f SCALE,  $L_{IS}$  x, HP FILT and a double integrator block  $(\frac{1}{s^2})$ . The input of this channel is specific force  $(f_{AA})$  in Figure 2-2) and the ouputs are simulator displacements  $(S_I)$  in Figure 2-2). The f SCALE block is used to scale the specific force that comes from the vehicle model (or from recorded data). The specific force that come from the vehicle model is in the simulator cabin frame of reference while the cueing will be performed in the inertial frame of reference like it is said in Grant [Grant, 1995]. Therefore, block  $L_{IS}$  x changes the frame of reference of the specific force coming from the block f SCALE using a rotation matrix. The gravity component is taken from the specific force that is between blocks  $L_{IS}$  x and HP FILT. This gravity component is designated by  $g_I$  in Figure 2-2. The input of the HP FILT block is then acceleration (since the gravity component is no longer present) in the inertial frame of reference. The HP FILT block contains the high pass filters that cut-off the low frequency component of the acceleration,

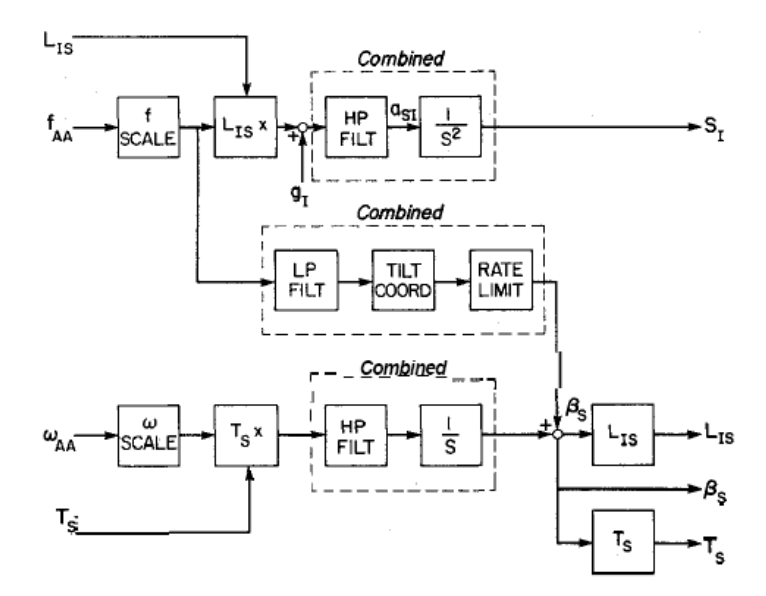


Figure 2-2: Classical Washout Algorithm structure [Nahon and Reid, 1990].

leaving only the high frequency component. The double integrator block is used to convert the high frequency acceleration into simulator displacements.

The high-pass rotational channel is constituted by the following blocks:  $\omega$  SCALE,  $T_S$  x, HP FILT and an integrator  $(\frac{1}{s})$ . The inputs of this channel are body rates ( $\omega_{AA}$  in Figure 2-2) and the outputs are simulator Euler angles. These angles are summed to the simulator angles coming from the low-pass translational channel forming then the total simulator angles ( $\beta_S$  in Figure 2-2). The  $\omega$  SCALE block is used to scale the body rates that come from the vehicle model. The body rates are transformed into Euler angle rates in block  $T_{SX}$ . This transformation is done using a rotation matrix. The HP FILT block contains the high pass filters that will cancel the low frequency component of the Euler angle rates. The integrator is used to convert the Euler angle rates into simulator Euler angles.

The low-pass translational channel is composed by the following blocks: LP FILT, TILT COORD, RATE LIMIT. The input of this channel is the scaled specific force that comes from the f SCALE block. The outputs are simulator Euler angles. Remember that the sum of these angles with the ones outputted by the high-pass rotational channel is equal to the total simulator angles ( $\beta_S$  in Figure 2-2). Block LP FILT contains low pass filters that will cut off the high frequency component of the specific force. These filters guarantee that only the sustained cues are simulated by this channel. TILT COORD contains the tilting coordination mechanism described previously in the beguinning of Chapter 2. The RATE LIMIT block contains the limiters that make sure that the angular motion created by the tilting coordination technique is below the human perception threshold. This channel connects the high-pass translational channel with the high-pass rotational channel.

The rotation matrices used by block  $L_{IS}$  x and block  $T_S$  x are created in blocks  $L_{IS}$  and  $T_S$  present in Figure 2-2. These transformation matrices can be found in Grant PhD thesis [Grant, 1995].

This algorithm as the advantage of being simple, since is created mostly with linear elements.

The tuning of the algorithm is not complicated since it is done directly in the algorithm filters, allowing then fast adjustments whenever they are needed. However, this algorithm has to be tuned for the worst case scenario, which means that the motion space (the space that the simulator has to move without violating its limits) is not fully exploited. This algorithm also does not take into account the nonlinearities of the human perception system [Nahon and Reid, 1990].

## 2-2 Coordinate Adaptive

The adaptive algorithms have a great potential since they can adapt the filter parameters while the simulation is running. In this way, a better use of the motion space is expected. The Coordinate Adaptive (CA) algorithm was first presented by Parrish [Parrish et al., 1973]. Since then, updates to this algorithm can be found in literature like the Reid and Nahon Coordinated Adaptive Washout Algorithm [Reid and Nahon, 1985] or the NASA Coordinated Adaptive Washout Algorithm [Telban et al., 2000b]. Figure 2-3 shows the Coordinate Adaptive algorithm block diagram.

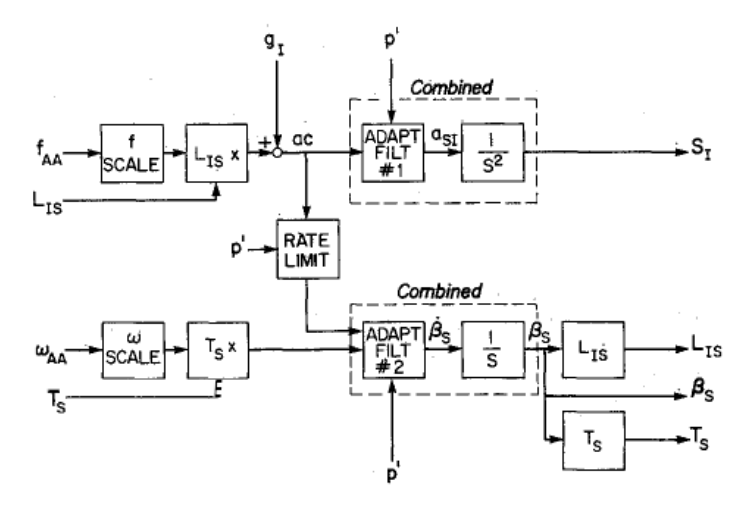


Figure 2-3: Coordinate Adaptive algorithm structure [Nahon and Reid, 1990].

From Figure 2-3 we can also observe three different channels like in the CW algorithm. The channels can be designated by: high-pass translational channel, high-pass rotational channel and a tilt channel.

The high-pass translational channel is constituted by the following blocks: f SCALE,  $L_{IS}$  x, ADAPT FILT #1 and the double integrator. The channel input is specific force ( $f_{AA}$  in Figure 2-3) and the outputs are simulator displacements ( $S_{I}$  in Figure 2-3). The f SCALE block scales the specific force that comes from the vehicle model. The  $L_{IS}$  x block is again used to transform the specific force from the simulator frame of reference into the inertial frame of reference. The input of the ADAPT FILT #1 (ac in Figure 2-3) is an acceleration (like the input for the HP FILT in the CW algorithm) because the gravity vector component ( $g_{I}$  in Figure 2-3) was taken from the specific force that is coming from the  $L_{IS}$  x block. The ADAPT FILT #1 contains the adaptive high pass filters that cut off the low frequency

component of the acceleration, ac. The adaptive high pass filters have adaptive parameters that vary during the simulation. These filters are more permessive (i.e. the frequency is cut at a lower frequency) when the simulator is near the neutral position and are more restrict (i.e. the frequency is cut at a higher frequency) when the simulator approaches the actuator limits. The adaptive parameters are represented in Figure 2-3 by p'. A cost function is minimization is used to calculate the adaptive parameters at each time step. The double integrator block transforms the high frequency acceleration ( $a_{\rm SI}$  in Figure 2-3) into simulator displacements.

The high-pass rotational channel is composed by the following blocks:  $\omega$  SCALE,  $T_S$  x, HP FILT and an integrator. The inputs of this channel are body rates while the outputs are the simulator total angles. The blocks  $\omega$  SCALE and  $T_S$  x have the same function as the ones with the same name in the CW algorithm, i.e., the former scales the body rates that come from the vehicle model while the latter transforms the body rates into Euler angular rates. The ADAPT FILT #2 block contains two different inputs. The first input correspond to the Euler angular rates that come from the tilt channel, while the second correspond to the Euler angular rates that come from the  $T_S$  x block. Both these inputs are summed before they are fed into the high pass filters present in this block. The high pass filters included in this block are adaptive like the ones in the ADAPT FILT #1. The integrator is used to convert the filtered Euler angular rates into simulator total angles ( $\beta_S$  in Figure 2-3).

The tilt channel contains the RATE LIMIT block. The input of this channel is the acceleration ac shown in Figure 2-3, which was already described before. The outputs of this channel are Euler angular rates. Two different tasks are performed in the RATE LIMIT block. The first is the scaling of the acceleration ac by an adaptative parameter that transforms it into Euler angular rates. The second task has to do with limiting these new angular rates in order to guarantee that they are below the human perception threshold. This channel obtains a similar effect in simulating the translational sustained cues as the low-pass translational channel in the CW algorithm and also connects the high-pass translational channel with the high-pass rotational channel.

The rotation matrices used by block  $L_{IS}$  x and block  $T_S$  x are created in blocks  $L_{IS}$  and  $T_S$ . The matrices are the same as the ones used in the CW algorithm.

This algorithm has the advantage changing the filter parameters during the simulation, which permits the use of the motion space in a more realistic way. Nevertheless this algorithm is difficult to adjust since the tuning is not done directly on the algorithm filters.

## 2-3 Optimal Control

The Optimal Control (OC) algorithm is designed based on the aircraft simulation problem shown in Figure 2-4. According to Ish-Shalom [Ish-Shalom, 1982] this algorithm tries to match the output of the inertial motion sensory model of an aircraft pilot with the one of a simulator pilot. Because it is not possible to obtain the exact output of the pilots vestibular system (one would have to measure directly from the pilots organs), mathematical vestibular models are created to perform this comparison. The objective of this algorithm is to create a transfer function W(s) (like the one present in Figure 2-4) that transforms the aircraft motion into simulator motion by minimizing the error between the aircraft pilot sentation and the simulator pilot sensation (like is shown in Figure 2-4). Note that this sensation is related to the

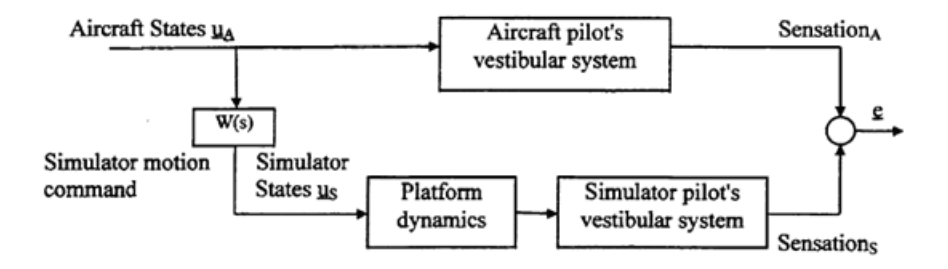


Figure 2-4: Aircraft simulation problem structure [Telban et al., 2000b].

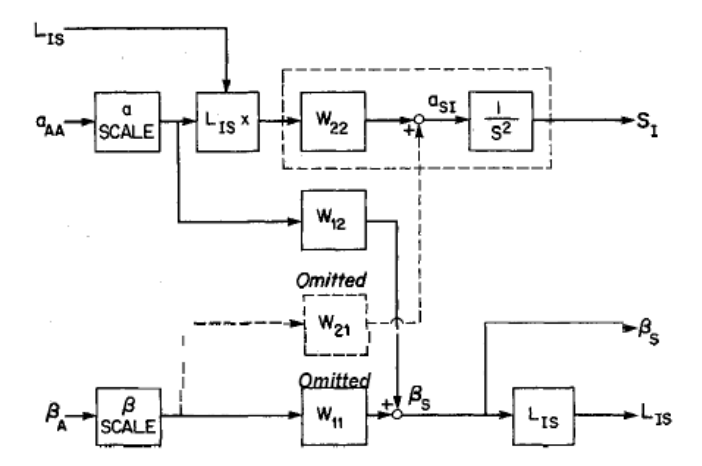


Figure 2-5: Optimal Control algorithm structure [Nahon and Reid, 1990].

output of the pilots vestibular system. Solving the aircraft simulation problem like is shown in Figure 2-4, has the advantage of using the limitations of the human sensory system to improve the simulation motion quality. The quality of the simulation will then be dependent on the quality of the used vestibular model. A linear optimal control theory can be used to solve the problem described in Figure 2-4. Nahon and Reid [Nahon and Reid, 1990] used an off-line design algorithm to obtain W(s). According to them, the "design algorithm solves the linear quadratic optimization problem that resuslts in the optimal form, order, and characteristics for the filters given the underlying assumptions". The OC algorithm block diagram is shown in Figure 2-5.

From Figure 2-5 we can also observe three different channels like in the CW algorithm. The channels can be designated by: high-pass translational channel, high-pass rotational channel and a tilt channel. In fact, a fourth channel is present in Figure 2-5 and is constituted by block  $W_{21}$ . However this channel will not be considered since is usually omitted from the final OC algorithm solution. This happens because of the extremely small gains of the transfer function present in this block, as is pointed out by Nahon and Reid [Nahon and Reid, 1990].

The high-pass translational channel is composed by the following blocks: a SCALE,  $L_{IS}$  x,  $W_{22}$  and a double integrator block. This channel input is given by the aircraft body-axis cockpit acceleration (a<sub>AA</sub> in Figure 2-5) while the outputs are simulator displacements (S<sub>I</sub> in Figure 2-5). The a SCALE block, scales the acceleration coming from the aircraft model. The block  $L_{IS}$  x transforms the scaled acceleration from body-axis into simulator inertial-axis. The

block  $W_{22}$  contains part of the transfer function W(s), that was obtained using optimal control techniques.  $W_{22}$  contains a transfer function that as the form of a high pass filter. Therefore, the low frequency component of the acceleration is cut off in this block. The double integrator block is used to convert the high frequency acceleration into simulator displacements.

The high pass rotational channel is constituted by the following blocks:  $\beta$  SCALE and  $W_{11}$ . The channel inputs are Euler angles ( $\beta_{\rm A}$  in Figure 2-5) while the channel output are simulator Euler angles. These angles will be sumed with the ones coming from the tilt channel resulting in the total simulator angles ( $\beta_{\rm S}$  in Figure 2-5). Block  $\beta$  SCALE is responsible for scaling the Euler angles coming from the aircraft model. Block  $W_{11}$  contains a transfer function that was obtained from the total transfer function W(s). According to Nahon and Reid [Nahon and Reid, 1990], this transfer function can be omitted in pitch and roll since it tends to be a unity gain. In yaw, this transfer function acts as an high pass filter.

The tilt channel is constituted by the  $W_{12}$  block. The input for this channel is scaled acceleration in the body-axis and the outputs are Euler angles. The transfer function present in  $W_{12}$  also comes from the total transfer function W(s). The  $W_{12}$  transfer function works as a low pass filter, which makes that this channel as similar properties to the low pass translational channel present in the CW algorithm.

The rotation matrix used by block  $L_{IS}$  x is created in blocks  $L_{IS}$  and is the same as the one used in the CW algorithm.

This algorithm uses an optimal solution to solve the vehicle simulation problem. The OC algorithm also takes into account the nonlinearities of the human perception system, which should be a major advantage versus other motion cueing algorithms. Some of the shortcomings of this algorithm have to do with using fixed parameters during the entire simulation, which means that the motion space is not used in an effective way. Tilt rate limiters are also not used, which leads to angular false cues.

# Motion Cueing Evaluation

One of the principal problems regarding motion cueing algorithms is their evaluation. Evaluation is needed in order figure out which algorithm suits best a certain motion platform. It is not trivial to assess the performance of a Washout filter. One of the difficulties has to the with the complexity of the human being, since what is good for one driver/pilot can be not sufficient for other driver/pilot. The motion cueing evaluation can be understood as an absolute or relative problem. In this document the following definitions are considered:

- Absolute evaluation is defined as an evaluation where the motion cues from the real vehicle are compared with the ones obtained from the motion cueing algorithm.
- Relative evaluation is defined as an evaluation where the motion cues of a motion cueing algorithm are compared with the motion cues of other motion cueing algorithm or the motion cues obtained from a mathematical model of a vehicle.

The cueing assessments vary from simple simulations - where designers compare the shape of the signals obtained from the simulator with the ones obtained from the real vehicle or a vehicle model - to simulator tests with subjects - where subjective scales are used to evaluate the simulation fidelity.

We could not find in literature a standard procedure to evaluate the performance of a motion cueing algorithm. Normally, the choice of the evaluation method depends on the adequacy to the study and on the available time. An evaluation of a motion cueing algorithm can take a few days, when simple computer simulations are used, or months when tests with individuals are performed. The fact that motion cueing evaluation is not a standard procedure, can create false judgments regarding some motion filters (because of that, these studies should always be analysed with extra criticism). For example, the fact that a given washout algorithm has performed better in one study than other algorithm, does not mean that the algorithm is better, it only means that for that specific study and with that specific tuning, the performance was better. For that reason, the designer when comparing two algorithms has to guarantee

that both algorithms are tuned in order to reach the highest level of performance for the manoeuvre(s) of relevance for that simulation.

Grant and Reid [Grant and Reid, 1997] pointed some difficulties in developing a pure mathematical solution to tune a motion cueing system. This situation is similar to evaluating a motion system since in both cases one wants to assess the best solution possible for a motion system. When a researcher is tuning a washout algorithm, intrinsically he is also evaluating it. Developing such a mathematical solution is extremely difficult due to the complexity of the human self-motion perception system. The human self-motion system is achieved by the integration and interpretation of different cues, like for example visual and vestibular cues. Some mathematical models of the human sensors have been developed [Zacharias, 1978, Gum, 1973], but these are still not accurate enough. A model of the Central Nervous System is also needed to understand how the information coming from the different systems is processed by the human being. The lack of good quality perception models is one of the reasons why motion algorithms tuning is still done iteratively by trial and error.

The evaluation techniques can be divided into two large groups, the objective evaluations and the subjective evaluations.

- The objective evaluation is based on objective measurements, where performance is assessed from mathematical variables involved in the simulation. As an example, the performance can be checked by analysing the difference in shape of specific force signals from the simulator and from the vehicle in study.
- The subjective evaluation is based on subjective measurements obtained from a group of test subjects, where performance is checked by analysing statistical variables created from the impression of those subjects.

Normally objective evaluation is cheaper and less time consuming since some of the tests can be made with computer simulations without requiring test subjects. On the other hand, subjective evaluation can be quite expensive and time consuming since normally an experiment has to be prepared where several test subjects will be used to evaluate the motion cueing algorithm. The time span of an experiment like this can vary from a few days to a few months.

This literature research will focus in the techniques used by motion cueing designers to evaluate different types of motion drive algorithms and at the end will try to achieve a standard protocol that should be used when a motion filter needs to be evaluated. The description will focus on several aspects like used manoeuvres, how results were analysed, which variables designers took into account. Experience has shown that every case is a case, and so it is difficult to group the evaluations done during the last years (even if the same evaluation techniques are used). For that reason, all the studies described in this literature will be analysed in detail with the purpose of gathering all the possible information for each type of simulation (car simulation, flight simulation, etc.). Before describing the evaluation techniques, a brief explanation of the motion cues errors that exist in simulations will be given so one can understand the problems inherent to a simulation. This is important since the motion cue errors will influence the motion cueing evaluation. For example, a motion cueing algorithm with several motion cueing errors should have a worst performing than a motion cueing algorithm with few motion cueing

errors. Therefore the evaluation method should be able to point out this difference between the two algorithms. The description of the evaluation methods will be made according to the definitions of objective evaluation and subjective evaluation given before.

## 3-1 Motion Cue Errors

Grant and Reid [Grant and Reid, 1997] categorized motion cue errors into three types, which are: false cues, scaling or missing cue errors and phase errors.

A false cue is a motion cue that exists in the simulator but not in the real vehicle. According to Grant and Reid [Grant and Reid, 1997] "false cues are the most destructive cueing errors from a perceived fidelity point of view". False cues can occur due to:

- Software or Hardware limiting, because the simulator has to stop in order not to reach its position, velocity or acceleration limits, situation that does not occur in the real vehicle.
- Return to Neutral, because the simulator cabin has to return to neutral position after an onset cue. If the washout is not performed, it is possible to reach a situation where there is not enough motion space to perform the next motion.
- Tilt coordination issues, because tilting coordination is an artefact to deceive the human perception system, used to obtain sustained cues of specific forces. These types of false cues include the perception of angular rate, which happens when the simulator tilts to provide sustained specific force. Abrupt specific force changes also induce false cues. This happens because the simulator cannot grapple with this change due to the rate limiter. Another false cue regarding tilt coordination has to do with false angular accelerations perceived when the tilt coordination is performed in a point not correspondent with the pilot-head, which generates extra specific forces.

Scaling or missing cues occur mainly due to the parameters of the motion cue algorithm. Scaling has to be done since the simulator is not able to achieved motion cues of the same order of magnitude of the real cues. Missing cues can happen when the scaling is so restrict that some cues disappear.

Phase errors have to do with the phase lead properties of the high-pass filters and phase lag properties of the low-pass filters present in some motion cueing algorithms.

## 3-2 Objective Evaluation

The objective evaluation can be divided into two groups: mathematical measurements and behavioural measurements. Mathematical measurements are related with mathematical variables that show motion cueing characteristics of the simulation, like for example specific forces or body rates. Behavioural measurements are related to subject behaviour in the simulator, in comparison with subject behaviour in the real world for absolute evaluations or subject behaviour in other simulator for relative evaluations. An example of behavioural variables are pilot inputs in an aircraft. Figure 3-1 shows how Section 3-2 is structured.

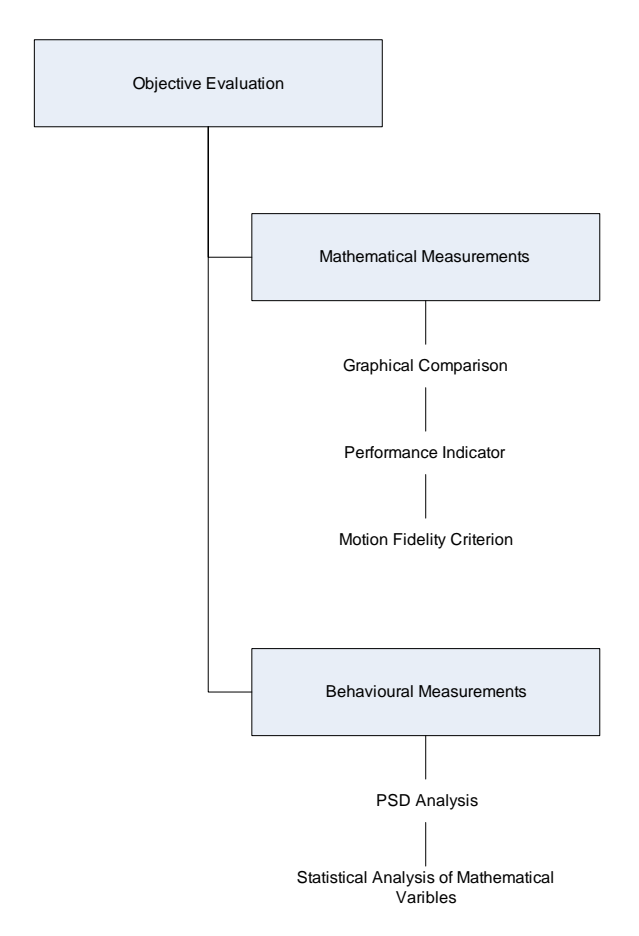


Figure 3-1: Objective evaluation structure.

## 3-2-1 Mathematical Measurement

In this section, different methods of mathematical evaluation will be described. This type of evaluation is more related with motion cueing algorithms outputs. It is possible to conduct these evaluations with off-line tests, which is cheaper and less time consuming than online experiments, where subjects are used.

## **Graphical Comparison**

This method is normally used in preliminary studies of motion filters. It is based in direct comparison of the motion cues felt in the vehicle and the motion cues felt in the simulator cabin using time history plots. This evaluation technique can be done using software simulations. From these simulations is possible to obtain the vehicle motions (using real data or using mathematical models) and the approximate motions that subjects would feel in the simulator cabin. Online simulations can also be used by this evaluation method. Then the graphical comparison is based in signals obtained from online simulations where test subjects perform a certain task, like in the Colombet et al. [Colombet et al., 2008] study.

Normally the analysis is made for specific forces and body rates but sometimes time histories of other variables are also analysed, like simulator displacements [Idan and Nahon, 1999, Barbagli et al., 2001, Zywiol and Romano, 2003, Wang and Fu, 2004, Wentink et al., 2005, Nehaoua et al., 2006, Grant, 1995, Chapron and Colinot, 2007 which helps to draw conclusions about the motion envelope usage. Idan and Nahon [Idan and Nahon, 1999] used these plots to hypothesise if the use of an algorithm that produces more motion is benefitial to the overal motion quality of the simulation. The choice of specific forces and body rates makes sense since these motion cues are normally used as inputs for the washout algorithm and are the motion cues perceived by the human vestibular system. Pouliot et al. [Pouliot et al., 1998], Telban et al. [Telban et al., 1999] and Kim et al. [Kim et al., 2006] also compared the specific force and angular rate sensed by the human, instead of only comparing the specific force and angular rate generated by the vehicle/simulator. In this way, they could see if the motion cueing algorithm is using the vestibular system nonlineaties to obtain a better match in motion. Telban et al. [Telban et al., 1999] used the plots of the sensed motion cues to draw conclusions about the signals shape differences between the vehicle and the simulator driven by different washout algorithms. Kim et al. [Kim et al., 2006] used the sensed motion cue plots to draw conclusions about phase and magnitude differences between the vehicle signals and the signals generated by the motion cueing algorithms.

Most of the graphical comparison studies found are relative evaluations. But absolute evaluations were also found like in the Zywiol and Romano [Zywiol and Romano, 2003] study.

A graphical comparison should be done using vehicle specific manoeuvres as inputs because it helps to infer the motion fidelity of the simulator for a certain type of simulation, i.e. one will not tune a motion cueing algorithm for an aircraft using car breaking data. Nevertheless, some authors prefer to use other inputs that are not vehicle manoeuvres to show their algorithm performance. For example Wentink et al. [Wentink et al., 2005] used step inputs and Chen and Fu [Chen and Fu, 2007] used a sinusoidal input.

From the graphical comparison method, it is possible to take information about false cues, signal delays, amplitude differences and shape errors. For example, Telban et al.

[Telban et al., 1999] used this method to point out the "sag (decrease followed by increase)" false cue that the adaptative algorithm produces in specific forces. Zywiol and Romano [Zywiol and Romano, 2003] also made a similar coment about the Classical Washout algorithm. Several authors also discussed about the specific force amplitude differences based in the graphical comparison plots, like in references [Dagdelen et al., 2004, Valente Pais et al., 2007]. It is also possible to notice the onset and sustained cues zones of the specific forces and angular rates. This information is used to show the transition between onset cues and sustained cues done by the washout algorithm. From this evaluation method, it is also possible to see the tilting coordination effects in the translational and angular motion cues. For example, Pouliot et al. [Pouliot et al., 1998] showed that the tilting coordination rate limit is an handicap to build up specific force as fast as in a real airplane.

Graphical comparison evaluation seems suitable for preliminary designs of motion filters. A standard that seems to be followed by most of the authors is to use an already known motion cueing algorithm for benchmarking purposes. It is advisable to show the filter parameters in the study, so one can infer how well the algorithms have been tuned. The results are normally assessed from plots that contain specific forces and angular rates for the three inertial axes. It is advisable to show these plots, even if the test manoeuvre is focused one type of motion cue. In this way, one can check if false cues exist in other motion cues due to simulation artefacts. Graphical comparison should also include plots of the sensed cues because in that way is easier to check if the cues performed by the simulator are taking into account the nonlinearities of the human motion perception system. By analysing plots, it is easy to observe differences between real cues and simulated cues. However knowing if those differences influence the human perception of motion, just by observing these graphics is extremely difficult. Sometimes one design seems much better than other "in paper" but when these designs are tested in the simulator the differences seem no longer noticeable. Because of that, better evaluation methods than graphical comparison are needed in order to guarantee that the designed motion filter is the best fit that one can get. That is why some studies do not use the graphical comparison as a stand alone method of draw conclusions about washout algorithms performance [Reid and Nahon, 1988, Pouliot et al., 1998, Liao et al., 2004, Colombet et al., 2008]. Some authors also noted that a subjective study should be done in order to draw better conclusions [Idan and Nahon, 1999, Chapron and Colinot, 2007].

The following authors conducted this evaluation in the subsequent way:

Crosbie and Kiefer [Crosbie and Kiefer, 1985] developed a controller for a dynamic flight simulator. The objective was to use the human centrifuge not only as a tool for physiological research studies but also as a dynamic flight simulator used for pilot training. For comparison effects, time history plots of roll manoeuvres were shown. These plots compare the cues felt by pilots in the dynamic flight simulator with predicted cues felt by pilots in an aircraft. The plots show roll angles, roll rates and specific forces. In these plots, authors show the effect that changes in the initial algorithm have in the simulator response. This was not the only evaluation method used in this paper. The other evaluation method can be found in section 3-3-2.

Reid and Nahon [Reid and Nahon, 1988] evaluated three different motion filter algorithms: Classical Washout Algorithm, Coordinate Adaptive Algorithm and the Optimal Algorithm.

This study is a summary of the more detailed evaluation made in [Reid and Nahon, 1986]. The study was conducted in the University of Toronto Institute for Aerospace Studies (UTIAS) Flight Research Simulator. The simulated aircraft was a Boeing 747. Seven airline pilots were invited to participate in the study but none of them with experience in a Boeing 747. The task was to perform a typical flight sequence. The detailed sequence consisted of:

Maintaining altitude and heading in a turbulence field, intercept a VOR and decelerate
while tracking the VOR radial. Then initiate the descent and do a sidestep manoeuvre
to capture an ILS. Perform an ILS approach to touchdown, then takeoff and climb-out
while an engine fails. Wheel and rudder contained induced transients.

Ten different motion drive configurations assigned in a random order where flown by the pilots. Only one morning/afternoon session per day was allowed for each pilot. In one single session, five flights were performed, so each pilot needed two sessions, each of them lasting 2.5 hours. Objective and subjective evaluations were used in this study. The graphical analysis was performed for a turn entry manoeuvre. The data for this analysis was taken from one pilot. Time histories were presented for the three motion cueing algorithms as well for the aircraft model in separate plots. The shown plots included roll rates, bank angles and lateral specific forces. From these plots, it was possible observe false cues. The other evaluation methods used in this study will be reported in the respective sections.

Pouliot et al. [Pouliot et al., 1998] compared the motion cues generated by three different motion base architectures. The motion platforms where the Stewart Platform (STW) with 6 degrees-of-freedom (DoF), the Spherical Platform (SPH) with 3 DoF and the Heave-Pitch-Roll (HPR) Platform also with 3 DoF. Three characteristic flight manoeuvres where used to evaluate the motion cues. The manoeuvres as described in [Pouliot et al., 1998] are:

- Take-Off Manoeuvre (TOM): The aircraft has an initial speed of 50 m/s on the runway and the throttle lever at 15% of maximum power. At t=3s, the throttle is set to 100%. At t=11s the aircraft reaches its rotation speed. The nose of the aircraft lifts and takes of at a pitch angle of 10°. At t=17s the right outboard engine fails and the elevator is eased to avoid stalling. At t=25s the manoeuvre finishes.
- Turn Entry Manoeuvre (TEM): The simulation starts with the aircraft in a cruise condition. First the aircraft rolls to the right, then left and then right again. The manoeuvre ceases at t=40s. The maximum bank angle is 40° and the throttle lever is set to 55% of maximum power for the entire manoeuvre. The elevators are adjusted during the manoeuvre to maintain constant altitude.
- Throttle Impulse manoeuvre (TIM): Initially the aircraft is flying at a cruise condition with throttle lever at 55% of maximum power. Then the throttle is set to maximum, and the aircraft is kept with constant altitude by moving the elevators accordingly. Seventeen seconds later the throttle is set to idle until the end. The manoeuvre finishes at t=40s.

The authors considered that these manoeuvres provided a wide range of motions in all DoFs. The aircraft motions where obtained from a nonlinear model of a Boeing 747. Plots of angular rates are not part of this study since the 3 DoF platforms present the same level of

angular motions of the 6 DoF platforms as is stated in reference [Pouliot et al., 1998]. For the TOM, four plots were analysed. The first and third plots contain respectively longitudinal and vertical specific force information of the aircraft. The second and forth plots contain respectively the longitudinal and vertical sensed specific force. The sensed specific force was obtained by passing the specific forces trough a human vestibular model. In the sensed specific force graphics, there is a shaded zone which defines the place where the human does not feel motion, i.e. the human thresholds. All these four plots contained four lines which stand for: aircraft motion cues, STW motion cues, SPH motion cues and the last one represented the difference between the motion cues obtained from the two platforms (second and third lines). The lines referent to the motion platforms can be read from different positions in the simulator (pilot head, centroid of the platform or center of gravity of the simulator), and that position choice depends from plot to plot. Only longitudinal and vertical directions were presented for this manoeuvre since these are the directions were the most important motion cues of the manoeuvre are present. From these plots, it was possible to draw conclusions about tilting coordination issues. The TEM evaluation contains four plots like the ones from the TOM where the vertical cues plots were substituted by lateral cues plots. The longitudinal plots contain information about the HPR 3 DoF platform instead of the SPH platform. From the plots, the authors took conclusions about the different amplitudes of the specific force signal (aircraft versus simulator). For the TIM evaluation, only two plots were shown from where delay conclusions were taken. These contained respectively longitudinal specific force information and longitudinal sensed specific force information. The plot lines were the same as the ones in the TOM. In this manoeuvre, they could also conclude that some false cues (amplitude peaks) existent in the specific force plots disappear when motion cues are processed by the vestibular model. The evaluation of the motion cues was done based in these plots and was supported by the performance index method described in section 3-2-1.

Idan and Nahon [Idan and Nahon, 1999] compared the RC algorithm with the CW algorithm. Three specific flight manoeuvres where used since the objective was to check the performance of these algorithms for flight simulators. The manoeuvres as described in [Idan and Nahon, 1999] are:

- Take-off manoeuvre: The aircraft has an initial speed of 50 m/s on the runway and the throttle lever at 15% of maximum power. At t=3s, the throttle is set to 100%. At t=11s the aircraft reaches its rotation speed. The nose of the aircraft lifts and takes of at a pitch angle of 10°. At t=17s the right outboard engine fails and the elevator is eased to avoid stalling. At t=25s the manoeuvre finishes.
- Turn entry manoeuvre: The simulation starts with the aircraft in a cruise condition with initial altitude of 6280m and initial speed of 212m/s. Right after a roll to the right is initiated and a steady state roll angle is maintained. At t=12 a left roll manoeuvre is initiated. This sequence is repeated a second time and the manoeuvre ceases at t=40s. The maximum bank angle is 40°.
- Throttle pulse manoeuvre: The initial condition is equal to the one of the Turn entry manoeuvre with throttle lever at 55% of maximum power. At t=1.5s the throttle is set to maximum, and the aircraft is kept horizontal. At t=8.5s the throttle is set to idle. The manoeuvre finishes at t=40s.

The test manoeuvres specifications are very similar to the ones used in [Pouliot et al., 1998]. The aircraft data was obtained from a Boeing 747 model. Twelve graphics where obtained from each manoeuvre. The first six graphics contained the specific forces in the three inertial directions and the three body rates. Each of these graphics enclosed the real aircraft signal and the signal generated by each of the motion cueing algorithms tested. The last six graphs contained the angular and translational displacements for each motion cueing algorithm. The cueing evaluation was obtained separately for each manoeuvre and was based on the graphics described before, by comparing which algorithm provided closer results to the real aircraft motion cues. This was done by comparing the shape of the different signals. The displacement plots were used to conclude about motion envelope usage and its effectiveness. At the end of the study, the authors emphasize that further work will include piloted evaluations.

Telban et al. [Telban et al., 1999] compared the performance of two different OC algorithms and then compared the "best" of those with an AC algorithm. Again flight manoeuvres where used since the study was performed for flight simulation. Two manoeuvres were used to compare an OC algorithm with angular acceleration as input and an OC algorithm with angular velocity as input. The manoeuvres were an aircraft surge input and an aircraft pitch input. The results were assessed from a specific force graphic in longitudinal direction for the first manoeuvre and an angular velocity graphic in pitch for the second manoeuvre. The main conclusions taken from them were about false cues. When comparing the OC algorithm with the AC algorithm, the authors included a piloted simulated manoeuvre in the test, which was a column manoeuvre (other manoeuvres were done, but were not included in the article). The results were assessed from four graphics for each manoeuvre. The graphics presented the longitudinal specific force, the longitudinal sensed specific force, the pitch angular velocity and the pitch sensed angular velocity. Each graphic contained the Aircraft signal as well as the AC algorithm and the OC algorithm signals. Signal shape and false cues conclusions were taken from these plots. "Sag's" were also identified in the motion cues. Telban and Cardullo [Telban and Cardullo, 2002] also performed a study where they compared the Nonlinear algorithm with the CA and the OC algorithms. The evaluation process was made in a very similar way to the one in [Telban et al., 1999].

Spenny et al. [Spenny et al., 2000] graphically evaluated two different motion controllers for a dynamic flight simulator. The first is a G-pointing architecture that uses PID control compensation while the second is a G-pointing architecture that uses inverse dynamic control. A pop-up manoeuvre was used to test the algorithms. The manoeuvre consists of a pull-up from low altitude with thrust applied, followed by a roll-over and after a pull-down. Thrust is reduced followed by another roll-over and a final pull-up. Four time history plots were shown. The first two contain z acceleration information for the two motion controllers and for the aircraft model, being the second plot a zoom of the first plot near the third second of simulation. The other two plots contained respectively the angular roll acceleration and the angular pitch acceleration for the aircraft model, PID controller and Inverse Dynamics controller. The authors also show a plot of the rectilinear z acceleration, but in this case for two imprecise forms of inverse dynamics control. Another study was presented in this paper with the objective of assessing the human sensitivity to centrifuge artefacts using the Dynamic Environment Simulator. This subjective study is analysed in section 3-3-1.

Barbagli et al. [Barbagli et al., 2001] designed a washout filter for a motorcycle simulator. Graphical analysis was used to assess the new algorithm. No online testing was performed, so the study was based in off-line simulations. The results of the off-line tests are in some degrees approximated since platform dynamics were not included. Three manoeuvres were performed: the first was a longitudinal acceleration followed by a deceleration. This manoeuvre lasted 55 seconds. The second manoeuvre simulated the motorcycle moving longitudinally at a constant velocity while being influenced by a truck wave. This manoeuvre lasted 10 seconds. The last manoeuvre consisted of a longitudinal acceleration followed by a deceleration ended with a hard stop. The manoeuvre duration was equal to the duration of the first manoeuvre. For the first manoeuvre four time history plots were shown. The information present in them was respectively: linear acceleration in the head longitudinal axis, linear acceleration in the head vertical axis, pitch rate in the driver head axis and actuator lengths. In these first three plots, the designers showed the real motion cues (data generated by the motorcycle model) against the simulator motion cues. The fourth plot showed the lengths for all the actuators. The second task was also analysed by four time histories plots: linear acceleration in the head longitudinal axis, linear acceleration in the head lateral axis, linear acceleration in the head vertical axis and roll rate in the driver head axis. All these plots showed the real motion cues versus the simulator motion cues. For the last manoeuvre two plots were shown, both of them regarding the longitudinal head axis, where the former contains information for all the manoeuvre and the latter contains information for part of the manoeuvre. Both of them included the real motion cues against the simulator motion cues. The head axes are defined in [Barbagli et al., 2001]. The conclusions of this study were taken from this analysis.

**Zywiol and Romano [Zywiol and Romano, 2003]** performed a study to evaluate the best motion cueing algorithm to implement in the Ride Motion Simulator of the TARDEC National Automotive Center. The objective was to simulate the motion cues felt in the passenger back compartment of a military transport vehicle. The two motion cueing algorithms used in the evaluation are: a classical washout filter and a washout algorithm based on a new tilt coordination method [Romano, 2003]. Two manoeuvres were used for evaluation. The first manoeuvre was a simulated longitudinal acceleration step input of  $2m/s^2$  while the second manoeuvre data was obtained from a real vehicle. This makes the evaluation absolute for the second manoeuvre and relative for the first manoeuvre. The real manoeuvre was collected from an eight-wheeled, Infantry Fighting Vehicle called Stryker. The real vehicle drove trough two real courses: Perryman A and Perryman 1. The collected data included: vehicle speed, vehicle body rate in pitch, roll and yaw, vehicle linear acceleration in lateral, longitudinal and vertical. The data was collected at 500 samples per second. For the first manoeuvre, the classical washout was graphically compared with the new motion cueing algorithm. Three time histories plots were presented containing respectively the specific force, angular velocity and the position displacement of the classical algorithm versus the new washout algorithm. For the real manoeuvre the new algorithm outputs were compared with the real data outputs. The first two plots show specific force time histories of the new algorithm versus the real data, where the second plot is a time constriction of the first plot (authors did this for zoom purposes). The last two plots present in the paper are the tilt rate and linear displacement time history responses generated by the new algorithm. From the plots, they were able to get information about sagging cues existent in the CW algorithm. This new washout algorithm was further developed by Romano [Romano, 2005].

Liao et al. [Liao et al., 2004] compared a new washout filter design with a classical washout filter. This new design was developed for a small entertainment 6 DoF simulator. In this study the new algorithm was evaluated against a typical classical washout algorithm. A virtual reality (VR) motion of an automotive system was used as system input for both algorithms. Time history plots of the longitudinal accelerations and pitch angular velocities containing information of the classical washout, the new washout algorithm and the dynamic model output were used for assessment. Both of these plots were followed by two plots containing the segmental errors of the classical washout and the new algorithm respectively. The authors also compared the new algorithm with different adaptive scaling factors. The same time history plots were shown but this time the classical washout information was substituted by a different tuning of the new algorithm. Other assessments were made for this study and will be presented in section 3-2-1.

Wang and Fu [Wang and Fu, 2004] used graphical comparison to evaluate a new Predictive Washout Filter Design. Simulations were done to show the algorithm effectiveness. The evaluation was divided in a simulation section and an experiments section using a Stewart platform. In the simulations section, two manoeuvres were performed. First a time history plot of the senseless manoeuvre that the cueing algorithm produces was shown. In this plot it is possible to observe the manoeuvre in the inertial coordinate frame as well as in the body coordinate frame. After, a throttle-pulse manoeuvre was created in order to test the algorithm in a realistic environment. Three plots were presented to evaluate the algorithm behaviour in this manoeuvre. The first plot contained information regarding the longitudinal acceleration of the model, the acceleration of a CW without parameter tuning and a CW with parameter tuning. The second plot shows the platform position for three different cases: CW before parameter tuning, CW after parameter tuning and CW using the new predictive tuning algorithm. The last time history plot contains the desired Euler angle along the vaxis. False cues conclusions were drawn from these plots. The experiment section is divided in two parts. In the first part, the new algorithm is evaluated using two tracking manoeuvres, a longitudinal sinusoidal and a longitudinal step. Three plots are used to assess results from the manoeuvres. The first plot shows the longitudinal acceleration with and without the predictive algorithm, the second plot shows the platform position in the longitudinal axis, while the third plot shows the platform rotation angle that happens when the predictive algorithm is used. The second part of the experiment section contains a realistic throttle-pulse manoeuvre. Three plots were shown containing information of the platform displacement, accelerations in the body frame and pitch motion in the lateral axis for different motion cueing algorithms and configurations. The conclusions taken in this section were similar to the ones of the simulation section.

Dagdelen et al. [Dagdelen et al., 2004] performed a graphical analysis to assess the performance of the MPC based washout algorithm. The test manoeuvre was a car accelerating from 0 to 70km/h using the first three gears of the car. The manoeuvre ended at t=10s. It was used a car manoeuvre since the algorithm is being developed for car driving simulation. The results were derived from a longitudinal acceleration plot, where the vehicle signal was compared with the motion cue algorithm signal. The authors also compared the new motion cueing solution with a classical washout algorithm. The same manoeuvre was used in this comparison and the results were shown in a time history plot of the longitudinal specific force

containing the motion cueing algorithm signals, as well as the signal coming from the car model. From this plot, the authors conclude about false cues and amplitude errors.

Wentink et al. [Wentink et al., 2005] designed a new washout algorithm for Desdemona simulator called spherical washout. The algorithm obtains sustained cues using simulator tilting or using the centrifugal capabilities of Desdemona. The authors used step inputs and compared them with the simulator response. Three different types of plots were shown during the paper: one containing the Desdemona trajectory, one containing the x and y specific forces and one with the angular rates around x, y and z. The first manoeuvre consisted of a longitudinal step of 0.3g, which is similar to the acceleration of a Boeing 747 during the take-off run [Wentink et al., 2005]. The manoeuvre was analysed for two different high-pass filter frequencies (2 and 1 rad/s). The three plots were shown for each high-pass condition. A new step input was created, consisting of a longitudinal 0.3g step at t=1s and a lateral 0.3g step at t=3s. Again the same plots were shown for this manoeuvre. A second manoeuvre of this type was analysed, but now containing the lateral step in the opposite direction. The last manoeuvre analysed in this paper used the centrifugal motion to generate the sustained cues. A lateral step starting at t=1s and finishing at t=6s was used for the cueing analysis. Again the three plots were used for evaluation. The conclusions of this study were about signal shape, motion space use and sustained cues generation.

Nehaoua et al. [Nehaoua et al., 2006] conducted a study to evaluate the best motion cueing algorithm to be used in a 2 DoF small driving simulator. Three algorithms were tested: Classical Washout algorithm, Coordinate Adaptive algorithm and the Optimal algorithm. The test manoeuvres were typical for car driving (accelerations, decelerations and braking). The results were assessed from four different plots. The first two plots contained longitudinal accelerations, where the former contained vehicle accelerations against the ones obtained by the classical and adaptive algorithms while the latter contained vehicle accelerations against the ones obtained by the classical and optimal algorithm. The last two plots show the platform displacement respectively for classical versus adaptive algorithms and classical versus optimal algorithm. Performance of the motion filters was assessed from graphical comparison. The conclusions were mostly regarding signal shape differences (between the car motions cues and the simulator motion cues).

Kim et al. [Kim et al., 2006] developed a new Washout algorithm for the KATECH Advanced Automotive Simulator (KAAS). They developed a new tilt coordination method for a washout algorithm as well as a Robust Control controller for the motion platform. The tilt coordination algorithm was evaluated using four motion cues plots of a driving circumstance. The plots contain the sensation felt by the human for the following cues: surge acceleration sensation, sway acceleration sensation, roll rate sensation and pitch rate sensation. All these plots contained three different signals: Human real sensation, Human sensation in the Classical algorithm and Human sensation in the new washout algorithm. Conclusions about magnitude and phase were taken from the plots. The authors also decided to include a table containing the correlation coefficient between human sensation in the real situation and human sensation for both algorithms. The robust controller for the motion platform was evaluated with five time histories plots. The first two represent respectively the translational and rotational cues

of the test manoeuvre. The last three plots contain respectively the desired actuator lengths, the actual actuator lengths and the error between these. All six actuators were represented in these last three plots. No other type of evaluation method was used by the authors.

Grant and Clark [Grant, 2006] did a relative study for a new motion drive algorithm developed for a car driving Large Displacement Simulator. The test manoeuvre was a lowspeed J-turn. In this manoeuvre, the car speed in the turn is of 36 km/h, the lateral force is of 0.25g and it has a steady state yaw rate of approximately 14°/s. Ten graphics were obtained from this manoeuvre. The first three graphics contain the specific forces of the car versus the specific forces of the simulator for each inertial axis (x, y and z). The second set of three graphics contains the angular rates of the car versus the angular rates obtained from the motion drive algorithm for each inertial axis. The third set of graphics contains respectively the simulator motion in position, velocity and acceleration. The simulator motion is displayed in x and y for these last three plots. The last graphic of this study shows a comparison of the simulator internal pitch and roll angles with the ones from the vehicle. The intention of this plot was to demonstrate the match between these angles. The results assessment was done based in these plots. The authors noted that more driving manoeuvres should be tested in order to approve the motion drive algorithm. The suggestions for further testing were a lower speed J-turn manoeuvre, a stop-and-go manoeuvre and a turn manoeuvre.

Valente Pais et al. [Valente Pais et al., 2007] evaluated four different types of motion cueing algorithms for curve driving in Desdemona. The algorithms were: a classical washout algorithm, a classical washout algorithm that uses Desdemona central yaw to generate lateral sustained cues, a centrifuge solution that makes Desdemona curve like a real car but constrained to the simulator maximum radius and a centrifuge solution that uses motion along the simulator radius. A simple car model was created to simulate curve driving. The car model was designed based on data obtained from an instrumented Volkswagen Passat. The test manoeuvre consisted of a 90 degrees curve to the left with a curve radius of 8 meters. The car had a constant velocity of 15 km/h. For simplification purposes, the car model only outputted lateral specific force and car yaw rate, being the other angular rates and the longitudinal specific force equal to zero. Four figures were shown for each motion cueing configuration. The first figure contained simulator movement during the curve and when returning to neutral. The second figure contained x and y specific forces in the simulator versus the x and y specific forces of the car model. The third figure represented the angular velocities of the car versus the angular velocities of the simulator, while the fourth figure contained the same information but now for angular accelerations. The authors used these plots to discuss about magnitude fits of the different motion cueing solutions. Signal shape and false cues were also issues focused in their analysis. These could be seen on the specific force and angular rate plots described before.

Chapron and Colinot [Chapron and Colinot, 2007] designed a motion filter for the new PSA Advanced Driving Simulator. The motion filter was based on a classical washout, but contains some new features like a lane change algorithm [Grant et al., 2002]. Offline simulations were performed to assess the motion filter. Two driving manoeuvres were used in this study. The manoeuvres consist of a double lane change manoeuvre, followed by a curve with

100m of radius. The driving speed is of 70km/h and the profile was obtained from a driver driving in other dynamic simulator. The difference between the first and the second manoeuvre lies whether the lane change occurs right before the curve or not. The results were assessed from time history plots of the lateral acceleration and the actuator displacement. These type of plots were show for both manoeuvre and they contained the cues of the new algorithm, the cues of a standard classical algorithm and the cues provided by the data of the car model. The authors noted that subjective evaluation should be done when the new simulator is fully operational in order to tune the motion cueing algorithm. This is because they don't know the impact of some filter parameters (that are related with human perception thresholds) in subjects.

Chen Fu [Chen and Fu, 2007] improved the predictive filter washout [Wang and Fu, 2004] by using Kalman filter techniques to estimate the platform position. They used graphical comparison to assess the washout filter. A sine wave was used as input to check the advantages of the new algorithm, both in z and x axis. For the z axis, three plots were presented. The first and the third plot contained z displacement information both for classical algorithm with and without prediction, being the latter a zoom of a section of the former. The second plot contained the acceleration generated by both of the algorithms. For the x axis, only two plots were shown, being the first one for the longitudinal displacement of the simulator and the last one for the accelerations felt in this direction. Both plots contained the results of the classical algorithm with and without the prediction algorithm. The evaluation of this new predictive method was made based on these plots.

Fischer and Werneke [Fischer and Werneke, 2008] used the graphical comparison method to evaluate the performance of a new motion cueing algorithm. This new fast tilt coordination (FTC) algorithm was compared with a CW algorithm. Two driving manoeuvres were used to do the comparison. The first was a full gas depression while the second was a slalom driving with rising steering frequency. Two plots were created for each manoeuvre. The plots of the first manoeuvre contained respectively longitudinal specific force and pitch angular velocity. The plots of the second manoeuvre contain respectively lateral specific force and roll angular velocity information. All plots contain 3 signals: the car cues generated by the car model, the cues generated by the CW algorithm and the cues generated by the FTC algorithm. The plots were mainly used to show shape error differences in the motion cues generated by both algorithms. This paper also contains results from a tilting study, assessed by other evaluation methods.

Colombet et al. [Colombet et al., 2008] performed a study that analyses the impact of three motion cueing algorithms in driver's behaviour. The motion cueing algorithms were: a static configuration that does not use platform motion, a classical washout algorithm and an adaptive algorithm. The task was to maintain a constant distance of 15 m from a leading car over 5 minutes using the three different motion cueing algorithms. Seven individuals participated in the experiment. Three figures were shown for graphical comparison. In the first figure, time histories of the platform longitudinal acceleration were presented for three situations: the vehicle acceleration, the accelerations obtained with the adaptive algorithm and the accelerations obtained with the classical algorithm. This figure was used only to show

the final tuning obtained for the motion cueing algorithms. The manoeuvre described in this figure corresponds to a car acceleration from 0 to 100 km/h. The second figure contains two time histories plots. The first one shows the driven velocity against the lead car velocity, while the second plot contains the platform longitudinal acceleration of this situation for the adaptive motion cueing algorithm and the vehicle acceleration. The last figure contains the platform longitudinal acceleration in function of its longitudinal position, both for the classical and the adaptive algorithm. The Statistical Analysis evaluation method and the subjective comment method were also used to measure the performance of the algorithms.

#### Performance Indicator

This evaluation method uses a quality criterion to rate the performance of a motion cueing algorithm. Two performance indicators were introduced by Pouliot et al. [Pouliot et al., 1998] to evaluate motion filters.  $\lambda_1$  is the performance indicator responsible for giving information of the average error between motion cues occurring in the vehicle (or vehicle model) and motion cues from a simulator.  $\lambda_2$  is related with the average error of the time variation of the variables in  $\lambda_1$  (vehicle motion cues and simulator motion cues). Therefore the value of  $\lambda_1$  gives information of how close are the simulator motion cues to the real motion cues. If  $\lambda_1$  is equal to zero, it means that the motion cue error between the simulator and the vehicle is zero, which says that the motion cues in the simulator are equal to the ones in the vehicle. Because  $\lambda_2$  measures the average error of the rate of change of the motion cues, if  $\lambda_2$  is equal to zero, it means that the error of the motion cue variation between the simulator and the vehicle is zero.

 $\lambda_{1f}$  is the performance index that gives information about the average error between the specific forces of the vehicle and of the simulator. If  $\lambda_{1f}$  is zero, it means that there is no difference between the specific forces of the vehicle and of the simulator.  $\lambda_{1f}$  is given by equation (3-1), where N is the total number of data points. Equation (3-3) defines the specific force error, where  $f^{veh}$  is the specific force of the real vehicle and  $f^{MCA}$  is the specific force obtained with the motion cueing algorithm.

$$\lambda_{1f} = \frac{1}{N} \sum_{j=0}^{N} \sqrt{\Delta f_{xj}^2 + \Delta f_{yj}^2 + \Delta f_{zj}^2}$$
 (3-1)

$$\triangle f = (\triangle f_x, \triangle f_y, \triangle f_z) \tag{3-2}$$

$$\triangle f = f^{veh} - f^{MCA} \tag{3-3}$$

 $\lambda_{1\omega}$  is the performance index that gives information about the average error between the angular rates of the vehicle and of the simulator. It can be obtained by substituting the

specific forces in equations (3-1) for angular velocities. Then  $\lambda_1$  is given by equation (3-4), where  $a_{max}$  and  $\omega_{max}$  are respectively the acceleration and angular rate limits of the simulator. These limits are used for normalization reasons.

$$\lambda_1 = 100 \times \left( \frac{\lambda_{1f}}{a_{max}} + \frac{\lambda_{1\omega}}{\omega_{max}} \right) \tag{3-4}$$

 $\lambda_{2f}$  is the performance index that gives information about the average error between the rate of change of the specific forces of the vehicle and of the simulator. If  $\lambda_{2f}$  is zero, it means that there is no difference between the rate of change of the specific forces of the vehicle and of the simulator.  $\lambda_{2f}$  is given by equation (3-5), where N is the total number of data points. Equation (3-7) defines the difference between the derivatives of the specific force of the vehicle and simulator.

$$\lambda_{2f} = \frac{1}{N-1} \sum_{j=1}^{N} \sqrt{\delta \dot{f}_{xj}^{2} + \delta \dot{f}_{yj}^{2} + \delta \dot{f}_{zj}^{2}}$$
 (3-5)

$$\delta f = (\delta f_x, \delta f_y, \delta f_z) \tag{3-6}$$

$$\delta f = \left(\frac{\triangle f^{veh}}{\triangle t} - \frac{\triangle f^{MCA}}{\triangle t}\right) \tag{3-7}$$

 $\lambda_{2\omega}$  can be obtained by substituting the specific forces in equations (3-5) by angular velocities.  $\lambda_2$  is defined by equation (3-8).

$$\lambda_2 = 100 \times \left( \frac{\lambda_{2f}}{a_{max}} + \frac{\lambda_{2\omega}}{\omega_{max}} \right) \tag{3-8}$$

This evaluation method gives a very objective result, since the motion filter is evaluated based on a number given by the method. Pouloit et al. [Pouliot et al., 1998] chosed to use this method because of that reason, since the information that we can take from graphical comparison is based on a visual analysis which sometimes can lead to some misjudgements (The designer could forget to point out some performance issues, which would bias the evaluation). From this method, designers can have an idea of what motion cueing algorithm perform better

in the global picture. The studies were this method was found have also used other evaluation methods to complete the motion filters analysis.

Nevertheless, with this method we could only get a rating for the motion algorithm performance, losing information regarding specific motion cue errors, like false cues or scaling errors. Therefore, this evaluation method is sort of a "compact" method of graphical comparison. This method is more like a complement to graphical analysis than a stand alone evaluation method. Therefore, all the information that this method gives, can also be taken by graphical comparison, the difference is that in the former one gets a mathematical value for that information, while in the later this information has to be inferred from observing the plots.

The following authors used this evaluation in the subsequent way:

Pouliot et al. [Pouliot et al., 1998] used the performance indicator to evaluate the motions cues generated by three different motion platforms designs. This study was already discussed in section 3-2-1 since graphical comparison was also used for assessment. Regarding the performance indicator method, one plot was presented for each of the three manoeuvres (TOM, TEM and TIM). The x axis of the plot represented  $\lambda_1$  while the y axis represented  $\lambda_2$ . Each plot contained the rating for all the tested platforms designs (STW@PH, STW@CP, SPH@CG, SPH@PH, SPH@CP, SPH+HF, HPR@PH, HPR@CP, HPR+HF). This method was used to show the global performance of the different motion solutions.

Liao et al., [Liao et al., 2004] also used a performance indicator to evaluate their new motion filter. The performance indicator used in [Liao et al., 2004] is given by equation (3-9), where  $W_a$  and  $W_b$  are weighting parameters. The RMS functions present in equation (3-9) are given by equations (3-10) and (3-11), where  $E_{a,k}$  and  $E_{\omega,k}$  are cost functions defined in reference [Liao et al., 2004].

$$PI = W_a \cdot RMS(E_a) + W_{\omega} \cdot RMS(E_{\omega}) \tag{3-9}$$

$$RMS(E_a) = \sqrt{\frac{\sum_{k=0}^{N} E_{a,k}^2}{N}}$$
 (3-10)

$$RMS(E_{\omega}) = \sqrt{\frac{\sum_{k=0}^{N} E_{\omega,k}^{2}}{N}}$$
(3-11)

The performance indicator was shown in two tables that also contained the root mean square errors of the accelerations and the angular velocities. These results were shown for different

linear scaling of the filters in one table and for different adaptive scaling factors in other table. The method was used to support the conclusions obtained with the other evaluation methods present in the study.

Fischer and Werneke [Fischer and Werneke, 2008] used this technique to evaluate a CW algorithm with different tilt rate limit and different tilt point. Four different CW algorithms were developed, the first has a tilt rate of 3°/s and a tilt point above the subject head (UpL), the second has a tilt rate of 30°/s and a tilt point under the subject head (LowL), the last has a tilt rate of 30°/s and a tilt point under the subject head (LowL), the last has a tilt rate of 30°/s and a tilt point under the subject head (LowU). They used slightly different equations for the performance indicators in order to differentiate shaping errors from scaling errors.  $\triangle f$  present in equation (3-3) can also be given by equation (3-12), where  $f^{veh,sc}$  is the scaled specific force of the real vehicle,  $\triangle f_{sc}$  is the specific force scaling error and  $\triangle f_{sg}$  is the specific force shaping error.

$$\Delta f = \Delta f_{sc} + \Delta f_{sh} = \left( f^{veh} - f^{veh,sc} \right) + \left( f^{veh,sc} - f^{MCA} \right)$$
 (3-12)

With these last two variables, one can relate the performance indicators to scaling and shape errors. The same reasoning was applied to  $\Delta_{\omega}$ ,  $\delta_f$  and  $\delta_{\omega}$ . The experiment data was achieved from simulator runs with driver in the loop. The test manoeuvre consisted of doing an emergency brake (total brake pedal depression) with an initial speed of 80 km/h. The authors presented the performance indicators results in four bar plots, where each bar plot contained the four algorithms. The performance indicators represented were:  $\lambda_{1f,sh}$ ,  $\lambda_{1\omega,sh}$ ,  $\lambda_{2f,sh}$ ,  $\lambda_{2\omega,sh}$ . The authors also presented a plot of  $\lambda_{1f,sh}$  versus  $\lambda_{2f,sh}$ . Evaluation of these cueing algorithms was not made exclusively with this method, since the authors also conducted a subjective evaluation using the test subjects.

## Motion Fidelity Criterion

Motion fidelity criteria evaluate the simulator motion according to the motion filter properties. Scaling, break frequencies and phase distortion are parameters that influence the criterion. This section is structured in a different way when compared to the other sections. Presenting how designers used these criteria during years is very straight forward and does not have much scientific interest. Instead, we will show how some motion fidelity criteria were created. Despite being an objective method, motion fidelity criteria are most of the times created recurring to subjective evaluations.

The motion fidelity criteria presented in this section are usually not used in motion filter evaluations. This occurs because these criteria are too generalist while motion filter evaluations should be specific (every case is a case). It can happen that the zone defined has high fidelity (as well as the other zones) in these studies cannot be applied in other studies, due to, for example, the specific nature of some manoeuvres. As an example, we have Schroeder [Schroeder, 1999] who did a study similar to the one done by Sinacori [Sinacori, 1977] and discovered that the

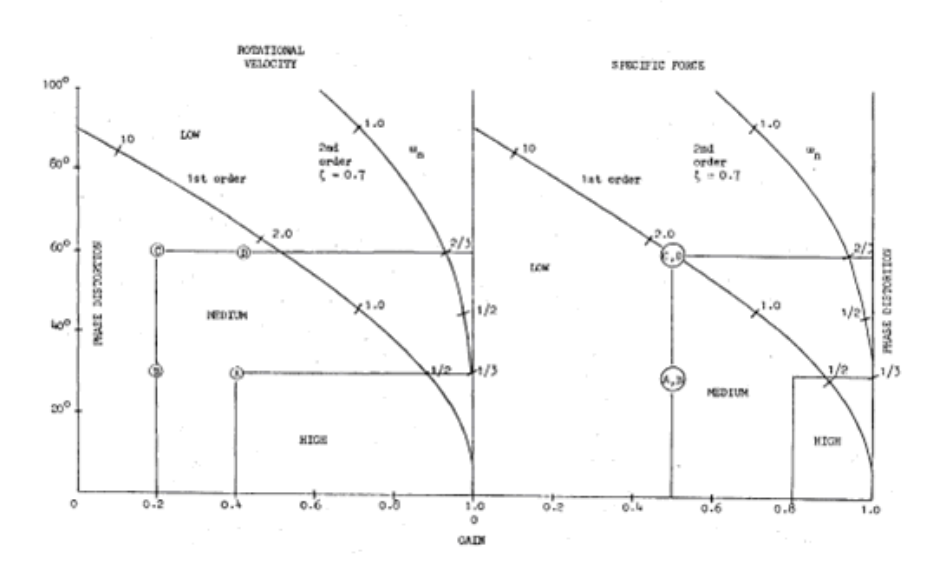


Figure 3-2: Motion fidelity criterion for different gains and phase distortions[Sinacori, 1977].

Sinacori criterion should be adjusted. Nevertheless these criteria are good guidelines in the design phase of a motion filter, since designers can use them to choose the initial parameters of the washout filter, even though in the evaluation phase other methods are advisable to check the performance of a motion filter.

Sinacori [Sinacori, 1977] developed a helicopter motion fidelity criterion at a frequency of 1 rad/s. The results were obtained from piloted manoeuvres. One task consisted of performing an "S" turn down a runway at approximately 60 knots while in the other task pilots had to perform a precision hover. Different motion configurations were used during the runs where the designer changed motion filters gains and break frequencies. After each trial, pilots had to rate motion according to the following criteria:

- High Fidelity: Motion sensations are close to those of visual flight.
- Medium Fidelity: Motion sensations differences are noticeable but not objectionable.
- Low Fidelity: Differences are noticeable and objectionable, loss of performance, disorientation.

From the results, Sinacori created the criteria for lateral specific forces and roll motions shown in Figure 3-2.

The author made some recommendations for further development, like for example, using other manoeuvres as well as real flight data, creation of a motion fidelity criterion that uses objective measurements in its development among other recommendations. Schroeder changed the Sinacori motion fidelity criterion due to the results obtained from the helicopter flight simulation motion platform requirements study [Schroeder, 1999]. The study will be analysed in section 3-2-2 and section 3-3-1. The obtained fidelity criterion is shown in Figure 3-3.

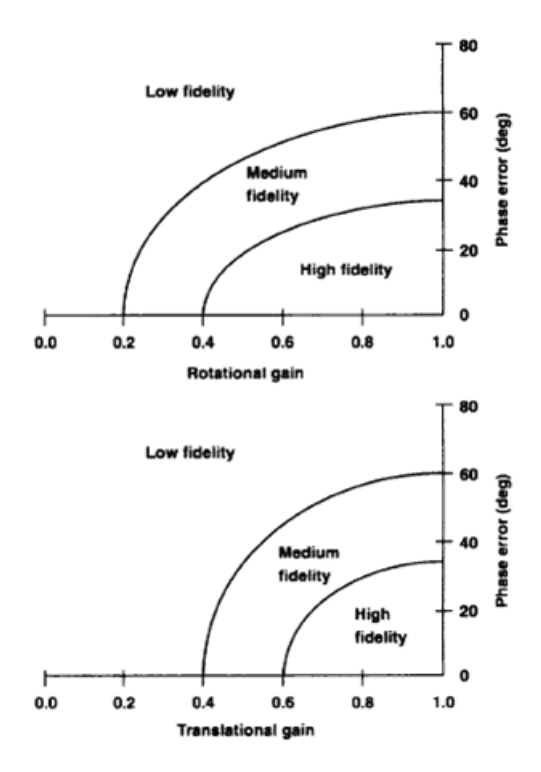


Figure 3-3: Modified motion fidelity criterion [Schroeder, 1999].

White and Rodchenko [White and Rodchenko, 1999] developed a motion criterion that helps selecting filter parameters. The study was developed for the lateral control axis. The authors divided motion cues into two types: beneficial and negative. In lateral control, beneficial motion cues reduce pilot's pure time delay since these are perceived faster than visual cues. Other beneficial effect is that these motion cues are perceived even if the pilot is not focused on the visual scene, increasing pilot awareness. Negative motion cues are the ones that result from high-frequency pilot control inputs. The criterion was developed for the break frequencies; filter order and scaling of the washout filters for the two different types of motion cues. For beneficial motion cues, the filter order and break frequencies were analysed using angular motion simulation. A logarithmic plot containing the relative roll stabilization precision versus the filter break frequency was used to infer the high fidelity specifications. For the negative motion cues, only the break frequencies were analysed. A logarithmic plot containing the pilot ratings versus the filter break frequency was shown. The high fidelity specifications were taken from this plot. For scaling a new criterion was proposed based in the ratio of the simulator motion cues to their threshold values. For angular rates, the ratio is given by equation (3-13), where  $m\sigma_p$  is the simulator angular rate and  $\sigma_{pth}$  is the angular rate threshold. For specific forces, the ration is given by equation (3-14), where  $m\sigma_{n_z}$  is the simulator specific force and  $\sigma_{n_z th}$  is the specific force threshold.

$$\mu_p = m \frac{\sigma_p}{\sigma_{nth}} \tag{3-13}$$

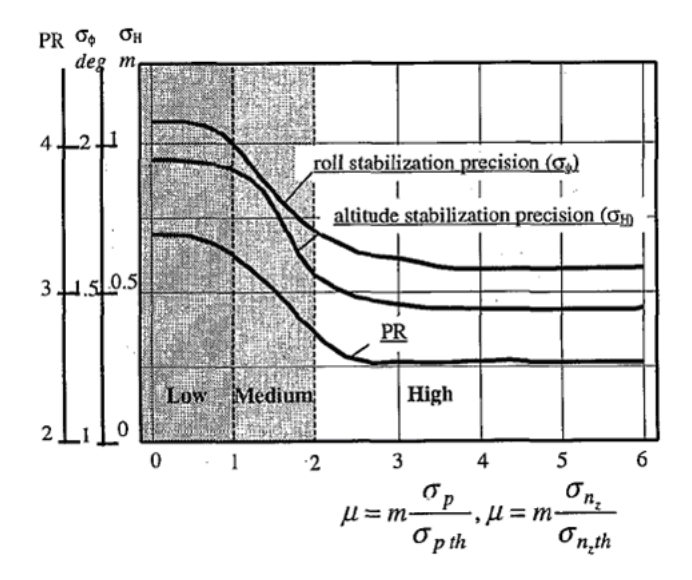


Figure 3-4: Beneficial motion cues criterion for scaling [White and Rodchenko, 1999].

$$\mu_{n_z} = m \frac{\sigma_{n_z}}{\sigma_{n_z th}} \tag{3-14}$$

The beneficial cues criterion is shown in Figure 3-4 and the negative cues criterion is shown in Figure 3-5.

The authors also created a motion fidelity criterion for tilting coordination based in human thresholds. Figure 3-6 shows this criterion.

Tran et al. [Tran et al., 1999] did an experiment with the objective of creating a motion fidelity criterion for a pitch-longitudinal translational task in a helicopter. The experiment task was to perform a 20 ft dash-and-stop at a constant altitude of 23 ft. The pilot starts the manoeuvre by doing a 20 ft longitudinal movement followed by 20 seconds of hovering in the final position. The manoeuvre had to be done in one smooth movement and respecting the performance standards shown in [Tran et al., 1999]. Two washout filters were implemented in the simulator. One washout was responsible for pitch motions while other was responsible for longitudinal translational motions. Two different configurations were used for the pitch filter and eleven different configurations were used for the longitudinal filter. Four pilots practiced with a random motion configuration. For the experiment, every pilot flew all the configurations in a random order. Every configuration had to be flown three times and had to be evaluated at the end of the third trial. Subjective rating scales were used in this process. Pilot had to give handling qualities using the Cooper-Harper [Cooper and Harper, 1969] rating scale and also had to rate the motion fidelity according to the following definitions [Tran et al., 1999]:

• High Fidelity: Motion sensations are not noticeably different from those of visual flight.

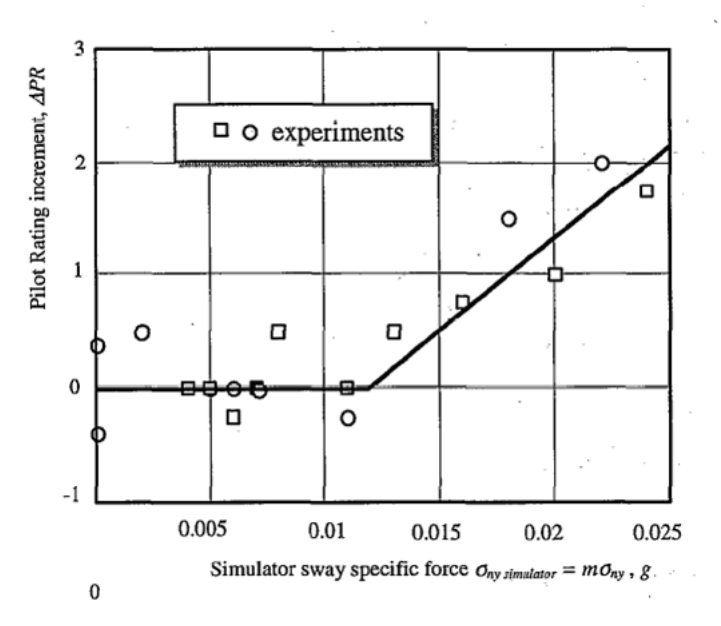


Figure 3-5: Negative motion cues criterion for scaling [White and Rodchenko, 1999].

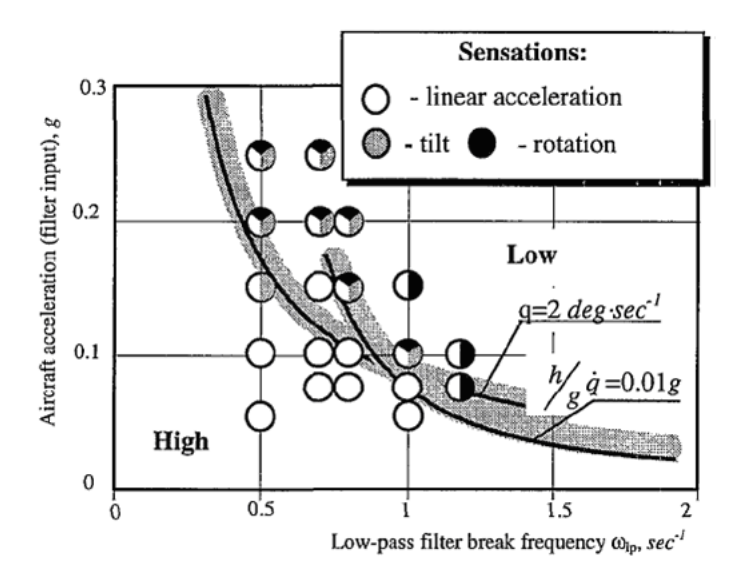


Figure 3-6: Tilting coordination criterion [White and Rodchenko, 1999].

- Medium Fidelity: Motion sensations are noticeably different from those of visual flight, but not objectionable.
- Low Fidelity: Motion sensations are noticeably different from those of visual flight and objectionable.

These definitions are very similar to the ones in [Sinacori, 1977]. The results of the ratings were plotted in a phase distortion versus gain plot, like in the Sinacori motion fidelity criteria [Sinacori, 1977]. Four extra plots were added regarding two different situations: full pitch motion and attenuated pitch motion. The plots show the break frequency of the longitudinal filter versus the motion fidelity ratings as well as the longitudinal gain versus the motion fidelity ratings. The authors noted that the results are similar to the ones for the roll-lateral motion requirements [Sinacori, 1977], nevertheless more testing is recommended.

Padfield and White [Padfield and White, 2005] are designing an adaptive pilot model that will be used to evaluate simulator motion. The study will focus on using the pilot model to detect differences from visual and motion cues and also to compare the fidelity of an aircraft model with real data.

#### 3-2-2 Behavioural measurements

In this section, different methods of behavioural evaluation will be analysed. This type of evaluation is related to simulation inputs, and control techniques used by subjects in simulators. Normally test subjects are needed, which makes these evaluation methods more expensive and time consuming than the ones using the mathematical evaluations.

### Power Spectral Density Analysis

The Power Spectral Density (PSD) can be used as a measure of workload. The PSD function is the average amount of power per unit of frequency. If the PSD is applied to the control inputs, one gets a measure of the amount of power that the pilot/driver uses in the simulator and so, a measure of workload. Guo et al. [Guo et al., 2003] pointed out that a higher PSD normally reveals higher workload.

In references [Guo et al., 2003, Telban et al., 2005, Soparkar and Reid, 2006] the PSD analysis was used to obtain workload measures of the pilot inputs for different motion cueing algorithms. Groen and Bos [Groen and Bos, 2008] used this method to observe the frequency content of linear acceleration in the vehicle and in the simulator.

Using this method, it is possible to observe which motion cueing algorithm has a higher workload. It is also possible to know which control inputs are more used for the different motion filters as we see in references [Guo et al., 2003, Telban et al., 2005]. Telban et al. [Telban et al., 2005] used the PSD plots to observe the pilot performance variations among the different motion algorithms. Guo, et al. [Guo et al., 2003] noted that the frequency range can vary for different motion cueing algorithms. They also draw some conclusions about the frequency content of the control inputs based on the highest peak of the PSD. Groen and Bos

[Groen and Bos, 2008] used this method to obtain information about motion sickness, but how they do it could be an idea to evaluate motion cueing algorithms.

With the PSD analysis it is possible to have a notion of the subject workload when controlling a vehicle. One also gets information about the frequency content of the control inputs. Using PSDs, one can compare the control inputs of the simulator versus the control inputs of the real vehicle and assess the motion cueing algorithm from there. It is also possible to assess the washout algorithms by checking which one delivers a lower workload, or a workload level similar to the real task. Therefore this evaluation method evaluates the performance of a motion cueing algorithm in terms of subject workload. A drawback of the PSD method is that phase information is lost. The results obtained from this method are difficult to analyse when we are talking about motion evaluation, since it is difficult to compare workload levels for this case (one motion filter can have low subject workload, but can also deliver poor motion cues, like a fixed base simulator). Normally one wants low workload, but when performing simulations, it is desirable to have workload levels similar to the ones of the real vehicles. It is also not possible to identify motion cue errors using this method, which means that if we wanted to improve the motion cueing algorithm, we would have to use another method to identify these errors. For these reasons, this method is good to check how hard is the task for the subject, but is not straightforward to use it has a motion filter evaluation method.

The following authors used this evaluation method in the subsequent way:

**Guo, et al. [Guo et al., 2003]** conducted a study to analyse pilot performance using two different algorithms, a new OC algorithm and the NASA CA algorithm. The study was done with three pilots flying in the NASA Visual Motion Simulator (VMS). The simulator contains a nonlinear model of a Boeing 747-200, with landing gear dynamics, gust and wind models, flight management systems and flight control computer systems. The study was made using three flight manoeuvres:

- Straight-in Approach (SA): This manoeuvre consisted of doing a visual approach into the Runway 18R of the Dallas/Fort Worth Airport. PAPI lights are available as well as Glideslope and Localizer needles. The flight initial conditions are:
  - Altitude: 1300 ft BARO, 697 ft AGL.
  - Airspeed: 135 kts. o Heading: 180°.
  - Distance to runway: 2 nm.
  - Flaps: Full.
  - Gear: Down.
  - EPR: 1.19.
  - Wind conditions: 10 kts, Begins as a head wind, swings around to a 90 deg wind from the left at 1 nm and continues to swing around to a tail wind as the aircraft crosses the threshold.
- Offset Approach (OA): In this manoeuvre the pilot is aligned with one runway and then has to change its heading when the red light on instrument panel illuminates, which happens at 7500 ft from threshold, and align the aircraft with Runway 18R. Again

PAPI lights are available on runway 18R as well as Glideslope and Localizer needles on the Primary Flight Display. The flight initial conditions are:

- Altitude: 1300 ft BARO, 697 ft AGL.

- Airspeed: 135 kts.

Heading: 180°, aligned with Runway 18L.

- Distance to runway: 2 nm.

Flaps: Full.Gear: Down.EPR: 1.19.

- Wind conditions: Severe turbulence. Lateral gust from the left, 90° to runway centreline, turns on at 3000ft from runway threshold, turns off at the runway threshold.

• Takeoff (with or without engine failure)(TO): In this manoeuvre the pilot has to perform a takeoff. The following procedure has to be followed: Pilot has to apply brakes and then advance the throttles from idle to Takeoff EPR. After the brakes are released. At VR, pilot has to rotate 15° in pitch and then as to climb to 2000ft BARO while accelerating to 200 kts. The runway heading of 180° has to be maintained while landing gear and flaps have to be used normally. The initial conditions are:

- Aircraft positioned at runway 18R

- Flaps: 15°.

- Takeoff EPR: 1.60.

- VR: 126kts.

- Engine failure cases: Left engine failure at 1300 ft BARO, 697 ft AGL.

Each pilot did 56 test runs in a single day, being 16 of these for the SA, 16 for the OA and 24 for the TO. The first two manoeuvres contained three varying simulation conditions: four different time delays (0, 50, 100 and 200 ms), the two motion cueing algorithms referred before (OC and CA) and the simulation could be with or without compensation. The TO manoeuvre has more cases because of the extra condition (with or without engine failure). All the needed variables were stored in order to do the PSD evaluation after the piloted tests. The authors used two different methods to calculate the PSD. The first one was the direct method, also known as periodogram and the second method was the indirect method. The periodogram is an estimate of the PSD obtained by the Discrete Fourier Transform (DFT), this technique suppresses some random details (peaks) because of smoothing properties. The indirect method first calculates the autocorrelation and only then calculates the DFT. In both methods the average of the signal is taken from the signal in order to eliminate the frequency peak at 0 Hz due to offsets existent in the signal. The Hamming method was adopted for the PSD calculation. The authors noted that the interval [0 1] Hz is where most of the control input occurs, and then the PSD was calculated in this interval range. This study did not aim only the evaluation of the motion filter, but also the study of the effects of time delays, compensation and engine failure in pilot workload. The PSD analysis was shown in three different forms of data presentation. The first is a bar plot where the PSD was integrated.

This gives the amount of power spent by the pilot in a control input, e.g. roll stick, pitch stick, ruder, pedals; for any situation that the designers want to test, e.g. a simulator run, a specific motion filter, a run with/without time delay or compensation. A table was also shown where one could get information about the frequency range of a control input for a manoeuvre and for both tested motion cueing algorithms. The last source of information were PSD plots in the frequency domain, so one can check at which frequencies the control inputs were more excited. Higher frequency range means that the pilot had to do more high frequency movements in order to control the aircraft. From this evaluation method, authors could draw conclusions about the different frequency ranges that the tested motion cueing algorithms operate. It was also used as a workload measure between the algorithms. Conclusions were also taken from a Copper Harper rating scale.

Telban et al., [Telban et al., 2005] conducted a study similar to [Guo et al., 2003] in order to evaluate the performance of three types of motion cueing algorithms: the NASA CA algorithm, an augmented form of the OC algorithm and the Nonlinear algorithm. Eleven pilots participated in this study. The study took part in the NASA VMS. The plane model and the test manoeuvres were exactly the same as the ones in [Guo et al., 2003]. Each pilot did a total of 96 manoeuvres: 24 for the SA, 24 for the OA, 24 for the TA without engine failure and 24 for the TA with engine failure. The manoeuvre distribution follows the same logic of [Guo et al., 2003], but with an extra motion cueing algorithm to evaluate. For the evaluation the pilots were separated into three distinct groups. Group one contained the most disciplined scan sample and control approach, group two contained a less disciplined flight approach than group one and group three was characterized by an erratic control approach. The PSD in [Telban et al., 2005] was obtained in the same way as in [Guo et al., 2003]. The SA manoeuvre was evaluated by three figures for Pilot Group 1 and Pilot Group 2 and one figure containing information of both these groups. The first figure contained two bar plots, one relative to the pitch stick and other to the roll stick. In each of these plots, the integral of the PSD is represented for each motion cueing algorithm regarding three different uncompensated delay situations (0, 100 and 200 ms). The second figure includes two plots, one showing the PSD of the aircraft pitch angle in the frequency domain with zero delay, and other showing the same thing, but for the aircraft roll. The average PSDs of the three motion cueing algorithms are presented together in these plots. The third figure shows the aircraft position at touchdown using the three different motion cueing algorithms for three different uncompensated delay situations (0, 100 and 200 ms). Two bar plots were present in this figure, one for the x direction and one for the y direction. The last figure used in the PSD analysis of the SA contained two bar plots, one for Pilot Group 1 and one for Pilot Group 2. The information in the plots was the aircraft vertical rate at touchdown, for the three motion cueing algorithms in three different uncompensated delay situations (0, 100 and 200 ms). Even though that these last two figures were not calculated using the PSD, the authors included them in the report to give extra information of the performance of the pilots. For example the figure of the touchdown position was used to check if the cueing algorithm influenced the pilot touchdown methodology, while the figure of the vertical rate at touchdown gives information about how much control of the airplane the pilot has. These figures continue to be behavioural measurements assessments, even though that they are in the wrong section of this literature study. For OA manoeuvre, the PSD analysis contained the same information as the one in the SA manoeuvre, so there is no need to describe all the figures again. The TO manoeuvre was divided into two section, one with engine failure and one without engine failure. Three figures are present in each section. The first two figures are equal to the first figure described for the SA manoeuvre, being one for Pilot Group 1 and other for Pilot Group 2. The last figure is equal to the second one described for the SA manoeuvre, but for Pilot Group 1 only. In the section of the engine failure, an extra figure was included describing the integral of the PSD for the rudder pedals. The figure contained one bar plot for Pilot Group 1 and other for Pilot Group 2. The three motion cueing algorithms were compared for three different uncompensated delay situations (0, 100 and 200 ms). A last section is present in the report to analyse the simulator attitude coherence. PSD plots of the average simulator pitch and roll angle for Pilot Group 1 for the OA with zero delay containing the three motion cueing algorithms were analysed, as well as the average simulator pitch and roll angle coherence. The coherence was defined as in equation (3-15), where  $\Phi_y(\omega)$ ,  $\Phi_u(\omega)$  are respectively the power spectral densities of the output and the input and  $\Phi_{yu}(\omega)$  is the cross-spectral density between the input and output.

$$\kappa_{yu} = \sqrt{\frac{\left|\Phi_{yu}\left(\omega\right)\right|^{2}}{\Phi_{y}\left(\omega\right)\Phi_{u}\left(\omega\right)}} \tag{3-15}$$

The conclusions were drawn from the PSD analysis method as well from the subjective evaluation of the NASA TLX scale analysis.

Soparkar and Reid [Soparkar and Reid, 2006] investigated the effects of simulator motion on handling qualities. The PSD analysis was used as a measure of the control input strategy of the pilot. Three pilots were used to evaluate different motion conditions of a motion base platform. The pilots had to in fly the University of Toronto Institute for Aerospace Studies (UTIAS) Flight Research Simulator (FRS). The aircraft model of the simulator was taken from a generic fixed-wing jet trainer. The pilot task was to perform an aerial refuelling. A performance definition was given to the pilots. Desired performance was defined as keeping the crosshairs in the inner portion of the basket for 40% or more of the total tracking time, while adequate performance was defined as keeping the crosshairs in the inner portion of the basket for 20% or more of the total tracking time. However the authors noted that this refuelling basket served only as an identifiable target and that the performance criteria were not based on aerial refuelling. The use of rudders was not allowed. Three types of motion were evaluated. The first one was a no motion condition, denominated as Fixed-Base; the second was a configuration with minimal roll washout, defined as Baseline Motion and the last one was a configuration with very high roll washout levels, called the Modified Motion. Four flight conditions were created for these motion configurations, each one with a different roll mode time constant (the last condition has the same roll mode time constant, but with increased disturbances). For the PSD analysis the plots of the Lateral control inputs PSDs were given for the three evaluation pilots in the four different conditions. One set of plots included the Fixed-Base signal and the Baseline Motion signal, while other set of plots included the Baseline Motion signal as well as the Modified Motion signal. The PSD method was used to draw conclusions about the different pilot control techniques for the different platform motion conditions. The conclusions were not totally taken from this method since this was not the main evaluation method used in this study. The authors assessed most of the results from subjective comments and Cooper-Harper ratings.

Groen and Bos [Groen and Bos, 2008] used PSD techniques to study what bad simulator motion is. The study was focused in simulator sickness; nevertheless the technique can also be used for simulator evaluation. The experiment was conducted in the TNO driving simulator. The simulator did not use tilt coordination due to visual constraints, so sustain cues are not present in the simulation. Two experiments were performed. The task of the first experiment was to drive the simulator using new driver support systems (different force feedback configurations on the car gas pedal) in a scenario that contains city and rural driving. Three sessions of 20 to 30 minutes were performed for each one of the 41 participants, changing the configurations between sessions (two different force feedback settings and one setting without force feedback). The second experiment consisted of highway driving using cruise control set to 120 km/h for 12 minutes. During this task 14 unexpected lateral disturbances occurred. Only 17 individuals participate in this experiment. The assessment of simulator motion was made based on the PSDs of the motion cues signals. The study was made for translational motion cues since the authors stated that these are the cues that hexapods mostly fail to correctly reproduce. The PSDs of the specific force signals of the vehicle and motion platform were calculated for the three axes (x, y and z). Then the evaluation of the motion quality is made based in the frequency content of the vehicle dynamics that lacks in the moving platform dynamics.

### Statistical Analysis of Mathematical Variables

The statistical analysis is used by designers to check performance of individuals in simulators and then assess motion filter based in the individual's behaviour. The analysis methods that authors use in this evaluation method depend from study to study. This evaluation is normally used to check the advantages of motion in simulators and to obtain a balance of the needed motion cues in certain manoeuvres, since until now is impossible to have one to one simulations.

Root Mean Square (RMS) and Standard Deviation (STDV) analysis are what authors usualy use. For example, Reid and Nahon [Reid and Nahon, 1988] used the RMS of the actuator length to conclude about simulator motion. Schroeder [Schroeder, 1999] and Beykirch et al. [Beykirch et al., 2007] draw conclusions from the RMS of helicopter control inputs. Siegler et al. [Siegler et al., 2001] used the RMS and STDV of four manoeuvre characteristics: linear velocity, angular velocity, lateral acceleration and distance to road side in their study. Some studies [Siegler et al., 2001, Greenberg et al., 2003, Brünger-Koch et al., 2006b] used an analysis of variance (ANOVA) to draw conclusions about the effect of motion in some variables like heading error in Greenberg et al. [Greenberg et al., 2003]. Absolute evaluations were also found for this evaluation method, like in Brünger-Koch et al. [Brünger-Koch et al., 2006a, Brünger-Koch et al., 2006b] where a real driving section was included in the study for comparison purposes.

This method helps to obtain conclusions about the benefitial effect of having motion in a simulator, like the vehicle control conclusions taken by Greenberg et al. [Greenberg et al., 2003].

We can see which motion cueing algorithm delivers a better driving/flying experience by analysing specific manoeuvres. Brünger-Koch et al. [Brünger-Koch et al., 2006b] analysed specific moments in a braking manoeuvre to assess the driving performance of a simulator tuned with different parameter sets. It is also possible to draw conclusions about the pilot/driver control input performance (mostly in terms of the input amplitude), like it was done in references [Schroeder, 1999, Beykirch et al., 2007].

With this evaluation method, it is possible to compare manoeuvre characteristics of a certain vehicle. Using this, motion cueing evaluation is done by comparing the manoeuvre characteristics of the simulator against the same characteristics in a real vehicle. One of the main problems of using this method is that these characteristics change from vehicle to vehicle and from manoeuvre to manoeuvre. Therefore is not straightforward to know which variables to choose and what type of analysis one should perform to obtain significant results regarding motion cueing evaluation (or other type of study that we want to do, like the impact of motion in driver/pilot performance). To effectively use this method, we need to know manoeuvre and vehicle specifications. This makes the Statistical analysis method too specific to use in a more general evaluation of a motion filter. In this context, general is related with a motion cueing algorithm that does not have a specific purpose, e.g. the Classical Washout algorithm is more general than the Lane Change algorithm (used only in driving simulators in lane change simulations).

The following authors used this evaluation method in the subsequent way:

Reid and Nahon [Reid and Nahon, 1988] performed a study to evaluate three different kinds of motion cueing algorithms like it was described in section 3-2-1. The authors used this evaluation method to study the simulator motion and the pilot's control activity and performance. For simulation motion, a plot of the Average RMS actuator length for each motion cueing configuration was analysed, while for the pilot's control activity and performance a plot of the touchdown rate of descent was analysed.

**Schroeder** [Schroeder, 1999] performed a study regarding the need of motion in helicopter flight simulators and the requirements for a motion platform of this kind. The experiments were conducted in the NASA Vertical Motion Simulator for three types of motion cues. These were yaw cues, vertical cues and roll-lateral cues. The yaw cue experiment had three tasks:

- 15° yaw rotational capture: The pilot controlled the vehicle only in the yaw axis. The objective was to obtain a north heading from 15° yaw offsets from the east or west. The task should be performed as fast as possible. The desired performance was to perform the manoeuvre and stay within  $\pm 1^{\circ}$  about north with a maximum of two overshoots. Six captures had to be performed for each motion configuration, alternating between west and east.
- 180° hover turn: In this manoeuvre the pilot had to perform a 180° pedal turn over a runway in 10 seconds. Only pedals were used as control input. The desired performance was to stabilize at the end of the turn within ±3° in 10s. Six 180° turns were performed.
- Yaw rotational regulation: The task was to perform a fast 9-ft climb while attempting to maintain a constant heading. Full vertical, yaw-rotational and lateral-roll motion

were allowed. The desired performance was to do the task as fast as possible while maintaining a  $\pm 1^{\circ}$  heading direction about north.

Each task had four different configurations. For the first task, two plots that use RMS analysis were presented. The first one was related to the number of overshoots that the pilots did during the task. The graphic compared the number of over shoots for four different motion configurations. The motion configurations were: no motion situation, the situation with only translational motion, the situation with only rotational motion and the full motion situation. The second plot showed the RMS of the rudder pedal rate for the same motion conditions. Schroeder [Schroeder, 1999] also assessed results from time histories of some variables and from subjective evaluations. The second and third tasks were assessed the same way as the first task. The vertical cue evaluation was obtained by three different experiments. For each of these experiments, ten different configurations of filer gain and natural frequency were used. The first experiment did not use any RMS evaluation method and so will not be described in this section. The second experiment task required the pilot to null the error present in the compensatory display. The moving target moved according to a sum-of-sines input, while the vehicle was perturbed by a sum-of-sines disturbance. The disturbance was created in a way to prevent that the pilot separates the motion of the target (visual) from the motion generated by the disturbance (visual and vestibular). The desired performance for this task was to keep the error one-half the height of the target vertical tail for half of the total run time. The target was at 100 ft in front of the aircraft with a vertical tail height of 3 ft. The six pilots that participated in this study had to fly all the configurations. Two different open-loop pilot-vehicles describing functions were analysed, because the sum-of-sines functions for the target and for the disturbance were independent. The first loop was the target following loop. For this loop, two bar plots were used for result assessment. The first contained the RMS and STDV of the crossover frequency for all the ten different configurations. The second plot contained the RMS and STDV but for the phase margin instead of the crossover frequency. The second loop was relative to disturbance rejection. The plots generated for this loop were the same. The statistical analysis assessment for this experiment finished with a plot showing the total vertical tracking error for the ten configurations. This experiment assessment was also completed with subjective evaluation. The third vertical cue experiment contained two tasks:

- Altitude repositioning task: The objective was to double or halve the initial altitude of the vehicle. The initial altitudes were 15.6, 18.3 and 21.0 ft. Altitude was the only thing that the pilot was able to change. No time or adequate performances were introduced in this study.
- Altitude-rate control task: In this manoeuvre, pilots had to climb or descent at a fixed rate of 3 ft/s. The climbs had an initial position of 7.5 ft and a final position of 42.5 ft, while the descends had an initial position equal to the climbs final position and a final position equal to the climbs initial position. These altitudes allowed a one to one simulation.

Five pilots participated in this experiment, doing one or two sessions per day, each of them lasting one to two hours. Two motion conditions were evaluated, one with motion and one

without motion. Three levels of visual detail were used (low, medium and high). Two figures were shown for the first task. The first one presented the mean percent repositioning error for three (of five) experimental factors: vertical motion presence, repositioning direction and initial altitude. This mean is defined in [Schroeder, 1999]. The data of this figure is presented in bar plots, each bar regarding one experimental factor. The second figure contained the final altitude of the climbs or ascents for different initial altitudes and different level of detail visuals. The second task contained two figures. The first figure represents the vertical speed for the two different types of motion and the second figure represents the mean vertical speed versus the vehicle altitude either for the climb and descent situations. This experiment conclusion was obtained from these graphics. The last experiment of this report had to do with roll-lateral cues. In this experiment the pilot had to do constant-altitude lateral side steps between two points 20 ft apart from each other. The desired positioning performance was  $\pm 3$  ft about the desired final hover point, while the adequate performance was  $\pm 8$  ft. Eleven different motion configurations were tested. These configurations were obtained by varying two different gains, K<sub>lat</sub> and K<sub>roll</sub>. Three test pilots were used in this study. The experiment was evaluated from three figures. The first one showed a plot of the pilot positioning performance described before, for the eleven different performances. The second plot contains information about the RMS of the lateral stick position for the eleven conditions while the last figure contain information about the RMS of the lateral stick rate for the same conditions. In this experiment, also subjective evaluation methods were used.

Siegler et al. [Siegler et al., 2001] analysed the roll of motion in car simulation. Two experiments were done to obtain the results. The Renault Dynamic Driving Simulator was used to conduct the experiments. The task of the first experiment was to execute a car braking manoeuvre. Participants had to drive the simulator on a country road that contained signposts. During the run, subjects had to make eight consecutive braking and had to stop as near as possible of the signposts. For the first four braking, the deceleration started where it looks best for the subject, while for the other four, the deceleration spot was indicated by specific signposts. A speed of 80 km/h had to be reach before braking. This experiment was executed by eleven individuals, three females and eight males. Two conditions were used during the experiment: a configuration where platform dynamics were used and a static configuration. These configurations were denominated respectively, ON and OFF. The analysis was focused in the first seconds of the driver action on the brake pedal. Two plots and one table were used for assessment. The first plot shows the deceleration profiles of one subject for the two motion configurations, while the second plot shows the deceleration mean in the first three seconds of the manoeuvre for both motion configurations. The table contained the mean and standard deviation of manoeuvre characteristics for both configurations. The characteristics are: initial velocity, initial distance to target, final distance to target, maximal deceleration and the mean onset jerk. An ANOVA study was used in this data to check significance levels. For this experiment, the authors decided to divide the data into two groups, to see the influence of starting the experiment with the ON or with the OFF condition. Two plots where presented. The first plot contains the first run in the simulator for both groups and shows the average and standard deviation of the maximal deceleration done by these groups. The second plot shows the same thing but for the second simulator run. The task of the second experiment involved cornering. Subjects had to drive around a square city block. The manoeuvre had to be done twice, so eight curves were done per trial. Four configurations were used in this experiment:

- ON configuration: translational motion in x and y; rotational motion around x, y and z.
- LA configuration: translational motion in y; rotational motion around x and z.
- LO configuration: translational motion in x; rotational motion around y.
- OFF configuration: no motion.

The mean driving trajectories were shown in an x and y plot for all the motion configurations. From these plots is possible to see the driving approaches for each configurations. Four plots containing the mean, standard error and standard deviation of four manoeuvre characteristics for all motion configurations were shown. The manoeuvre characteristics are: linear velocity, angular velocity, lateral acceleration and distance to road side. The authors used the data to take conclusions about the influence of lateral cues on driver's behaviour.

Greenberg et al. [Greenberg et al., 2003] performed a study about the effects of lateral motion cues in driving simulators. Although this paper is not a motion cueing assessment study, it is interesting to reference it since the idea can be adapted for motion evaluation. Two experiments were done at the VIRTTEX simulator. For the experiments, a 2000 Ford Taurus cabin was used. The first experiment objective was to see motion cueing effects in secondary tasks. The results of this experiment were obtained from six participants. The used secondary tasks in this experiment are:

- Radio tuning: Subjects has to find a specified radio station using a switch on the radio.
- Climate control adjustments: Subjects had to adjust the air system in the car by adjusting three dials into the experiment required position.
- Incoming calls: Subjects had to answer incoming calls using hand-held or hands-free cellular phones.
- 10-digit dialling: Subjects had to call to the voicemail service using hand-held or handsfree cellular phones.
- Retrieving and responding to voicemail: Subjects had to retrieve a specific message from the voicemail server and then had to reply it.

Two different cueing configurations were used, one without motion a one motion configuration based on a classical washout algorithm. The first measure used to evaluate motion effects was the number of lane violations per trial for each secondary task. A plot containing this information was shown. An analysis of variance was made to show the effect of motion in the secondary tasks. In this analysis, secondary tasks were divided into four groups. Radio and climate control were referred as "trad", hands-free tasks were in the "hands free" group while hand-held tasks were in the "hands held" group. Driving without secondary task was denominated by "norm". The interactions of these secondary task groups with the motion

conditions were graphically presented. Another measure used in this experiment was the heading error. In [Greenberg et al., 2003] heading error is defined as "the difference between the instantaneous roadway tangent and the current vehicle heading measured in degrees". This measure was also evaluated using an analysis of variance and the results were graphically presented with the secondary tasks divided in the described groups. In the second experiment participants had to follow a certain path defined by cones in a virtual world. The cones were placed on the road in pairs with a lateral separation of 9.5 ft and a longitudinal separation of 12.5 ft. The virtual world was a straight flat road with a wide of 9.5 ft. For this experiment, 24 subjects were used. The objective in this experiment was to measure the effect of lateral motion magnitude on the driver disturbance rejecting ability while performing the manoeuvre described before. Cruise control was used to maintain a constant speed of 60 mph during the tests. Trials were structured in 4 blocks of 24 manoeuvres each. Each block contained 8 training manoeuvres and 16 disturbance rejection manoeuvres. During the disturbance rejection manoeuvres a 2 second lateral wind gust was applied to the vehicle. Four different wind gust configurations were used during the trials with peaks of -55, -25, +25 and +55 mph. For this experiment a positional motion drive algorithm with four different levels of scaling was used. The scaling levels were: 0%, 25%, 50% and 70%. Two different measures of lateral control were used in the evaluation. The first measure was the RMS heading error which is defined by the "difference between the instantaneous vehicle yaw angle and the heading angle of the cone path center". The second measure was the RMS path error which is defined by "the difference between the lateral position of the vehicle CG and the lateral position of the cone path center". An analysis of variance was used in these measures and the results were graphically presented. The plots shown represent the two different measures used versus several variables, like for example the different scale factors or the different subjects in the experiment. The plots used in [Greenberg et al., 2003] will not be described in detail here since they are numerous and that would involve a deep description already done in the paper. The study was used to check how motion influence driver vehicle control.

Brünger-Koch et al. [Brünger-Koch et al., 2006a] performed a motion assessment study, using objective evaluation and subjective evaluation. The subjective evaluation of this study will be described in the respective section. The experience was divided in real world driving and simulated driving in a 6 DoF simulator. The real world driving consisted of a 10 to 15 minutes drive in a road with several curves and areas with different speed limits. In the simulator trials, three different scenarios were presented. The first scenario (S1) was an exact copy of the real world driving. This was included to directly assess driver behaviour differences. The second scenario (S2) was a curvy road with different velocity limits. This scenario was included with the aim of evaluating car lateral control in the simulator. The last scenario (S3) was focused in longitudinal control, and was based in a long straight section with different speed limits. Three classical washout configurations were used in the simulator, which were denominated by the authors by parameter set a, b and c respectively. Parameter set 'a' was optimized for longitudinal manoeuvres, parameter set 'b' was optimized for curve driving and parameter set 'c' was tuned to handle both longitudinal and lateral driving manoeuvres. Twelve subjects (eight male and four female) participated in the experiment, with an age varying from 25 to 50 years. The objective evaluation starts with the comparison of the real driving task with simulator driving in scenario S1. Four bar plots show the results of this comparison. The first plot shows the average speed in straight sections for the three motion cueing configurations in scenario S1 and for the real driving section while the second plot contains the standard deviation of the speed in straight sections for the same situations of the first plot. The other two plots represent respectively the standard deviation of the lateral position and the steering wheel reversal rate in straight sections for the tree motion configurations and the real drive situation. Scenarios S2 and S3 were used to analyse the lateral and longitudinal control. Analysis was made for the average speed and the standard deviation of speed. Only three bar plots were shown for these driving scenarios. The first plot contains the standard deviation of the lateral position in straight sections of scenario S2 for the three motion configurations. The other two plots are relative to scenario S3. They show respectively the standard deviation of the average speed and the steering wheel reversal rate for all the parameter sets. The data used in these plots was taken from different track sections for each of them. The conclusions were taken from these assessments as well as from the subjective assessments.

Brünger-Koch et al. [Brünger-Koch et al., 2006b] evaluated three classical washout configurations in a braking manoeuvre. Two of this configurations contained specific tuning for this type of manoeuvre (parameter set 'a' and 'c' in [Brünger-Koch et al., 2006a]) while the other configuration was badly tuned (parameter set 'b'). The simulator driving behaviour was compared with real driving behaviour, which transforms this study in an absolute evaluation. Two virtual courses were described in this study. The first course forces the driver to perform six braking sequences. Three different approaching speeds were used (50, 80 and 120 km/h). The drivers had to perform a full stop. For comparison purposes, the second course was similar to the real driving situation. In this case the driver only had to stop due to traffic. Twelve subjects participated in the experiment, each of them driving the two different courses three times, each time with one of the three parameters set. These motion configurations were presented in a random order. The authors pointed out three important moments in a braking manoeuvre: the time when the driver releases the gas pedal (t0), when the braking is initiated (t1) and when the vehicle stops (t2). The following characteristics can be measured for posterior data analysis: approaching speed (v), stopping time (ST), stopping distance (SD), time to collision (TTC) transition time (TT) and the maximum deceleration (amax). The analysis of the cueing configurations was based in six bar plots. Every bar plot contains the mean and standard deviation of a certain braking manoeuvre characteristic for the all the motion parameters for the two virtual tracks and also for the real world. The plotted braking manoeuvres characteristics are: approaching speed at t0, stopping distance at t0, stopping time at t0, time to collision at t0, transition time and maximum deceleration. Further evaluation continued with a two-way analysis of variance. Two analysis of variance were shown in the paper. The first one checked the effects that the two virtual scenes had with the different parameter sets (track vs parameter set). A table was presented with the values of the analysis for the six different braking manoeuvre characteristics described before. Two plots were also shown containing the mean of the stopping time at t0 and the mean of the maximal deceleration for the two different tracks and the three parameter sets. The second analysis of variance was regarding the effects of speed for the different parameter sets (speed vs parameter). The results were presented in the same way as the ones for the first analysis.

Beykirch et al. [Beykirch et al., 2007] conducted a study to evaluate the suitability of a new simulator physical design in a helicopter simulation. The task of this study was to perform constant altitude side-steps between two targets. At the start of each trial, the individual had

to acquire a steady state position at the starting target. After that, the individual pressed a button of the centre stick which would make the target move to a new position. The pilot had then to do a side-step in order to move to the new position. When reaching the final position, the pilot had to hover for about 5 sec before pushing the button of the centre stick to sign the end of the trial. Twelve conditions were created by varying two different gains,  $K_{lat}$  and  $K_{roll}$ . The RMS analysis was used to create four plots. The first two plots contained the RMS of the lateral stick position and lateral stick rate respectively. These values were evaluated for the twelve conditions. The third plot contained the RMS of the value of the lateral helicopter position for the hovering that occurred at the end of the trials for all the test conditions. The last plot shows the RMS of the lateral position versus  $K_{lat}$ , for three different  $K_{roll}$  curves. Here, this motion evaluation method was used to assess pilot workload for the different motion configurations. The study was completed with a subjective evaluation.

Colombet et al. [Colombet et al., 2008] used this method to assess some results regarding their study of motion cueing impact in the driver's behaviour. This study was already referenced in section 3-2-1. Two tables contain the results of this analysis. The first table contains the mean and standard deviation of the driven vehicle speed, the mean and standard deviation of the speed difference between lead vehicle and driven vehicle and the mean and standard deviation of the platform longitudinal acceleration. This information was shown for all the subjects and all the motion cueing configurations. The second table shows the mean of the simulated vehicle and platform accelerations for every acceleration step of the lead vehicle (nine speed variations in total). The values are shown for the three motion cueing algorithms as well as for the difference between the classical algorithm values and the adaptive algorithm values.

# 3-3 Subjective Evaluation

Subjective evaluation does not rely on mathematical functions or signal comparison, but on individuals opinion and "feeling". Therefore this evaluations are are a lot dependent on the capacity of the subjects to analyse the situations proposed by the experimenter. It is also also influenced by external factors that can be affecting subjects (like physical or emotional problems). Subject tendency to suffer from simulator sickness it could be also an issue, since subjects that suffer from it tend to give poorer ratings to the motion cueing algorithms than subjects that do not suffer severe sickness [Watson, 2000]. The subjective evaluation studies are structured like in Figure 3-7.

## 3-3-1 Rating Scales

In this type of evaluation, the individual is asked to rate the simulator motion based on a rating scale given by the experimenter. The scales should be consistent, easy to use and not ambiguous. The normal procedure in this method is that subjects rate the motion cueing algorithm after experiencing the simulation. Examples of used rating scales in flight simulation are the Cooper-Harper [Cooper and Harper, 1969] handling characteristics scale and the NASA Task Load Index (TLX) [Hart and Staveland, 1988] scale.

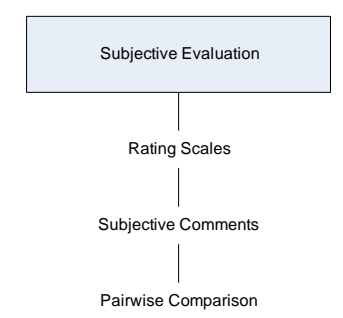


Figure 3-7: Subjective evaluation structure.

The Cooper-Harper [Cooper and Harper, 1969] rating scale is a one-dimensional rating scale and is used to obtain the pilot rating regarding the handling qualities of an airplane. This rating scale is also used in flight simulators evaluation, so that designers can compare aircraft pilot ratings with simulator pilot ratings. The individuals after a flight task evaluate how the flight was by choosing the correct Copper-Harper rating. Figure 3-8 contains the Cooper-Harper rating scale description. In literature it was found that references [Schroeder, 1999, Guo et al., 2003, Soparkar and Reid, 2006, Beykirch et al., 2007] used the Cooper-Harper rating scale.

The NASA TLX [Hart and Staveland, 1988] scale is a multi-dimension rating scale. It has six subscales and is applied in three different steps. In the first step, the individuals have to evaluate by pair-wise comparison the contribution of the parameter being evaluated in each subscale for their mental load. This assigns a weight to each subscale. The second step consists of rating each subscale. The third step consists of combining the weights with the ratings of each subscale. This process is made for each experimental condition. Figure 3-9 and Figure 3-10 contain respectively the NASA TLX subscale description and the NASA TLX rating sheet that individuals have to fill. Telban et al. [Telban et al., 2005] used this rating scale in their study.

There are rating scales that are used in conjunction with questionnaires [Brünger-Koch et al., 2006a, Fischer and Werneke, 2008, Wentink et al., 2008b]. This type of evaluation helps to answer questions that motion filter engineers may have about their filter design or behaviour.

The other studies present in this section use different rating scales than the ones proposed before (Copper-Harper and NASA TLX). Nevertheless they work in a similar way but adapted to the reality of their study (Copper-Harper and NASA TLX are normally used for flyght analysis). Analysis of variance can also be used in this method to check the significant levels of the rates obtained from the subjects like in Fischer and Werneke [Fischer and Werneke, 2008].

Absolute evaluations can also be done using this method. Most of the times, this is done by asking the subject to compare the simulation motion with the real vehicle motion, like in references [Reid and Nahon, 1988, Brünger-Koch et al., 2006a, Wentink et al., 2008b].

Authors use rating scales to conclude about which motion filter delivers more realism to the simulation [Reid and Nahon, 1988, Molino et al., 2003, Guo et al., 2003, Soparkar and Reid, 2006, Wentink et al., 2008b]. Workload conclusions can also be obtained with this evaluation method like in Telban, et al. [Telban et al., 2005]. The questionnaires included in [Brünger-Koch et al., 2006a, Fischer and Werneke, 2008, Wentink et al., 2008b] can

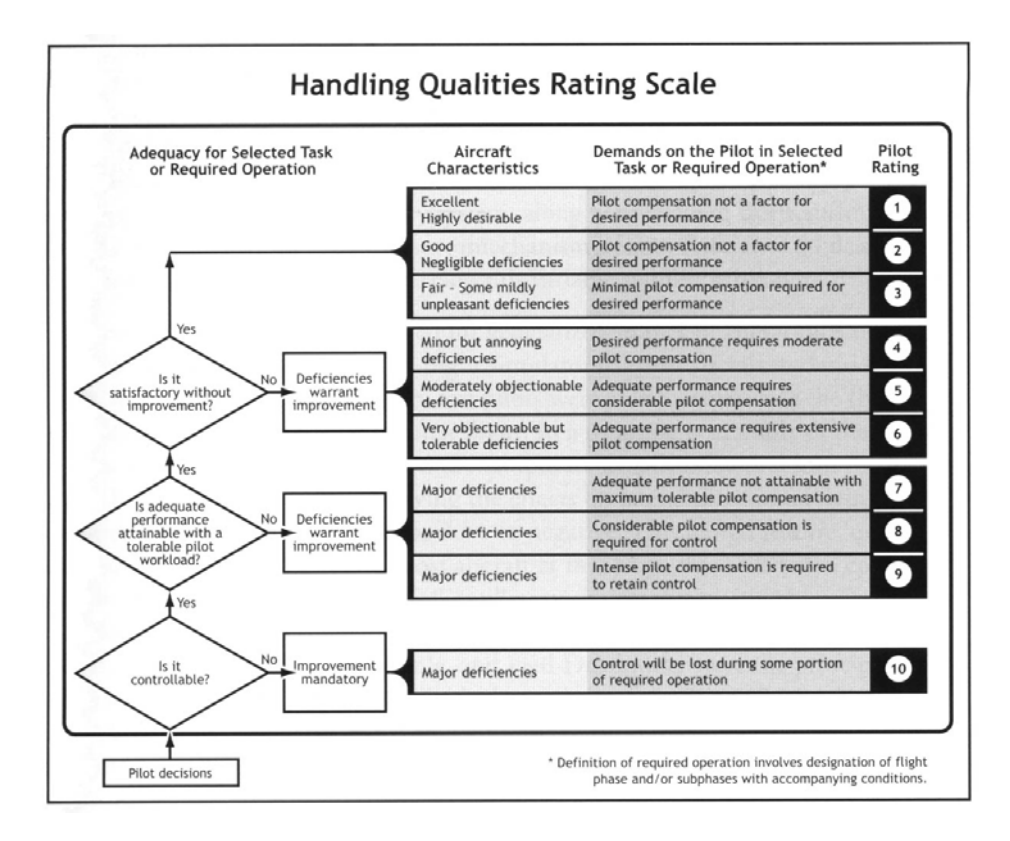


Figure 3-8: Handling qualities rating scale.

NASA TLX rating descriptions									
Title	Endpoints	Description							
Mental demand	Low, High	How much mental and perceptual activity was required? (e.g. thinking, deciding, calculating, remembering, looking, searching, etc.) Was the task easy or demanding, simple or complex, exacting or forgiving?							
Physical demand	Low, High	How much physical activity was required (e.g. pushing, pulling, turning, controlling, activating, etc.)? Was the task easy or demanding, slow or brisk, slack or strenuous, restful or laborous?							
Temporal demand	Low, High	How much time pressure did you feel due to the rate or pace at which the tasks or task elements occured? Was the pace slow and leisurely or rapid and frantic?							
Effort	Low, High	How hard did you have to work (mentally or physically) to accomplish your level of performance?							
Performance	Good, Poor	How successful do you think you were in accomplishing the goals of the task set by the experimenter (or yourself)? How satisfied were you with your performance in accomplishing these goals?							
Frustration Level	Low, High	How insecure, discouraged, irritated, stressed and annoyed versus secure, gratified, content, relaxed and complacent did you feel during the task?							

Figure 3-9: NASA TLX rating descriptions.

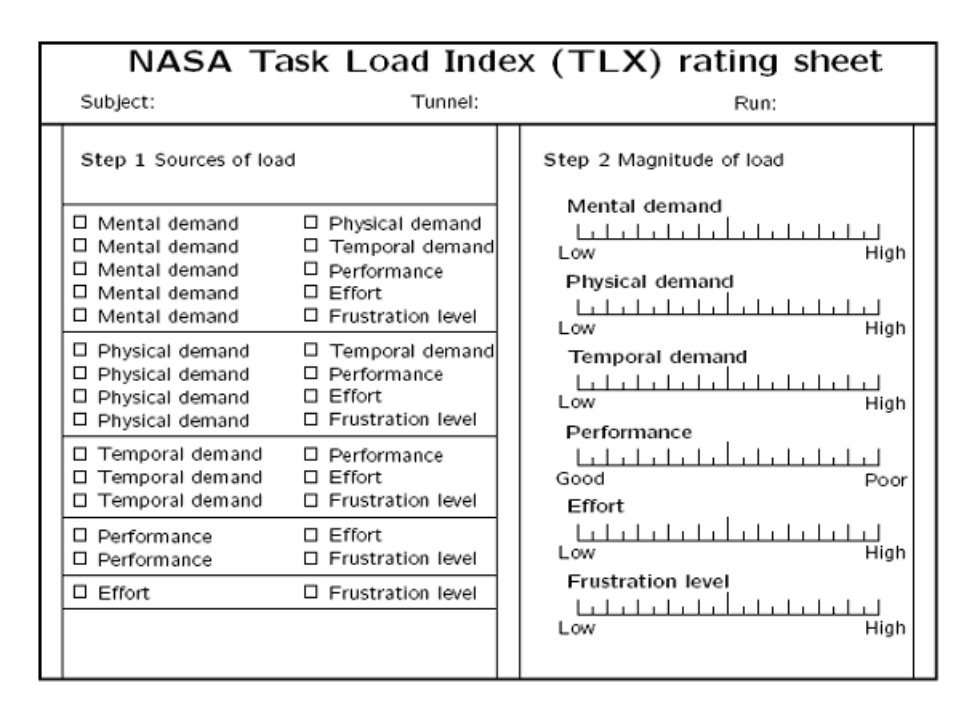


Figure 3-10: NASA TLX rating sheet.

be used to draw conclusions about specific situations, like for example questions about car handling in Brünger-Koch et al. [Brünger-Koch et al., 2006a].

The rating scale method is very useful since motion filter designers can obtain the opinion of subjects regarding the performance of motion filters. One of the biggest shortcomings of objective measurements has to do with the difficulty to know how the human perception system will react to the motion filter. This makes the evaluation difficult since improvements in a motion cueing filter that are visible, for example in a graphical comparison, may not be felt by the human being. With subjective ratings, the human perception system is used in the evaluation and then one can obtain results that are more meaningful. Nevertheless effectiveness of this method depends of many parameters like: subject susceptibility to motion sickness, mood of the subject in the trial day, capacity of the subject to distinguish between different solutions and capacity to give an objective and conscious answer while rating the motion filter. To have better results, designers should give to the subject a rating scale that is consistent and not ambiguous.

The following authors used rating scales in their studies:

Reid and Nahon [Reid and Nahon, 1988], in continuation of their study to evaluate three motion cueing algorithms for the Flight Research Simulator of the Toronto University, used subjective rating scales to assess most of their conclusions. The experimental design was already described in section 3-2-1, so one will only focus on the subjective evaluation method used by the authors. Two rating scales were used in order to obtain information about the simulation motion quality. The first one was the UTIAS [McDonnell, 1969] rating scale while the second was the MIT [Bussolari et al., 1986]. Figure 3-11 and Figure 3-12 show the UTIAS and the MIT rating scale respectively.

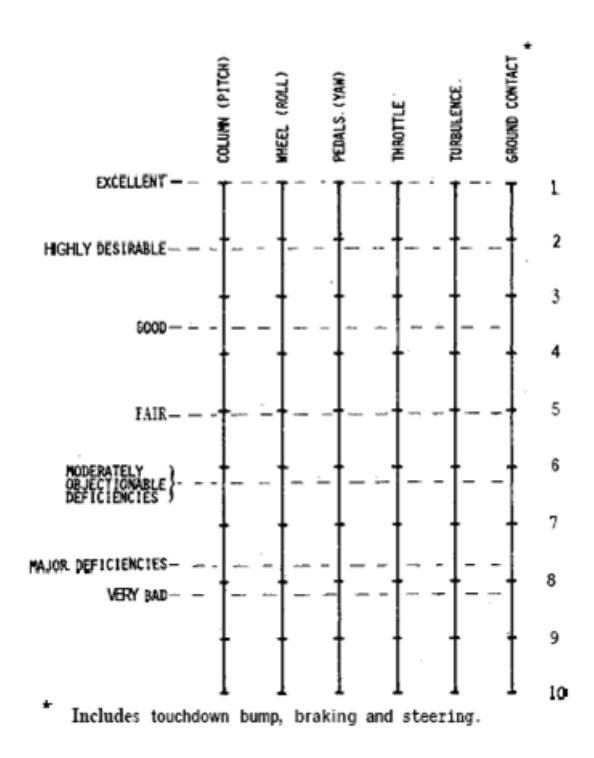


Figure 3-11: UTIAS rating scale [Reid and Nahon, 1988].

Attribute	Rating		Response	
SMOOTHNESS:	extremely smooth-comparable with fixed base	extremely jerky limit of tolerance		
SENSE:	definitely correct as in aircraft	totally reversed	<u> </u>	
AMPLITUDE:	no motion experienced	at least twide that expected		
PHASE LAG:	none experienced	at least 180°	ì	
DISCOMPORT;	none experienced	cannot continue		
DISORIENTATION:	none experienced	cannot perform		
OVERALL:	excellent	extremely poor		

Figure 3-12: MIT rating scale [Reid and Nahon, 1988].

Pilots were asked to compare the simulator motion relative to the real aircraft motion and not to motion in other simulators. This makes the subjective evaluations in [Reid and Nahon, 1988] absolute. The results of the rating scales were presented in two plots and four tables. The first plot showed the pilot ratings, using the UTIAS scale, of the response to wheel inputs for every motion configuration. The second plot contained the overall pilot ratings, using the MIT rating scale, for all the motion cueing configurations. The first table showed a variance analysis for the UTIAS rating scale while the second and third tables are a summarization of the of the variance analysis for the UTIAS and MIT rating scales respectively. The last table consists of a summary of the average pilot ratings, coming from the best rating motion cueing configurations to the worst motion cueing configurations. The authors pointed that more detailed results of this study can be found in [Reid and Nahon, 1986].

Schroeder [Schroeder, 1999] used rating scales in the helicopter flight simulation study described in section 3-2-2. For the yaw cue experiment, pilots had to fill a sheet after each run of each task. Three different rating scales were present in this sheet. First pilots had to rate the task level of required compensation according to the following definitions taken from the Cooper-Harper Handling Qualities Scale [Cooper and Harper, 1969]: not-a-factor, minimal, moderate, considerable, extensive and maximum-tolerable. Numerical values were assigned from -1 to 4 respectively. The next scale, rated the motion fidelity in three different categories: Low fidelity, where the cues differences between real flight and simulated flight were noticeable and objectionable; Medium fidelity, where the cues differences between real flight and simulated flight were perceived but not objectionable; High fidelity, where motion cues differences between real flight and simulated flight were minimal. These definitions were given by Sinacori [Sinacori, 1977] and were slightly modified by Schroeder [Schroeder, 1999]. The last scale had to do with perceived translational or rotational cues in the simulator. Pilots had to assign zero if any of these cues were not perceived. The response of the pilots for these three questions had to be based in real flight experience, making this an absolute evaluation. The performed data analysis was equal for the three tasks. Four plots were created based in the subjective questions described before. The y axis of the first plot contained the values of compensation, while the x axis contained two points, one for the no rotation condition and other for the rotation condition. Two lines were shown in the plot, one for the translational condition and other for the no translational condition. The second plot showed a fidelity plot, containing the fidelity levels in the y axis and the two rotational situations in the x axis. This plot also contained two lines, one for each translational motion situation. The third plot contains information about the percentage of time that lateral translational motion was reported by pilots. Again this plot contains the rotational information in the x axis and the translational information separated in two different lines in the plot. The fourth plot is equal to the third one, but now containing the percentage of time of rotational motion detection instead of translational one. The first vertical cue experiment consisted in increasing the aircraft altitude in 10 ft. The pilot had to visually place the horizon between two red squares on an object which was 50 ft away. The red squares had a height of 0.75 ft. The 10 ft 1:1 bobup was performed in the NASA Vertical Motion Simulator. The desired performance of this task permitted only two reversals outside the red region before stabilization. The adequate performance was defined by permitting only two reversals outside the top and bottom of the horizontal objects placed above and under the red squares. These objects were 2.25 ft apart. The task had to be performed as fast as possible. Five manoeuvres were performed for each of the ten motion configurations. In this experiment, a baseline condition was set at the beginning of the test, so the subjective measurements obtained in this study will be relative. The pilot rated the motion-fidelity according to the Sinacori [Sinacori, 1977] definitions given before. The subjective analysis contained also some questions answered by the pilot regarding aircraft characteristics, the awareness of their performance, and the compensation needed to perform the task. The results of the motion-fidelity rating were shown in a Sinacori [Sinacori, 1977] criterion figure similar to the one of Figure 3-2. The figure contains the pilot ratings for each pilot and for each condition. For the second vertical experiment described in section 3-2-2 the pilots had to rate the motion-fidelity of each configuration like they did in the first vertical experiment. The results were again present in a figure similar to Figure 3-2. All the configurations are shown in the figure as well as the motion-fidelity ratings that the pilot has given to the configuration. A new rating called "split" was added since pilots sometimes have given inconsistent ratings in repeated runs for the same configuration. The third vertical experiment contained in this study does not contain subjective evaluations. The Roll-Lateral experiment explained in section 3-2-2 also contained subjective ratings to evaluate the motion cues in the simulator. Pilots were asked to rate the task according to motion-fidelity and handling qualities. Motion-fidelity was again rated according to the Sinacori [Sinacori, 1977] criteria while for handling qualities the Copper-Harper [Cooper and Harper, 1969] rating scale was used. For presentation purposes, numbers were given to the motion-fidelity ratings. Values 1.2 and 3 were assigned respectively to Low, Medium and High. A plot containing the  $K_{roll}$ versus K<sub>lat</sub> is shown with the numerical motion-fidelity ratings given by the pilots. A second plot of the same type is present in [Schroeder, 1999], but containing the Cooper-Harper ratings instead of the motion-fidelity ratings. A third plot was included equal to the first one, but containing lines that represent the boundaries that separate each motion-fidelity area. These area definitions come from the proposed modifications by Schroeder [Schroeder, 1999] to the Sinacori [Sinacori, 1977] criteria.

Spenny et al. [Spenny et al., 2000] discovered angular artefacts in their motion controller analysis for a dynamic flight simulator. Because of that reason a subjective study was conducted at the Dynamic Environment Simulator at Wright Patterson AFB, in order to see if these artefacts were disconcerting or not. The artefacts are obtained from Gx or Gy pulses. In this experiment, subjects were feed with a series of  $0.75~G_z/s$  onset ramps until reaching steady accelerations of 1.4, 2, 4, 6 and 8  $G_z$  as well as a control condition of 1  $G_z$ . Each of these steady accelerations lasted 12 seconds. During these seconds a  $G_x$  or  $G_y$  pulse was felt by the subject. The pulse was sustained for the 4, 6 and 8  $G_z$  situations and quick for the other situations. The study contained 26 profiles, distributed in four different experiments. Each of these experiments had one fixed factor ( $\alpha$ =4,  $G_z$ =2 or 4 and  $G_x$ =0.5) so that the assessment could be performed for the non-fixed factors. The study was made recurring to 7 subjects. They had to rate the experiences recurring to the artefact response rating (ARR) scale. This scale was defined in [Spenny et al., 2000] in the following way:

- 0 = did not feel at all,
- 2 =noticed it,
- 4 = felt but not disruptive,

- 6 = felt and caused some distress,
- 8 = felt and caused significant discomfort,
- 10 = totally unacceptable.

The results were shown in four bar plots, one for each experiment. The plots contain the mean ARR rating for the two non-fixed parameters of the experiment. Two tables were included to summarize the findings of the  $G_x$  and  $G_y$  analysis.

Molino et al. [Molino et al., 2003] evaluated two different motion cueing algorithms for car simulation in a 3-DOF driving simulation. The first motion cueing algorithm, denominated in [Molino et al., 2003] by vector substitution method, was based on replacing the total force vector of the car with gravity when sustained cues are not available (this method is normally denominated by tilting coordination). The second motion cueing algorithm, denominated in [Molino et al., 2003] by leaning vehicle method, uses the model of a bicycle or a motorcycle and correctly leans the vehicle in curves like it happens in two wheels vehicles. This experiment objective is similar to the one proposed by Heyde and Riecke [von der Heyde and Riecke, 2001] in which the "fun ride" approach of motion would be compared with the "engineering" approach. The study started with 14 participants, but two had to be left out which lead to a final test population of 12 subjects, 6 males and 6 females with an age average of 32.6 years. The experiment took place in the FHWA Highway Driving Simulator (HDS) which consists of a 1998 Saturn SL sedan car cabin mounted on a motion base. The screen is decoupled from the cabin and contains an 88 degree field of view. The vehicle dynamics model is provided by Illusion Technologies International (ITI), Inc. and contains simulation of the following five components: engine, transmission, steering, suspension and brakes. The experiment consisted of three driving condition for each subject:

- Steering condition: Each subject steered the vehicle trough 16 random curves at a constant speed of 45 mph (cruise control in the vehicle was on).
- Riding condition: Each subject sat passively in the seat while the vehicle drove trough the same series of 16 curves existent in the steering condition at a constant speed of 45 mph.
- Blindfolded condition: Equal to the riding condition, but this time the subject worn a blindfold.

During the trials, the passenger seat was occupied by an experimenter who carried all the experiment necessary paperwork. Four different types of curves were present in the simulation: right hand with 30 and 10 degrees of curvature and left hand with 30 and 10 degrees of curvature. All curves had a 90 degree deflection angle, zero superelevation and high luminance pavement markings. The simulations were carried out in a night time environment. Each driving condition contained 16 trials (four different curve types paired with two different motion cueing algorithms which gives 8 combinations, each one with one repetition which gives the final 16 trials per subject). The subjects were divided into 3 different groups, each group starting with a different driving condition. For the first two driving conditions, drivers

had to rate the motion after each curve as natural or unnatural and as sharp or shallow. For the last motion condition, subjects had to rate each curve as if it was perceived to the left or to the right as well as if it was sharp or shallow. Two measures were created for assessment. The first one is the Leaning In Quotient (LIQ) and was defined as the "proportion of curves that were judge as "natural" based on an assumed perfect "leaning in" criterion". Subjects with a LIQ=1 means that the leaning vehicle algorithm was the one with a more natural feeling while subjects with a LIQ=0 means that the vector substitution algorithm was the more natural one. An LIQ=0.5 indicates random guessing. The second measure is called Curve Sharpness Quotient (CSQ) and is defined as "the proportion of times each participant judged the curves correctly". A CSQ=1 means that the subject correctly judged all the 16 curves while CSQ=0.5 is associated to random guessing. Both measures were presented in two tables. The first table contained the LIQ or CSQ for each subject and each driving condition. The second table contained the same information as table, but only for the statistical significant data. In the LIQ table if LIQ was superior to 0.75 an "I" would appear, if it was lower than 0.25 an "O" would appear. For values between 0.25 and 0.75 nothing was written in the table. In the CSQ table if CSQ was higher than 0.69 a "C" would appear in the table, while for values lower than this nothing would be written. A plot was shown in the paper containing the frequency distribution of the LIQ scores. The conclusions were obtained from these assessments.

Guo et al. [Guo et al., 2003] concluded their motion cueing study described in section 3-2-2 with a Cooper-Harper rating scale analysis. The pilots had to rate all the manoeuvres for all the conditions present in the study. Two figures were used to show the subjective data. The first contained eight bars grouped two by two (each bar of the two by two groups represent respectively the adaptive and the optimal algorithms). The figure contained then the three pilot Cooper-Harper rating means and standard deviation as well as the Cooper-Harper rating mean and standard deviation of all the pilots together. This plot contained the zero time delay situation. The second plot also contained eight bars grouped two by two, but in this case the bars represent if there is or there isn't compensation in the simulation. The Cooper-Harper rating means and standard deviations were shown for four different time delay situations: 0 ms, 50 ms, 100 ms and 200 ms. This method was used to conclude about the motion cueing algorithm performance. The conclusions of [Guo et al., 2003] were obtained from the PSD analysis and from the subjective rating scales.

Telban, et al. [Telban et al., 2005] used the NASA TLX subjective scale in their motion cueing algorithm study referenced in section 3-2-2. Eight bar plots were created based on the data taken from the TLX results. The first four plots are similar, changing only the flight manoeuvre (SA, OA, TO and TO with engine failure). These plots show the average of the TLX ratings versus the three pilot groups. For each pilot group the plot shows how these rated each motion cueing algorithm (Adaptive, Optimal and Nonlinear). The last four plots are also similar to each other, changing again the flight manoeuvre between them. This type of plot compares the average of the TLX ratings of a manoeuvre with three different time delays (0 ms, 100 ms and 200 ms), for the three motion cueing algorithms evaluated in [Telban et al., 2005]. The TLX rating scale was used to conclude about pilot workload. Like it was said before, final conclusions of [Telban et al., 2005] were made based on NASA TLX subjective rating scales as well as in the PSD analysis.

Category	Description	Colour	no.
A lot too much	Clearly perceptible and very unpleasent	Red	2
A little too much	Perceptible, but not unpleasant	Yellow	1
Ok	Comes up to the expectations	Green	0
A little too little	Perceptible, but not unpleasant	Yellow	-1
A lot too little	Clearly perceptible and very unpleasant	Red	-2

**Table 3-1:** Rating scale used during the experiment [Fortmüller and Meywerk, 2005].

Fortmüller and Meywerk [Fortmüller and Meywerk, 2005] studied the influence of the yaw movements in the subjective impression of driving. The objective was to check how subjects would rate different yaw configurations of a motion cueing algorithm. A one degree-of-freedom simulator was used to provide the different yaw motions. The vehicle model had a behavior similar of a middle class passenger car, and the yaw acceleration outputs ranged between 0 and 12  $\deg/s^2$ . For these yaw accelerations, the motion filter of the simulator outputted values between -2 and 24 deg/s<sup>2</sup>. This means that the driver would feel yaw cues that were in the opposite direction, scaled according to the real yaw cue and also yaw cues that were amplified. Clothoid curves were used in the simulation since in those the yaw acceleration is constant. The circuit contained 34 vertex clothoid curves with 5s-sections in between. The curves demanded different yaw accelerations. The different motion cueing configurations were randomly chosen for each participant. The number of participants was 40, being 26 of them casual drivers and 14 professional test drivers. Steering wheel and pedals were operated by the drivers and they were instructed to drive at maximum speed unless they had any kind of difficulties to do it. The assessments were made trough the rating scale present in Table 3-1. The subjects rated the curves by pushbutton method. The results were presented in a plot that contained the driver average ratings for all the motion conditions. The plot contained the model yaw accelerations in the x axis and the corresponding simulator yaw accelerations in the y axis. A plot containing the acceptable offset factors was also shown. This experiment was recently conducted in a simulator with lateral accelerations capability [Fortmüller et al., 2008].

Brünger-Koch et al. [Brünger-Koch et al., 2006a] used subjective ratings to evaluate three different classical washout configurations. This study was already described in section 3-2-2 since objective measurements were also used for assessment. Because of that, the experimental setup will not be described again. The subjects had to answer a questionnaire after each run. The motion fidelity was evaluated based in the following questions [Brünger-Koch et al., 2006a]:

- How realistic is the motion experience during driving?
- How accurately can the car be handled?
- How well the movements match with reality?
- How does the driver feel?

These questions were answered recurring to a two-level assessment scale (Figure 3-13). For scenario S1, a plot containing the mean of the subjective ratings for the different parameters

	very poor		poor		okay			good			very good				
	-1	0	1	-1	0	1	-1	0	1	-1	0	1	-1	0	1
Ξ															
	1	2	3	4	5	6	7	8	9	10	11	12	13	14	15

Figure 3-13: Two-level assessment scale [Brünger-Koch et al., 2006a].

sets and for the four questions answered in the questionnaire was shown. In scenario S2, a track which was especially designed for curve driving, the authors only showed data regarding the handling accuracy. A plot containing the handling accuracy for the three parameter sets and for three different speed limits (50, 80 and 120 km/h) was shown. For the last scenario only the results from the motion experience realism were presented. A plot containing the ratings from this question for all the parameter sets and for three different speeds limits (50, 80 and 120 km/h) was analysed. The conclusions were based in these subjective ratings as well as in the statistical analysis evaluation described before.

Soparkar and Reid [Soparkar and Reid, 2006] also used subjective rating scales in their experiment described in section 3-2-2. In this study, pilots had to rate the trials according to the Cooper-Harper [Cooper and Harper, 1969] rating scale. Subjective comments were also recorded, but these will be analysed in the respective section of this literature research. Four plots were shown in this study, each one for the four different flight conditions. Each plot contained the Cooper-Harper values (from 1 to 10) in the y axis and the three different motion configurations in the x axis. The plots contained the rating given by each of the three pilots for each motion configuration, as well as the average of the pilot ratings. Conclusions were draw from other evaluation methods as well.

Beykirch et al. [Beykirch et al., 2007] used subjective ratings in the study described in section 3.2.2.2 about new platform solutions for a helicopter simulation. A baseline condition was given to the participants before the measured experiment, which was called "real world". The objective was to familiarize the participants with the task and to give them a reference for the subjective analysis. This study is relative since it was not asked to the participants to compare the task with a similar task in a real vehicle. The individuals had to fill subjective rating scales after each trial. Three different scales were used. The first scale rated the pilot performance: 1 for good, 2 for adequate and 3 for inadequate. The second scale measured the motion fidelity: 1 for "comparable to real world", 2 for "different from the real world but not distracting" and 3 for "different from the real world and distracting". The last scale was the Cooper-Harper Handling Qualities Rating Scale [26]. The results were presented with two plots for each rating scale. The first plot was a  $K_{roll}$  versus  $K_{lat}$  plot of the rating scale method in question. The second type of plot contained the rating scale in the y axis of the plot and K<sub>lat</sub> in the x axis of the plot. Three lines were present in this plot, each one for a different K<sub>roll</sub> value. Conclusions were draw from these results as well from the results obtained by the objective evaluation methods.

Fischer and Werneke [Fischer and Werneke, 2008] completed the study described in section 3-2-1 with a subjective rating scale analysis. The objective of the study was to evaluate

a classical washout algorithm with four different parameter settings for tilting coordination. Twelve drivers were used in this study. Like it was said before, the manoeuvre consisted of an emergency braking with a starting speed of 80 km/h. Eight runs in varying order were performed by each participant with each parameter set introduced twice. The results were assessed from the magnitude and timing of the perceived force during three phases of a brake manoeuvre (beginning of the manoeuvre, ongoing manoeuvre and ending of the manoeuvre [Fischer and Werneke, 2008]). The parameter sets were rated with a questionnaire after each run. The rating scale present in the questionnaire rates the manoeuvre in terms of perceived force. The scale ranged from 1 to 15, being 1 a force that is too low/slow, 8 a force that is correct and 15 a force that is too high/too fast. The ratings were analysed recurring to analvsis of variance for repeated measures. Two different bar plots were used to show the results obtained from the questionnaire. The first plot shows the average rating for each of the four parameter sets. Both timing and magnitude results were present in the plot. The second plot shows the average rating for the three phases of the manoeuvre. Again magnitude and timing results are present (except for the on going phase where no timing can be assessed). The conclusions were based in the results obtained with this evaluation method as well as with the objective performance indicator evaluation method.

Wentink, et al. [Wentink et al., 2008b] conducted a curve driving experiment in Desdemona simulator, using three different motion cueing conditions. The conditions were denoted as: road rumble, classical washout and car yaw to centrifuge. The first condition only has road rumble motion, the second condition was a typical classical filter and the last condition was a Desdemona solution that uses the simulator central yaw to generate lateral onset cues without needing to washout to a neutral position. The driving task was to drive a square circuit in a city block scenario. Two of the curves had a radius of 20 meters in the road middle section while the other two were city crossings with rounded shoulders. Each curve was separated by a straight section of 150 meters. Twelve subjects participated in the study. Each subject had a test run and then drove the conditions in a random order. For each condition a questionnaire had to be filled. A sickness scale was also filled after the first and third conditions runs. At the end of the experiment, subjects had to rank the conditions by answering the following question: "Which of the motion conditions felt most like driving a real car, especially with regard to driving curves?" The motion cueing results were presented in a graph that shows the ranking given by each of the subjects for each motion cueing conditions. The ranking had three possible choices that go from the worst motion cueing to the best motion cueing. A plot of the sickness score per subject was also shown. The conclusions of the study were made based in these plots as well as on some subjective comments taken during the trials.

### 3-3-2 Subjective Comments

In some studies, motion cueing designers also include subjective comments from the simulation participants in their motion cueing analysis. These comments are used as assistance to the other subjective measurements and are helpful to check the state of mind of the individual. Although it was not found in literature, experience has shown that comments done by subjects can also be used to point out problems in the simulator motion that were not yet thought of.

This method is normally used as a support to other methods and not a stand alone method to evaluate motion filters. Designers should know how to "filter" the feedback given by subjects,

since sometimes the comments may not have any scientific significance or may be only based in guessing.

Crosbie and Kiefer [Crosbie and Kiefer, 1985] included some pilot subjective comments in the conclusion of the paper to support the effectiveness of the algorithm developed for using the human centrifuge as a dynamic flight simulator. The comments were not only regarding the performance of the motion cueing algorithm, but also regarding motion sickness issues.

Reid and Nahon [Reid and Nahon, 1986], in their study relative to the CW, CA and OC algorithms assessed some of the conclusions based in pilot subjective comments. These comments were included as an annex of [Reid and Nahon, 1986]. The authors in [Reid and Nahon, 1988] made reference to some of the subjective comments of [Reid and Nahon, 1986].

**Soparkar and Reid [Soparkar and Reid, 2006]** present a table in their study with the pilot comments regarding the simulator runs for all the configurations and all the motion cueing solutions. Conclusions of the study were taken from this table, as well from the PSD analysis and the rating scale use to quantify the handling qualities.

Colombet et al. [Colombet et al., 2008] used driver subjective comments to assess some of the conclusions of the motion cueing study done in the Renault CARDS simulator. The task was already explained in section 3-2-1. After the end of the second and third sessions (each session uses a different motion cueing algorithm) the drivers were asked to say if there was any noticeable difference in vehicle dynamics feedback between sessions and which one was the more realistic one (comparing to the real world). These comments were used to assess some of the conclusions.

#### 3-3-3 Pairwise Comparison

Because in the pairwise comparison method, motion filters are compared in pairs, the number of simulator runs that we have to do increases with the number of motion cueing algorithms that we want to evaluate. In one simulator run, subjects are presented with a pair of motion cueing filters. At the end of the run subjects have to tell which motion cueing filter was better (like in references [Reid and Nahon, 1988], [Grant et al., 2002] and [Grant et al., 2003]). The experiment ends when all the possible pairs of motion cueing filters have been rated by subjects (normally the pairs are presented in a randomized order). The results are then assessed in order to obtain conclusions about subject consistency in assigning motion cueing algorithms. Reid and Nahon [Reid and Nahon, 1988] used a concordance coefficient (W) defined in reference [Seaver and Stillwell, 1983] to conclude about pilot consistency. Grant, et al. [Grant et al., 2002] show the subject scores and repeatability (which is the ability of the subject to distinguish between different motion configurations) to conclude about the fidelity level of the used motion filters in the study. With pairwise comparison they can show if subjects were confused in differentiating the motion filters by showing their consistency and repeatability.

It is very important to know about subject consistency since most of the times designers are not sure if subjects felt the difference between motion filters, and if they can distinguish the best motion cueing algorithm. This method is not affected by the order that motion cueing algorithms are presented to subjects, since all the possible orders will be tested. This eliminates incongruence's that subjects normally have in rating scales due to the different orders that motion cueing algorithms are proposed to them. One shortcoming of this method has to do with the numerous simulator runs that have to be done, in order to present all possible pairs to subjects. This makes this method one of the most time consuming methods shown in this literature research.

The following authors used this evaluation method:

Reid and Nahon [Reid and Nahon, 1988], used pair wise comparison to check pilot consistency in assigning subjective ratings in the evaluation of the three different motion cueing algorithms described before sections 3-2-1, 3-3-1 and 3-3-2. For these tests new flight manoeuvres, different from the ones used in the other evaluation methods, were used. The pilots had to fly three short flight segments of about four minutes each one. The first segment consisted of deceleration and descent, the second segment contained an ILS approach and takeoff and the last segment consisted of test manoeuvres [Reid and Nahon, 1988]. The three segments were studied as a block of experimental trials. A trial consisted of flying a particular segment twice, with different motion cueing configurations each time. Then the pilots were asked which configuration generated better motion. Only four motion cueing configurations were used for this test. All possible pairs were flown by each pilot. These were presented to the pilot using a randomized Latin-Square design. A table containing the rating sequences from the paired comparison tests was present in the paper. The pilot consistency was measured using a coefficient of concordance (W) deffined in reference [Seaver and Stillwell, 1983]. From this coefficient, the authors conclude about pilot variability in the rating process.

Grant, et al. [Grant et al., 2002] conducted a study that compares a classical washout based algorithm with a lateral lane position washout algorithm. Six parameter configurations were tested for the former and four parameter configurations were tested for the latter. The study was conducted at the VIRTTEX simulator and the car model used in this simulation belongs to a 2002 Ford Taurus. The driving manoeuvre consisted of a lane change in a straight road. Cones were used to signalize the beginning and end of the lane change manoeuvre. These were spaced 9 ft apart laterally and 15 ft apart longitudinally. The vehicle used speed control to maintain a constant speed of 60 mph. The time that took to change between filter conditions was 6 seconds. According to the authors, this time span was long enough to switch between motion cueing configurations but short enough to allow reliable comparisons between conditions. The manoeuvre is repeated every 3000 ft intervals and is driven for a pair of tuning conditions. A left lane change is performed for one tuning condition and a right lane change is performed for other. After one pair, the driver has to say which manoeuvre was better. Twelve individuals were used in the evaluation process: six vehicle test drivers and six research engineers. The participants had eight trials for practice. The experiment had 30 trials for the CW configurations, consisting of 15 different pairs which were randomized and then repeated in the reverse order, and 12 trials for the lane change algorithm configurations, consisting of 6 pairs randomized and then repeated in the reverse order. The experiment took approximately 35 minutes for each participant. The results were divided into two sections, one for the lane change motion cueing algorithm and other for the classical washout motion cueing algorithm. In the lane change algorithm section the results of the experiment were used to create three different plots. The first plot shows the sum of the scores given by the drivers for the four parameter configurations. The second plot shows the repeatability rate for each subject. The repeatability measures the ability of the subject to distinguish between different motion configurations. The third plot shows the time history of the lateral specific force for a given motion configuration. Three different specific forces can be read in this plot: model lateral specific force, commanded lateral specific force and measured lateral specific force. Although this last plot is a graphical analysis evaluation, there is no need to describe it in section 3-2-1 of this literature research since it was only used to point out a problem existent for high lateral velocities in the simulator. In the classical washout algorithm section three plots were shown. The first plot contained the sum of the scores given by the drivers for the six parameter configurations while the second plot shows the repeatability rate of each subject. The third plot contains again the sum of the scores for the six parameter configurations, but this time only for the drivers with repeatability higher than 59%. The results and conclusion of the study were assessed only by this evaluation method. A very similar study [Grant et al., 2003] was also conducted by the authors, but in this case the analysis of the motion cueing algorithms was done together.

# Extreme Manoeuvres in Curve Driving

Cornering is were a race driver should be more concentrated in order to feel all the important cues associated to it. During a curve, a driver as to use the tires traction limit [Bentley, 1998], while in a straight track segment, drivers just have to concern about keeping the car running as fast as possible, since the tires traction limit is normally not violated due to minor forces involved in the manoeuvre. The traction limit is violated when the force in the tire is higher than the tire adhesion. The adhesion is given by Equation (4-1), where W is the car weight and  $\mu$  is the coefficient of adhesion. The coefficient of adhesion is dependent of the tire type and the pavement condition. Note that in a car, all the forces are applied on the tire (except aerodynamic forces or wind gusts).

$$A = W \times \mu \tag{4-1}$$

It is important to define two different interactions on the car wheels: slipping and sliding, in order to understand how can a driver drive on the tire traction limit.

# 4-1 Slipping

Slipping happens every time that a lateral force is applied to the lateral plane of the wheel. This lateral force will create a deflection on the tire, like in Figure 4-1. This deflection disaligns the contact surface of the tire since it is no longer in line with the wheel vertical plane of symmetry [Frère, 1992]. This tire deflection will induce a deviation in the wheel path, i.e. the wheel will no longer move in the direction of the wheel lateral plane but in a deviated direction of this plane. The angle that the wheel plane does with this new direction is called slip angle (Figure 4-1). The slip angle is dependent of the following factors:

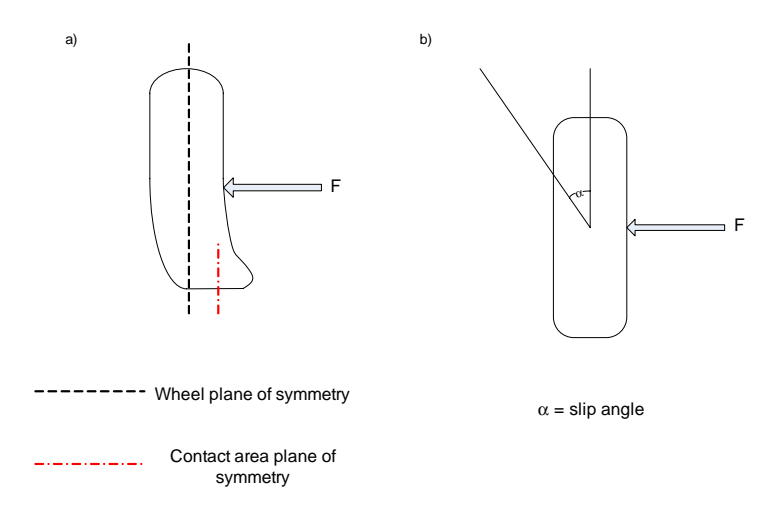


**Figure 4-1:** a) The Force F will disalign the planes of symmetry of the wheel and of the contact area. b) Slip angle of the whell when a lateral force F is applied.

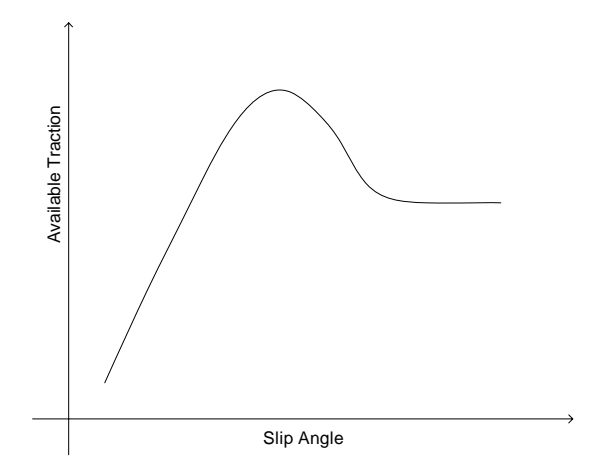
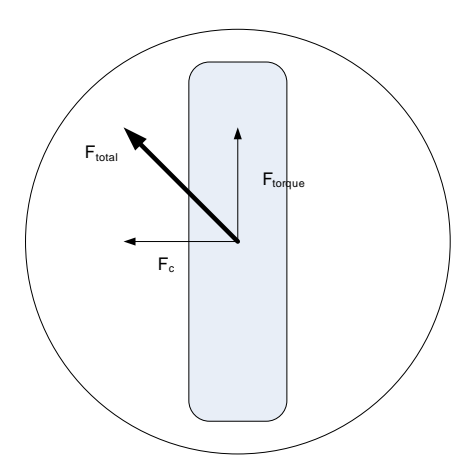


Figure 4-2: Example of slip angle versus available traction.

- Side force on the wheel: When the lateral force increases, the slip angle also increases.
- Tire pressure: When the tire pressure decreases, the slip angle increases.
- Weight carried by the tire: Tires are designed to carry a certain weight. The slip angle will be minimum if the weight carried by the tire is arround the designed weight. Larges changes on the weight will augment the slip angle.
- Wheel chamber: Positive wheel chamber will increase the slip angle while negative wheel chamber will decrease it.

The slip angle is very important to drive in the limit of traction, since it directly influenciates the amount of available traction that a tire still has. Figure 4-2 is an example of how the available traction on a tire varies with the slip angle. The available traction increases with the slip angle until a certain slip angle value that changes from tire to tire. Therefore, to take advantage of the tire, a driver should perform a curve using the slip angle that ensures the

4-2 Sliding 131



**Figure 4-3:** Total force acting on a wheel due to torque and centrifugal forces. The circle aroung the wheel represents the total adhesion of the wheel (This circle is also known as traction circle).

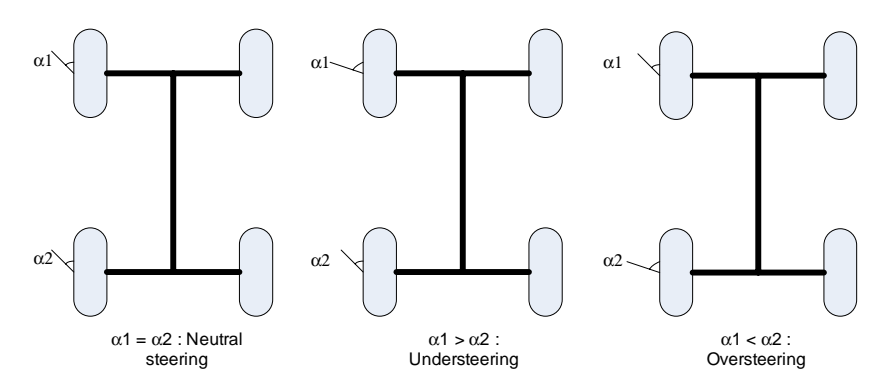


**Figure 4-4:** Neutral steering on the left, understeering in the middle and oversteering on the right.

maximal available traction. In this way, more forces can be applied to the tire before it loses adhesion.

# 4-2 Sliding

When the total force acting on a tire is higher than the adhesion of the tire, the tire will slide (Figure 4-3). Slipping can become sliding when the lateral force applied his higher than the adhesion. The wheel path will be deviated, not only by the slip angle but also by the slide angle. While splipping was only affected by the lateral force applied on the wheel, slidding is a phenomenom that depends on the total force applied on the wheel. This means that we also have to take into account the torque applied on the wheel. Note that the adhesion of the wheel is the same in all the directions.

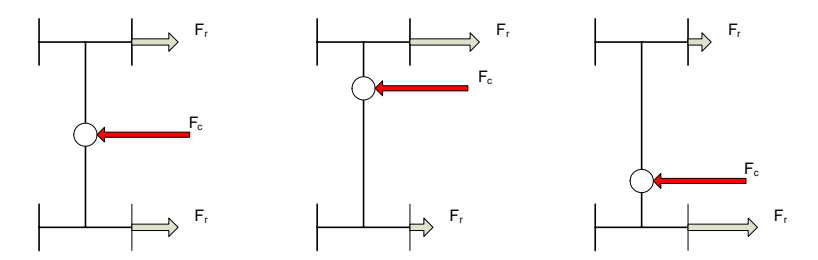


**Figure 4-5:** Center of gravity position.  $F_c$  is the centrifugal force of the curve applied in the car CG during a curve.  $F_r$  is the wheels reaction force. Note that  $F_c$  is an imaginary force and does not exist in an inertial frame of reference.

## 4-3 Understeer/Oversteer

In normal conditions, the forces applied on the front wheels are the same as the ones applied on the rear wheels. If this balance changes we can end up in understeer or oversteer conditions. According to [Frère, 1992] understeer happens when the slip angle of the front tires is higher than the slip angle of the rear tires. On the other way around, oversteer occurs when the slip angle of the rear tires is higher than the slip angle of the front tires. When both slip angles are the same, we have neutral steering. In understeer/oversteer the slip angle increases fast which can make the tires to start sliding, i.e. the forces applied on the tires are higher than the tire adhesion. In understeer, the front of the car will slide, which will make it to do a curve with an higher radius (in relation to the radius in neutral steering). The car will also not react to steer inputs. In oversteer, the back of the car will slide, which decreases the radius of the curve (again comparing it to the radius of the curve in neutral steering). In some cases, the driver loses the control and the car starts to spin. Below we can find examples of situations that induce understeer/oversteer.

## 4-3-1 Position of the center of gravity (CG)

The position of the CG influences the existent reaction forces on the wheels [Frère, 1992]. If the CG is near the front wheels, these will have a reaction force higher than the rear wheels. The car will then have a tendency to understeer. The car will have a tendency to oversteer if the CG is near the rear wheels.

#### 4-3-2 Torque

A car can be front wheel, back wheel or four wheel driven. This means that the necessaty torque to move a car can be applied in the front wheels, in the back wheels or in all the four wheels of the it. The place were the torque is applied is important to check if the car as a tendency to oversteer/understeer. Like it was said in section 4-2, slidding depends on the total force applied to the wheel. The wheels where the torque is applied will be subject to a higher total force than the other wheels of the car. Therefore if the car is back wheel driven, it will have a tendency to oversteer, since the rear wheels will be subjected to a higher total force and these will have a tendency to slide first than the front wheels. The same reasoning is used for a front wheel driven car, which has a tendency to understeer.

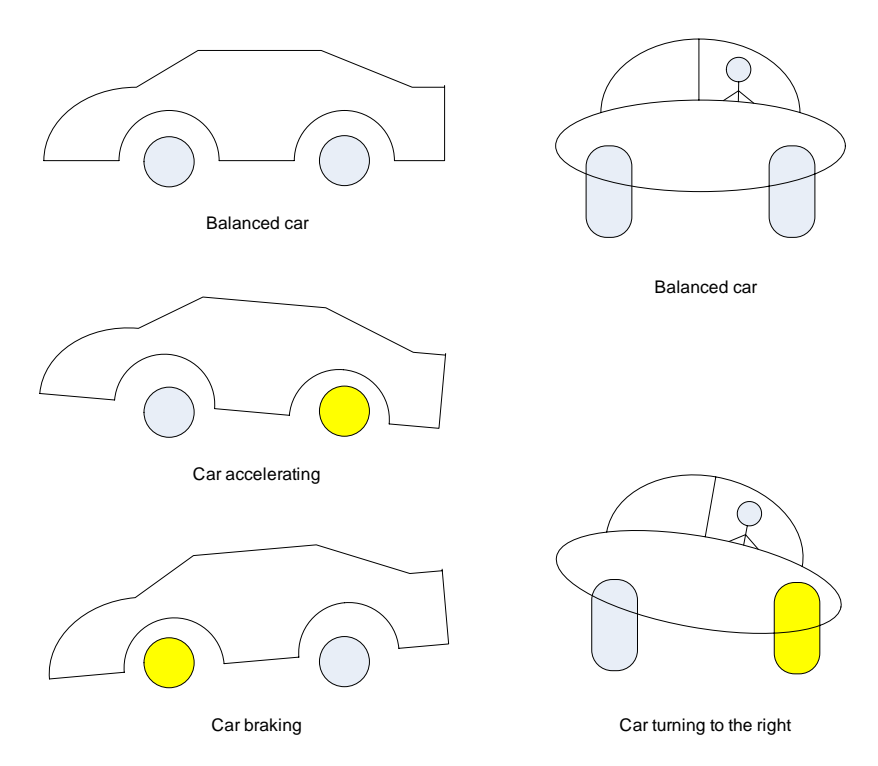


**Figure 4-6:** Weight transfers in a car. On the left we have weight transfer to the front or rear of the car while in the right we have lateral weight transfer. The yellow tire is the one supporting more weight.

### 4-3-3 Wheight transfer

The initial wheight distribution that a car has in rest will change when forces are applied to the car. The adhesive forces on a car are applied on the tire surface in contact with the pavement. Because the car CG is above the contact point of these forces [Beckman,], momentus are induced around it which provoques weight transfer due to car inertia. When weight transfers occur during break or accelerating manoeuvres, cars will also have a tendensy to oversteer/understeer. During a brake manoeuvre, the weight is transfered from the rear wheels to the front wheels, which will increase the adhesion of the front wheels and decrease the one of the rear wheels. In this case the car will have a tendency to oversteer. During an accelerating manoeuvre, the weight will be transfered from the front wheels to the rear wheels, which increase the adhesion of the latter and reduces the adhesion of the former. In this case, the car will have a tendency to understeer. Weight transfer also occurs lateraly when the car rolls in a curve. Figure 4-6 illustrates these cases.

# 4-4 Oversteer dynamics

It is easier to lose the control of the car in a oversteer situation than in an understeer situation. This has to do with the tendency of the car to spin in oversteer. Therefore the driver needs to feel when he is near an oversteer situation in order not to lose the control of the car. With this disadvantage it was expected that most of racing cars were front wheel driven (in

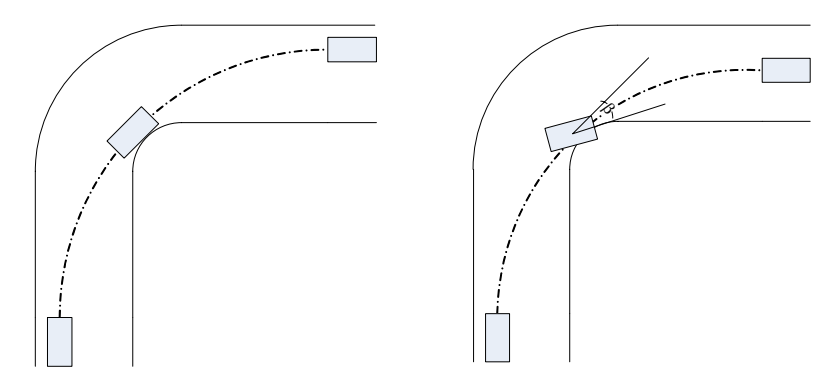


**Figure 4-7:** On the left, the car is in a normal steer situation. On the right, the car oversteers during the curve.

order to induce an understeer tendency), but that is not what happens. In race driving, more important than doing the curve in the traction limit of the tires it is to accelerate as soon as possible in the end of the curve. This will allow the car to achieve a higher velocity in the straight track segment that normally follows up a curve. One of the reasons why rear wheel driven cars are preferable in this case has to do with weight transfer. When we accelerate a car, the weight is transferred from the front to the rear of the car and therefore, acceleration can be applied sooner and with more itensity. There are other reasons that make cars with oversteer tendency more adequate for certain race types (they obtain drift angles easily or can do curves with a smaller radius), but they will not be discussed in this study.

During a neutral steering curve, the path that the car follows is equal to the path given by the front wheels angle plus some deviation due to the slip angle. This means that the yaw angle of the car is proportional to the yaw angle of the path that the car is following. In a oversteer situation, the yaw angle of the car will be higher than in a neutral steer situation. The total yaw angle of the car would be proportinal to the yaw angle of the path the car is following plus a sideslip angle ( $\beta$  on Figure 4-7). Figure 4-7 contains the neutral steering and the oversteering situations.

The forces acting on the car will also change in a oversteer situation. For simplicity purposes, lets assume that the only force acting on a car during a curve is the centrifugal force (in the car frame of reference, since in an inertial reference frame the centrifugal force does not exist). In a neutral steering situation, this force will act on the car lateral plane. In a curve where oversteer occurs, the centrifugal force will be decomposed in a lateral and longitudinal component (in the car reference axis). The lateral component will act the same way as in the neutral steering situation (same direction, but different magnitude) but the longitudinal component will act against the car movement. Figure 4-8 illustrates this. Oversteer will also influence the roll and pitch angle of the car.

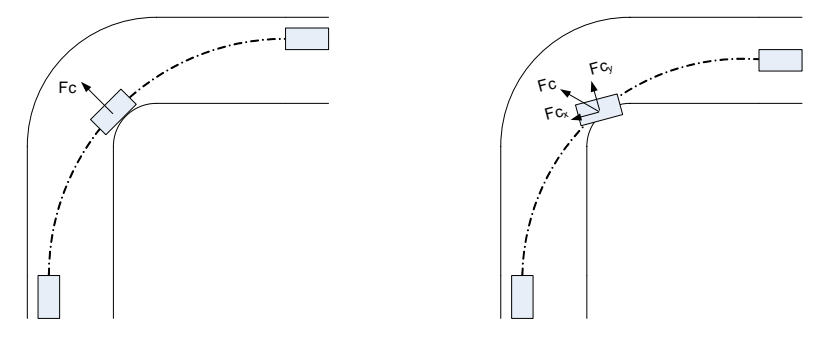


**Figure 4-8:** On the left, the car is in a curve without oversteering. On the right, the car is in a curve with oversteering.

# Design of Racing Motion Cueing Algorithms for Desdemona

Nowadays, it is not possible to develop a one to one racing simulation (in terms of motion) due to the physical constraints of the motion platform. Therefore false cues will always be present. In order to discover which false cues are more acceptable for this type of simulation, four motion cueing solutions were developed, each one with different pros and cons.

# 5-1 Desdemona Specifications

Desdemona (Figure 1-1 and Figure 5-1) is a simulator with specifications much different from a conventional hexapod. Physically, Desdemona has a cabin that is suspended in a gimballed 3 DoF system. These 3 DoF are denominated by cabin roll  $(\phi_{cab})$ , cabin yaw  $(\psi_{cab})$ , cabin pitch  $(\theta_{cab})$  and give Desdemona capability to rotate the cabin. The gimballed system is mounted in a heave axis (H) that enhances the simulator with vertical translation capabilities. The system moves horizontally over a sledge. This DoF is called radius (R). The last DoF is the central yaw  $(\psi_{centr})$  which is responsible for rotating the sledge. Table 5-1 shows Desdemona actuator limits in terms of position, velocity and acceleration.

## 5-2 Motion Cueing Solutions

#### 5-2-1 Solution 1:

This solution uses car yaw rate to drive Desdemona. The yaw rate is used without scaling. Low frequency yaw rate is fed to the simulator central yaw while high frequency yaw rate is fed to the simulator cabin yaw. The low frequency yaw rate is obtained using a second order low-pass filter while the high frequency yaw rate is obtained using a second order high-pass filter. The cabin should be positioned at 0° in yaw for left curves and at -180° for right

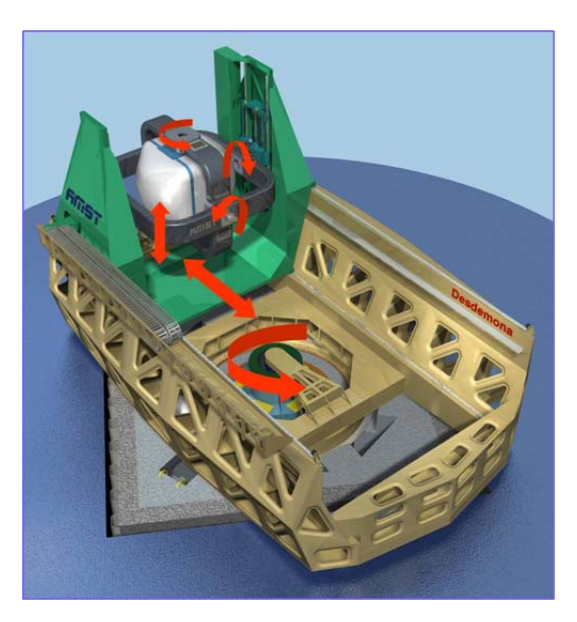


Figure 5-1: Desdemona DoF's.

	$\psi_{centr}$	R	Н	$\phi_{cab}$	$\theta_{cab}$	$\psi_{cab}$
Max.	>360[°]	±4[m]	±1[m]	>360[°]	>360[°]	>360[°]
Position						
Max.	155[°/s]	$3.2[\mathrm{m/s}]$	2[m/s]	180[°/s]	180[°/s]	180[°/s]
Velocity						
Max.	$45[^{\circ}/{\rm s}^{2}]$	$4.9[{ m m/s^2}]$	$4.9[{ m m/s^2}]$	$90[^{\circ}/\mathrm{s}^2]$	$90[^{\circ}/\mathrm{s}^2]$	$90[^{\circ}/\mathrm{s}^2]$
Acceleration						

**Table 5-1:** Desdemona technical specifications.

curves to benefit from lateral force correct direction since the cabin will be fixed at -3m in radius. The transition between the cabin positions is obtained using the steering wheel angle of the car multiplied by a gain. These yaw angle positions are added up to the high frequency yaw rates fed to the cabin. The neutral position of the cabin yaw is at -90 degrees which enables the use of tangential accelerations induced by the rotation of the central yaw as onset cues for the curves.

Figure 5-2 shows a simplified block diagram of this solution. The Limiter block is used to guarantee that the signal sent to Desdemona is not above the simulator limits of position, velocity and acceleration. A low pass filter is used in the steering wheel angle channel for smoothing purposes. The transfer function of the HP Filter 2 order block is given by (5-1) while the transfer function of the LP Filter 2 order is given by (5-2), where  $\omega$  is the natural frequency and  $\varsigma$  is the damping of the filter (the values of  $\omega$  and  $\varsigma$  can be different for each block).

$$H(s) = \frac{s^2}{s^2 + 2s\omega\varsigma + \omega^2} \tag{5-1}$$

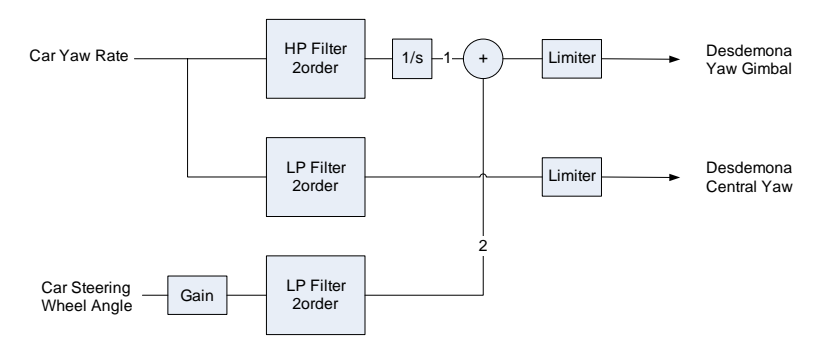


Figure 5-2: Solution 1 block diagram.

$$H(s) = \frac{\omega^2}{s^2 + 2s\omega\varsigma + \omega^2} \tag{5-2}$$

The high-pass filter is second order which guarantees that Desdemona cabin returns to neutral position. This can be shown by applying the final value theorem (5-3).

$$f(t)|_{t\to\infty} = sF(s)|_{s\to 0} \tag{5-3}$$

The yaw angle of the Desdemona cabin is the sum between the yaw angle induced by the steering wheel (2 in Figure 5-2) and the yaw angle coming from the car yaw rate (1 in Figure 5-2). The transfer function of the yaw angle coming from the car yaw rate in order to the car yaw rate is given by equation (5-4).

$$\frac{Y(s)}{U(s)} = \frac{s^2}{s^2 + 2s\omega\zeta + \omega^2} \frac{1}{s}$$
 (5-4)

Applying the final value theorem (5-3) to equation (5-4), we will get the steady state position of the yaw angle coming from the car yaw rate. The final value is then given by (5-5).

$$sF(s)\|_{s\to 0} = s \frac{s^2}{s^2 + 2s\omega\varsigma + \omega^2} \frac{1}{s} U(s)\|_{s\to 0} = \frac{s^2}{s^2 + 2s\omega\varsigma + \omega^2} U(s)\|_{s\to 0}$$
 (5-5)

If we use a unitary step input in (5-5) we get the solution in (5-6).

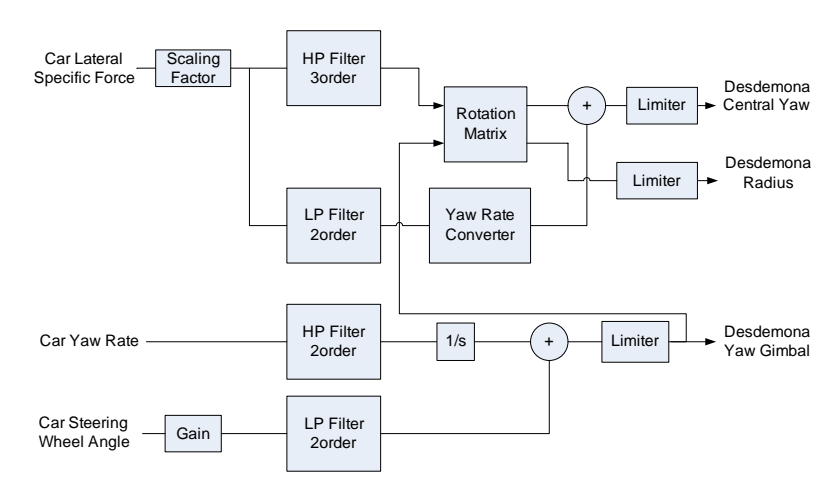


Figure 5-3: Solution 2 block diagram.

$$sF(s)\|_{s\to 0} = \frac{s^2}{s^2 + 2s\omega\varsigma + \omega^2} \frac{1}{s}\|_{s\to 0} = \frac{s}{s^2 + 2s\omega\varsigma + \omega^2}\|_{s\to 0} = \frac{0}{\omega^2} = 0$$
 (5-6)

Therefore, the steady state yaw angle of the Desdemona cabin will be given by the yaw angle induced by the steering wheel. If we used a first order filter instead, the steady state position would no longer be zero, and therefore the neutral position would vary from the pretended one.

This solution has the advantage of using the car yaw rate without any scaling, which will induce correct yaw cues in the driver. Nevertheless the cabin preposition will generate some false cues. In this solution, the lateral force is not directly cued, however the lateral force generated by the simulator movement is in the correct direction (when compared with the specific force on the car).

#### 5-2-2 **Solution** 2:

This solution uses Desdemona centrifuge capabilities. The yaw rate fed to the simulator central yaw is calculated using the low pass component of the car lateral force. This means that the sustained lateral force cues are simulated using a centrifugal force. The radius of Desdemona is used to generate lateral onset cues when the cabin is perpendicular to it. The radius neutral position will be at -3m. The lateral force used for the calculations is scaled. In this solution, the cabin should be placed in the same way as solution 1 in order to obtain the lateral forces in the correct direction. The steering wheel angle was again used as a control input for the cabin position. The cabin yaw is again fed with high frequency yaw rates (that is believed to be one of the cues that triggers the perception of oversteering).

Figure 5-3 shows the block diagram of this solution. The Scaling Factor block is used to scale the car specific forces, since these are too high to simulate them one to one. The filter present in the HP Filter 3 order block is a second order filter in series with a first order filter. The

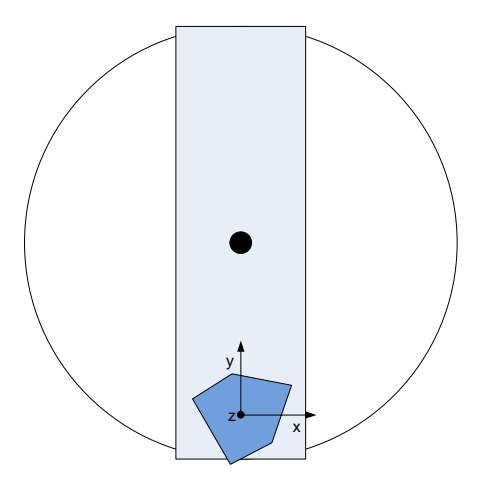


**Figure 5-4:** Desdemona top view. Desdemona cabin is represented in dark blue while Desdemona radius is represented in light blue. The z axis is perpendicular to x and y and is represented as a point in the origin.

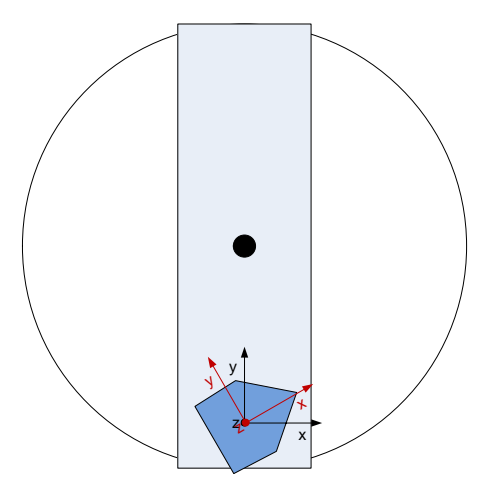


**Figure 5-5:** Desdemona top view. In red we have the Desdemona cabin reference frame and in black we have the Desdemona inertial reference frame.

transfer function is given by equation (5-7), where  $\omega$  is the natural frequency and  $\varsigma$  is the damping of the second order filter and  $\omega_b$  is the natural frequency of the first order filter.

$$H(s) = \frac{s^2}{s^2 + 2s\omega\varsigma + \omega^2} \frac{s}{s + \omega_b} \tag{5-7}$$

In this case, a third order filter is necessary to ensure that the actuator position returns to zero. This has to do with the fact that we are using accelerations as inputs for the filter. Therefore, and according to the Final Value theorem (5-3), we need at least a third order filter to ensure that no deviations occur in the actuator position, and that it returns to neutral. The reasoning of this is similar to the one done with equations (5-5) and (5-6).

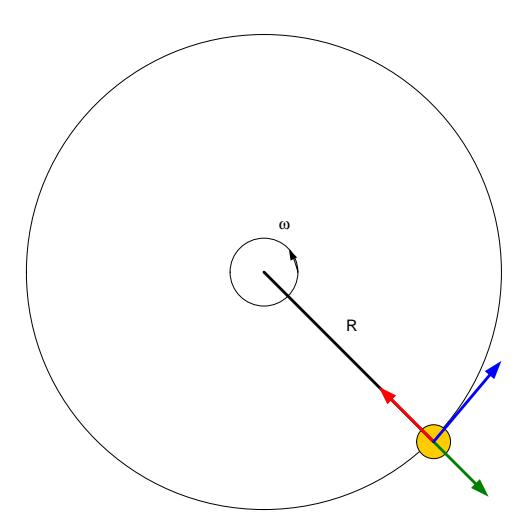


**Figure 5-6:** Rotation of a mass point (yellow) on the tip of a string. The blue arrow stands for the particle velocity, the green arrow shows the centrifugal force (which is a fictional force, that has to be considered in non-inertial frames of reference) and the red arrow shows the centripetal force. R stands for the radius of the circle that the mass point is doing and  $\omega$  stands for the angular velocity.

Desdemona has only three inertial sources to generate specific force onset cues. These are the Heave, the Radius and the Central Yaw. The heave generates cues in the z axis, while the radius generates cues in the y axis and the central yaw in the x axis. These axis are defined in Figure 5-4. The Rotation Matrix block is used to transform the specific forces in the Desdemona cabin (red reference frame in Figure 5-5) to specific forces in the Desdemona inertial axis (black reference frame in Figure 5-5). The Rotation Matrix block includes equations (5-8) and (5-9) to perform the transformation, where  $x_i$  is the x inertial axis,  $y_i$  is the y inertial axis,  $y_{cab}$  is the y cabin axis and  $\psi_{cab}$  is the Desdemona gimbal yaw angle (note that this motion filter only cues lateral specific force. To cue longitudinal specific forces, the equations have to be substituted by a solution that includes the longitudinal specific force in the cabin).

$$x_i = y_{cab} \sin \psi_{cab} \tag{5-8}$$

$$y_i = y_{cab}\cos\psi_{cab} \tag{5-9}$$

Like it was said before, the sustained lateral specific forces will be created using Desdemona centrifuge capabilities. Therefore, Desdemona central yaw will be used. The Yaw Rate Converter block calculates the necessary yaw rate to achieve the wanted specific force. To understand this block, one should first understand the difference between centrifugal and centripetal force. Consider the rotation of a mass point on the tip of a string shown in Figure 5-6. The centripetal force (red in Figure 5-6) is the force needed to force a mass point to follow a circular path, without this force, the mass point would move in the same direction of its velocity

vector (blue arrow in Figure 5-6). Imagine now that the mass point is big enough that we can put an object on top of it. If at a certain time the friction between the object and the mass point is lost, the object will follow a path tangentional to the circular movement. Considering this phenomenon in the inertial frame of reference, it is easy to understand that the object separated from the mass point due to a lack of centripetal force. However if we now consider a non-inertial frame of reference with origin in the mass point, we have to consider the centrifugal force in order to explain the decouplement of the object and the mass point. In the case of Figure 5-6, the magnitude of the centripetal force can be given by (5-10), where m is the mass of the mass point, R is the radius of the circle that the mass point is doing and  $\omega$  is the angular velocity.

$$Force_{centripetal} = ma_{centripetal}^2 = m\omega^2 R \tag{5-10}$$

In Desdemona, we want to have the correct magnitude of the lateral specific force in the cabin (since the direction will be given by the steering wheel angle interaction). Using equation (5-10), the necessary yaw rate is given by (5-11), where  $f_{yLP}$  is the low passed lateral specific force and  $R_{Desd}$  is the Desdemona radius at a certain time instant.

$$\omega = \sqrt{\frac{f_{yLP}}{R_{Desd}}} \tag{5-11}$$

The main advantage of this motion cueing solution, has to do with the lateral force cueing, namelly the sustained cues. This is because we are using centrifuge techniques to obtain these cues (which is something not possible in an hexapod). However this design contains false yaw cues since the radius of Desdemona is much of the times smaller than the radius of curves in a track, which means that the yaw rate necessary to achieve the same specific force is higher. That can be seen in equation (5-10), since if we want to maintain the force and decrease the radius, we have to increase the angular velocity. Other false cue that we have in this solution has to do with the steering wheel interaction, which will induce the same problems already stated in the first motion cueing solution.

#### 5-2-3 Solution 3:

This method brings some hexapod characteristics to Desdemona. The radius neutral position will be at the center of the radius rail. Onset cues will be performed by this actuator. For that, the lateral specific force is high passed in a second order filter. Sustained cues will be simulated using tilting coordination. Lateral force is then low passed by a second order complementary filter. The low frequency component of the yaw rate is fed one to one to the central yaw while the high frequency component of the yaw rate is fed one to one to the cabin yaw. Complementary filters are used which guarantees that the yaw rate in the cabin

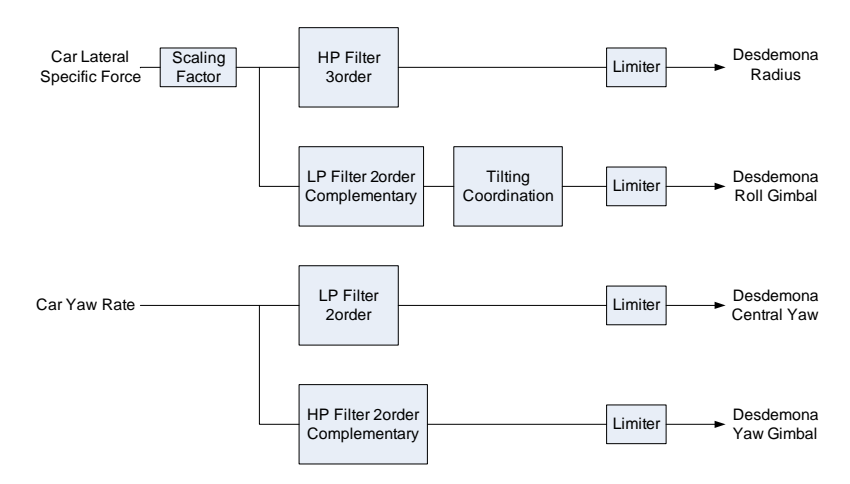


Figure 5-7: Solution 3 block diagram.

is extremely similar to car yaw rate. This solution can be downtuned to fit motion envelopes smaller than the one of Desdemona.

Figure 5-7 shows the block of this solution. The transfer functions of the blocks HP Filter 3 order and LP Filter 2 order are defined by equations (5-7) and (5-2) respectively. In both channels (the specific force channel and the angular rates channel) complementary filters are used to obtain the sustained cues (in the specific force channel) and the onset cues (in the angular rate channel). Two filters are complementary if the sum of their transfer functions is equal to unity. Explained this, the transfer functions of blocks HP Filter 2 order Complementary and LP Filter 2 order Complementary are respectively (5-12) and (5-13).

$$H(s) = \frac{s^2 + 2s\omega\varsigma}{s^2 + 2s\omega\varsigma + \omega^2}$$
 (5-12)

$$H(s) = \frac{2s\omega\varsigma + \omega^2}{s^2 + 2s\omega\varsigma + \omega^2}$$
 (5-13)

If we sum equation (5-2) with equation (5-12) the final value is one (5-14).

$$H_{2ndLP}(s) + H_{2ndHP}(s) = \frac{\omega^2}{s^2 + 2s\omega\zeta + \omega^2} + \frac{s^2 + 2s\omega\zeta}{s^2 + 2s\omega\zeta + \omega^2} = 1$$
 (5-14)

Note that if we sum the transfer function of the third order high pass filter (5-7) with the complementary second order low pass filter (5-13) we obtain the first order filter instead of one. This happens because of the different filter order. The complementary low pass filter only compensates the second order part of the third order high pass filter.

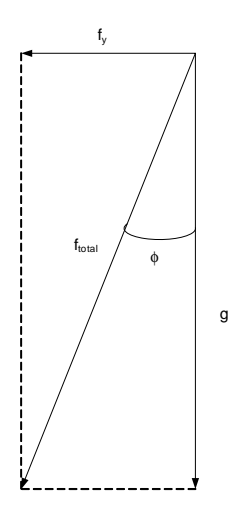


Figure 5-8: Total force decomposed into lateral force and gravity.

The Tilting Coordination block uses the gravity vector to create sustained cues. The objective is to match the total force vector direction with the gravity vector. In Figure 5-8 we can see that the total force ( $f_{total}$  in the figure) can be decomposed into the lateral force component and the gravity vector (respectively  $f_y$  and g in the figure). From Figure 5-8 it is possible to write equation (5-15).

$$\tan \phi = \frac{f_y}{g} \tag{5-15}$$

Therefore the roll angle necessary to match the total force direction is given by (5-16). The Tilting Coordination block calculates this angle and sends it to the Desdemona roll gimbal. This block also contains a rate limiter to guarantee that the roll rate is never above the human threshold.

$$\phi = \arctan\left(\frac{f_y}{g}\right) \tag{5-16}$$

This filter delivers very good onset cues regarding lateral specific force and yaw rate. In fact, due to the complementary filters, yaw rate is almost equal to the one in the car. Nevertheless the tilting coordination techniques deliver sustained cues with the same shortcommings as the ones found in normal classical washout filters.

#### 5-2-4 Solution 4:

Solution 4 uses the idea of Desdemona three different inertial sources of motion that were briefly described in Section 5-2-2. First we define Desdemona frame of reference like in Figure

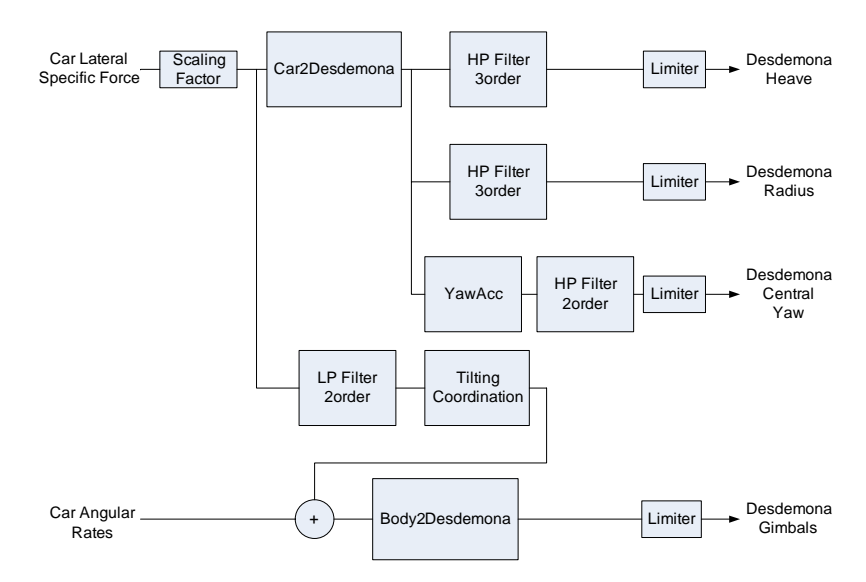


Figure 5-9: Solution 4 block diagram.

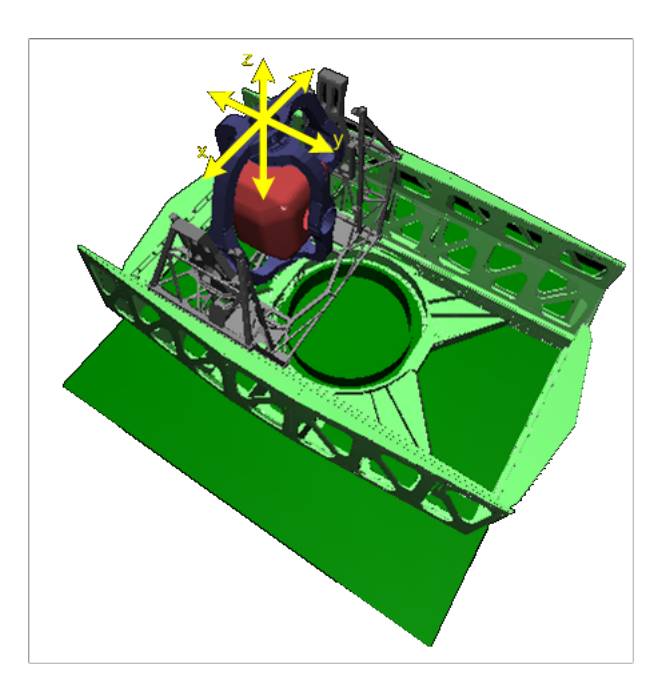
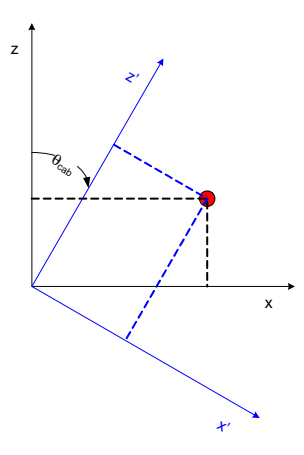


Figure 5-10: Desdemona frame of reference.



**Figure 5-11:** Desdemona pitch rotation. x and z represent Desdemona frame of reference while x' and z' represent Desdemona cabin position.

5-10. Therefore one rotation matrix will be used to convert the car specific forces from the body frame of reference into Desdemona frame of reference. In this way the motion filters can be applyed directly to Desdemona actuators. High pass filters are used in the three inertial directions to guarantee onset cues. The sustained cues are simulated using tilting coordination techniques. A second rotation matrix is used to convert the car body rates into Desdemona rates. In this way we have the correct angular body motion in Desdemona cabin.

The change from car reference frame to Desdemona frame of reference has to respect the gimbal order. The first gimbal is the  $\theta_{cab}$  and rotates Desdemona like is show in Figure 5-11.

The coordinates in the cabin frame of reference (x' and z' in Figure 5-11) of the red point in Figure 5-11 in order to Desdemona frame of reference and the cabin pitch angle ( $\theta_{cab}$  in Figure 5-11) is given by equations (5-17) and (5-18).

$$x' = x\cos\theta_{cab} - z\sin\theta_{cab} \tag{5-17}$$

$$z' = x \sin \theta_{cab} + z \cos \theta_{cab} \tag{5-18}$$

Equations (5-17) and (5-18) can be written in matrix notation (5-19), where  $Rot_{\theta}(\theta_{cab})$  is the matrix that defines a rotation of  $\theta$  radians in Desdemona.

$$\begin{bmatrix} x' \\ y' \\ z' \end{bmatrix} = \begin{bmatrix} \cos \theta_{cab} & 0 & -\sin \theta_{cab} \\ 0 & 1 & 0 \\ \sin \theta_{cab} & 0 & \cos \theta_{cab} \end{bmatrix} \begin{bmatrix} x \\ y \\ z \end{bmatrix} = Rot_{\theta} (\theta_{cab}) \begin{bmatrix} x \\ y \\ z \end{bmatrix}$$
 (5-19)

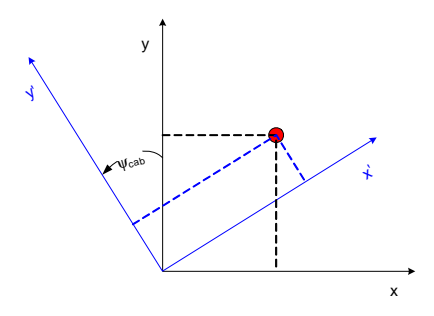


**Figure 5-12:** Desdemona yaw rotation. x and y represent Desdemona frame of reference while x' and y' represent Desdemona cabin position.

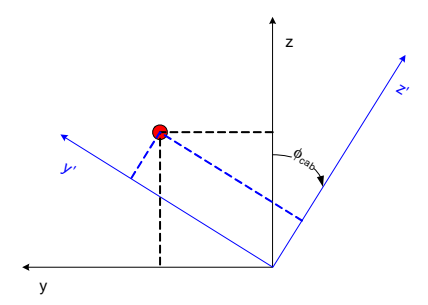


**Figure 5-13:** Desdemona roll rotation. y and z represent Desdemona frame of reference while y' and z' represent Desdemona cabin position.

A Desdemona rotation in yaw (performed with the  $\psi_{cab}$  gimbal) is defined in Figure 5-12. The reasoning to obtain the coordinates in the cabin frame of reference is the same as in the theta rotation, therefore we will only write the equation in matrix notation (5-20), where  $Rot_{\psi}(\psi_{cab})$  is the matrix that defines a rotation of  $\psi$  radians in Desdemona.

$$\begin{bmatrix} x' \\ y' \\ z' \end{bmatrix} = \begin{bmatrix} \cos \psi_{cab} & \sin \psi_{cab} & 0 \\ -\sin \psi_{cab} & \cos \psi_{cab} & 0 \\ 0 & 0 & 1 \end{bmatrix} \begin{bmatrix} x \\ y \\ z \end{bmatrix} = Rot_{\psi} (\psi_{cab}) \begin{bmatrix} x \\ y \\ z \end{bmatrix}$$
(5-20)

A Desdemona rotation in roll (performed with the  $\phi_{cab}$  gimbal) is defined in Figure 5-13. The reasoning to obtain the coordinates in the cabin frame of reference is the same as in the theta rotation, therefore we will only write the equation in matrix notation (5-21), where  $Rot_{\phi}(\phi_{cab})$  is the matrix that defines a rotation of  $\phi$  radians in Desdemona.

$$\begin{bmatrix} x' \\ y' \\ z' \end{bmatrix} = \begin{bmatrix} 1 & 0 & 0 \\ 0 & \cos \phi_{cab} & \sin \phi_{cab} \\ 0 & -\sin \phi_{cab} & \cos \phi_{cab} \end{bmatrix} \begin{bmatrix} x \\ y \\ z \end{bmatrix} = Rot_{\phi} (\phi_{cab}) \begin{bmatrix} x \\ y \\ z \end{bmatrix}$$
(5-21)

The block Car2Desdemona in Figure 5-9 is the one responsible for converting the specific forces from car frame of reference into Desdemona frame of reference. The block perfoms this

transformation using a rotation matrix based on the ones described before  $(Rot_{\theta}, Rot_{\psi})$  and  $Rot_{\phi}$ . In Desdemona, the rotations follow the gimbal order, therefore to change from cabin reference frame to Desdemona reference frame we have to multiply the rotation matrices using that order (5-22), where  $Rot_{total}(\theta_{cab}, \psi_{cab}, \phi_{cab})$  is the total rotation matrix from car frame of reference into Desdemona frame of reference.

$$\begin{bmatrix} x' \\ y' \\ z' \end{bmatrix} = Rot_{\theta} (\theta_{cab}) Rot_{\psi} (\psi_{cab}) Rot_{\phi} (\phi_{cab}) \begin{bmatrix} x \\ y \\ z \end{bmatrix} =$$

$$= Rot_{total} (\theta_{cab}, \psi_{cab}, \phi_{cab}) \begin{bmatrix} x \\ y \\ z \end{bmatrix}$$
(5-22)

However, what we want is a matrix that transforms the car frame of reference into the Desdemona reference frame. This matrix is defined in equation (5-23) has  $Rot_{total}$  ( $\theta_{cab}, \psi_{cab}, \phi_{cab}$ )<sup>-1</sup> and is the rotation matrix used in block Car2Desdemona present in Figure 5-9.

$$\begin{bmatrix} x' \\ y' \\ z' \end{bmatrix} = Rot_{total} (\theta_{cab}, \psi_{cab}, \phi_{cab}) \begin{bmatrix} x \\ y \\ z \end{bmatrix} \iff$$

$$\iff \begin{bmatrix} x \\ y \\ z \end{bmatrix} = Rot_{total} (\theta_{cab}, \psi_{cab}, \phi_{cab})^{-1} \begin{bmatrix} x' \\ y' \\ z' \end{bmatrix}$$
(5-23)

The Body2Desdemona block included in Figure 5-9 uses a different rotation than the Car2Desdemona block. The pitch gimbal is directly connected to Desdemona cabin, allowing to establish equation (5-24).

$$q = \dot{\theta}_{cab} \tag{5-24}$$

The Desdemona yaw gimbal is connected to the pitch gimbal instead of being connected to Desdemona cabin, which means that if we want to obtain the correct r rate, we cannot directly couple it with the  $\dot{\psi}_{cab}$  like in (5-24). Therefore we first have to rotate the frame of reference in pitch like in Figure 5-11.

The Desdemona roll gimbal is connected to the yaw gimbal, which means that we have to do two reference frame rotations (one in pitch and one in yaw) to obtain the correct p. Equation

(5-25) correctly transforms body rates into Desdemona gimbal rates, where I is the identity matrix. Equation (5-25) can also be written as (5-26).

$$\begin{bmatrix} p \\ q \\ r \end{bmatrix} = Rot_{\theta} (\theta_{cab}) Rot_{\psi} (\psi_{cab}) \begin{bmatrix} \dot{\phi} \\ 0 \\ 0 \end{bmatrix} + I \begin{bmatrix} 0 \\ \dot{\theta} \\ 0 \end{bmatrix} + Rot_{\theta} (\theta_{cab}) \begin{bmatrix} 0 \\ 0 \\ \dot{\psi} \end{bmatrix}$$
(5-25)

$$\begin{bmatrix} p \\ q \\ r \end{bmatrix} = \begin{bmatrix} \cos \theta_{cab} \cos \psi_{cab} & 0 & -\sin \theta_{cab} \\ -\sin \psi_{cab} & 1 & 0 \\ \sin \theta_{cab} \cos \psi_{cab} & 0 & \cos \theta_{cab} \end{bmatrix} \begin{bmatrix} \dot{\phi} \\ \dot{\theta} \\ \dot{\psi} \end{bmatrix}$$
 (5-26)

The function of the Body2Desdemona block is to transform body rates into Desdemona rates and not the opposite like in equation (5-26). Then the rotation matrix included in this block is denominated by  $Rot_{ang}(\theta_{cab}, \psi_{cab})^{-1}$  and is given by (5-27).

$$\begin{bmatrix} p \\ q \\ r \end{bmatrix} = \begin{bmatrix} \cos \theta_{cab} \cos \psi_{cab} & 0 & -\sin \theta_{cab} \\ -\sin \psi_{cab} & 1 & 0 \\ \sin \theta_{cab} \cos \psi_{cab} & 0 & \cos \theta_{cab} \end{bmatrix} \begin{bmatrix} \dot{\phi} \\ \dot{\theta} \\ \dot{\psi} \end{bmatrix} \iff$$

$$\iff \begin{bmatrix} \dot{\phi} \\ \dot{\theta} \\ \dot{\psi} \end{bmatrix} = \begin{bmatrix} \cos \theta_{cab} \cos \psi_{cab} & 0 & -\sin \theta_{cab} \\ -\sin \psi_{cab} & 1 & 0 \\ \sin \theta_{cab} \cos \psi_{cab} & 0 & \cos \theta_{cab} \end{bmatrix}^{-1} \begin{bmatrix} p \\ q \\ r \end{bmatrix} =$$

$$= Rot_{ang} (\theta_{cab}, \psi_{cab})^{-1} \begin{bmatrix} p \\ q \\ r \end{bmatrix}$$
(5-27)

The YawAcc block transforms longitudinal specific force into angular acceleration. This has to be done because Desdemona central yaw will provide this cue. Figure 5-6 was used to explain the concept of centripetal force. In that case, the mass point had always a constant velocity represented by the blue arrow. If this velocity varies, we will have a new acceleration (which is in the same direction of the velocity vector, i.e., tangent to the trajectory) that is called tangentional acceleration and is given by (5-28), where  $\dot{\omega}$ is the angular acceleration and R is the radius of the string.

$$a_t = \dot{\omega}R \tag{5-28}$$

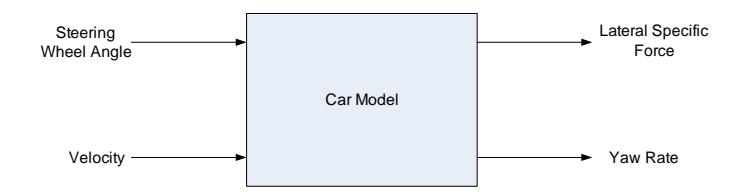


Figure 5-14: Car model.

Using Equation (5-28) in Desdemona reality, we end up with an angular acceleration given by (5-29).

$$\dot{\omega} = \frac{f_{xi}}{R_{Desd}} \tag{5-29}$$

This transformation is done before passing throught the second order high-pass filter since this motion cueing algorithm uses the filters in the Desdemona actuators. Note also that for this channel, the high-pass filter is second order instead of third order. This has to do with the fact that Desdemona central yaw has unlimited displacement capabilities, therefore there is no need to return to neutral in postion. All the other blocks of this motion cueing solution have already been described for the other solutions, and no differences are present (even in the Tilting Coordination, which still only works for lateral cues). This filter allows to insert an initial condition for the gimbals which can be used to achieve motion cueing solutions with different characteristics.

# 5-3 Preliminary motion cueing analysis

The motion cueing solutions described in Section 5-2 are analysed using two different datasets. The first dataset is based on a really simple car model, in order to obtain similar motion cues to the ones that one have in a chicane. The second dataset was available at TNO, and was recorded from a car driving in a big roundabout. This datasets were used exclusively to show how the motion cueing solutions work. For future work, race driving datasets will be used.

The used evaluation method in this section is the graphical comparison, since is a good method for a preliminary analysis and that easily shows how the different motion filter work. Nevertheless, for future work a more exhaustive analysis has to be made in order to choose the motion cueing filter that is more adequate for the racing simulation. For all the motion filters, graphical comparison is made using specific forces and angular rates plots of the simulator motion versus the "real" motion.

#### 5-3-1 Car model

The car model developed is based on the centripetal force that affects a wheel in a curve. Figure 5-14 shows a simple block diagram of the model. The model inputs are steering wheel

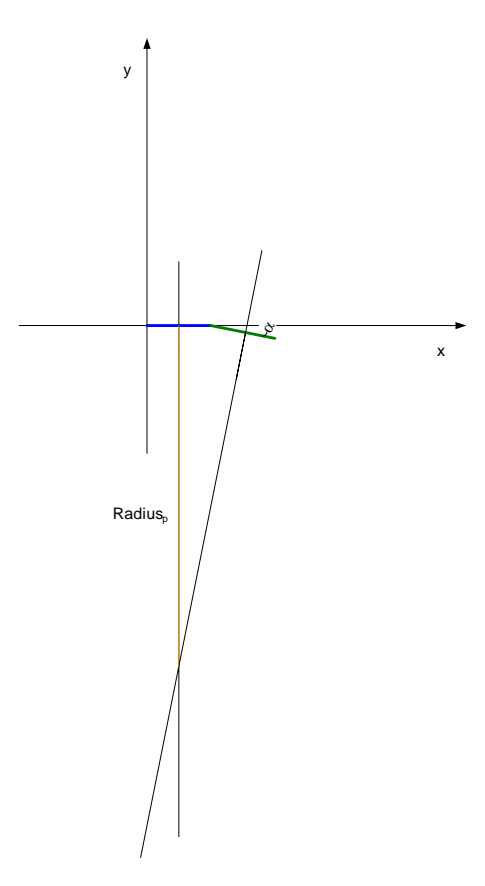


Figure 5-15: Radius of a curve. The blue vector represents the tire in a time instant. The green vector represents the tire in a future time instant, making an angle  $\alpha$  with the blue vector. The orange line is proportional to the real curve radius.

angle and vehicle velocity, while the outputs are lateral force and yaw rate. The model is based in equation (5-10), which can also be written as equation (5-30), where m is the car mass, v is the car velocity and R is the curve radius.

$$Force_{centripetal} = m \frac{v^2}{R} \tag{5-30}$$

Because we want specific force instead of force, the only unknown in equation (5-30) is the curve radius. This model assumes that the car path is equal to the front wheel path (which is wrong due to slip angles, tire-pavement interactions, inertia issues, etc.). Other assumption is that the steering wheel angle is proportional to the tire angle. Therefore, the curve radius is calculated based in Figure 5-15.

The calculations of the variable Radius<sub>p</sub> of Figure 5-15 are done in Appendix A. The model was tweaked using car data present at TNO, but that cannot be used in this study. Therefore the lateral specific force and yaw rate outputted by the model are given by equation (5-31) and equation (5-32) respectively, where v is the car velocity and R is a radius proportional to Radius<sub>p</sub> of Figure 5-15.

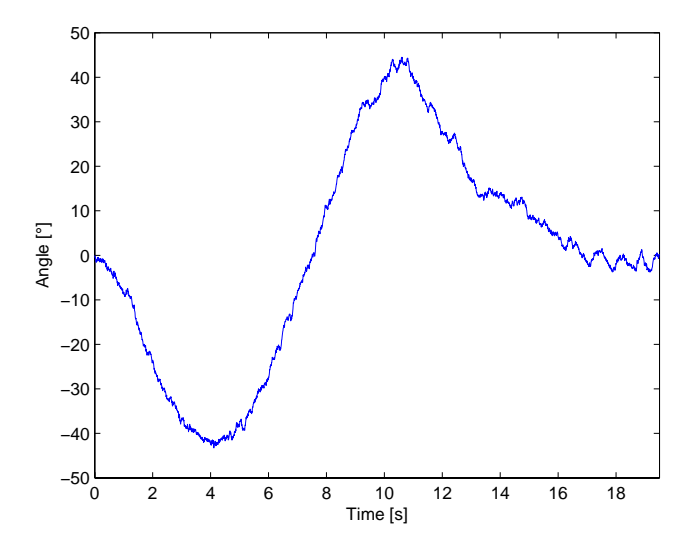


**Figure 5-16:** Steering wheel input.

$$lateral_{sf} = \frac{v^2}{R} \tag{5-31}$$

$$yaw_{rate} = \frac{v}{R} \tag{5-32}$$

#### 5-3-2 Datasets

#### Car model

The car model inputs are respectively steering wheel angle and car velocity. The steering wheel angle was obtained from the sum of a sinusoidal input with random noise and then smoothing it. The sinusoid had an amplitude of 60 degrees and a period of 12 seconds. Figure 5-16 shows this input. The steering wheel input had this shape in order to simulate a chicane.

The velocity input was built from the smoothing of a step input. The step input contained random noise. Figure 5-17 shows the velocity input. The velocity was kept constant during the all chicane, which is not quite realistic, but is good enough for a preliminary study.

The car model outputs, lateral specific force and yaw rate, are shown respectively in Figure 5-18 and Figure 5-19. No more cues were created to use as inputs for the motion cueing solutions since these are still only cueing lateral motions.

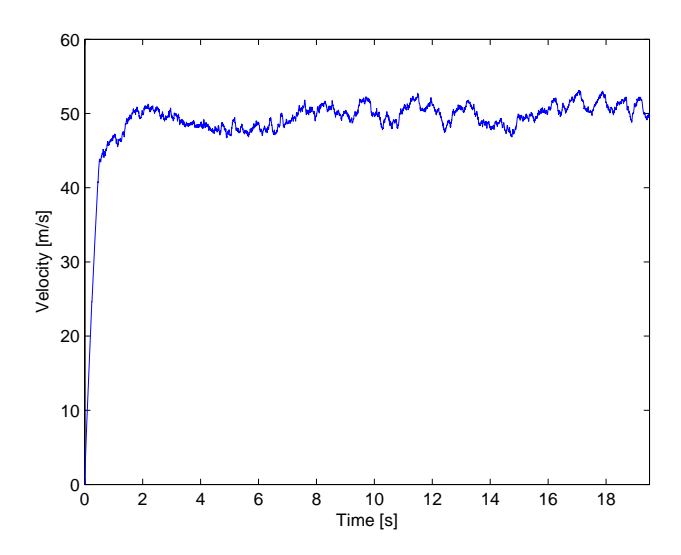


Figure 5-17: Velocity input.

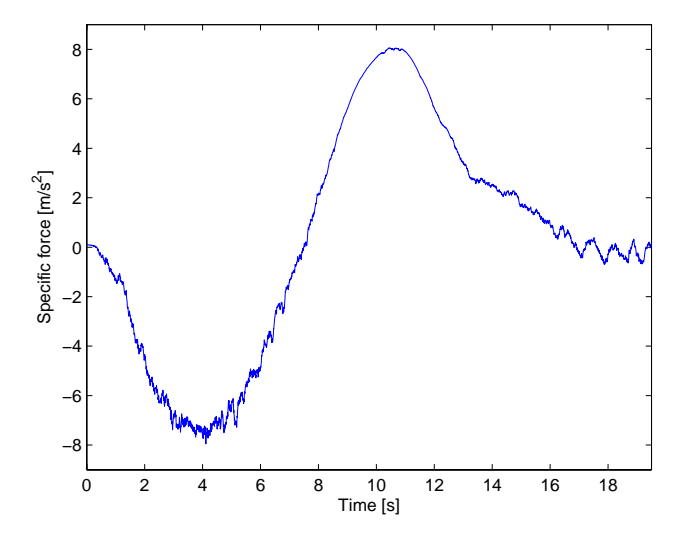


Figure 5-18: Car model lateral specific force.

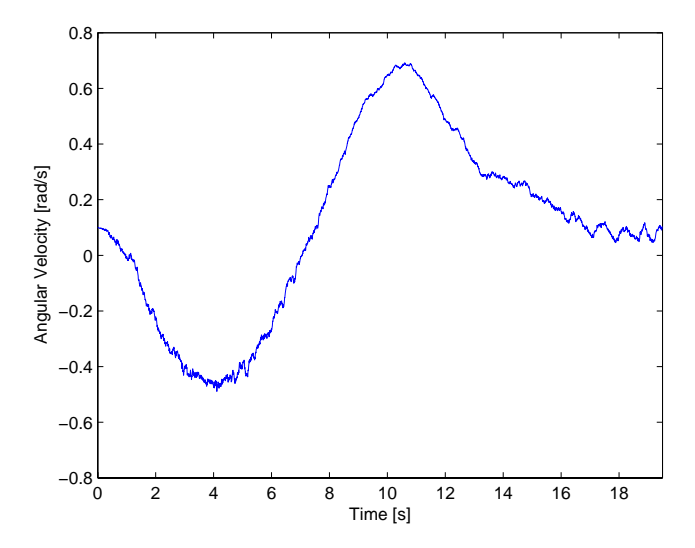


Figure 5-19: Car model yaw rate.

#### Roundabout dataset

The inputs needed from the motion cueing filters are: steering wheel angle, lateral specific force and yaw rate. For this dataset, these variables are shown in Figures 5-20, 5-21 and 5-22.

#### 5-3-3 Solution 1:

#### Car model results

Figure 5-23 contains the simulator specific forces versus the scaled lateral specific force from the car model. We can observe that the simulator specific force values have low amplitude (the values are between 2 and -2  $\rm m/s^2$ ) when compared with the car model ones (the scaled values are between 4 and -4  $\rm m/s^2$ ). Nevertheless the lateral specific force is most of the time in the correct direction. The simulation induces longitudinal specific force, which is a false cue. However, a judgement can not be made since the car model does not output longitudinal specific force, which in real car data could have similar direction to the one that is being generated by the simulator. We should also take into account that the developed motion cueing solutions are not yet cueing longitudinally. The introduction of a longitudinal channel will change the behaviour of the simulator.

The angular rates involved in this simulation are shown in Figure 5-24. Although the angular rates are being feed one to one to the simulator, the differences between the car model yaw rate and the simulator yaw rate are noticeable. The main reason of this has to with the steering wheel interaction (2 in Figure 5-2) that is used to position the simulator cabin in the correct curve direction so that the lateral specific forces induced by the rotation of Desdemona central yaw are also in the right direction. However, this creates the spurious yaw rates that we see in Figure 5-24.

From Figure 5-25 we can see that Desdemona movement is rather simple, since the simulator only uses the central yaw and the yaw gimbal actuators. Desdemona radius is constant dur-

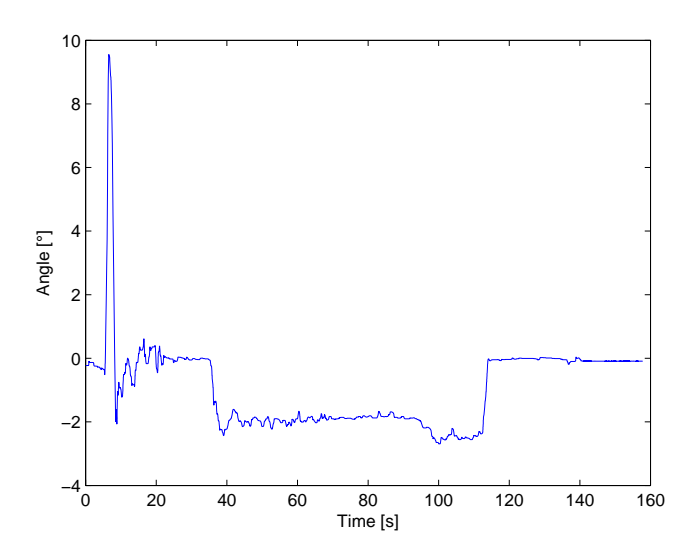


Figure 5-20: Roundabout dataset steering wheel angle.

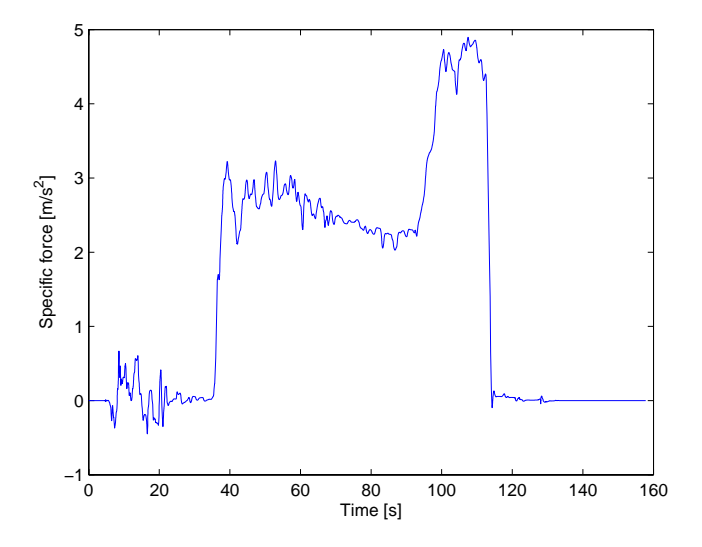


Figure 5-21: Roundabout dataset lateral specific force.

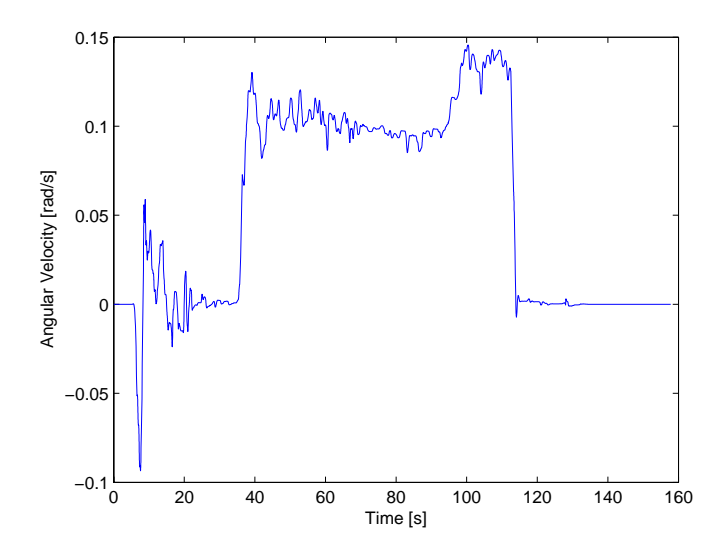
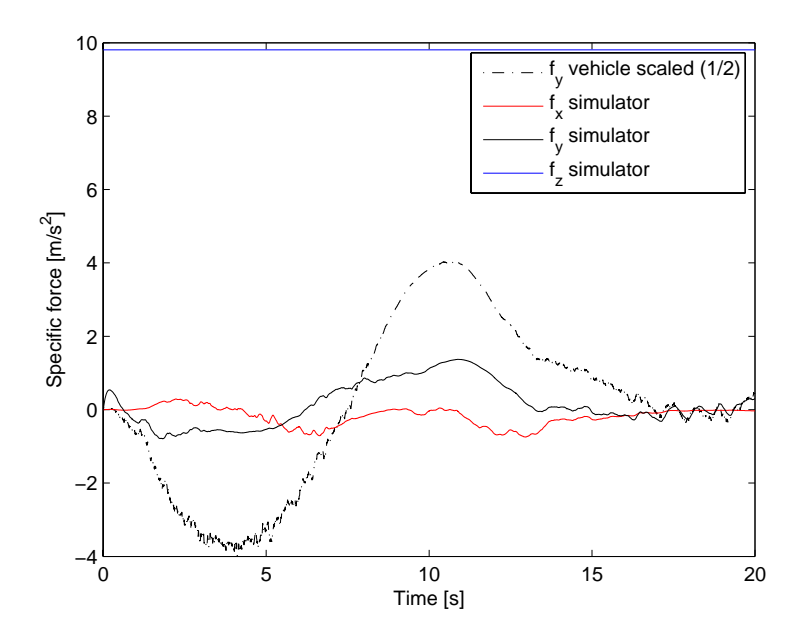
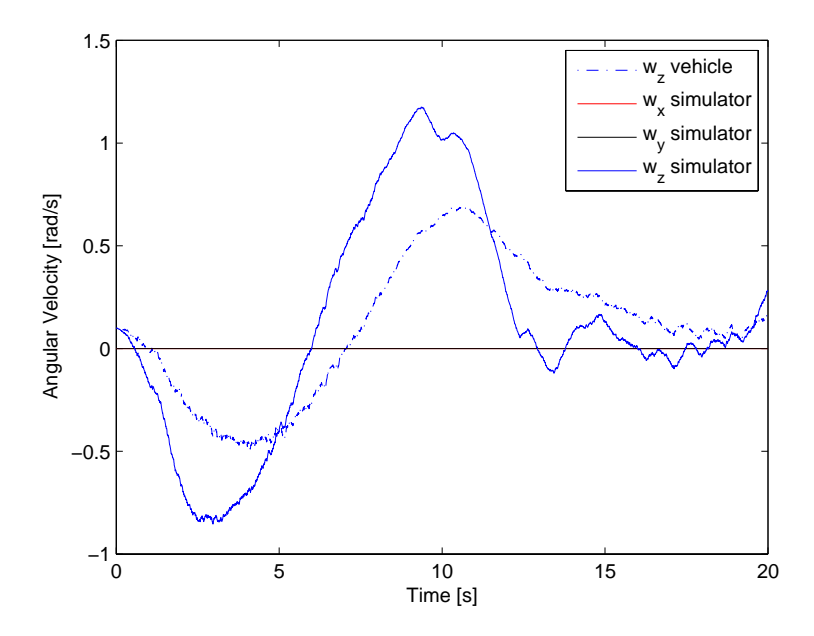


Figure 5-22: Roundabout dataset yaw rate.



**Figure 5-23:** Specific forces of the car model data versus simulated data using motion cueing solution 1.



**Figure 5-24:** Angular rates of the car model data versus simulated data using motion cueing solution 1.

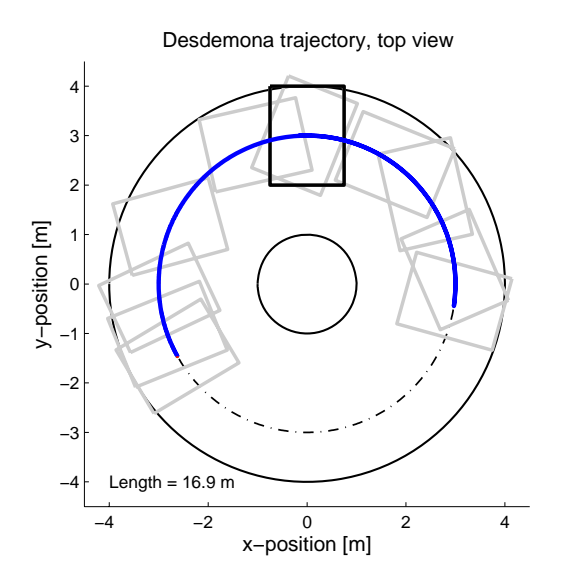
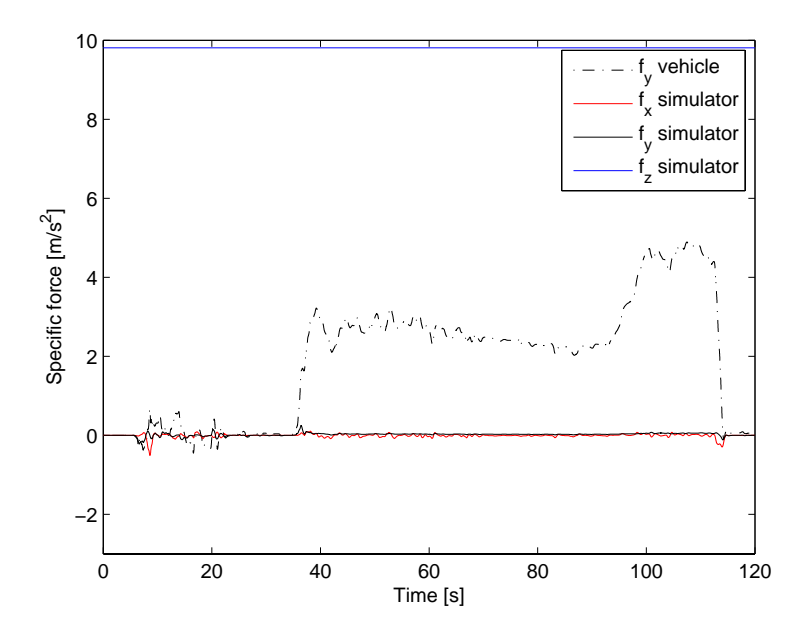


Figure 5-25: Desdemona displacement using motion cueing solution 1 (car model data).



**Figure 5-26:** Specific forces of the roundabout data versus simulated data using motion cueing solution 1.

ing the simulation, which means that this actuator can be used for lateral (or longitudinal, depending on the cabin position) onset cues. The relatively high number of DoF's that are not being used leave options for further developments in the algorithm.

#### Roundabout dataset results

For this dataset, the specific force built by the rotation of Desdemona central yaw is extremely low has we can see from Figure 5-26. These low specific forces are induced by the low yaw rate values (Figure 5-27) present in this dataset. Note that this motion cueing solution is not triggered by specific forces, but by angular rates only. From Figure 5-22 we can see that the maximal yaw rate present in the dataset is of approximately 0.15 rad/s during the roundabout. Using equation (5-10) and knowing that Desdemona radius is fixed on 3 meters, the maximal specific force that we would obtain with this configuration is of about  $0.0675 \text{ m/s}^2$ , which is too low when compared with the roundabout data lateral specific force (the maximum is around the  $5 \text{ m/s}^2$ ).

One of the possible reasons for the low yaw rate present in the roundabout data has to do with a large roundabout radius. From equation (5-32) we can observe that for a constant velocity v, if the radius increase, the angular rate decreases, which explains the existence of low angular rates for rotations with a large radius. The peaks of yaw rate seen in Figure 5-27 are induced by the steering wheel channel (2 in Figure 5-2). The variations that happen around the first 20 seconds of simulation, come from the large steering wheel input that the driver has done before driving in the roundabout. Such input can be seen in Figure 5-20.

Desdemona displacement in this case (Figure 5-28) is similar to the one in Figure 5-25, which is expected since the motion cueing algorithm is the same. The length however is much higher

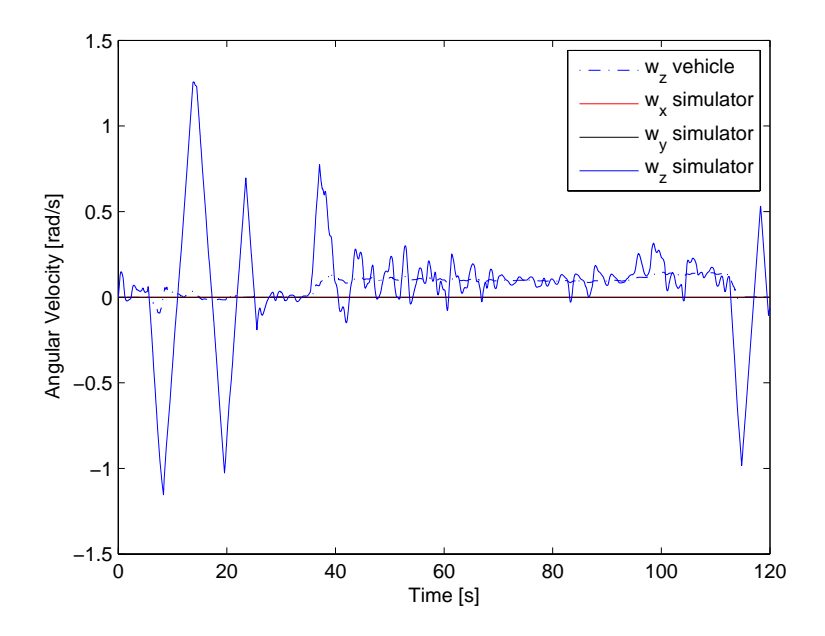


**Figure 5-27:** Angular rates of the roundabout data versus simulated data using motion cueing solution 1.

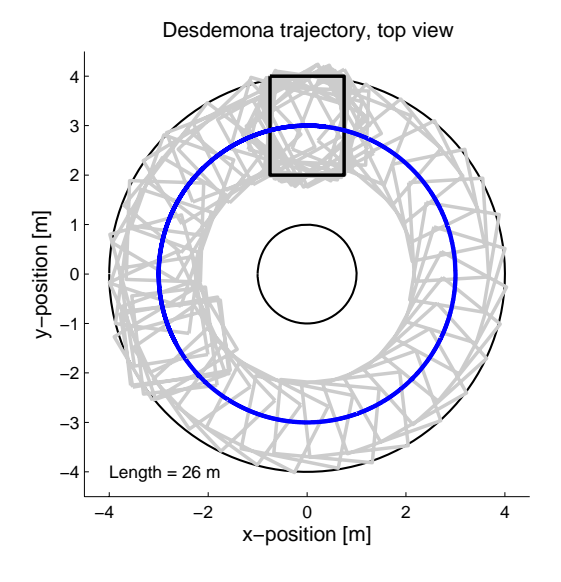
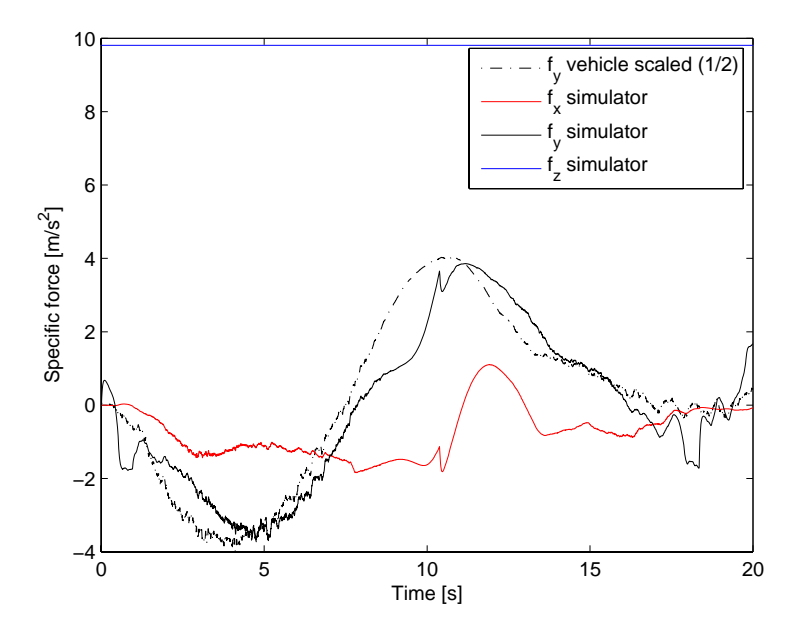


Figure 5-28: Desdemona displacement using motion cueing solution 1 (roundabout data).



**Figure 5-29:** Specific forces of the car model data versus simulated data using motion cueing solution 2.

due to the longer simulation time for this data (120 seconds versus the 20 seconds of the car model data).

#### 5-3-4 Solution 2:

#### Car model results

This motion cueing solution tries to match the car lateral specific force instead of the car yaw rate. This solution reaches specific force values (Figure 5-29) of the same magnitude order of the scaled specific force coming from the car model (the specific force input for the motion filter had a gain of 0.5). The solution introduces longitudinal specific force false cues due to the steering wheel method that is being used to turn the cabin to the correct direction (method that is also used on solution 1). These false cues, can however be decreased with the use of a better car model and the implementation of longitudinal cueing in the motion cueing solution. The steering wheel interaction and limiting introduce some discontinuities in the signal like the one around 10 seconds. From 5-29 we can also observe that the simulator lateral specific force has delay when compared with the car model lateral specific force.

The yaw rate generated by this solution is much higher than the car model yaw rate, since Desdemona central yaw is used, not to match the yaw rate, but to match the lateral specific force. In Figure 5-30 we can also find angular rate peaks similar to the ones of solution 1, due to the steering wheel interaction. High frequency yaw rate continues to be simulated without any scaling.

Desdemona displacement continues to be radial, with a radius around 3 meters, which is the neutral position defined for this solution. Nevertheless, radius variations occur in this solution

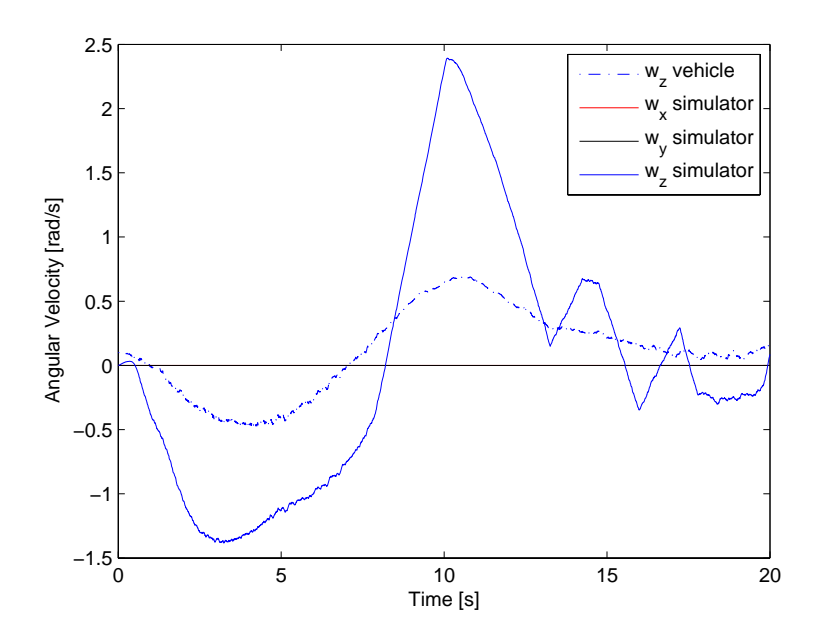


**Figure 5-30:** Angular rates of the car model data versus simulated data using motion cueing solution 2.

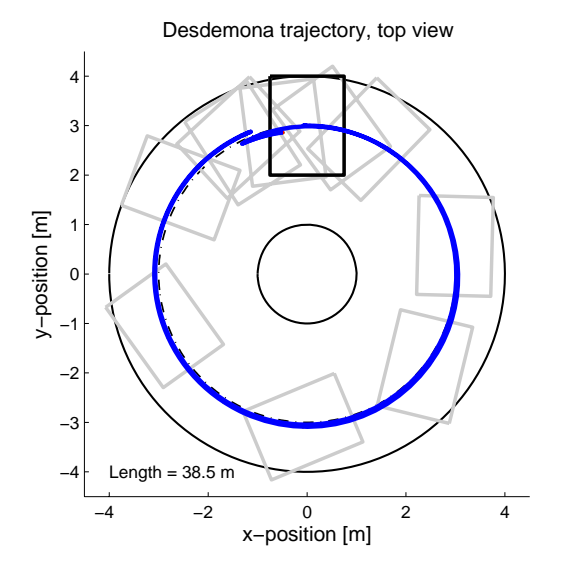
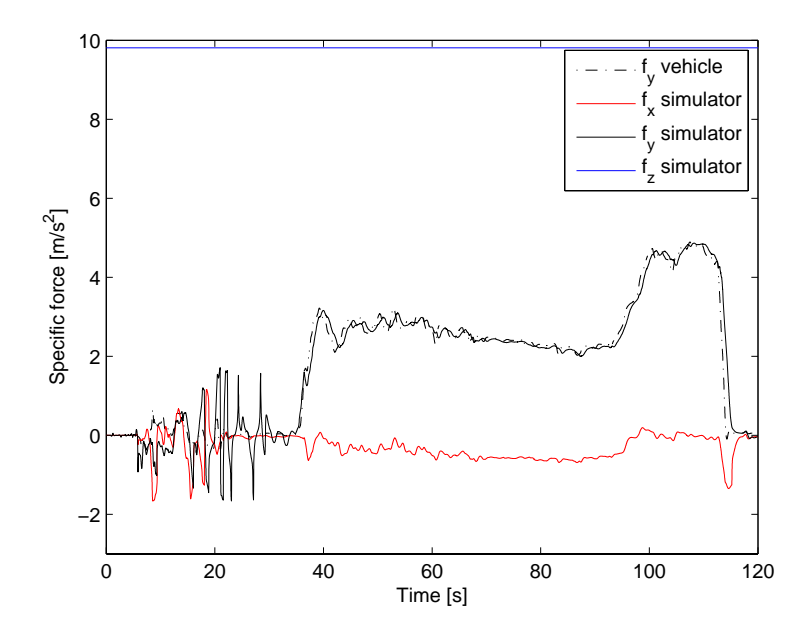


Figure 5-31: Desdemona displacement using motion cueing solution 2 (car model data).



**Figure 5-32:** Specific forces of the roundabout data versus simulated data using motion cueing solution 2.

due to the use of Desdemona radius to generate onset cues. In Figure 5-31 it is possible to see that the radius is not always 3 meters. We can also observe that this solution generates large Desdemona travelling, which happens because of the higher angular rates used in Desdemona central yaw. This solution still presents free DoF's which can be used to improve the algorithm in the future.

#### Roundabout dataset results

According to Figure 5-32 the lateral specific force during the roundabout shows a good fit in terms of signal amplitude and shape. Nevertheless, the simulation continues to contain delay. The level of longitudinal false cues during the roundabout is low (the biggest variation occurs at the end of the roundabout). At the initial seconds of simulation, the simulator signals are a little noisy, due to Desdemona central yaw acceleration. This situation can be solved with some smoothing filters, but this solution will introduce more delay in the simulation.

In Figure 5-33 it is easier to observe that the simulator yaw rates are much higher than the roundabout data yaw rates. This is expected due to the use of the Desdemona centrifuge capabilities to obtain sustained specific forces. The signal is noisy, during the roundabout, due to the steering wheel interaction used to rotate the cabin. In the first simulation seconds, the peaks in Figure 5-33 occur due to an interaction between the steering wheel method (which has large initial steering wheel inputs shown in Figure 5-20) and the angular accelerations of Desdemona central yaw needed to follow specific force in the beginning of the dataset (which can be seen in Figure 5-21).

Figure 5-34 does a better job than Figure 5-31 in showing the radius variation for this motion cueing solution. Again, we can also see the large simulator displacements obtained by this

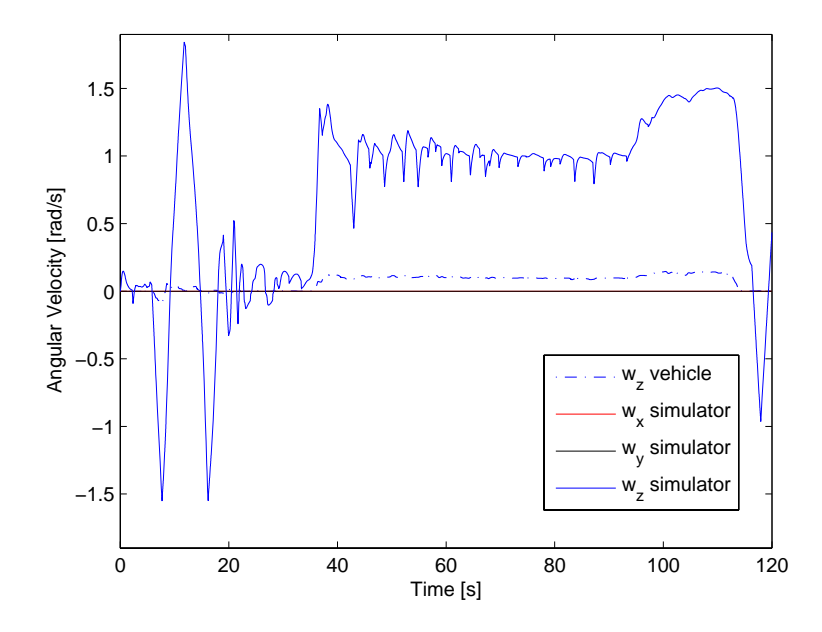


**Figure 5-33:** Angular rates of the roundabout data versus simulated data using motion cueing solution 2.

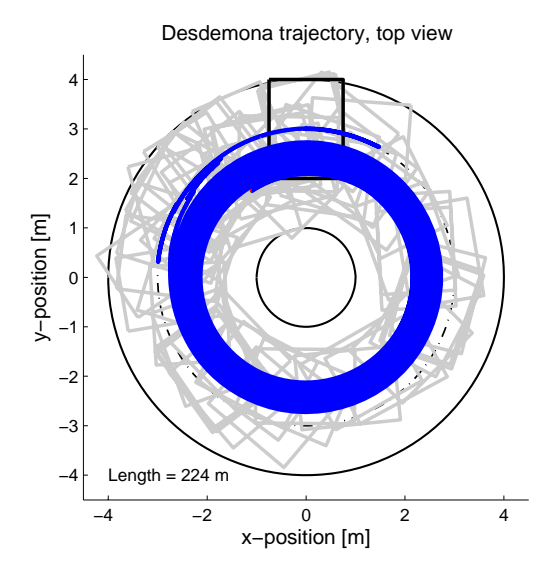


**Figure 5-34:** Desdemona displacement Desdemona displacement using motion cueing solution 2 (roundabout data).

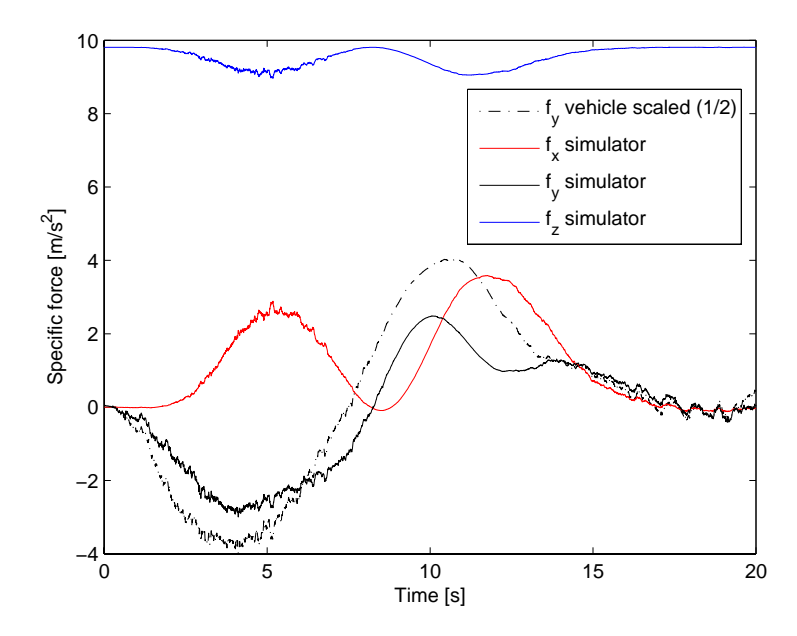


**Figure 5-35:** Specific forces of the car model data versus simulated data using motion cueing solution 3.

solution.

#### 5-3-5 Solution 3:

#### Car model results

Figure 5-35 shows the specific forces generated by motion cueing solution 3. We can see that the lateral onsets cues are quite good and that the sustained cues respect the movement direction, even though that they are not a perfect fit. However, this solution introduces longitudinal false cues mainly because no rotation matrix is being used to convert the tilting coordination body rates into Desdemona rates. In this case, that is a problem because the used complementary filters will create large displacements in Desdemona yaw gimbal. If the roll gimbal has already some displacement (due to tilting coordination) the variation on the yaw gimbal will induce cabin pitch variations, as we can see in Figure 5-36. Note that the longitudinal false cue of Figure 5-35 is in phase with the pitch rate of Figure 5-36. Future work is needed to correct these false cues. The most direct solution is to use the rotation matrices in order to produce the correct body rotations in the cabin. Nevertheless it is important to analyse a more complete car model first (with longitudinal specific force output) in order to see if we can take advantage of these false cues to improve the simulation.

The yaw rate fit is quite impressive as we can see from Figure 5-36, where the signal shape and amplitude are very similar to the car model ones. The spurious angular rates introduced by the interaction of the tilting coordination with the complementary yaw rate high pass filters are relatively high (around 12 °/s) which can be disorienting for the driver, since the standard used in simulations is near 3 °/s (human threshold for angular motion).

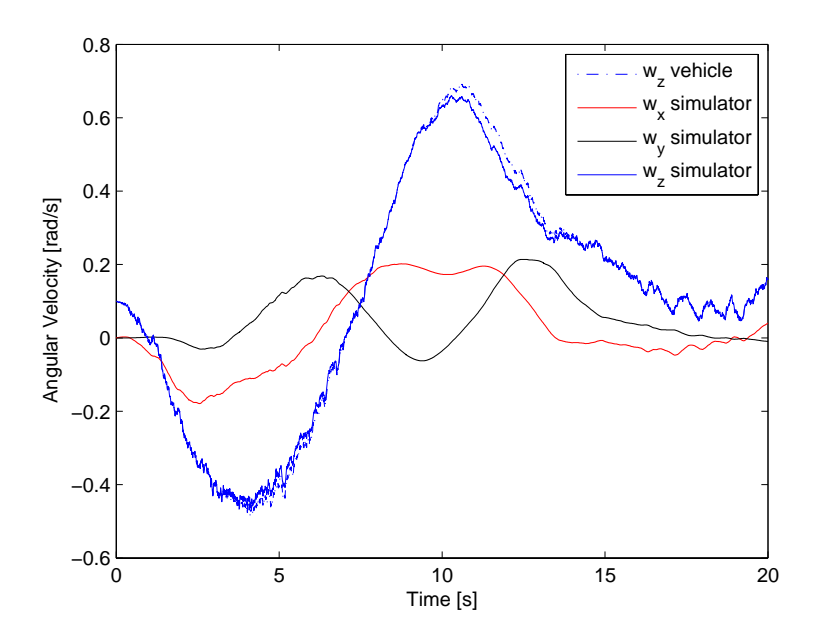


**Figure 5-36:** Angular rates of the car model data versus simulated data using motion cueing solution 3.

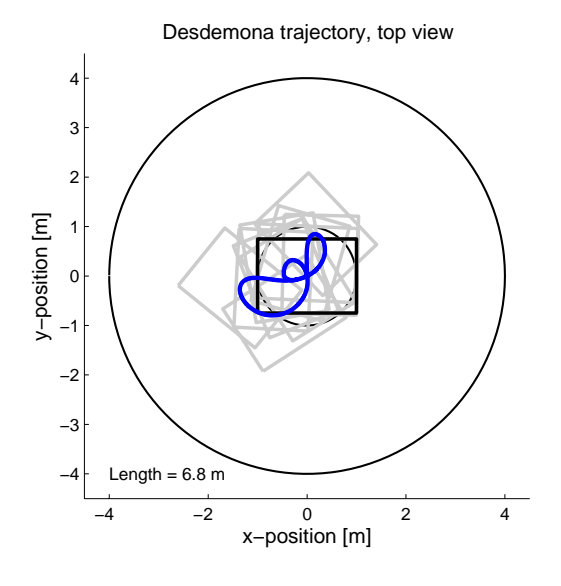
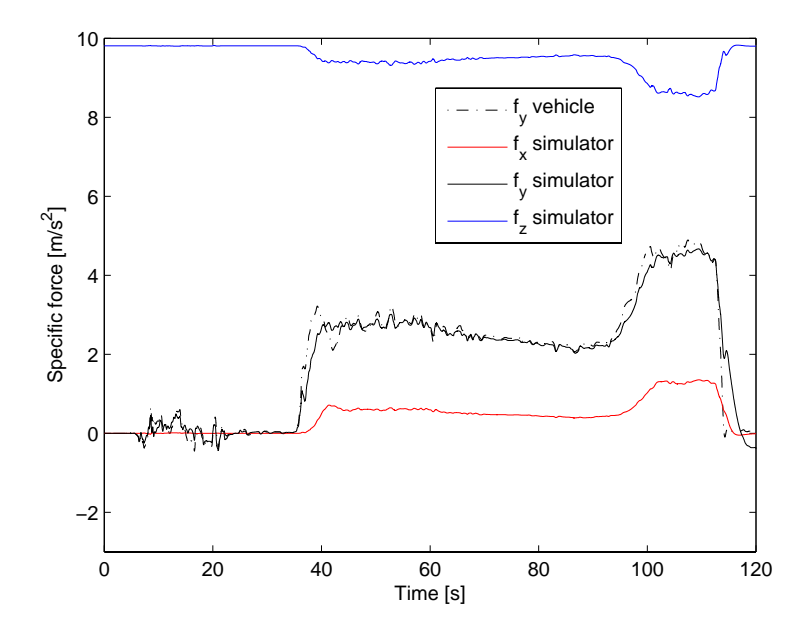


Figure 5-37: Desdemona displacement using motion cueing solution 3 (car model data).



**Figure 5-38:** Specific forces of the roundabout data versus simulated data using motion cueing solution 3.

This solution uses a smaller motion space, than the previous solutions. This situation can change with a more effective tuning, but it is desirable to have this motion space flexibility in order to do direct comparisons between Desdemona and smaller simulators.

#### Roundabout dataset results

Figure 5-38 shows that the lateral specific force contains a good fit regarding onset cues, but that the tilting coordination introduces some delays in the lateral sustained cues. It is possible to see the tilting coordination interferences in the beginning and in the end of the roundabout (around second 36 and second 114 of the simulation). Note that tilting coordination will also change the vertical specific force component. Longitudinal false cues continue present, but now the signals order of magnitude is lower than the lateral cues order of magnitude, while for Figure 5-35 the orders of magnitude were similar.

Figure 5-39 shows the simulation angular rates. The yaw angular rate has a good fit with the roundabout data yaw rate, which was expected due to the complementary filters described before. Again, we can also observe the spurious angular rates due to the interaction of these filters with the tilting coordination block used to create sustained lateral specific forces.

Figure 5-40 shows again that this solution uses fewer motion space than solutions 1 and 2. The simulator action zone continues to be mostly in the middle of the radius sledge (which was defined has the neutral position), leaving the extremes of the radius sledge for more demanding manoeuvre during the simulation.

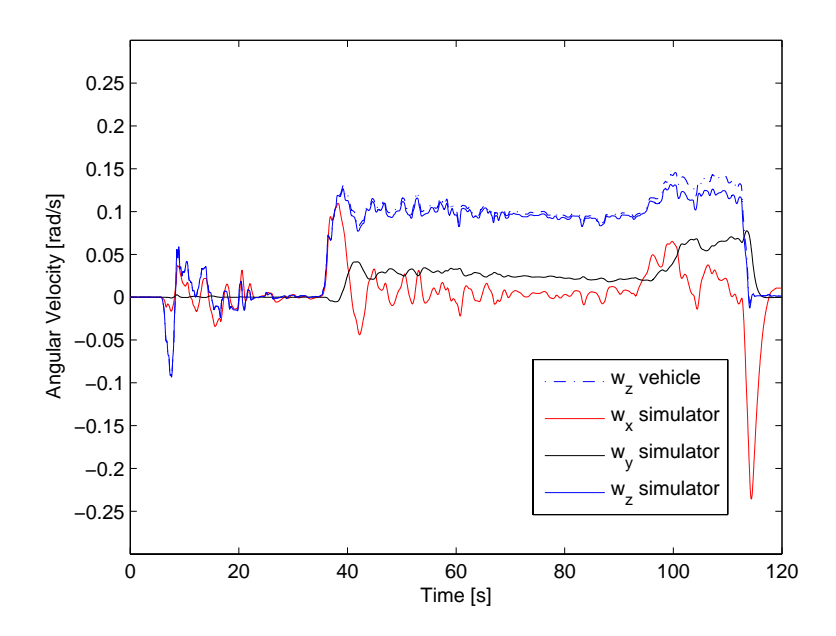


**Figure 5-39:** Angular rates forces of the roundabout data versus simulated data using motion cueing solution 3.

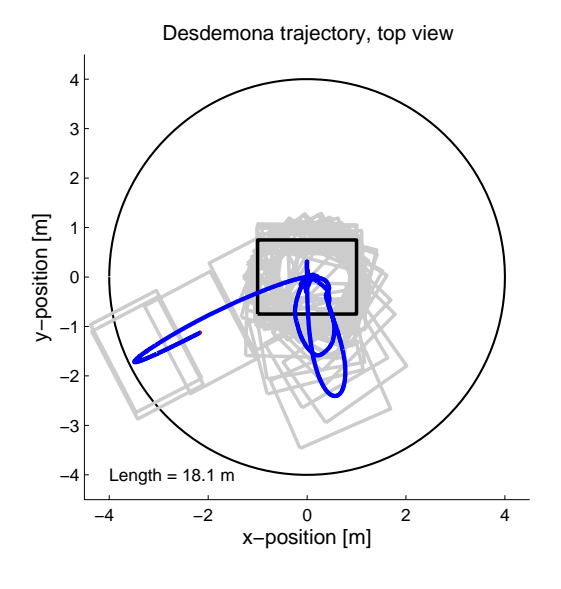
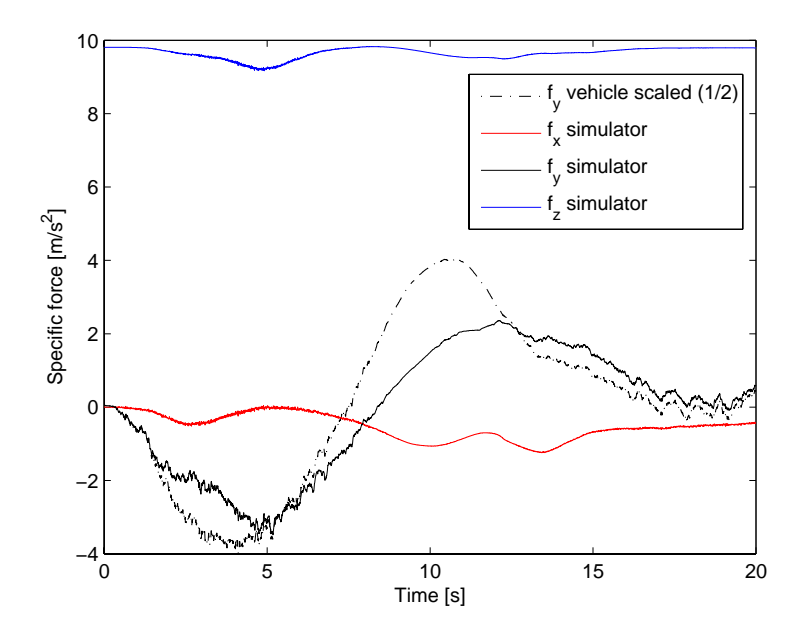


Figure 5-40: Desdemona displacement using motion cueing solution 3 (roundabout data).



**Figure 5-41:** Specific forces of the car model data versus simulated data using motion cueing solution 4.

#### 5-3-6 Solution 4:

#### Car model results

This motion cueing solution has the particularity of allowing assigning initial positions to Desdemona gimbals. Therefore, different cueing solutions can be built based on this motion cueing filter. For this situation, the cabin initial position is 0 degrees for the roll and pitch gimbals and -65 degrees for the yaw gimbal. This configuration is used to take advantage of the Desdemona central yaw since this actuator does not need position washout. The simulator specific forces in Figure 5-41 show a good match regarding onset cues. The sustained cues suffer from the normal problems introduced by tilting coordination techniques (signal delay and difficulties to reach the maximal amplitudes of the car model). The longitudinal false cues are very low and are generated by the central yaw acceleration used to produce lateral onset cues. This generates longitudinal specific forces because the rotation of the central yaw actuator will create centripetal forces in the cabin.

The yaw angular rates have a similar shape to the car model yaw rate as we can observe from Figure 5-42. Nevertheless this situation occurs just because we are using Desdemona central yaw to generate the lateral specific force, since this solution only cues high frequency yaw rates. The spurious angular rates due to tilting coordination achieve limits near the 6  $^{\circ}$ /s which is a little high for tilting coordination standards (due to human thresholds for angular rates) but those limits have already been used in other studies [Wentink et al., 2008b].

For this simulation, a neutral position of -2 meters in radius was used. According to Figure 5-43 a larger radius could be used since the simulator was always quite far from its position limits. This would allow the use of a lateral onset force with a higher amplitude as we can show from equation (5-28) (when R increases,  $a_c$  also increases for a constant  $\dot{\omega}$ ).

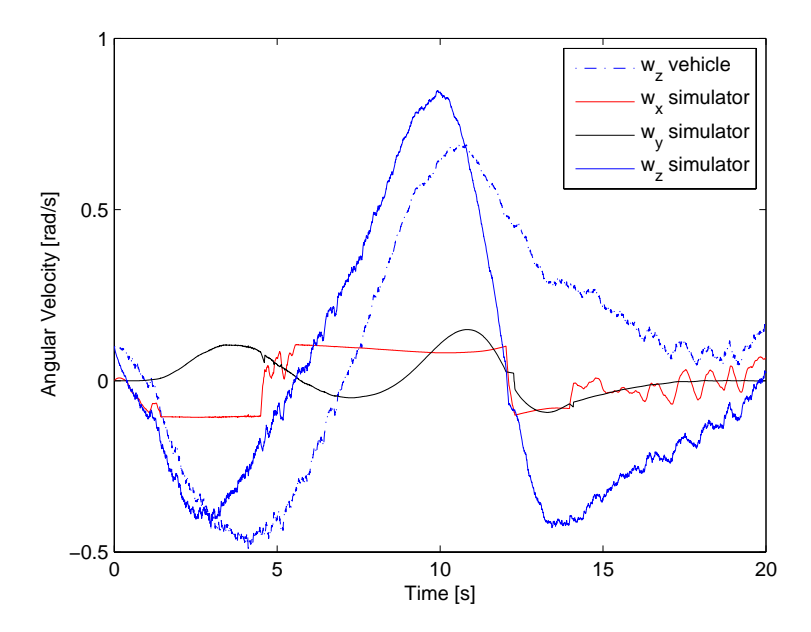


**Figure 5-42:** Angular rates of the car model data versus simulated data using motion cueing solution 4.

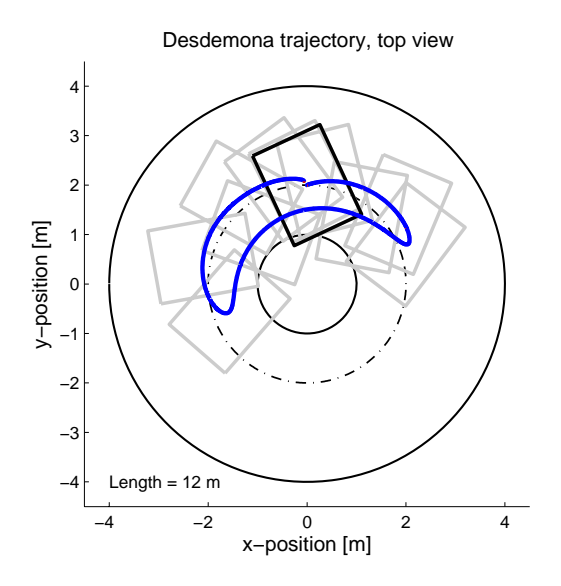
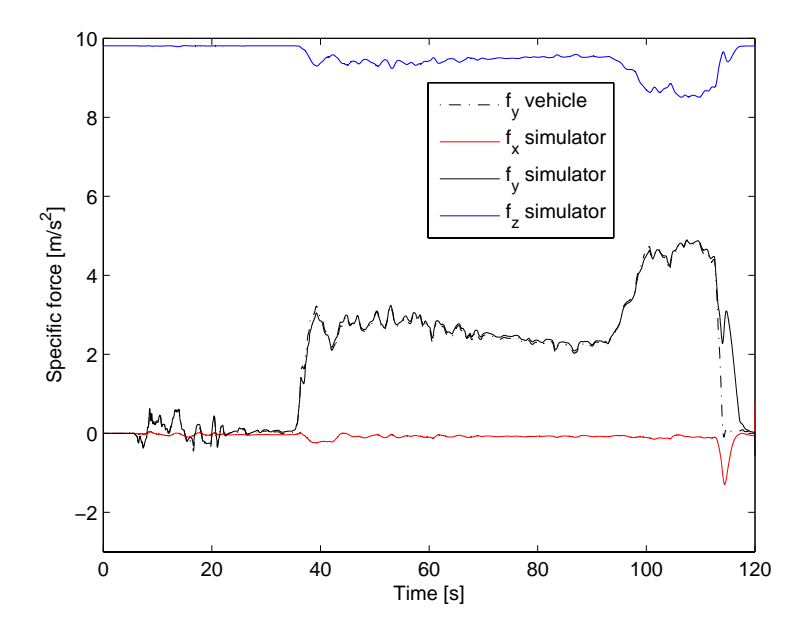


Figure 5-43: Desdemona displacement using motion cueing solution 4 (car model data).



**Figure 5-44:** Specific forces of the roundabout data versus simulated data using motion cueing solution 4.

#### Roundabout dataset results

The gimbals initial positions used for this dataset are the same as the ones used in section 5-3-6. The lateral specific force match shown in Figure 5-44 is quite good, only showing some tilting coordination issues, especially at the end of the roundabout. We can also see that this simulation does not present any considerable amount of delay (except around the 114 second due to tilting coordination issues). The onset and sustained cues show a very good fit and the longitudinal false cue is minimal (showing problems only at the end of the roundabout). The vertical false cues occur because of tilting coordination.

The yaw angular rate in this case does not show a nice fit when compared with the yaw rate of the roundabout data. The reason for that is the fact that only the high frequency yaw rate is being cued. The peaks in yaw rate that we see in Figure 5-45 at the beginning (approximately at t=38s), middle (approximately at t=96s) and end (approximately at t=114s), come from the generation of lateral onset cues performed by Desdemona central yaw actuator. The other angular rates are near the 6  $^{\circ}$ /s limit already discussed in section 5-3-6.

From Figure 5-46 we can conclude again that the radius neutral position can be increased to take advantage of a larger motion space which allows the use of a higher lateral specific force onset.

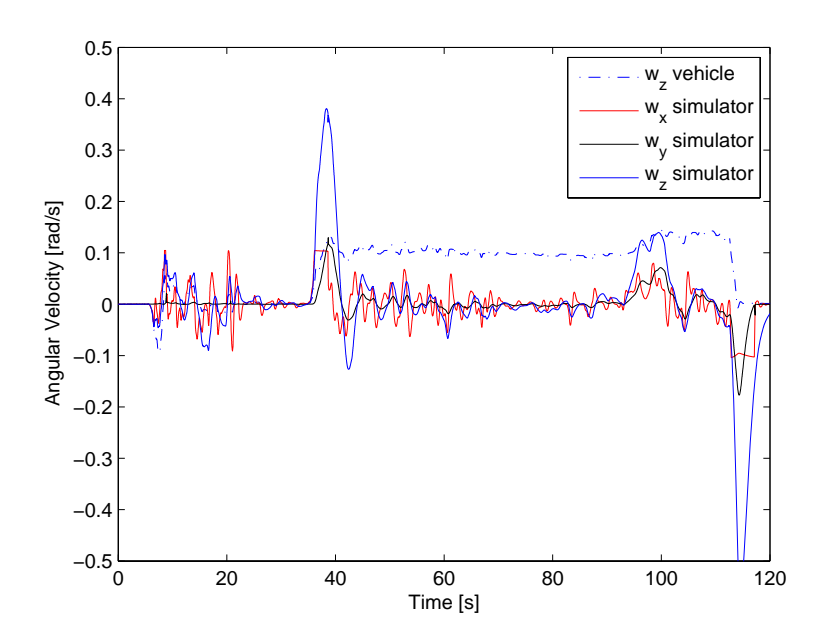


**Figure 5-45:** Angular rates of the roundabout data versus simulated data using motion cueing solution 4.

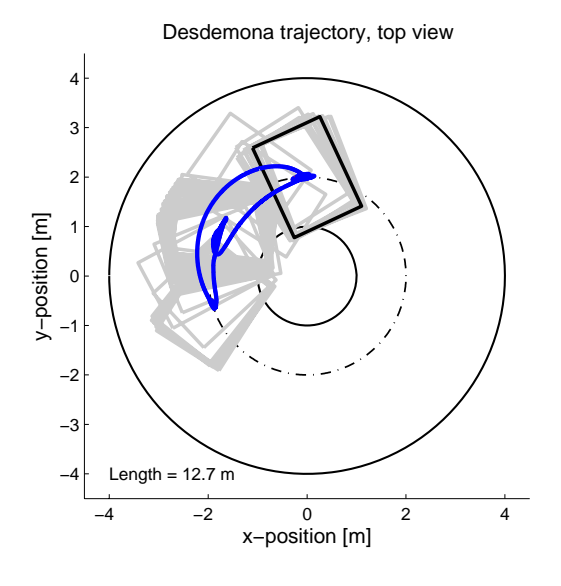


Figure 5-46: Desdemona displacement using motion cueing solution 4 (roundabout data).

### Conclusion and Future Guidelines

#### 6-1 Literature Research

The literature review performed in this research covers some of the most important studies regarding motion cueing evaluation. Some evaluation methods may not be mentioned here, but we believe that the most relevant are present. The evaluation methods were divided into objective evaluations and subjective evaluations. In the objective evaluations we found the following methods: graphical comparison, performance indicator, motion fidelity criterion, PSD analysis, statistical analysis of mathematical variables.

Graphical comparison is a method that uses time history plots to draw performance conclusions. The most used variables in this method are specific forces and angular rates. When comparing the motion cues from the vehicle with the ones delivered by the motion cueing algorithm, it is possible to draw conclusions about false cues, scaling errors and signal shape errors. From this method it is hard to know how humans will react to the simulation. We also can't get workload measures from it.

Performance indicator is a method that uses a mathematical formula to give a rating to the motion cueing algorithm. In this way it is possible to have a global notion of how good algorithm is. Nevertheless, this is the only information that is possible to take from this method, losing then other relevant knowledge (regarding false cues, scaling errors, workload, among others).

Motion fidelity criterion evaluates the motion cueing algorithm based in its filter properties (scaling, break frequencies, phase distortion). Normally, this evaluation method uses a fidelity plot with fidelity zones where motion filters are rated. These fidelity zones are most of the time obtained recurring to subjective evaluations. This method only tells the designer where the washout filters would fit in the fidelity plot (according to the used parameters in the filter). However the validity of this information is somehow questionable because the fidelity plots where created based on specific manoeuvres that could be irrelevant to our study.

PSD analysis (and the statistical analysis) is an objective behavioural evaluation because it is based on the subject behaviour in the simulator. The PSD analysis measures the amount of

power that subjects dispend in the control inputs. With this is possible to obtain a workload measure and then conclude about the pilot performance for different motion filters. With this method it is not possible to conclude about false cues or signal shape errors.

The statistical analysis of mathematical variables method is used to assess the subject performance in the simulator for different motion situations. The statistical techniques that are most used are the RMS and STDV of manoeuvre characteristics, like braking distances, heading error, linear velocity among others. The used variables depend from study to study, nevertheless this method is used most of the times to check if motion improves a certain task (like negotiating velocity in curve driving) in the simulator. Therefore the use of this method to gather information about false cues, scaling errors or signal shape errors was not found in literature.

The subjective evaluations methods found in literature are the following: rating scales, subjective comments and pairwise comparison.

Rating scales are used in simulation in order to know the motion filter performance based in the subject's opinion. In this way, it is possible to infer if the interaction between the motion filter and the human vestibular system is done in a realistic way. This method however is dependent on the subject capability to distinguish motion filters. The order that the motion filters are presented to the subject can influence the rating. The use of questionnaires can increase the number of conclusions that we can take from this method.

Subjective comments is a method used to support other methods. Here conclusions are taken based on commentaries done by subjects during the simulation. The conclusions of this method depend on the nature of the commentaries.

Pairwise comparison is used to decrease the errors that result from presenting the motion filters in different orders. From this method it is possible to conclude about subject consistency in assigning rates to motion cueing algorithms. Therefore, conclusions about which motion filter performs better in a certain situation are more meaningful, since we can check if subjects were aware of which motion filter they were perceiving.

#### 6-2 Preliminary Analysis

Regarding the preliminary analysis, motion cueing solutions were developed with the objective of finding a design that best suits a racing simulation. Extreme manoeuvres need to be understood in order to be correctly simulated. The focus on this preliminary design was to develop a solution that ensures realistic lateral cues in order to obtain good results in curve driving. Therefore the longitudinal cueing will be developed in the future. Four solutions were developed, each one with different pros and cons.

Solution 1 should deliver a good yaw rate cue due to the one to one coupling existent between the vehicle model and the Desdemona actuators. The lateral specific force that this solution offers is of very low amplitude when compared with the one of the vehicle model. The steering wheel method used to turn the cabin introduces false cues.

Solution 2 is driven by lateral specific force which guarantees that the simulation will have higher amplitude values of specific force when compared with solution 1. This solution uses Desdemona centrifuge capabilities to generate lateral specific force which is useful to create

high amplitude sustained cues. The drawback is that high rotations are needed to accelerate the simulator. Subjective tests should be done in order to see how disturbing these false cues are. The steering wheel interaction also creates false cues.

Solution 3 delivers good onset cues. The specific force sustained cues are achieved using tilting coordination techniques. The yaw rate is simulated one to one. Because Desdemona pitch gimbal is not used to compensate roll and yaw gimbals interaction (between tilting coordination (roll) and high frequency yaw rate), false cues exist in this method. This situation should be solved in future designs.

Solution 4 uses rotation matrices to transform car body-axis into Desdemona inertial axis. Therefore this design delivers very good onsets. It is also possible to change cabin initial conditions in order to choose which Desdemona actuators we want to use. Tilting coordination is used in this solution to deliver specific force sustained cues. This will introduce the normal tilting coordination false cues in this solution. Future designs can try to couple a centrifuge design in this solution with the intention of generating produce sustained specific forces.

The solutions were not exhaustively tuned to fit the datasets present in section 5-3 because the objective of that section was only to show how the motion cueing solutions work. Race driving datasets (or a racing vehicle model) are needed to choose the solution that best simulates a car driving in the traction limit. The graphical comparison method was used with the same objective (showing how the solutions work). For future work, we want to design an experiment which helps us to discover which algorithm is best suited for a race driving simulator. This experiment will also be used to identify the motion cues that best describe an oversteer manoeuvre. All the motion cueing solutions need to be upgraded with simulation of longitudinal motion cues and an exhaustive tuning has to be made in order to guarantee that the solutions are in top of their performance.

- [Baarspul, 1990] Baarspul, M. (1990). A review of flight simulation techniques. *Progress in Aerospace Sciences*, 27(1):1–120.
- [Barbagli et al., 2001] Barbagli, F., Ferrazzin, D., Avizzano, C. A., and Bergamasco, M. (2001). Washout filter design for a motorcycle simulator. In *Virtual Reality*, pages 225–232. IEEE.
- [Beckman, ] Beckman, B. The physics of racing. 1991.
- [Bentley, 1998] Bentley, R. (1998). Speed Secrets: Professional Race Driving Techniques. MO-TORBOOKS INTERNATIONAL.
- [Beykirch et al., 2007] Beykirch, K., Nieuwenhuizen, F. M., Teufel, H. J., Nusseck, H. G., Butler, J. S., and Bülthoff, H. H. (2007). Control of a lateral helicopter side-step maneuver on an anthropomorphic robot. In *Modeling and Simulation Technologies Conference and Exhibit*, Hilton Head, South Carolina. AIAA.
- [Brünger-Koch et al., 2006a] Brünger-Koch, M., Briest, S., and Vollrath, M. (2006a). Do you feel the difference? a motion assessment study. In *Driving Simulation Conference Asia/Pacific*, Tsubaka, Japan.
- [Brünger-Koch et al., 2006b] Brünger-Koch, M., Briest, S., and Vollrath, M. (2006b). Virtual driving with different motion characteristics braking manoeuvre analysis and validation. In 2006 Driving Simulation Conference.
- [Bussolari et al., 1986] Bussolari, S. R., Sullivan, R. B., and Young, L. R. (1986). Vestibular models for design and evaluation of flight simulator motion. In *Royal Aeronautical Society conference on Advances in Flight Simulation Visual and Motion Systems*, London.
- [Chapron and Colinot, 2007] Chapron, T. and Colinot, J.-P. (2007). The new psa peugeotcitroën advanced driving simulator overall design and motion cue algorithm. In *DSC 2007 North America*, Iowa City.

[Chen and Fu, 2007] Chen, S.-H. and Fu, L.-C. (2007). Predictive washout filter design using the forward kinematics and a kalman filter. In *Control Applications*, Singapore. IEEE.

- [Colombet et al., 2008] Colombet, F., Dagdelen, M., Reymond, G., Pere, C., Merienne, F., and Kemeny, A. (2008). Motion cueing: what is the impact on the driver's behaviour? In DSC 2008 Europe, pages 171–181, Monaco.
- [Conrad and Schmidt, 1970] Conrad, B. and Schmidt, S. F. (1970). Motion drive signals for piloted flight simulators. Technical Report CR-1601, NASA.
- [Conrad et al., 1973] Conrad, B., Schmidt, S. F., and Douvillier, J. G. (1973). Washout circuit design for multi-degrees-of-freedom moving base simulators. In *Visual and Motion Simulation Conference*, number 73-929, Palo Alto, California. AIAA.
- [Cooper and Harper, 1969] Cooper, G. E. and Harper, R. P. (1969). The use of pilot rating in the evaluation of aircraft handling qualities. Technical Report TN D-5153, NASA.
- [Crosbie and Kiefer, 1985] Crosbie, R. J. and Kiefer, D. A. (1985). Controlling the human centrifuge as a force and motion platform for the dynamic flight simulator. In *Flight Simulation Technologies Conference*, number 85-1742, St. Louis, MO.
- [Dagdelen et al., 2004] Dagdelen, M., Reymong, G., Kemeny, A., Bordier, M., and Maïzi, N. (2004). Mpc based motion cueing algorithm: Development and application to the ultimate driving simulator. In *Proceedings of the DSC Europe Conference*, pages 221–233, Paris, France.
- [Fischer and Werneke, 2008] Fischer, M. and Werneke, J. (2008). The new time-variant motion cueing algorithm for the dlr dynamic driving simulator. In *Proceedings of the DSC Europe Conference*, pages 57–68, Monaco.
- [Fortmüller and Meywerk, 2005] Fortmüller, T. and Meywerk, M. (2005). The influence of yaw movements on the rating of the subjective impression of driving. In *DSC2005 North America*, Orlando.
- [Fortmüller et al., 2008] Fortmüller, T., Tomaske, W., and Meywerk, M. (2008). The influence of sway accelerations on the perception of yaw movements. In *DSC 2008 Europe*, pages 161–170. Monaco.
- [Frère, 1992] Frère, P. (1992). Sports Car and Competition Driving. Bentley Publishers.
- [Grant, 1995] Grant, P. R. (1995). The development of a tuning paradigm for flight simulator motion drive algorithms. PhD thesis, Institute for Aerospace Studies, University of Toronto.
- [Grant, 2006] Grant, P. R. (2006). Motion drive algorithm development for a large displacement simulator architecture with redundant degrees of freedom. In *DSC Asia/Pacific 2006*, Tsubaka, Japan.
- [Grant et al., 2002] Grant, P. R., Artz, B., Blommer, M., Cathey, L., and Greenberg, J. (2002). A paired comparison study of simulator motion. In *DSC2002 Proceeding*, Paris, France.

[Grant et al., 2003] Grant, P. R., Blommer, M., Cathey, L., Artz, B., and Greenberg, J. (2003). Analyzing classes of motion drive algorithms based on paired comparison techniques. In *DSC North America 2003 Proceedings*.

- [Grant and Reid, 1997] Grant, P. R. and Reid, L. D. (1997). Motion washout filter tuning: Rules and requirements. *Journal of Aircraft*, 34(2):145–151.
- [Greenberg et al., 2003] Greenberg, J., Artz, B., and Cathey, L. (2003). The effect of lateral motion cues during simulated driving. In *Driving Simulator Conference North America* 2003 Proceedings, Dearborn, Michigan.
- [Groen and Bos, 2008] Groen, E. L. and Bos, J. E. (2008). Identification of "bad simulator motion". In *DSC 2008 Europe*, pages 237–245, Monaco.
- [Gum, 1973] Gum, D. R. (1973). Modeling of the human force and motion-sensing mechanics. Technical report, U. S. Air Force Human Resources Lab.
- [Gundry, 1976] Gundry, A. J. (1976). Thresholds to roll motion in a flight simulator. In *Visual and Motion Simulation Conference*, Dayton, Ohio. AIAA.
- [Guo et al., 2003] Guo, L., Cardullo, F. M., Telban, R. J., Houck, J. A., and Kelly, L. C. (2003). The results of a simulator study to determine the effects on pilot performance of two different motion cueing algorithms and various delays, compensated and uncompensated. In *Modeling and Simulation Technologies Conference*, Austin, TX. AIAA.
- [Hart and Staveland, 1988] Hart, S. G. and Staveland, L. E. (1988). Development of nasa-tlx (task load index): Results of empirical and theoretical research. *Human Mental Workload*, P. A. Hancock and N. Meshkati (Eds.):139–183.
- [Idan and Nahon, 1999] Idan, M. and Nahon, M. A. (1999). Off-line comparison and robust flight simulator motion control. *Journal of Guidance*, *Control and Dynamics*, 22(5):702–709.
- [Idan et al., 1998] Idan, M., Nahon, M. A., and Sahar, D. (1998). A comparison of classical and robust flight simulator motion control. In *Modeling and Simulation Technologies Conference and Exhibit*, number 98-4366, Boston, MA. AIAA.
- [Idan and Sahar, 1996] Idan, M. and Sahar, D. (1996). Robust controller for a dynamic six degree of freedom flight simulator. In Flight Simulation Technologies Conference, San Diego, CA. AIAA.
- [Ish-Shalom, 1982] Ish-Shalom, J. (1982). Design of Optimal Motion for Flight Simulators. PhD thesis, Technion, Israel Institute of Technology.
- [Kim et al., 2006] Kim, K. D., Kim, M. S., Moon, Y. G., and Lee, M. C. (2006). Application of vehicle driving simulator using new washout algorithm and robust control. In *SICE-ICASE*. *International Joint Conference*, pages 2121–2126, Busan. IEEE.
- [Liao et al., 2004] Liao, C.-S., Huang, C.-F., and Chieng, W.-H. (2004). A novel washout filter design for a six degree-of-freedom motion simulator. *JSME International Journal Series C*, 47(2):626–636.

[McDonnell, 1969] McDonnell, J. D. (1969). An application of measurement methods to improve the quantitative nature of pilot rating scales. *IEEE Transactions on Man-Machine Systems*, 10(3):81–92.

- [Molino et al., 2003] Molino, J. A., Liao, D., Williams, J. R., and Wink, J. M. (2003). Motion cues for a 3-dof driving simulator. In *Driving Simulator Conference North America 2003 Proceedings*, Dearborn, Michigan.
- [Nahon and Reid, 1990] Nahon, M. A. and Reid, L. D. (1990). Simulator motion-drive algorithms: A designer's perspective. *Journal of Guidance, Control and Dynamics*, 13(2):356–362.
- [Nahon et al., 1992] Nahon, M. A., Reid, L. D., and Kirdeikis, J. (1992). Adaptive simulator motion software with supervisory control. *Journal of Guidance, Control and Dynamics*, 15(2):376-383.
- [Nehaoua et al., 2006] Nehaoua, L., Arioui, H., Espie, S., and Mohellebi, H. (2006). Motion cueing algorithms for small driving simulator. In *Robotics and Automation*, pages 3189–3194. IEEE.
- [Padfield and White, 2005] Padfield, G. D. and White, M. D. (2005). Measuring simulation fidelity through an adaptive pilot model. *Aerospace Science and Technology*, 9(5):400–408.
- [Parrish et al., 1973] Parrish, R. V., Dieudonne, J. E., Bowles, R. L., and Martin, D. J. (1973).
  Coordinated adaptive washout for motion simulators. In *Visual and Motion Simulation Conference*, number 73-930, Palo Alto, California. AIAA.
- [Pouliot et al., 1998] Pouliot, N. A., Gosselin, C. M., and Nahon, M. A. (1998). Motion simulation capabilities of three-degree-of-freedom flight simulators. *Journal of Aircraft*, 35(1):9–17.
- [Reid and Nahon, 1985] Reid, L. D. and Nahon, M. A. (1985). Flight simulation motion-base drive algorithms: part 1 - developing and testing the equations. Technical Report 296, Institute for Aerospace Studies, University of Toronto.
- [Reid and Nahon, 1986] Reid, L. D. and Nahon, M. A. (1986). Flight simulation motion-base drive algorithms: part 3 pilot evaluations. Technical Report 319, Institute for Aerospace Studies, University of Toronto.
- [Reid and Nahon, 1988] Reid, L. D. and Nahon, M. A. (1988). Response of airline pilots to variations in flight simulator motion algorithms. *Journal of Aircraft*, 25(7):639–646.
- [Romano, 2003] Romano, R. (2003). Non-linear optimal tilt coordination for washout algorithms. In Simulation and Modeling Conference, Austin, TX. AIAA.
- [Romano, 2005] Romano, R. (2005). Minimum time control system for use in driving simulator washout algorithms. In DSC 2005 North America, Orlando.
- [Schroeder, 1999] Schroeder, J. A. (1999). Helicopter flight simulation motion platform requirements. Technical Report TP-1999-208766, NASA.

[Seaver and Stillwell, 1983] Seaver, D. A. and Stillwell, W. G. (1983). Procedures for using expert judgment to estimate human error probabilities in nuclear power plant operations. Technical report, U.S. Nuclear Regulatory Commission.

- [Siegler et al., 2001] Siegler, I., Reymond, G., Kemeny, A., and Berthoz, A. (2001). Sensorimotor integration in a driving simulator: contributions of motion cueing in elementary driving tasks. In *DSC2001*, Sophia Antipolis.
- [Sinacori, 1977] Sinacori, J. B. (1977). The determination of some requirements for a helicopter flight research simulation facility. Technical Report CR-152066, NASA.
- [Soparkar and Reid, 2006] Soparkar, S. and Reid, L. D. (2006). The influence of simulator motion on handling qualities. *Canadian Aeronautics and Space Journal*, 52(1):21–29.
- [Spenny et al., 2000] Spenny, C. H., Liebst, B. S., Chelette, T. L., Folescu, C., and Sigda, J. (2000). Development of a sustainable-g dynamic flight simulator. In *Modeling and Simulation Technologies Conference*, number 00-4075, Denver, CO.
- [Telban and Cardullo, 2002] Telban, R. J. and Cardullo, F. M. (2002). A nonlinear, human-centered approach to motion cueing with a neurocomputing solver. In *Modeling and Simulation Technologies Conference and Exhibit*, Monterey, California.
- [Telban and Cardullo, 2005] Telban, R. J. and Cardullo, F. M. (2005). Motion cueing algorithm development: Human-centered linear and nonlinear algorithms. Technical Report CR-2005-213747, Nasa, Langley Research Center.
- [Telban et al., 2000a] Telban, R. J., Cardullo, F. M., and Guo, L. (2000a). Investigation of mathematical models of otolith organs for human centered motion cueing algorithms. In *Modeling and Simulation Technologies Conference*, number 00-4291, Denver, CO. AIAA.
- [Telban et al., 1999] Telban, R. J., Cardullo, F. M., and Houck, J. A. (1999). Developments in human centered cueing algorithms for control of flight simulator motion systems. In *Modeling and Simulation Technologies Conference and Exhibit*, number 99-4328, Portland, OR. AIAA.
- [Telban et al., 2005] Telban, R. J., Cardullo, F. M., and Kelly, L. C. (2005). Motion cueing algorithm development: Piloted performance testing of the cueing algorithms. Technical Report CR-2005-213748, Nasa.
- [Telban et al., 2000b] Telban, R. J., Wu, W., and Cardullo, F. M. (2000b). Motion cueing algorithm development: Initial investigation and redesign of the algorithms. Technical Report NASACR-2000-209863, Nasa, Langley Research Center.
- [Tran et al., 1999] Tran, D. T., Mikula, J., and Chung, W. W. (1999). Preliminary investigation of the motion fidelity criterion for a pitch-longitudinal translational task. In *Modeling and Simulation Technologies Conference and Exhibit*, number 99-4333, pages 503–511, Portland, OR. AIAA.
- [Valente Pais et al., 2007] Valente Pais, A. R., Wentink, M., Mulder, M., and van Paassen, M. M. (2007). A study on cueing strategies for curve driving in desdemona. In *Modeling and Simulation Technologies Conference and Exhibit*, number 07-6473, Hilton Head, South Carolina. AIAA.

[von der Heyde and Riecke, 2001] von der Heyde, M. and Riecke, B. E. (2001). How to cheat in motion simulation - comparing the engineering and fun ride approach to motion cueing. Technical Report 089, Max Planck Institut, Tübingen, Germany.

- [Wang and Fu, 2004] Wang, S.-C. and Fu, L.-C. (2004). Predictive washout filter design for vr-based motion simulator. In *International Conference on Systems, Man and Cybernetics*, volume 7, pages 6291 6295, The Hague, The Netherlands. IEEE.
- [Watson, 2000] Watson, G. S. (2000). A synthesis of simulator sickness studies conducted in a high-fidelity driving simulator. In *Proceedings of the Driving Simulation Conference 2000*, Paris, France.
- [Wentink et al., 2005] Wentink, M., Bles, W., Hosman, R. J. A. W., and Mayrhofer, M. (2005). Design & evaluation of spherical washout algorithm for desdemona simulator. In *Modeling and Simulation Technologies Conference and Exhibit*, San Francisco, CA.
- [Wentink et al., 2008a] Wentink, M., Correia Grácio, B. J., Groen, E. L., Feenstra, P., and Bles, W. (2008a). New technologies & applications in the desdemona simulator. In RAeS Spring 2008 Flight Simulation Conference, Expanding Horizons: Technology Advances in Flight Simulation.
- [Wentink et al., 2008b] Wentink, M., Valente Pais, A. R., Mayrhofer, M., Feenstra, P., and Bles, W. (2008b). First curve driving experiments in the desdemona simulator. In *DSC* 2008 Europe, pages 135–146, Monaco.
- [White and Rodchenko, 1999] White, A. D. and Rodchenko, V. V. (1999). Motion fidelity criteria based on human perception and performance. In *Modelling and Simulation Technologies Conference*, number 99-4430, pages 485–493, Portland, OR. AIAA.
- [Wu and Cardullo, 1997] Wu, W. and Cardullo, F. M. (1997). Is there an optimum motion cueing algorithm? In *Modeling and Simulation Technologies Conference*, New Orleans, LA. AIAA.
- [Zacharias, 1978] Zacharias, G. (1978). Motion cue models for pilot-vehicle analysis. Technical report, Aerospace Medical Research Laboratory.
- [Zywiol and Romano, 2003] Zywiol, H. J. and Romano, R. (2003). Motion drive algorithms and simulator design to study motion effects on infantry soldiers. In *Driving Simulator Conference North America 2003 Proceedings*, Dearborn, Michigan.

## Part V

## **Appendices**

### Appendix A

### Car model radius calculation

Consider the vector  $\overrightarrow{AB}$  defined in Figure A-1. If point A coordinates are (1,0) and  $\overrightarrow{AB}$  is an unitary vector, then point B coordinates are  $(\cos \alpha + 1, -\sin \alpha)$ . Vector  $\overrightarrow{AB}$  is then defined by  $(\cos \alpha, -\sin \alpha)$ . Now lets define a new vector perpendicular to  $\overrightarrow{AB}$  and with coordinates (a,b). From the inner product formula (A-1) we know that the dot product of  $\overrightarrow{AB}$  with a perpendicular vector is equal to zero. Therefore we can write equation (A-2).

$$\cos \theta = \frac{x \cdot y}{|x| |y|} \tag{A-1}$$

$$a\cos\alpha - b\sin\alpha = 0 \iff a = \frac{\sin\alpha}{\cos\alpha}b$$
 (A-2)

The vector perpendicular to  $\overrightarrow{AB}$ ,  $\overrightarrow{AB_{\perp}}$ , can be defined as  $(\frac{\sin \alpha}{\cos \alpha}b, b)$ . The mid point of  $\overrightarrow{AB}$  is given by  $(\frac{2+\cos \alpha}{2}, \frac{-\sin \alpha}{2})$ . With this information it is possible to define a straight-line perpendicular to  $\overrightarrow{AB}$  and that passes throught the mid point of  $\overrightarrow{AB}$ . This straight-line is defined by equation (A-3).

$$y = \frac{\cos \alpha}{\sin \alpha} x - \frac{(2\cos \alpha + 1)}{2\sin \alpha}$$
 (A-3)

If the blue vector of Figure A-1 is also a unitary vector. Then to obtain Radius<sub>p</sub> we only need to substitute x in equation (A-3) by 1/2.

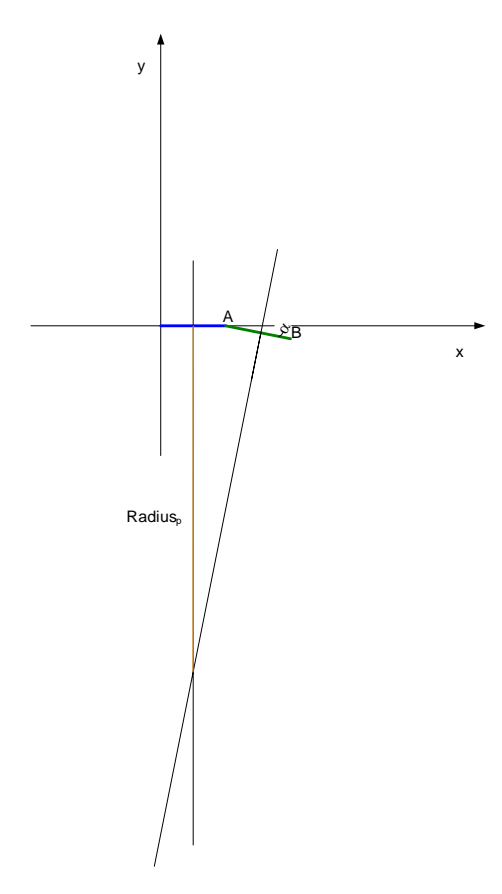


**Figure A-1:** Radius of a curve. The blue vector represents the tire in a time instant. The green vector represents the tire in a future time instant, making an angle  $\alpha$  with the blue vector. The orange line is proportional to the real curve radius.

## Appendix B

# Questionnaires (Dutch)

M.Sc. thesis

## Instructie experiment MOVES - rijsimulatorstudie-

Wilt u deze instructie zorgvuldig doorlezen.

Tijdens dit experiment rijdt u buiten de stad op een tweestrooksweg. In het midden van de weg staan pylonen waar u om heen dient te slalommen. De eerste pylon passeert u steeds van rechts naar links. De auto waar u in rijdt is een Volkswagen Passat automaat waarbij de snelheid begrensd is op 70 km/u.

In dit experiment zult u verschillende ritten rijden, waarbij de aangeboden beweging per rit verschillend is. Elke rit bevat een aantal slalom parcoursen. U zult beginnen met een slalom oefenrit. Daarna beginnen de ritten van het echte experiment. Hier zal per rit, bij ieder volgend slalomparcours, de afstand tussen de pylonen kleiner worden.

Uw doel is om de rit in een zo kort mogelijke tijd af te leggen. Dus probeer zo snel mogelijk te rijden zonder de auto te beschadigen. Verminder alleen de snelheid als u de auto niet meer onder controle heeft. Bijvoorbeeld als u van weg af dreigt te raken of de pylonen begint te raken.

Na iedere rit vragen wij uw mening over de gereden rit door middel van een vragenlijst. We zijn geïnteresseerd in uw mening!



#### **PROEFPERSOONVERKLARING**

Ondergetekend	e,		
Naam o Dhr o Mevrouw			
Geb. datum			
Rijbewijs sinds			19
Gemiddeld aan	tal kilometer rijervaring per j	aar:	
Rijsimulator er	varing in uren:		
Heeft u een nor	rmale nacht gehad:	□ ja	□ nee
Voelt u zich ok	ay:	□ ja	$\square$ nee
Desdemona simu experiment waar	ulator, uitgevoerd bij TNO te So	esterberg. Ik het op een weg bui	speriment m.b.t. onderzoek in de o begrepen dat het daarbij gaat om een ten de bebouwde kom, waarbij ik
uitgelegd, en mij op elk moment z kan de proefleide	conder opgaaf van redenen mijn	er bevredigend b deelname aan he mijn deelname a	eantwoord. Er is mij verzekerd dat ik et experiment kan beëindigen. Evenzo an het experiment beëindigen. Ik zal
	an de resultaten van het experim zijn op enigerlei wijze mijn ide		privacy beschermd in die zin dat het nalen.
Voorts verklaar	ik lichamelijk in goede gezondh	eid te verkeren.	
Soesterberg,	2008		
Handtekening pr	roefpersoon:		
Proefpersoon-nr	:		
TOELATING			
Naam proefleide	er:		
	rvan overtuigd dat deze proefper md experiment deel te mogen ne		n de selectiecriteria om aan
Soesterberg, date	um		
Handtekening pr	oefleider:		

Proefpersoonnummer:

Simulator rit: 1

In hoeverre bent u het eens met de volgende stellingen (omcirkel het nummer)?

1.	Ik was	echt aan	het rijden.
----	--------	----------	-------------

Helemaal niet mee eens 1 2 3 4 5 6 7 Helemaal mee eens

#### 2. Ik vergat dat ik in een simulator zat.

Helemaal niet mee eens 1 2 3 4 5 6 7 Helemaal mee eens

#### 3. Ik reed de auto zoals ik normaal ook zou doen.

Helemaal niet mee eens 1 2 3 4 5 6 7 Helemaal mee eens

#### 4. Ik had het gevoel dat ik gewond kon raken tijdens het uitvoeren van de rijtaak.

Helemaal niet mee eens 1 2 3 4 5 6 7 Helemaal mee eens

#### 5. Ik was best gespannen tijdens het uitvoeren van de rijtaak.

Helemaal niet mee eens 1 2 3 4 5 6 7 Helemaal mee eens

#### 6. Ik vond het rijden leuk.

Helemaal niet mee eens 1 2 3 4 5 6 7 Helemaal mee eens

#### 7. De auto stuurde normaal, zoals ik gewend ben.

Helemaal niet mee eens 1 2 3 4 5 6 7 Helemaal mee eens

#### 8. De bewegingen in de auto voelden zoals ik gewend ben.

Helemaal niet mee eens 1 2 3 4 5 6 7 Helemaal mee eens

Proefpersoonnummer: Simulator rit: 1 9. Ik voelde me vertrouwd met de auto. Helemaal niet mee Helemaal mee 7 4 5 6 eens eens 10. Soms had ik het gevoel de controle over de auto te verliezen. Helemaal niet mee Helemaal mee 1 2 3 5 7 eens eens 11. Ik heb het maximale uit de prestaties van de auto gehaald (in bochten). Helemaal niet mee Helemaal mee 7 1 2 3 4 5 6 eens eens 12. Het voelde alsof ik een echte auto bestuurde. Helemaal niet mee Helemaal mee 1 2 3 7 5 6 eens eens 13. De rijtaak was makkelijk. Helemaal niet mee Helemaal mee 7 1 2 3 5 6 4 eens eens 14. Ik heb de taakuitvoering aangepast aan de beperkingen van de simulator. Helemaal niet mee Helemaal mee 7 1 2 3 4 5 6 eens eens 15. Ik voerde de rijtaak goed uit. Helemaal niet mee Helemaal mee 7 1 2 3 5 6 4 eens eens

16. De bewegingen en krachten die ik voelde hielpen me bij de taakuitvoering. Helemaal niet mee 1 2 3 4 5 6 7 Helemaal mee

eens 1 2 3 4 5 6 7 Helenia eens 1 eens

17. De simulatie was realistisch.

Helemaal niet mee
eens
1 2 3 4 5 6 7

Helemaal mee
eens

Proefpersoonnummer:

Simulator rit: 1

18. De bewegingen	ı en kracht	en van	de sin	nulator	voeld	en real	ıstısch	aan.
Helemaal niet mee	1	2	3	4	5	6	7	Helemaal mee eens
19. Het buitenbeeld	l in de sim	ulator	was re	alistisc	ch.			
Helemaal niet mee	1	2	3	4	5	6	7	Helemaal mee eens
20. Het gezichtsvel	d in de sir	nulatoi	: was g	root ge	enoeg.			
Helemaal niet mee	1	2	3	4	5	6	7	Helemaal mee eens
21. Ik was heel gef								
Helemaal niet mee	1	2	3	4	5	6	7	Helemaal mee eens
22. Ik ben tot het u		aan.						
Helemaal niet mee	1	2	3	4	5	6	7	Helemaal mee eens
23. Ik werd uitgeda	agd om go	oed te j	prester	en.				
Helemaal niet mee	1	2	3	4	5	6	7	Helemaal mee eens
24. Ik ben steeds be	eter gewor	den.						
Helemaal niet mee	1	2	3	4	5	6	7	Helemaal mee eens
25. Na deze ervarir	ng, kan ik o	de rijta	ak ook	in het	echt b	eter ui	tvoerei	1.
Helemaal niet mee	1	2	3	4	5	6	7	Helemaal mee eens
26. Deze ervaring l	neeft me g	eholpe	n om d	le benc	odigde	rij-vaa	rdighe	id te ontwikkelen.
Helemaal niet mee	1	2	3	4	5	6	7	Helemaal mee eens

Proefpersoonnummer: Simulator rit: 1

#### Hoe voelt u zich (omcirkel het nummer):

- Okay, geen klachten.
   Voel m'n maag / licht in 't hoofd, maar niet misselijk.
- 3. Beetje misselijk
- 4. Misselijk
- 5. Erg misselijk
- 6. Braken

Proefpersoonnummer:

Simulator rit: 2

In hoeverre bent u het eens met de volgende stellingen (omcirkel het nummer)?

1.	Ik was	echt aan	het rijden.
----	--------	----------	-------------

Helemaal niet mee eens 1 2 3 4 5 6 7 Helemaal mee eens

#### 2. Ik vergat dat ik in een simulator zat.

Helemaal niet mee eens 1 2 3 4 5 6 7 Helemaal mee eens

#### 3. Ik reed de auto zoals ik normaal ook zou doen.

Helemaal niet mee eens 1 2 3 4 5 6 7 Helemaal mee eens

#### 4. Ik had het gevoel dat ik gewond kon raken tijdens het uitvoeren van de rijtaak.

Helemaal niet mee eens 1 2 3 4 5 6 7 Helemaal mee eens

#### 5. Ik was best gespannen tijdens het uitvoeren van de rijtaak.

Helemaal niet mee eens 1 2 3 4 5 6 7 Helemaal mee eens

#### 6. Ik vond het rijden leuk.

Helemaal niet mee eens 1 2 3 4 5 6 7 Helemaal mee eens

#### 7. De auto stuurde normaal, zoals ik gewend ben.

Helemaal niet mee eens 1 2 3 4 5 6 7 Helemaal mee eens

#### 8. De bewegingen in de auto voelden zoals ik gewend ben.

Helemaal niet mee eens 1 2 3 4 5 6 7 Helemaal mee eens

15. Ik voerde de rijtaak goed uit. Helemaal niet mee Helemaal mee 7 1 2 3 5 6 4 eens eens 16. De bewegingen en krachten die ik voelde hielpen me bij de taakuitvoering. Helemaal niet mee Helemaal mee 7 1 2 3 4 5 6 eens eens 17. De simulatie was realistisch. Helemaal niet mee Helemaal mee 1 7 2 3 4 5 6 eens eens

Proefpersoonnummer: Simulator rit: 2

18. De beweginge	n en kr	achter	n van d	le simu	ılator v	oelder	realis	tisch a	an.
Helemaal niet me een		1	2	3	4	5	6	7	Helemaal mee eens
19. Het buitenbeel		simu	lator w	as real	listisch	•			
Helemaal niet me een		1	2	3	4	5	6	7	Helemaal mee eens
20. Het gezichtsve		e simu	ılator v	was gro	oot gen	ioeg.			
Helemaal niet me een		1	2	3	4	5	6	7	Helemaal mee eens
21. Ik was heel ge	focuse	d.							
Helemaal niet me een		1	2	3	4	5	6	7	Helemaal mee eens
22. Ik ben tot het u	iiterste	gegaa	ın.						
Helemaal niet me een	e	1	2	3	4	5	6	7	Helemaal mee eens
23. Ik werd uitged	aagd o	m goe	d te pr	esterei	1.				
Helemaal niet me een		1	2	3	4	5	6	7	Helemaal mee eens
24. Ik ben steeds b	eter ge	eworde	en.						
Helemaal niet me een		1	2	3	4	5	6	7	Helemaal mee eens
25. Na deze ervari	ng, kai	ı ik de	rijtaal	k ook i	n het e	cht be	ter uity	oeren.	
Helemaal niet me een	e	1	2		4	5	6	7	Helemaal mee eens
26. Deze ervaring	heeft r	ne gel	nolpen	om de	benod	igde ri	i-vaaro	ligheid	l te ontwikkelen.
Helemaal niet me	e	1	2	3	4	5	6	7	Helemaal mee eens

Proefpersoonnummer: Simulator rit: 2

Hoe voelt u zich (omcirkel het nummer):

- 1. Okay, geen klachten.
- 2. Voel m'n maag / licht in 't hoofd, maar niet misselijk.
- 3. Beetje misselijk
- 4. Misselijk
- 5. Erg misselijk
- 6. Braken

Welke van de twee condities voelde het meest realistisch (benaderde het gevoel in een echte auto het best, omcirkel het nummer)?

- 1. Een na laatste rit
- 2. Laatste rit

Proefpersoonnummer:

Simulator rit: 3

In hoeverre bent u het eens met de volgende stellingen (omcirkel het nummer)?

1.	Ik was	echt aan	het rijden.
----	--------	----------	-------------

Helemaal niet mee eens 1 2 3 4 5 6 7 Helemaal mee eens

#### 2. Ik vergat dat ik in een simulator zat.

Helemaal niet mee eens 1 2 3 4 5 6 7 Helemaal mee eens

#### 3. Ik reed de auto zoals ik normaal ook zou doen.

Helemaal niet mee eens 1 2 3 4 5 6 7 Helemaal mee eens

#### 4. Ik had het gevoel dat ik gewond kon raken tijdens het uitvoeren van de rijtaak.

Helemaal niet mee eens 1 2 3 4 5 6 7 Helemaal mee eens

#### 5. Ik was best gespannen tijdens het uitvoeren van de rijtaak.

Helemaal niet mee eens 1 2 3 4 5 6 7 Helemaal mee eens

#### 6. Ik vond het rijden leuk.

Helemaal niet mee eens 1 2 3 4 5 6 7 Helemaal mee eens

#### 7. De auto stuurde normaal, zoals ik gewend ben.

Helemaal niet mee eens 1 2 3 4 5 6 7 Helemaal mee eens

#### 8. De bewegingen in de auto voelden zoals ik gewend ben.

Helemaal niet mee eens 1 2 3 4 5 6 7 Helemaal mee eens

Proefpersoonnummer: Simulator rit: 3 9. Ik voelde me vertrouwd met de auto. Helemaal niet mee Helemaal mee 7 4 5 6 eens eens 10. Soms had ik het gevoel de controle over de auto te verliezen. Helemaal niet mee Helemaal mee 1 2 3 5 7 eens eens 11. Ik heb het maximale uit de prestaties van de auto gehaald (in bochten). Helemaal niet mee Helemaal mee 7 1 2 3 4 5 6 eens eens 12. Het voelde alsof ik een echte auto bestuurde. Helemaal niet mee Helemaal mee 1 2 3 7 5 6 eens eens 13. De rijtaak was makkelijk. Helemaal niet mee Helemaal mee 7 1 2 3 5 6 4 eens eens 14. Ik heb de taakuitvoering aangepast aan de beperkingen van de simulator. Helemaal niet mee Helemaal mee 7 1 2 3 4 5 6 eens eens 15. Ik voerde de rijtaak goed uit. Helemaal niet mee Helemaal mee 7 1 2 3 5 6 4 eens eens

16. De bewegingen en krachten die ik voelde hielpen me bij de taakuitvoering.

Helemaal niet mee eens 1 2 3 4 5 6 7 Helemaal mee eens

17. De simulatie was realistisch.

Helemaal niet mee eens 1 2 3 4 5 6 7 Helemaal mee eens

Proefpersoonnummer:

Simulator rit: 3

18. De bewegi	ingen en kr	acnter	ı van a	e simu	nator v	oeiaen	reams	tisch a	an.
Helemaal niet	mee eens	1	2	3	4	5	6	7	Helemaal mee eens
19. Het buiten	beeld in de	simul	ator w	as real	istisch				
Helemaal niet	mee eens	1	2	3	4	5	6	7	Helemaal mee eens
20. Het gezich	tsveld in d	e simu	ılator v	vas gro	oot gen	oeg.			
Helemaal niet	mee eens	1	2	3	4	5	6	7	Helemaal mee eens
21. Ik was hee	l gefocuse	d.							
Helemaal niet	mee eens	1	2	3	4	5	6	7	Helemaal mee eens
22. Ik ben tot l	het uiterste	gegaa	ın.						
Helemaal niet	mee eens	1	2	3	4	5	6	7	Helemaal mee eens
23. Ik werd ui	tgedaagd o	m goe	d te pr	esterer	1.				
Helemaal niet	-	1	2	3	4	5	6	7	Helemaal mee eens
24. Ik ben stee	eds beter ge	eworde	en.						
Helemaal niet	_	1	2	3	4	5	6	7	Helemaal mee eens
25. Na deze er	varing, ka	n ik de	rijtaak	c ook i	n het e	cht bet	er uitv	oeren.	
Helemaal niet	_	1	2	3	4	5	6	7	Helemaal mee eens
26. Deze ervai	ring heeft r	ne geh	olpen	om de	benod	igde ri	j-vaard	ligheid	te ontwikkelen.
Helemaal niet	mee	1	2	3	4	5	6	7	Helemaal mee eens

Proefpersoonnummer: Simulator rit: 3

Hoe voelt u zich (omcirkel het nummer):

- 1. Okay, geen klachten.
- 2. Voel m'n maag / licht in 't hoofd, maar niet misselijk.
- 3. Beetje misselijk
- 4. Misselijk
- 5. Erg misselijk
- 6. Braken

Welke van de twee **laatste** condities voelde het meest realistisch (benaderde het gevoel in een echte auto het best, omcirkel het nummer)?

- 3. Een na laatste rit
- 4. Laatste rit

Proefpersoonnummer:

Simulator rit: 4

In hoeverre bent u het eens met de volgende stellingen (omcirkel het nummer)?

1.	Ik	was	echt	aan	het	rij	iden.

Helemaal niet mee eens 1 2 3 4 5 6 7 Helemaal mee eens

#### 2. Ik vergat dat ik in een simulator zat.

Helemaal niet mee eens 1 2 3 4 5 6 7 Helemaal mee eens

#### 3. Ik reed de auto zoals ik normaal ook zou doen.

Helemaal niet mee eens 1 2 3 4 5 6 7 Helemaal mee eens

#### 4. Ik had het gevoel dat ik gewond kon raken tijdens het uitvoeren van de rijtaak.

Helemaal niet mee eens 1 2 3 4 5 6 7 Helemaal mee eens

#### 5. Ik was best gespannen tijdens het uitvoeren van de rijtaak.

Helemaal niet mee eens 1 2 3 4 5 6 7 Helemaal mee eens

#### 6. Ik vond het rijden leuk.

Helemaal niet mee eens 1 2 3 4 5 6 7 Helemaal mee eens

#### 7. De auto stuurde normaal, zoals ik gewend ben.

Helemaal niet mee eens 1 2 3 4 5 6 7 Helemaal mee eens

#### 8. De bewegingen in de auto voelden zoals ik gewend ben.

Helemaal niet mee eens 1 2 3 4 5 6 7 Helemaal mee eens

Proefpersoonnummer: Simulator rit: 4 9. Ik voelde me vertrouwd met de auto. Helemaal niet mee Helemaal mee 7 4 5 6 eens eens 10. Soms had ik het gevoel de controle over de auto te verliezen. Helemaal niet mee Helemaal mee 1 2 3 5 7 eens eens 11. Ik heb het maximale uit de prestaties van de auto gehaald (in bochten). Helemaal niet mee Helemaal mee 7 1 2 3 4 5 6 eens eens 12. Het voelde alsof ik een echte auto bestuurde. Helemaal niet mee Helemaal mee 1 2 3 7 5 6 eens eens 13. De rijtaak was makkelijk. Helemaal niet mee Helemaal mee 7 1 2 3 5 6 4 eens eens 14. Ik heb de taakuitvoering aangepast aan de beperkingen van de simulator. Helemaal niet mee Helemaal mee 7 1 2 3 4 5 6 eens eens 15. Ik voerde de rijtaak goed uit. Helemaal niet mee Helemaal mee 7 1 2 3 5 6 4 eens eens

17. De simulatie was realistisch.
Helemaal niet mee
eens 1 2 3 4 5 6 7 Helemaal mee
eens

4

5

6

Helemaal mee

eens

7

16. De bewegingen en krachten die ik voelde hielpen me bij de taakuitvoering.

3

1

2

Helemaal niet mee

eens

Proefpersoonnummer: Simulator rit: 4

18. De bewegn	ngen en kr	achten	van d	e simu	lator v	oelden	realist	asch aa	an.
Helemaal niet	mee eens	1	2	3	4	5	6	7	Helemaal mee eens
19. Het buitent		simul	ator wa	as real	istisch				** .
Helemaal niet	mee eens	1	2	3	4	5	6	7	Helemaal mee eens
20. Het gezicht		e simu	lator w	vas gro	ot gen	oeg.			
Helemaal niet	mee eens	1	2	3	4	5	6	7	Helemaal mee eens
21. Ik was heel		d.							Halamaal maa
Helemaal niet	eens	1	2	3	4	5	6	7	Helemaal mee eens
22. Ik ben tot h Helemaal niet		gegaa	n.						Halamaal maa
	eens	1	2	3	4	5	6	7	Helemaal mee eens
23. Ik werd uit		m goe	d te pre	esteren	l <b>.</b>				
Helemaal niet	mee eens	1	2	3	4	5	6	7	Helemaal mee eens
24. Ik ben stee	_	eworde	en.						Halamaal maa
Helemaal niet	mee eens	1	2	3	4	5	6	7	Helemaal mee eens
25. Na deze er	-	n ik de	rijtaak	ook ii	n het e	cht bet	er uitv	oeren.	
Helemaal niet	mee eens	1	2	3	4	5	6	7	Helemaal mee eens
	_	ne geh	olpen (	om de	benodi	igde rij	j-vaard	igheid	te ontwikkelen.
Helemaal niet	mee eens	1	2	3	4	5	6	7	Helemaal mee eens

Proefpersoonnummer: Simulator rit: 4

Hoe voelt u zich (omcirkel het nummer):

- 1. Okay, geen klachten.
- 2. Voel m'n maag / licht in 't hoofd, maar niet misselijk.
- 3. Beetje misselijk
- 4. Misselijk
- 5. Erg misselijk
- 6. Braken

Welke van de twee **laatste** condities voelde het meest realistisch (benaderde het gevoel in een echte auto het best, omcirkel het nummer)?

- 1. Een na laatste rit
- 2. Laatste rit

Algemene opmerkingen: